VOLUME 87, NO. 1
MAY 1961

JOURNAL of the

Hydraulics Division

PROCEEDINGS OF THE
AMERICAN SOCIETY
OF CIVIL ENGINEERS

Vol. 87 No. HY 3

Journal of the

HYDRAULICS DIVISION

Proceedings of the American Society of Civil Engineers

CONTENTS

May, 1961

Papers

(over)

Note.—Part 2 of this Journal is the 1961-17 Newsletter of the Hydraulics Division.

The three preceding issues of this Journal are dated November 1960, January 1961, and March 1961.

DISCUSSION

Journal of the
HYDRAULICS DIVISION
Proceedings of the American Society of Civil Engineers

MECHANICS OF WASHOUT OF AN ERODIBLE FUSE PLUG

By E. Roy Tinney,[1] M. ASCE, and H. Y. Hsu,[2] F. ASCE

SYNOPSIS

Laboratory and field experiments are described that were undertaken to demonstrate the feasibility of a fuse plug in the spillway of a major dam. From the data and from tractive force theory, similitude relationships are derived that permit the application of model test results to rates of washout.

INTRODUCTION

The Idaho spillway of the Oxbow project, on the Snake River between Idaho and Oregon, will have a fuse-plug control instead of conventional gates. The prototype fuse plug as designed and constructed for control of this spillway will provide an economical, safe, and effective control for the maximum designed flow of 150,000 cfs. The combined design capacity of the fuse-plug spillway and the conventional spillway is 300,000 cfs.

The fuse plug is simply a rockfill dam with special arrangement of the impervious core and strict control of the rockfill and filter materials. It has a factor of safety equal to that for ordinary rockfill or earth dams when it functions as a dam; however, it will be washed out by the reservoir water automatically at a suitable rate when the spillway capacity is required.

The general arrangement of the fuse plug controlled Idaho spillway is shown in Fig. 1. The fuse plug, located across the upper end of the approach channel,

Note.—Discussion open until October 1, 1961. To extend the closing date one month, a written request must be filed with the Executive Secretary, ASCE. This paper is part of the copyrighted Journal of the Hydraulics Division, Proceedings of the American Society of Civil Engineers, Vol. 87, No. HY 3, May, 1961.

[1] Head, The R. L. Albrook Hydr. Lab., Div. of Industrial Research, and Prof., Dept. of Civ. Engrg., Wash. State Univ., Pullman, Wash.

[2] Proj. Engr., Internatl. Engrg. Co., San Francisco, Calif.

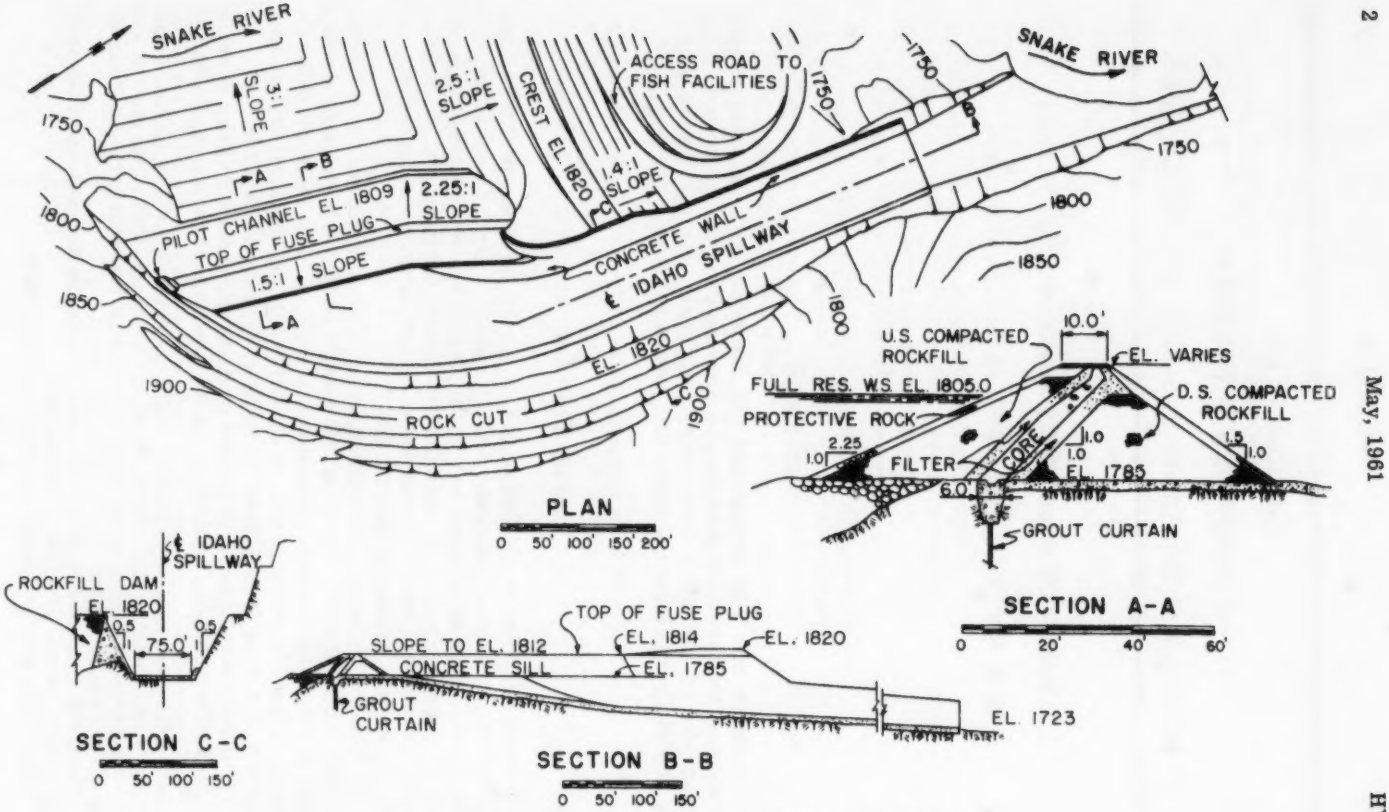

FIG. 1.—FUSE PLUG SPILLWAY GENERAL ARRANGEMENT

has a total length of 440 ft and varies in height from 27 ft to 29 ft above a level concrete sill.

At the upstream end of the embankment, a pilot channel, 10 ft wide with an invert 3 ft lower than the crest, is provided to start the washout of the fuse plug at a predesignated location. The location of this pilot channel is chosen so that the flow of water, during washout, will be smoothly channeled into the spillway chute.

When it is required to pass an extraordinary flood exceeding the capacity of the Oregon spillway, the fuse plug would be washed out to provide additional capacity. To initiate the fuse-plug breach, the Oregon spillway gates would be closed slightly raising the reservoir water surface to the required predetermined level, one foot above the invert of the pilot channel. After breaching, the fuse plug would wash out progressively from the upstream to the downstream end in an orderly manner. During the washout, the Oxbow reservoir would be kept more or less at constant level by closing the Oregon spillway gates, thus shifting the discharge from the Oregon spillway to the Idaho spillway with no appreciable variation of outflow.

Fuse-plug controlled spillways have previously been designed and constructed. The Aluminum Company of America has seven such spillways in service in North Carolina which were constructed under the direction of James P. Growdon, F. ASCE, the originator and pioneer in the use of the fuse plug for the control of spillways in the United States. Fuse-plug sections have been used on levees for passing extraordinary floods on major rivers in this country and abroad. In case of unusual floods, the fuse plug is designed to wash out either automatically or artifically to minimize flood damages.

As most existing fuse-plug spillways have not been in service long enough to pass their design floods, thereby demonstrating their washout performance, literature describing the mechanics of washout of a fuse plug is insufficient to provide practical data substantiating design assumptions. Although scattered information is known from observations of washout of cofferdams and levees, it would be difficult to arrive at any reliable statistical deductions as to the washout characteristics. A project as large as the Oxbow project on the Snake River required more thorough investigation.

Before the fuse-plug spillway could be approved for construction, several fundamental engineering aspects had to be thoroughly investigated, so that there could be no doubt that the fuse plug would function as designed.

1. How does the pilot channel breach? What is the water depth over the pilot channel before it breaches?
2. What is the nature of the washout process after the initial breach? What is the speed of washout?
3. How complete is the washout? Will any portion of the plug remain intact?

The fuse plug was designed according to theoretical computations based mainly upon bed load transportation principles and modern concepts of soil mechanics. However, the assumptions made by the design engineers required verification by a large scale model. Furthermore, some basic information, which could only be found through a large scale model test, was needed to finalize the design. After considerable planning, it was decided to conduct a 1/2-scale model test at the project site where the same materials could be used for both model and prototype, the construction equipment and control personnel

would be readily available, and a large quantity of water and constant head could be provided in the Oxbow reservoir upstream from the diversion cofferdam.

Because of the large expenditure involved in the construction and testing of the 1/2-scale model, as well as interference with upstream power generation at Brownlee Dam during the test, it was impractical to repeat the 1/2-scale model test. In other words, the information which was desired from the large scale model had to be obtained in one test. Therefore, preparatory tests of small scale models in the laboratory, and of large scale flume models in the field were deemed necessary.

From experience with river models which usually are of small scale and deal with small particle sizes, it is known that model results are, at best, only indicative. However, for large particle sizes and large scale models, model test results are surprisingly accurate, as demonstrated at the Fort Randall closure.[3]

It has also been established experimentally that the bed-load transport of non-cohesive material has a definite relationship to the tractive force. In order to avoid the troublesome problem of simulating the particle size, shape, and compaction, it was decided to use the same material and the same construction control for both the large scale field model and the prototype and to establish the similitude relationship by using the tractive force, the only predominant variable, as the basis. It was also considered important to have a scale ratio as large as possible, to minimize not only the scale effect, but also the influence of critical tractive force.

LABORATORY INVESTIGATIONS

Laboratory investigations, including experimental tests and theoretical derivations, were performed to determine (a) the mechanics of the washout process, and (b) the similitude relationship for the rate of washout.

For convenience, the model tests were made in the downstream portion of an existing model. A concrete pad and concrete blocks were placed to form a non-erodible base and a vertical wall was constructed on the right (looking downstream) bank.

The fuse plug models were constructed with axes angled 64° from the face of the right wall. The typical cross sections of the models are shown in Fig. 2. These are for 1:20 and 1:40 scale models of the proposed Oxbow fuse plug. The mechanical analysis of the materials used in each model are shown in Fig. 3.

No attempt was made to duplicate the density or other characteristics of the materials which would be used in the prototype. However, considerable effort was made in constructing the different 1:20 and 1:40 scale models to achieve identical placement and compaction of like materials.

In all, ten models were built and washed out as shown in Table 1. The normal core and thin core, referred to previously, represent the two types of cores used. In the thin core section, the rockfill material was increased to its maximum possible area for the purpose of testing its influence on washout time. The dimensions of these cores are given in Fig. 2.

---

[3] "Dredge Fill Closure of Missouri River at Fort Randall," by Lorenz G. Straub, Proceedings, Minnesota Internatl. Hydr. Convention, September, 1953.

In the 1:20 model, the invert of the pilot channel was 3 in. lower than the crest of the fuse plug, and the width (parallel to the axis of the fuse plug model) was 6 in. In the 1:40 model these dimensions were 2 in. and 3 in., respectively.

The operation of the tests was as follows:

1. The forebay was filled to the level of the invert of the pilot channel.
2. The forebay water level was then raised rapidly the prescribed amount (approximately 0.4 in.) to achieve initial breach action.
3. The forebay level was held more or less constant at this elevation during the washout process by continually increasing the inflow.
4. A record was kept of the time at which the top and bottom of rows of beads spaced at 1-ft intervals along the model were washed away.
5. Photographs were taken and the time recorded for each photograph.
6. A movie was taken of Test Nos. 3 and 5.

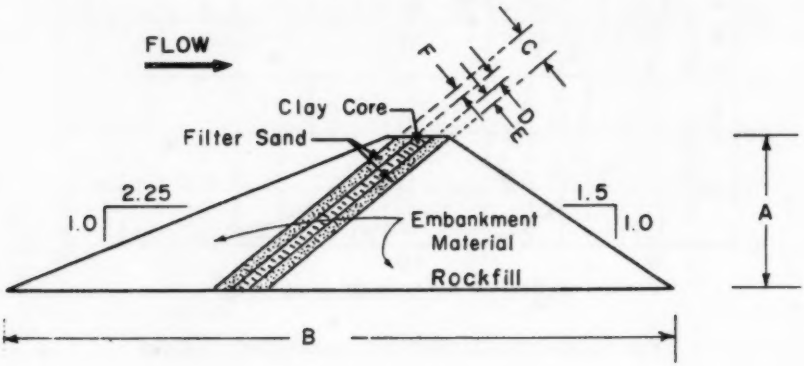

TYPICAL SECTION

	A	B	C	D	E	F
1:20 Normal Core	16.20	66.75	9.0	3.6	2.7	2.7
1:20 Thin Core	16.20	66.75	0.75	0.25	0.25	0.25
1:40 Normal Core	8.10	33.37	4.5	1.8	1.35	1.35

Dimensions of Model in Inches

FIG. 2.—DIMENSIONS OF LABORATORY MODELS

Test Results.

Description of Washout Process.—The washout process as observed in these tests consists essentially of two phases, (1) the breaching of the pilot channel, and (2) the eroding of embankment face. The breaching action starts with an initial slip at the downstream end of the pilot channel (Fig. 4). This slippage rapidly increases until the clay core is exposed. The flow then cascades over the clay core and begins to erode the material downstream nearly to the base of the model. At approximately this time the clay core, which is left

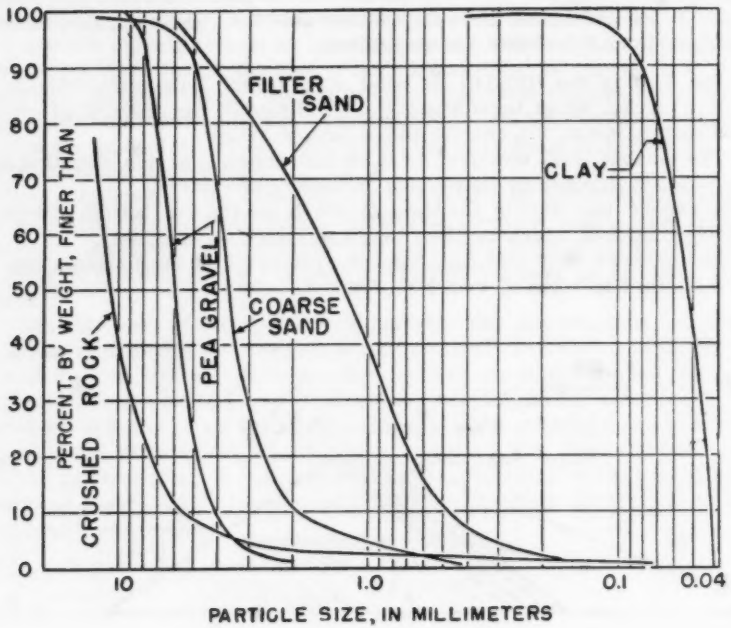

FIG. 3.—MATERIAL USED IN LABORATORY MODELS

FIG. 4.—INITIAL SLIP IN PILOT CHANNEL

standing as a cantilever by the removal of the supporting downstream material, fails under the water load and the breaching action is complete. The flow then begins to attack the base of the embankment, carrying away the material as it slides into the flow and producing a lateral advance of the eroding face along the length of the fuse plug. When a sufficiently large portion of the core is exposed, it breaks off. This process proceeds in a most regular manner gradually increasing the opening and washing out the fuse plug.

The shape of the eroding face depends on the nature of the materials. For uniformly graded material without fines, the slopes on the eroding face are gradual and the material rolls continuously into the flow (Fig. 5), but for materials that have some apparent cohesion or mechanical interlocking, the face stands nearly vertical (Fig. 6). With the latter materials, the face recedes by sudden large slips of the material and sudden failure of portions of the clay core.

Experimental Data.—The data on the rate of washout for each of the ten tests are plotted as graphs in Figs. 7, 8, and 9, which show the eroded length of the

TABLE 1

Composition of Model	Code Number of Test	
	1:20 Scale	1:40 Scale
Coarse sand - normal core	1	4
Pea gravel - normal core	2	5
Crushed rock - normal core	3	6
Filter sand - normal core	7	-
Crushed rock - thin core	8	-
Pea gravel - thin core	9	-
Crushed rock - normal core (Repeat of Test 3)	10	-

model as a function of time. In Fig. 7, R is the rate of recession of the eroding face, in feet per hour; and R_r denotes the ratio of the rate of recession for the 1:20 scale to the 1:40 scale model. The average values of the top and bottom washout times were used. Rows affected by breaching action were not included.

In the interest of determining laboratory test accuracy, the 1:20 crushed rock model test was repeated. The results of the two tests were remarkably close. The differences are well within the expected accuracy of measurement of this type of test (Fig. 10).

Analysis of Experimental Results.—Analysis of the laboratory washout tests results indicates the following:

1. The washout rate is a function of the grain size of the material; the larger the size, the slower the rate of washout. However, the effect is not pronounced.
2. The washout rate for a fuse plug is between 1.05 and 1.20 times faster than the corresponding half-scale model.
3. Increasing the volume of rockfill (reducing the thickness of the clay core) decreases the washout rate slightly.

Theoretical Analyses.—After the pilot channel has been breached, the main embankment washes out in a regular manner, as described previously. The following treatment of the mechanics of washout has been made to establish the similitude relationship.

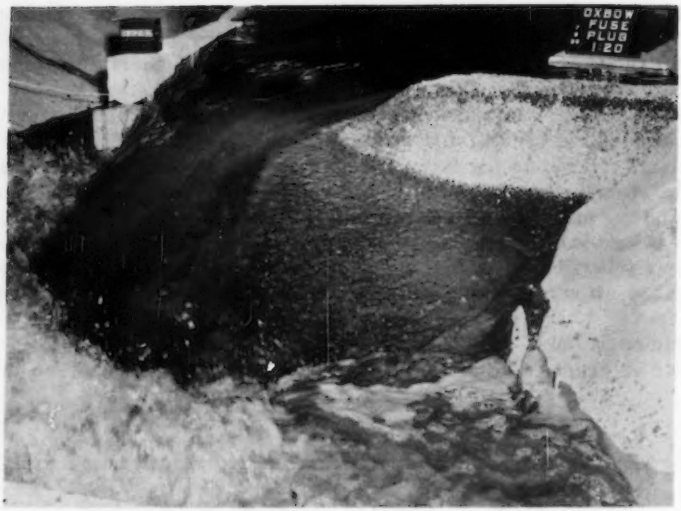

FIG. 5.—SLOPING FACE WITH UNIFORMLY GRADED MATERIAL

FIG. 6.—VERTICAL FACE WITH MATERIALS HAVING APPARENT COHESION OR MECHANICAL INTERLOCKING (TEST 3)

Referring to the definition sketch (Fig. 11) the rate of recession of the eroding face of the main embankment will be

$$R = \frac{q}{A} \quad \ldots\ldots\ldots\ldots\ldots\ldots\ldots \quad (1)$$

in which R is the rate of recession of the eroding face (L/T), q denotes the rate or erosion of material (L^3/T), and A refers to the cross-sectional area of fuse plug (L^2).

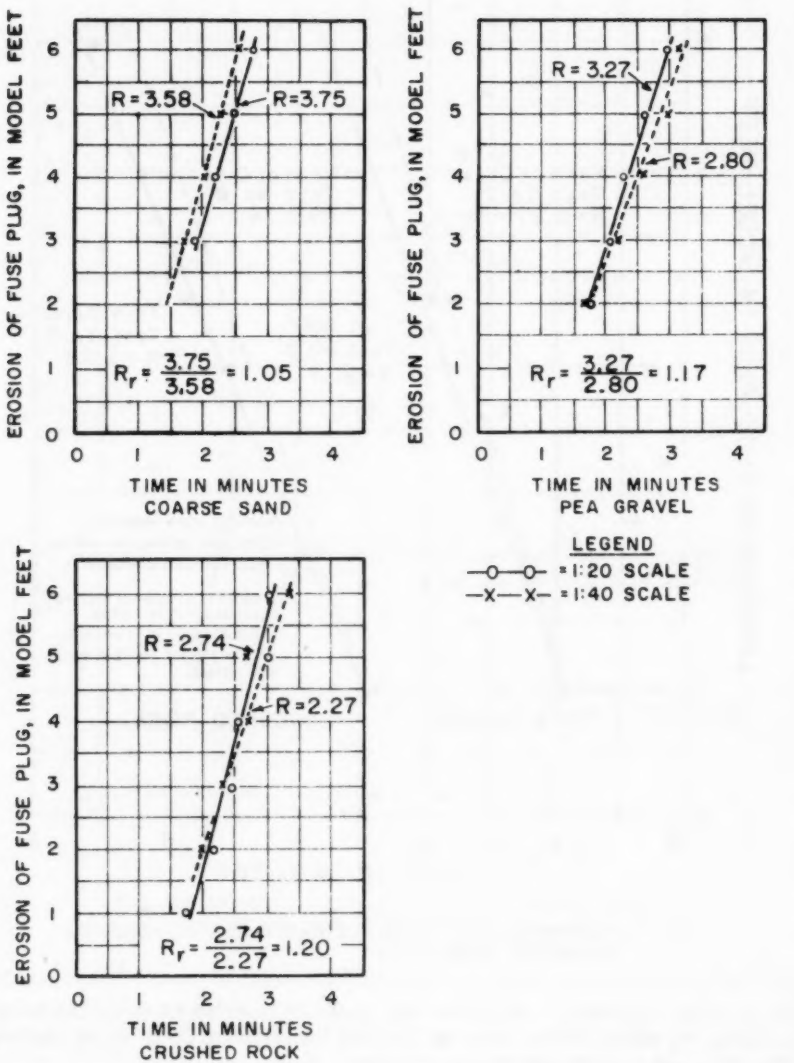

FIG. 7.—RELATIONSHIP BETWEEN 1:20 AND 1:40 MODELS OF IDENTICAL MATERIAL

The rate of erosion of material can be obtained from Du Boys equation

$$G = \frac{\psi}{\gamma^2} \tau(\tau - \tau_c) \quad \ldots\ldots\ldots\ldots\ldots\ldots (2)$$

in which G denotes the rate of erosion of material in weight per unit time/unit width of eroding face, ψ is the sediment transportation characteristic (Fig. 12)

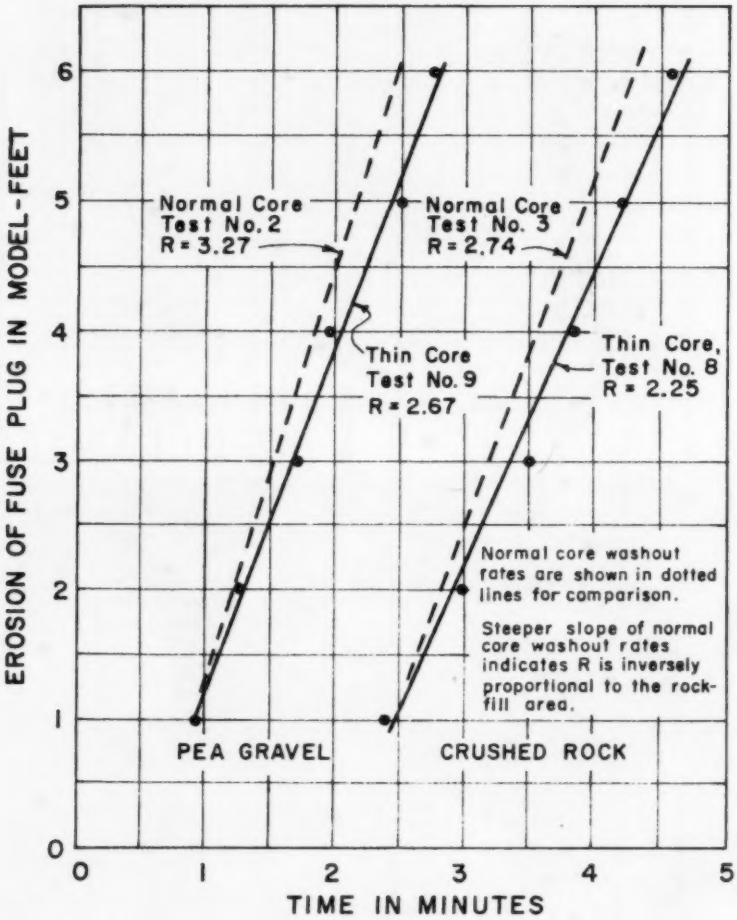

FIG. 8.—COMPARISON OF WASHOUT RATES FOR DIFFERENT ROCKFILL ZONE AREAS

for riverbed material, τ describes the shear or tractive force on the eroding material, τ_c refers to the critical tractive force required to move material, (Fig. 12), and γ is the unit weight of water. Now

$$q = \frac{G\,s}{\gamma_s} = \frac{\psi}{\gamma_s\,\gamma^2} \tau(\tau - \tau_c)\, s \quad \ldots\ldots\ldots\ldots\ldots\ldots (3)$$

in which γ_s is the dry unit weight of material, and s denotes the width of the eroding face.

The shear or tractive force, τ, for uniform flow in open channels is given by

$$\tau = \gamma y S \quad \ldots\ldots\ldots\ldots\ldots\ldots\ldots\ldots \quad (4)$$

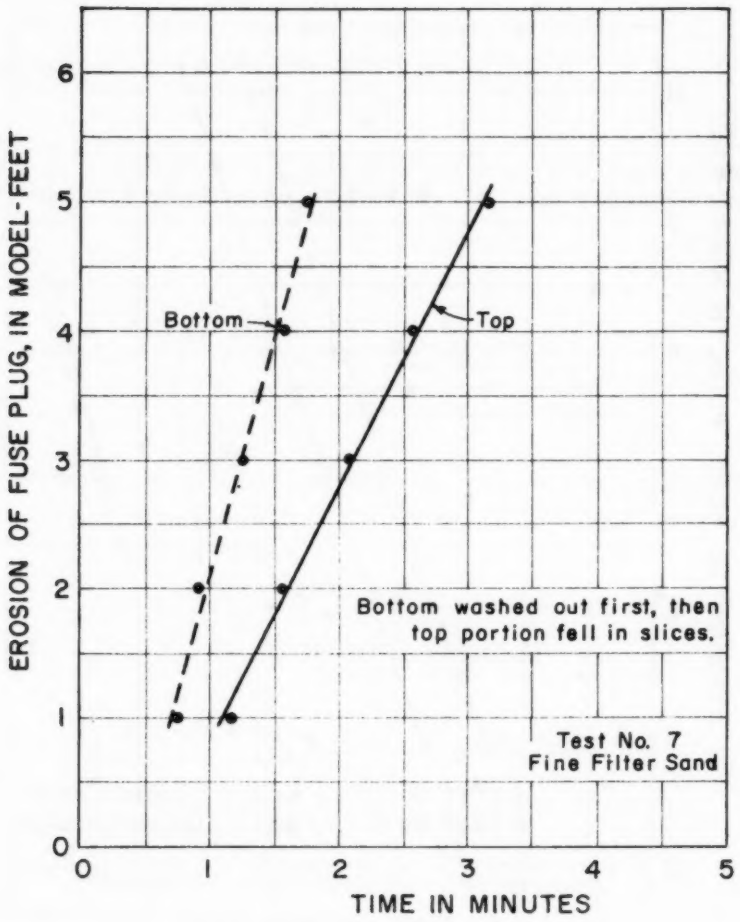

FIG. 9.—WASHOUT CHARACTERISTICS FOR MATERIAL WITH APPARENT COHESION

in which y is the depth of flow, and S denotes the slope of energy grade line (or water surface for uniform flow).

For flow around the eroding face of the fuse plug, however, a more general equation is required:

$$\tau = C_f \frac{\rho v^2}{2} \quad \ldots\ldots\ldots\ldots\ldots\ldots\ldots\ldots \quad (5)$$

in which C_f denotes the coefficient of drag, and ρ is the mass density of fluid. For uniform flow it can be shown that

$$C_f = \frac{f}{4} \quad \ldots\ldots\ldots\ldots\ldots\ldots\ldots\ldots (6)$$

in which f is the friction factor in the Darcy equation for head loss. Using the

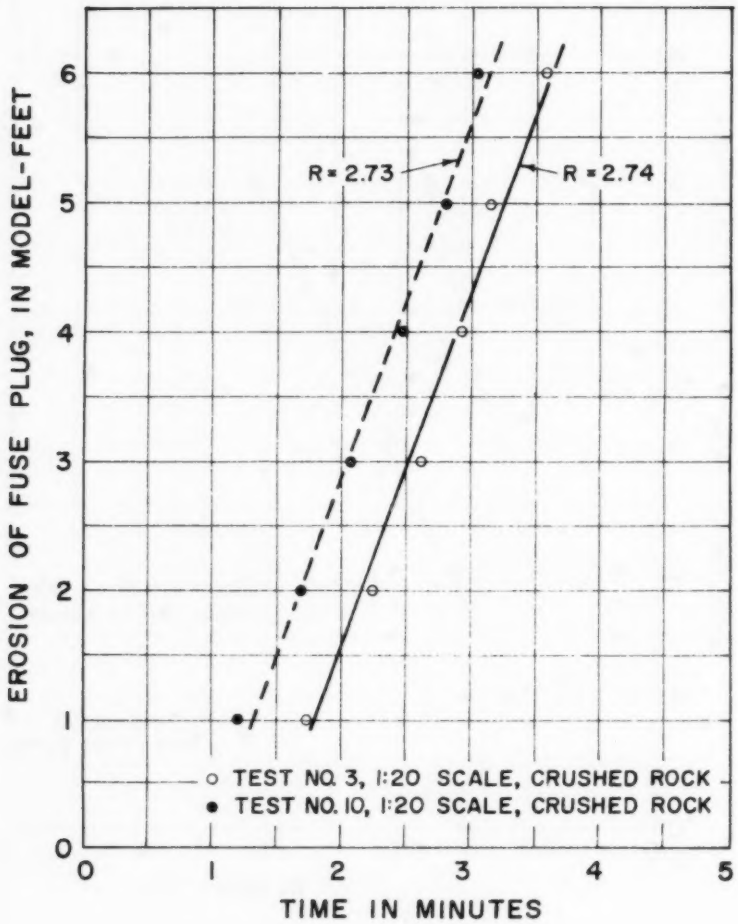

FIG. 10.—COMPARISON OF WASHOUT TESTS FOR IDENTICAL MODELS

maximum velocity available on the face, $V = \sqrt{2\,g\,h}$, the maximum tractive force is

$$\tau = C_f \gamma h \quad \ldots\ldots\ldots\ldots\ldots\ldots\ldots\ldots (7)$$

Combining Eqs. 1, 3, and 7

$$R = \frac{\psi}{\gamma_s \gamma^2} \frac{C_f \gamma h \left[C_f \gamma h - \tau_c\right] s}{K H^2} \quad \ldots\ldots\ldots\ldots (8)$$

in which K is the constant of proportionality in the formula for the cross-sectional area of the fuse plug

$$A = K H^2 \quad \ldots\ldots\ldots\ldots\ldots\ldots (9)$$

Generally speaking, s is proportional to h, that is,

$$s = a h \quad \ldots\ldots\ldots\ldots\ldots\ldots (10)$$

in which a is a constant.

Now, C_f is proportional to f, and f, in turn, is proportional to the 1/3 power of the relative roughness of the eroding face. This last relationship follows

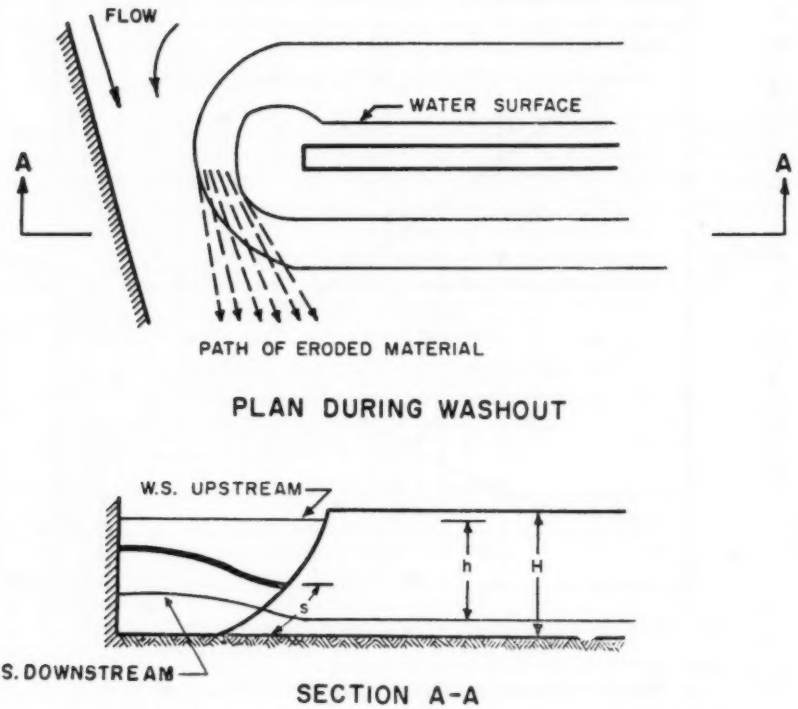

FIG. 11.—DEFINITION SKETCH FOR THEORETICAL CONSIDERATIONS

from the fact that Manning's "n" is proportional to the 1/6 power of the grain diameter for flows over unriffled sediment beds and from the fact that f is proportional to n^2. It follows then that

$$C_f = k\left(\frac{d}{h}\right)^{1/3} \quad \ldots\ldots\ldots\ldots\ldots (11)$$

in which d denotes the mean diameter of the material. Inserting Eqs. 10 and 11 into Eq. 8 yields

$$R = \frac{a\,\psi}{\gamma_s\,\gamma^2}\,\frac{k}{K}\left(\frac{d}{h}\right)^{1/3}\left(\frac{h}{H}\right)^2\gamma\left[k\left(\frac{d}{h}\right)^{1/3}\gamma\,h - \tau_c\right] \quad \ldots\ldots\ldots \quad (12)$$

Finally, for conditions in which τ_c is much smaller than τ (that is, small noncohesive material in large fuse plugs)

$$R = \frac{a\,\psi\,k^2}{\gamma_s\,K}\,d^{2/3}h^{1/3}\left(\frac{h}{H}\right)^2 \quad \ldots\ldots\ldots\ldots\ldots \quad (13)$$

Eq. 13 provides a basis for determining the similitude relationship for rate of recession between model and prototype. Let the subscripts r, p, and m, refer

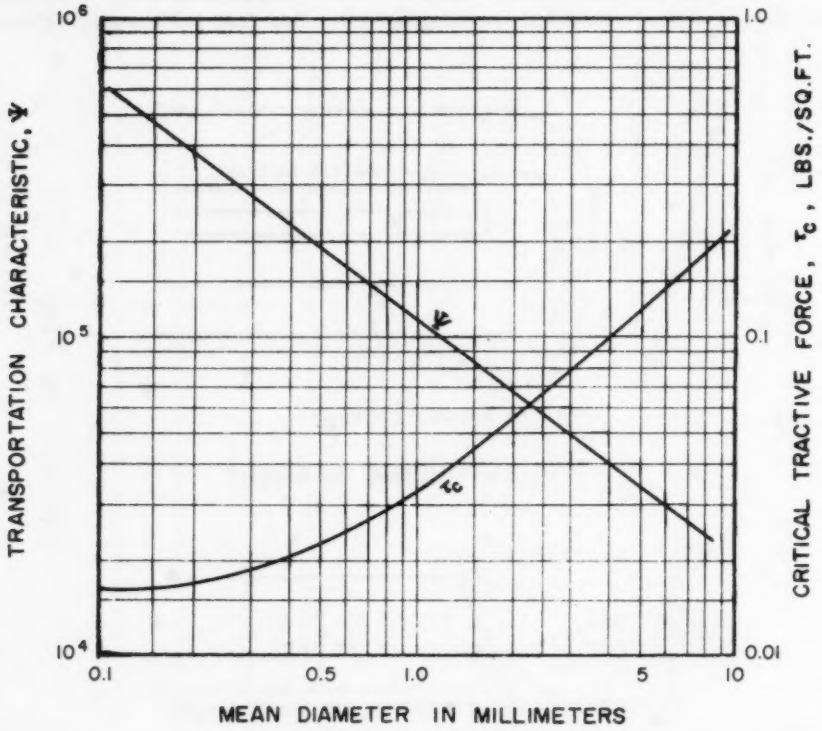

FIG. 12.—PARAMETERS FOR TRACTIVE FORCE THEORY

to the words "ratio," "prototype," and "model," respectively. Then, for geometrically similar models using identical materials (which must be relatively small in both model and prototype) it follows that

$$R_r = \frac{R_p}{R_m} = \left(\frac{h_p}{h_m}\right)^{1/3} = L_r^{1/3} \quad \ldots\ldots\ldots\ldots \quad (14)$$

as all other ratios are unity. (L_r is the scale ratio of the model.)

For two fuse plugs of identical materials with scale ratio of 1:2, the larger one will therefore erode $\sqrt[3]{2}$ or 1.26 times faster. This relationship is roughly verified by the laboratory tests described previously for which the 1:20 model eroded 1.05 to 1.20 times faster than the corresponding 1:40 model. Although the experiments indicate a rate of erosion for the larger model that is somewhat slower than the theory indicates, it should be remembered that neither the theory nor the experiments are precise and, at least from a practical standpoint, this agreement between theory and experiment is acceptable.

Summary.—From the laboratory tests and theoretical analyses on the mechanics of washout of fuse plugs, the following has been found:

1. The mechanics of washout can be explained on the basis of the laws for sediment transport.
2. The rate of recession of the eroding face varies approximately with the 1/3 power of the scale ratio for fuse plugs constructed with identical materials (non-cohesive) and methods.

LARGE SCALE FIELD MODEL TESTS

General Considerations.—The tests of small scale models in the laboratory had supplied the preparatory information necessary to correlate the results of the large scale model test to prototype performance. In order to finalize the design of the Oxbow Idaho spillway, the construction of the 1/2-scale field model was commenced in June 1959 with the test scheduled for late July.

Purposes of Large Scale Field Model Tests.—The main purposes of the large scale model test were to verify the design assumptions, and to seek additional information for the final design of the fuse plug.

The assumptions to be verified were as follows:

1. Mechanism of the breaching action at the pilot channel;
2. Depth of water required to effect a successful breach;
3. Completion of breach before lateral erosion; and
4. Washout process for lateral erosion.

The following additional information was needed:

1. Time function of the breach process;
2. Time function of the lateral washout process;
3. Effect of the core on rate of washout;
4. Completeness of washout; and
5. Anything unforeseen which could cause malfunctioning of the fuse plug.

Model Scale and Similarity.—The selection of a 1:2 ratio for the large scale field model was prompted by a number of considerations. The primary factor was the existence at the project of a readily adaptable site where a 1/2-scale model could be constructed with a suitable length-to-height ratio.

The predominant material in a fuse plug is the rockfill that occupies more than 75% of the volume (in the design shown), has relatively much larger size particles than the filter, and, therefore, controls the rate of washout. As determined by the laboratory investigations, the similitude relationships between the prototype and the 1:2 scale model with identical materials and construction methods would be the same as between the 1:20 and 1:40 models.

Because the impervious core material was to have the same inplace density and moisture content for both the model and the prototype and, thereby, the same unit strength, the similitude relationship of the impervious core had to be determined according to its failure action. In this design, the core is expected to break by cantilever load, both in breaching and lateral washout. Therefore, the core thickness was proportioned according to

$$t_r = (L_r)^{3/2} \quad \ldots\ldots\ldots\ldots\ldots\ldots \quad (15)$$

in which t_r is the thickness ratio, and L_r denotes the scale ratio. In order not to disturb the similarity of the rockfill, the reduced thickness of the core (more than the 1:2 ratio) was made up by the fine filter material, which has very little effect on washout rate.

For testing the initial breach action, the prototype head and dimensions of the pilot channel were used because the materials and slopes are identical in both model and prototype.

Flume Model of Clay Core.—After having studied the general breaching and washout action on small scale models in the hydraulic laboratory, it was more or less certain that the initial breach would start at the downstream edge of the pilot channel with a very small water head. However, because the impervious core material, the fine filter, and even the rockfill material may behave differently after being compacted to maximum density, it was proposed to test the breaching action in a wood flume at the site before proceeding with the large scale washout model test. The specific purpose of this model was as follows:

1. To observe closely the erosion phenomena of the downstream rockfill and filter material;
2. To verify the break-up action of the impervious core.

To avoid all complications, the model in the flume was to have the same scale as that of the large scale field model, with the same materials and compaction.

A wooden flume was constructed at the project site which was able to accommodate a 6 ft high crest section of the pilot channel portion of the 1/2-scale fuse plug.

Two flume tests were performed, from which sufficient information was obtained for the construction of the large scale model.

Test No. 1.—The flume model had a section as shown in Fig. 13. The impervious core was supported on processed fine filter material on the downstream side, and covered by the same material on the upstream side. Flume floor and walls are of 1 in.-by-6 in. tongue and groove with polyethylene sheet lining. The mechanical analyses are shown in Fig. 14.

The model was constructed so as to obtain the same compaction in the core and filter zones as in the prototype. After turning on the water and removing the downstream bulkhead, the downstream processed fine filter material eroded only to the extent of its contact with the lower nappe falling over the impervious core. Due to the apparent cohesion of the compacted, well-graded material, the processed fine filter material stood almost vertical for the entire height of the model.

After mechanically removing the processed fine filter material, the impervious core was tested to determine the point of failure under cantilever action. (The bond between the core and the walls of the flume was carefully broken at the top portion of the model.) The first break of the core occurred

about 18 in. from the top with less than a foot of water over the top. The second break occurred about 4.5 ft from the top.

Test No. 2.—The second flume model had a section as shown on Fig. 13. The impervious core was identical to that of Test No. 1, but the processed fine

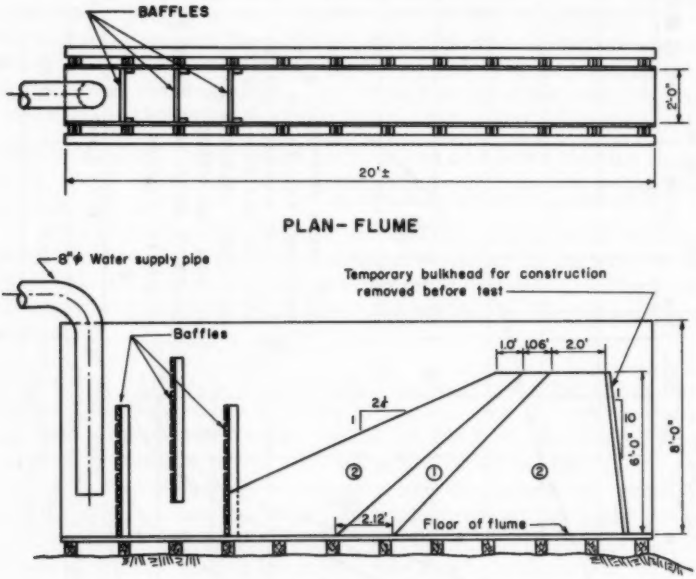

FIG. 13.—LARGE SCALE FLUME MODEL TEST

filter material was replaced with a downstream rockfill zone of concrete aggregate and a filter zone composed of a thin layer of concrete sand over pit-run fine gravel. The substitutes were of more or less uniform materials. Their gradations are shown on Fig. 14.

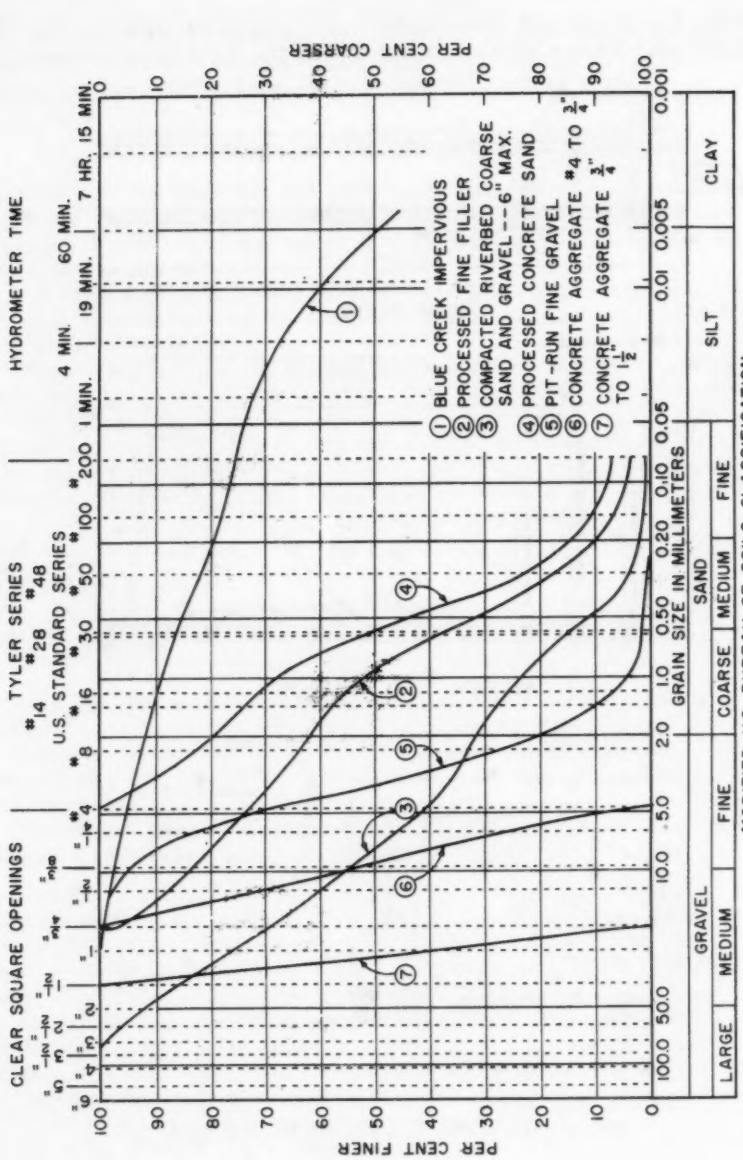

FIG. 14.—MECHANICAL ANALYSIS-LARGE SCALE FUSE PLUG MODELS

The materials were placed in the same manner as for Test No. 1, but with provisions to prevent bond and wedge action between the impervious core and the walls of the flume.

After the end bulkhead was removed and the test started, the material downstream of the core was gradually washed out from the top. As the water hit the downstream rockfill material and washed it out of the flume, the rockfill and filter material beneath the nappe gradually receded by surface sliding. The first break of the unsupported core occurred about 18 in. from the top. The washout cycle was then repeated. The second break of the core occurred at a height about 2.5 ft below the first.

On the basis of the flume model tests, it was concluded that the impervious core of the large scale model was satisfactory with respect to thickness and arrangement.

These tests also indicated that the compacted, well-graded riverbed sand and gravel, because of its apparent cohesion, would not be satisfactory for use in the pilot channel section. It was demonstrated that clean, uniform material was necessary for the downstream filter and rockfill to effect a rapid and successful breach.

Half Scale Field Model Tests.

Description of Half Scale Model.—The location chosen for the construction of the model was a natural rock saddle at the left abutment of the Oxbow cofferdam. Here a large water supply was available from the natural river flow and the Oxbow reservoir above the cofferdam could be used as a regulating pool to keep the water surface almost constant throughout the test. The pool between the cofferdam and the main dam could store all the water passing the model without any flow over the Oregon spillway.

The first step in preparing the model site was to remove part of the existing cofferdam, and expose the rock foundation. Because the rock surface was quite irregular, a concrete sill was poured for the cutoff under the impervious zone. The rock on the right side of the concrete sill sloped up to form a natural abutment. However, on the left side, the rock was lower and very irregular, so a vertical steel sheet pile wall was constructed to form the abutment for the model. The piling was set in a trench excavated to rock and backfilled with concrete. The top of the piling was securely anchored to logs buried well back in the cofferdam. Hand-tamped clay was placed in back of the piling.

The pilot channel in the model was adjacent to the sheet pile abutment. In the prototype, the pilot channel will be adjacent to a concrete-faced rock abutment, excavated as steeply as possible. No difference in breaching action is foreseen due to the probable minor difference in abutment slopes.

A compacted clay foundation pad, 1 ft to 3 ft thick, was placed under the entire model to the level of the concrete sill.

The length of the base of the fuse-plug model, measured along the concrete sill, was 51.6 ft. The crest length was 75 ft, and the height was 13.5 ft minimum, except at the pilot channel. The crest was 1-ft higher in elevation at the right abutment than it was adjacent to the pilot channel. The height at the pilot channel was 11.5 ft. Typical sections of the model as constructed are shown in Fig. 15, and a picture of the complete model is shown on Fig. 16.

In the lower 5 ft of the model, the rockfill materials were dumped directly in place by trucks, and spread by bulldozer. For the remainder of the model, the materials were stockpiled near the site, transferred to the embankment by clamshell as required, and spread by hand.

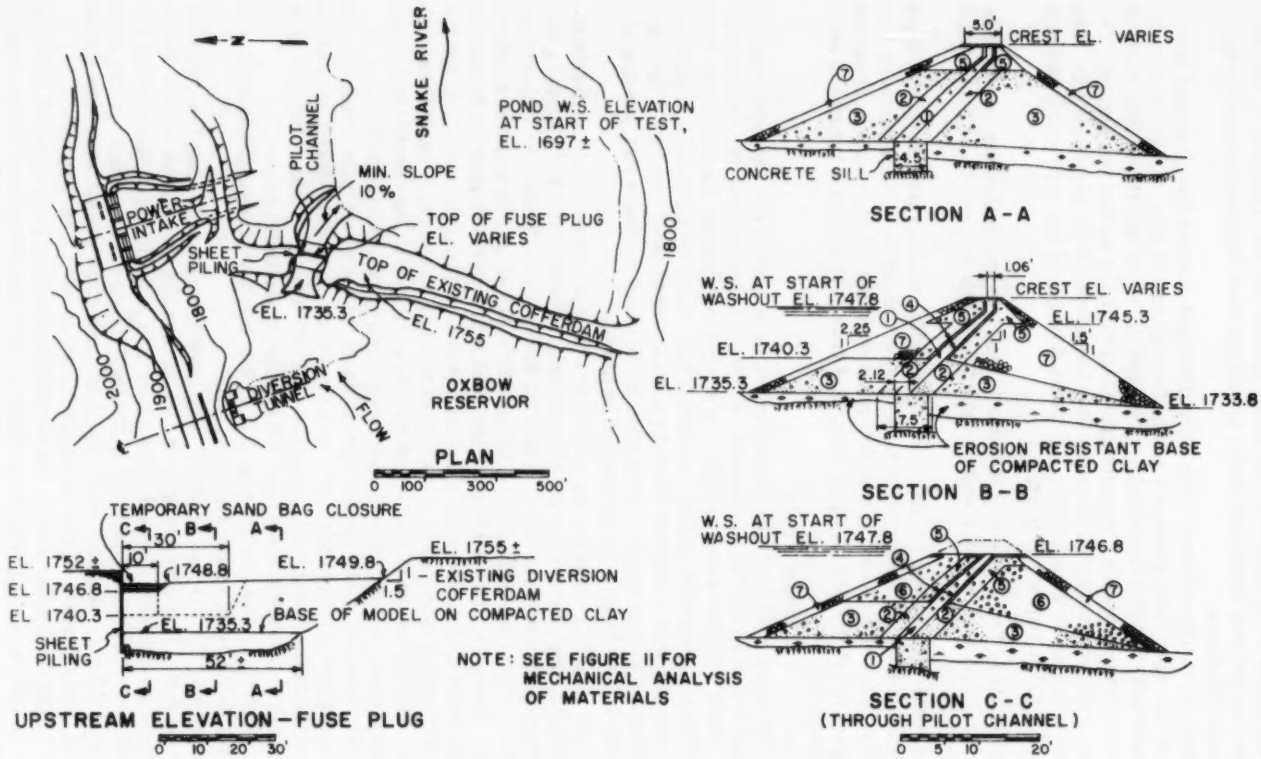

FIG. 15.—FUSE PLUG HALF SCALE MODEL

Compaction of the riverbed sand and gravel, and the processed fine filter, was accomplished by vibrating roller. Liberal quantities of water were applied to these materials. The concrete aggregates and fine gravel were heavily sluiced.

The clay core was spread in 3-in. lifts, sprinkled as required, and compacted by pneumatic hand tampers. In order to get satisfactory bond between lifts it was necessary to roughen the contact surface and moisten it before placing the next lift. In general, compaction was between 85% and 90% of peak modified American Association of State Highway Officials (AASHO) density, and the moisture content was within 1-1/2% of optimum.

Material Selection and Laboratory Tests.—The model was constructed of the same materials economically available for use in the prototype. The model was designed as a composite section, using several rockfill materials, in order that washout rates for the various materials could be established and thereby ensure selection of the most advantageous materials for the prototype.

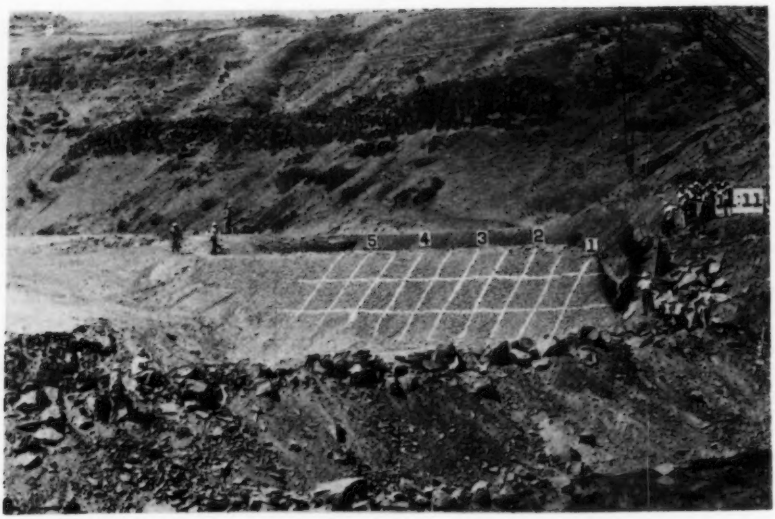

FIG. 16.—SANDBAGS JUST CLEAR OF PILOT CHANNEL

The flume model tests had indicated that pit-run riverbed sand and gravel, when placed wet and compacted, had considerable apparent cohesion. Because this property might slow the erosion process, it was decided to use this material where it would be the last to wash out; that is, at the end opposite the pilot channel.

At the pilot channel it was necessary to have an easily moved, cohesionless material. Concrete aggregate passing a 3/4-in. screen and retained on a No. 4 screen was sure to meet these requirements and was therefore used. Because there was an excess of the larger sizes of concrete aggregates available, it was decided to test a section using rock between the 3/4-in. and 1-1/2-in. sizes. This section, 20 ft long, was placed adjacent to the pilot channel section.

The processed fine filter used in the main dam showed the same property of apparent cohesion as the riverbed sand and gravel. Therefore, this filter material was restricted to use only in those sections using the sand and gravel. For the sections using concrete aggregates, a pit-run fine gravel with a minimum thickness of concrete sand on the face in contact with the impervious core, was used for the filter. The fine gravel showed no cohesion under any conditions. The impervious core was constructed of the same material as the main dam impervious core. The upstream and downstream slopes were faced with the 3/4-in. to 1-1/2-in. concrete aggregate.

For the results of standard laboratory tests performed on the various embankment materials, see Table 2, and mechanical analysis curves, Fig. 14.

In addition to the standard laboratory tests referred to previously, a series of special flexural tests were performed on the core material. The tests were

TABLE 2.—LABORATORY TESTS ON FUSE PLUG MATERIALS

Material	Specific Gravity	Maximum Density,[a] in pounds per cubic foot	Optimum Moisture Content, in percent	Coefficient Permeability, in centimeters per second	Shear Strength	
					Friction, $\phi°$	Cohesion, C, in kips per square foot
(1)	(2)	(3)	(4)	(5)	(6)	(7)
Clay core	2.80 ave	109.5 ave	19.0 ave	1×10^{-6} min	10° min	1.0 min
Fine Filter	2.75	129.8	-	2×10^{-5} ave	-	-
Riverbed Sand and Gravel	2.76	132.0	-	3×10^{-1}	39°	0
Processed Concrete Sand	2.70	115.7	-	-	-	-
Pit-run Fine Gravel	2.73	107.7	-	-	-	-
Concrete Aggregate No. 4 to 3/4 in.	2.72	106.0	-	-	-	-
Concrete Aggregate 3/4 in. to 1-1/2 in.	2.75	107.5	-	-	-	-

[a] Maximum density determined by: (1) Modified AASHO method for clay, (2) field density test after compaction for fine filter, and (3) dry, rodded method for all other materials.

required to quantitatively evaluate the maximum cantilever projection of the core that could occur in the pilot channel section during removal of the downstream supporting rockfill. This value, in turn, permitted a rough computation of the time required to start initial breakup of the core, and the effective breach of the section. Flexural strength values were desirable for both the as-placed material and the saturated material to get a comparison between the fuse-plug model, which would be tested with the core still in the as-placed condition, and the prototype, which would certainly be subjected to a prolonged period of submergence up to the full reservoir level at El. 1805, before it would be required to wash out.

The test specimens were prepared by compacting the soil to approximately the same density, and at about the same moisture content, as the material

placed in the model. The specimens were 2 in. square in section, and 10 in. long. The soil was placed and compacted in about five layers.

The test consisted of supporting the specimen at its ends, and applying a uniformly increasing load at the third points until rupture occurred. The load was applied normal to the direction of compaction, to reduce the effects of laminations in the test specimen.

The test results showed a modulus of rupture between 3000 psf and 4000 psf for the material as placed. No conclusive results were obtained on the effects of saturation. However, the tensile strength was apparently significantly reduced due to prolonged submergence.

Measuring Devices.

Embedded Washout Rate Indicators:—To get information on the rate at which the interior portions of the fuse plug were being eroded, a series of washout rate indicators were installed during the course of construction. These were simply electrical switches which were held closed by the earth pressure within the embankment. As the erosion progressed the earth pressure would be relieved, the circuit broken, and a light would go out at the observer's station.

The indicators were installed in a vertical plane along the center of the crest on three vertical lines as shown on Fig. 17. In general, they were installed at 2-ft increments of elevation. The wires from each indicator went vertically down to the clay foundation, upstream to the concrete sill and then out over the Idaho abutment. This routing prevented damage to the wiring before operation of the respective indicators.

Grid Lines on Downstream Face:—A 5-ft grid was painted on the downstream face of the fuse plug model, as shown in Fig. 16. Three independent observers recorded the elapsed time between the start of the test and the removal of the grid intersections, as an aid in establishing the washout rates for the various materials.

For the final determination of washout rates, a careful study of the motion picture, taken at the time of the large scale model washout, was made. The grid lines were the dimensional control, and repeated stop watch measurements established the time.

Description of Washout.

Provisions for Starting Test:—A 10-ft long section of the crest was left 2 ft lower in elevation than the remainder to form the pilot channel, through which the water would flow and start the breaching action. Close control of the reservoir water surface elevation was required, but difficult to achieve. In order to get the proper head for the test, without danger of premature washout, sandbags were employed in the pilot channel.

Four layers of sandbags were used to close the pilot channel to the model crest at El. 1748.8. The sandbags were arranged on a wire rope sling attached to a truck crane. After the reservoir stabilized at the desired elevation, the sandbags could be lifted quickly to start the test.

Final Test:—In the morning of July 22, 1959, all preparations for the final test had been completed. The reservoir water surface was brought up to the proper level, one foot above the invert of the pilot channel. At 30 sec after 11:11 a.m. the initial breach began with the lifting of the sandbags clear of the pilot channel (time consumed in clearing sand bags, 9 sec), as shown in Fig. 16.

As soon as the sandbags were lifted, the water gushed through the pilot channel and, flowing down the slope, commenced the erosion of downstream rock-

fill starting at the top of the slope. Within 35 sec after the start of the test the erosion had progressed to such an extent that the upper portion of the core was acting as a weir, with the nappe clear of the material below, Fig. 18 (time 11:12+). The first break of the core occurred 1 min and 7 sec after the start of the test. Fig. 19 (time 11:13+) shows the moment at which the second break of the core had just occurred. The time, as calibrated from the motion picture record was 1 min and 27 sec after the start of the test. The breach action was considered completed at this point as no further change occurred in surface profile of the water rushing through the gap or in the color of the water.

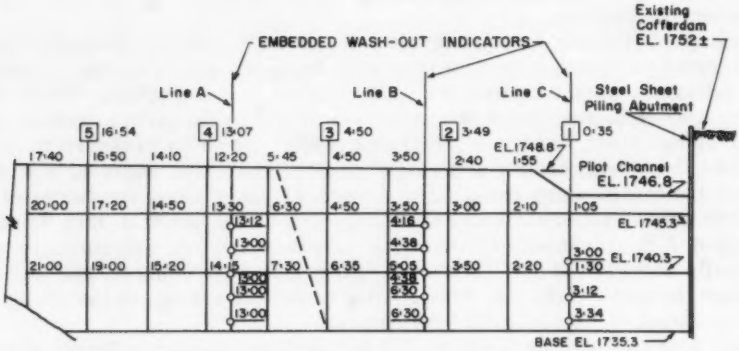

DOWNSTREAM ELEVATION OF MODEL
OBSERVED WASHOUT TIME

The numbers on the signs along the crest designate 10 foot stations from the Sheet Pile Abutment.
Time is in minutes and seconds from start of wash-out.
min:sec wash-out of grid intersections.
min:sec wash-out of embedded wash-out indicators

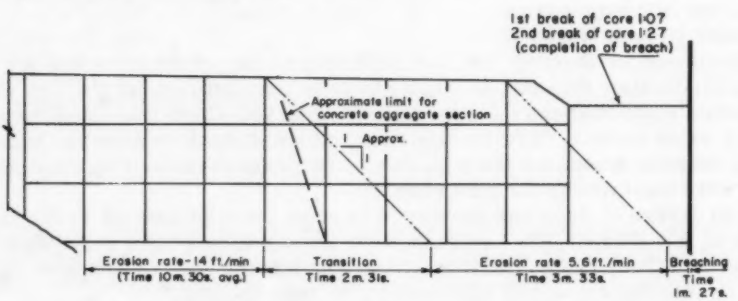

DOWNSTREAM ELEVATION OF MODEL

FIG. 17.—RECORD OF WASHOUT RATE

The lateral erosion of the model began during the initial breach period as the rockfill material along the side slid into the water rushing through the gap and the core was left overhanging along the side. As the uniformly-graded rockfill and filter slid out from underneath, the core was left cantilevered and sections would break off at intervals. The surface of the uniformly-graded

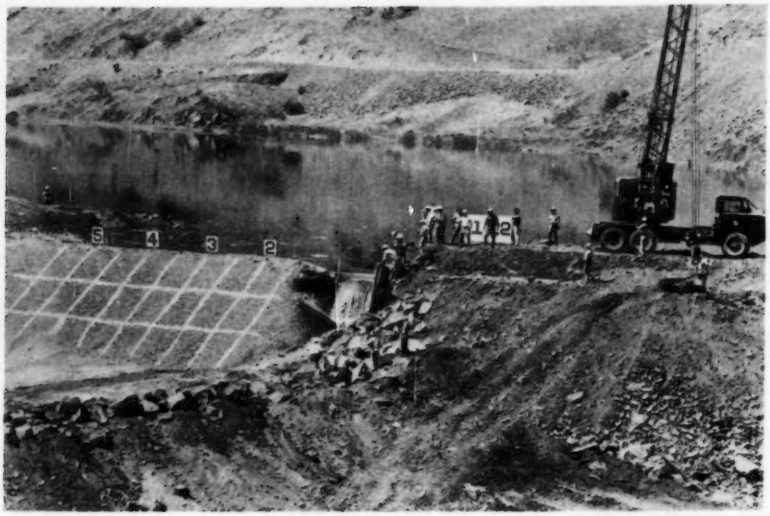

FIG. 18.—OVERHANGING OF CORE. FIRST BREAK OF CORE IMMINENT

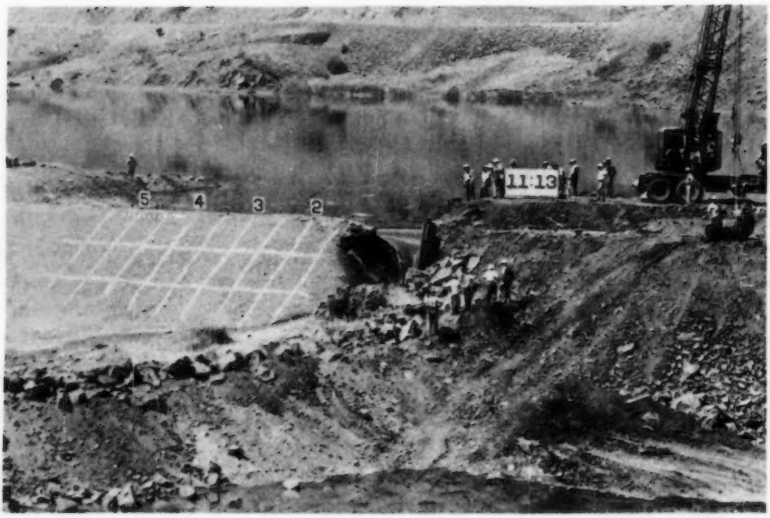

FIG. 19.—AT MOMENT OF SECOND BREAK OF CORE.
BREACH ACTION COMPLETE

material sliding into the water assumed a slope slightly steeper than the angle of repose of the material. This phase of the washout took approximately 6 min. Fig. 20 (time 11:17) shows the characteristic slope of the uniformly-graded rockfill and filter under full face lateral erosion. The change from the uniform to the well-graded material occurs at Station 35 and the vertical break can be seen at the downstream face above El. 1795, the upper white line.

The washout of the well-graded material is characteristically different from that of the uniform material. Due to apparent cohesion and a small amount of fine material in the well-graded riverbed sand and gravel, the end of the partially washed out fuse plug model assumed a nearly vertical attitude. The erosion of this portion of the fuse plug model proceeded as the churning water undermined the vertical face. At intervals the undermined portions of the downstream rockfill broke off and fell into the water and the material was carried away. As the core became exposed and was left unsupported, sections would break off. Fig. 21 (time 11:22) shows the vertical face of the well-graded material and the churning, undermining action of the water.

As soon as the test was over, the spillway gates at Brownlee were closed, and the powerhouse release was ordered cut down as much as possible so that the foundation could be examined as early as possible.

At 12:30 p.m., the powerhouse release was reduced to 6000 cfs, and kept there until 2:30 p.m. The Oxbow reservoir receded rapidly. At 3:15 p.m. the water surface downstream of the fuse plug was at the same elevation as the Oxbow reservoir, and the water started to flow into the reservoir. At this time the reservoir water surface, as well as the tailwater pool, was at El. 1738.5, 4 ft below the temporary crest of the Oregon spillway.

Analysis of Test Results.—The large scale field model test has clearly demonstrated the details of the washout action. Information which had previously been determined from the laboratory and flume model tests was confirmed, and some new information was revealed which could not be found from the other model tests due to their limitation in scale and size.

The continuous motion picture record has been found most valuable, because it enabled the engineer to study the washout action closely and repeatedly.

After the Oxbow reservoir and the pond downstream of the cofferdam had receded, the model foundation was examined.

All information obtained, including the river gage records at Oxbow and Hells Canyon, have been carefully analyzed, and the results are presented as follows:

Breach Action:—The breach action was entirely as expected. It showed close similarity to the small scale model. The core broke up exactly as in the flume model, first, a small break, then a large break, and then repetition of the breach action all the way to the base. There was no significant seepage into the rockfill at the downstream edge of the pilot channel before the initial breach.

Lateral Washout:—The uniform material washout process was exactly as estimated. The kinetic angle of repose was about 45° for the uniform material. For the material with apparent cohesion and a small amount of fines in it, the washout face was vertical, and the washout process was a three-step action; undermining the base of the vertical face, vertical slide of the rockfill and filter material, and the break of the impervious core. The embedded indicator record also indicated vertical face erosion under water.

Rate of Washout:—Based upon direct observations (three observers) and the motion picture record, the washout time function is shown in Fig. 13, and the

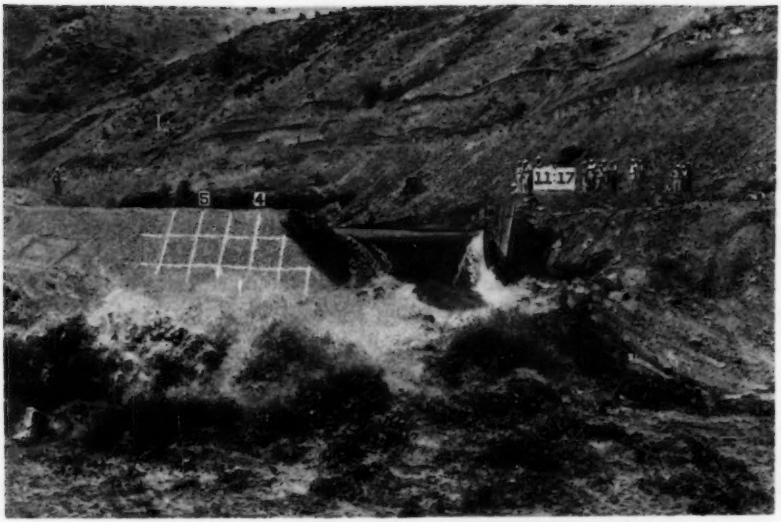

FIG. 20.—SLOPE OF UNIFORM MATERIAL (COMPARE WITH FIG. 5)

FIG. 21.—VERTICAL FACE OF WELL-GRADED MATERIAL
(COMPARE WITH FIG. 6)

results summarized as follows:

Breach (Complete)	1 min and 27 sec
Rate of washout, uniform material	5.6 ft per min
Rate of washout, well-graded material	1.4 ft per min

Hold-up time of the core was insignificant.

Order and Completeness:—The entire washout proceeded in an orderly manner. Breach was completed before lateral erosion. There was no evidence of any portion of the plug remaining beneath the water during the washout and Fig. 22 shows the completeness of the washout after the foundation was exposed next morning. The reservoir water surface at the start of test was El. 1747.80. The reservoir water surface at the end of test was El. 1747.98. The maximum water surface during test was El. 1747.98.

FIG. 22.—LOOKING TOWARD LEFT ABUTMENT OF STEEL SHEET PILING

Headwater and Tailwater:—From reservoir water gage records, it was found that during the entire test, the headwater varied only 0.18 ft. The breach head was 1 ft. The slope of the ground downstream of the model was approximately 10%. There was no settling of the material in the escape channel. The dike downstream of the model was constructed to study its effect on the washout, but no noticeable effect was found.

Summary.—The large scale field model test has conclusively demonstrated the following:

1. The structure showed the ability to withstand a water load with a reservoir surface at or above the pilot channel invert for 4.5 hr, and also a rapid drawdown actually more severe than expected for the prototype.
2. The breaching action was initiated with a water head one foot above the pilot channel, and completed to the base of the model in less than two minutes.

A uniform, cohesionless material is essential for the downstream filter and rockfill zones at the pilot channel to achieve a rapid and successful breach.

3. The lateral washout process for the two different types of materials was clearly demonstrated. The rate of washout for the uniform, cohesionless material was found to be 5.6 ft per minute, and for the well-graded material with apparent cohesion 1.4 ft per min. Through proper proportioning of the lengths involving the two kinds of materials, a suitable value for the total washout time of the prototype fuse plug can be achieved.

4. The impervious core design is satisfactory, because the "hold-up" action of the core was found to be insignificant.

5. The model fuse plug was completely washed out to the concrete foundation sill in an orderly fashion, without unforeseen developments.

CONCLUSIONS

The small scale washout tests in the laboratory have established a definite pattern of similarity between a 1:20 and 1:40 scale model, composed of the same materials and constructed in the same manner. The 1/2-scale field model test has also shown similar washout mechanics.

The ratio of washout rates from the small scale model tests, for identical materials and construction, and scale ratio of 1:2, checks very closely with the theoretically derived value. Therefore, it can be logically concluded that the actual washout rate of the prototype can be closely approximated by applying this ratio of washout rates to the results from the 1/2-scale field model test.

The design assumptions of the fuse plug have been verified, in all respects, by the actual large scale field test. Based upon the performance of this test, the prototype fuse plug design, including the selection of materials, will be entirely satisfactory in effecting a successful breach, and a complete washout, in an orderly manner, as planned.

By using two types of rockfill and filter materials, it is considered definitely feasible and practical to construct a fuse plug for suitable washout rates along different portions and an appropriate total duration of the washout.

ACKNOWLEDGMENTS

The laboratory investigations were performed in the R. L. Albrook Hydraulic Lab., Washington State Univ. at Pullman, Wash. Field models were constructed by the Morrison-Knudsen Company. Personnel of the engineering staff of Idaho Power Company conducted the final test of the field model. The entire testing program was under the direction of International Engineering Company's design engineers for the Oxbow Hydroelectric Project.

In the process of developing the fuse-plug spillway design and formulating the model test program, valuable and constructive suggestions were offered by the members of the consulting board, J. P. Growdon, F. ASCE, I. C. Steel, F. ASCE, and H. T. Stearns.

Journal of the
HYDRAULICS DIVISION
Proceedings of the American Society of Civil Engineers

SEEPAGE THROUGH LAYERED ANISOTROPIC POROUS MEDIA[a]

By David K. Todd,[1] M. ASCE, and Jacob Bear[2]

SYNOPSIS

The paper summarizes an investigation of seepage from leveed rivers into low-lying adjoining agricultural lands. Only the flow rate and distribution of seepage as a function of the surface and subsurface boundary conditions were studied. Flow nets in idealized cross sections were determined by an electric analogy model. Boundaries represented channel bed and bank, a levee base, a lower impermeable stratum, and the water table in adjoining drained agricultural land. Variables studied included two subsurface layers of different permeabilities and anisotropies, layer arrangements and thicknesses, channel depth and width, levee base width, and water table slope.

INTRODUCTION

Seepage from rivers and natural channels is a serious problem in many locations. Significant contributions to the literature on this and other types of seepage have been made by several engineers (1), (2), (4), (5), (6), (11), (15), (17), (21), (26).[3] When channel levels exceed the adjacent ground surface elevation, water moves through and under the confining levees into adjacent lands. If drainage facilities are inadequate, the soil becomes saturated,

Note.—Discussion open until October 1, 1961. To extend the closing date one month, a written request must be filed with the Executive Secretary, ASCE. This paper is part of the copyrighted Journal of the Hydraulics Division, Proceedings of the American Society Society of Civil Engineers, Vol. 87, No. HY 3, May, 1961.

[a] Presented at the March 1960 ASCE Convention in New Orleans, La.

[1] Assoc. Prof. of Civ. Engrg., Univ. of California, Berkeley, Calif.

[2] Formerly Graduate Research Engr., Univ. of California, Berkeley, Calif.; presently Lecturer, Technion, Israel Inst. of Tech., Haifa, Israel.

[3] Numerals in parentheses refer to corresponding items in the Appendix Bibliography.

water ponds on the surface, and crops are damaged. The Sacramento Valley of California is a typical example of an area which suffers extensive seepage damages. Losses in the period 1937-1953 (at 1953 prices) were reported as $1,834,000 per year, or $102 per acre affected (20). The problem of seepage in this area prompted the present investigation.

The purpose of the investigation was to study the physical picture of flow of water from stream channels through subsurface strata to the adjacent ground surface. Natural conditions governing these flows include geology and soils, topography, ground water, rainfall, runoff, and channel stage. The range of conditions for each of these variables, together with their possible combinations, makes it apparent that not all situations could be studied. Instead, key variables were selected for study so that results could be applied not only to the Sacramento Valley, but also to other areas with similar conditions. The present work deals, therefore, with general aspects of seepage from rivers.

Most seepage studies in the Sacramento Valley have been concerned with field conditions of the affected areas, periods and durations of flooding, and economic losses. Comprehensive surveys are summarized in reports by the Joint Committee on Water Problems of the California Legislature (9) and by C. E. Plumb, M. ASCE, and others (20). Because the present study was a laboratory investigation of seepage flow nets for steady flows, these reports and others (10), (16) furnished valuable information relating to construction of idealized cross sections. Results from an electric analogy model were analyzed and presented in graphical form to facilitate interpretation and application to various field conditions. In view of the number and complexity of cross sections to be investigated for quantities and distribution of seepage, model investigations rather than analytic studies were necessary (application of analytic techniques to two simplified special cases is shown in Appendix I). Hydraulic models have often served as a valuable tool to supplement analytic approaches (24, pp. 307-321). The electrical analogy was most suitable for the present investigation. Analysis of this type of model and its application to seepage studies have been presented by N. N. Pavlovsky (19), C. J. G. Vreendenburgh and O. Stevens (22), (27), (28) and others (8), (12). A recent summary of the theory of the analogy has been prepared by L. C. Malavard (14).

In most cases, subsurface strata through which seepage flows occur are nonhomogeneous and anisotropic. Therefore, the main emphasis in the present investigation was on seepage through layered anisotropic soils.

SEEPAGE CROSS SECTION

Conditions along the Sacramento River served as a basis for selecting cross sections to investigate. The variety, irregularity, and wide diversity of layered alluvial deposits along the river precluded the possiblity of determining seepage through actual geologic sections without having extensive field data available. Instead, about fifty representative hypothetical cross sections were constructed for model tests (25).

Almost all seepage occurs in the zone above the highest more or less continuous clay layer, which acts as a lower impermeable boundary. In the permeable zone various layers of deposits can be found. Based on types of geologic deposits, layers could be reduced to those having relative permeabilities of 50, 1, and 0. These layers are essentially horizontal, but may vary in thickness and in their relative vertical positions. As most seepage occurs within

less than a mile of the river, the model was limited to a maximum distance of 3,000 ft inland from the levee. A maximum depth of 100 ft from the water table to the impermeable clay layer was also selected. If symmetry is assumed about the center of the river, a section on only one side of the river need be investigated.

Other assumptions made for the model investigation were that the river channel is rectangular with a depth of 25 ft (a few cases of other depths were also studied) and a width of 600 ft. Levees were assumed to be situated adjoining the river channel, to be impermeable, and to have a base width of 100 ft at the elevation of the inland water table. An impermeable levee, of course, implies that all seepage passes under the levee. Depending upon the mode of construction and materials employed, seepage through the levee may or may not be a significant item.

A final variable necessary in evaluating seepage is that of the anisotropy of permeable zones. Most alluvial strata are deposited horizontally with a pronounced tendency for a greater uniformity in grain size and depositional structure horizontally than vertically. Commonly this results in a condition of anisotropic permeability where the horizontal permeability may greatly exceed that of the vertical. Ratios of vertical to horizontal permeability of 1, 0.1, and 0.01 were selected to give a range of representative conditions.

The position of the water table relative to river stage and to ground surface determines relative seepage rates and the length of time before seepage will appear at ground surface. Seepage to a deep water table from a short duration flood stage may not affect surface conditions, whereas at a location with a high water table it may have a marked surface effect.

In most irrigated agricultural land the water table is controlled to within narrow limits by subsurface drainage facilities. The level is commonly maintained at 3 ft to 4 ft below ground surface. For steady flow conditions studied in the electric analogy model, the water table was assumed to be stationary. This might represent levels controlled either by subsurface drains or by ponding at ground surface. Both horizontal and sloping water tables were investigated.

Field (9) and laboratory (23) investigations have confirmed that seepage from flood flows is proportional to a duration-height factor. This study was limited to the steady case with emphasis on the distribution of seepage inland from the river. Factors of river stage magnitude and duration are variables which are necessary in applying these results to obtain quantitative seepage for a given situation and location.

Based on these considerations the general cross section to be studied is shown in Fig. 1. From Fig. 1 the channel depth, d, has a range of values of 0 ft to 100 ft; the permeable zone depth, D, is a constant 100 ft; thickness of upper layer, u, ranges from 10 ft to 100 ft; thickness of lower layer, l, has a range of 0 ft to 90 ft; length of cross section from centerline of river, L, has a range of 1,000 ft to 3,300 ft; no range is assigned for the river stage above levee base, H; the range of channel half-width, B, is 100 ft to 300 ft; the levee base width, b, is a constant 100 ft; distance landward from toe to levee, x, ranges from 600 ft to 2,900 ft; no ranges are assigned for the permeability of the upper layer, K_U, or the lower layer, K_L; the ranges for both the anisotropy of the upper layer, K_{yU}/K_{xU}, and the lower layer, K_{yL}/K_{xL}, are 1/1 to 1/100; and the ranges for the ratio of permeabilities to the two layers, K_U/K_L.

The channel depth d and the channel half-width B were constant for all but a few model tests. Significant variables are the thicknesses of the upper and

lower layers, u and l, respectively. These are related by

$$D = u + l = 100 \text{ ft} \quad \ldots\ldots\ldots\ldots\ldots\ldots \quad (1)$$

The length of cross section L was varied as required to obtain a practical vertical scale to define the seepage flow pattern in each model test. Although the river stage H determines the rate of subsurface flow, no values were assigned since it has no effect on the distribution of seepage. Similarly, the permeabilities of the layers, K_U and K_L, were unassigned, but their relative values expressed by their ratio K_U/K_L form a key variable of the investigation. The

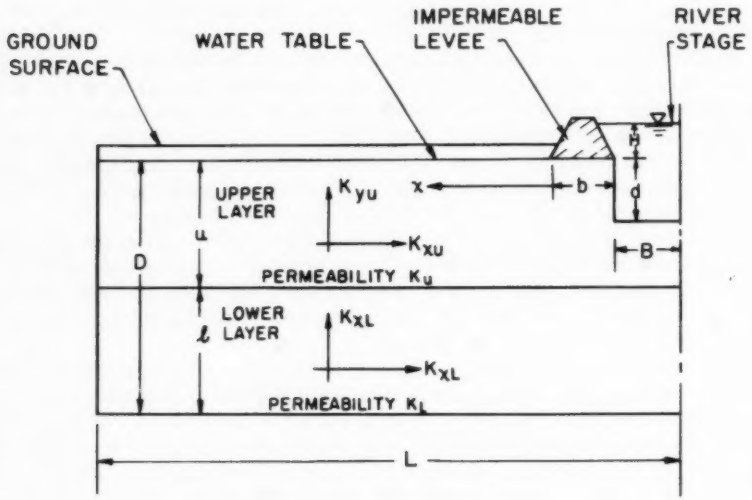

FIG. 1.—DEFINITION SKETCH OF CROSS SECTION ASSUMED FOR MODEL ANALYSIS

anisotropies of the individual layers are expressed by the ratio of their respective directional permeabilities, K_{yU}/K_{xU} and K_{yL}/K_{xL}. Based on the variables defined in Fig. 1 and on a study of field conditions in seepage areas of the Sacramento Valley, a series of model tests was outlined covering various combinations of the significant variables (25).

THEORY OF THE ELECTRIC ANALOGY

The electric analogy is a well-known device for studying the field of flow of fluid through porous media (8), (18). The analogy is based on the similarity between the differential equations which describe the flow of fluid through porous media, and those which govern the flow of electric current through conducting materials (14). Methods for treating anisotropic layered media by transformation into equivalent isotropic fields by scale distortion have been described by M. Maasland (13).

Model scales and dimensions were based on

$$\frac{X^2_{rU}}{Y^2_{rU}} = \frac{K_{yU}}{K_{xU}} \quad \text{.....(2a)}$$

and

$$\frac{X^2_{rL}}{Y^2_{rL}} = \frac{K_{yL}}{K_{xL}} \quad \text{.....(2b)}$$

in which the subscript r denotes a model-prototype ratio. By selecting

$$X_{rL} = X_{rU} = X_r \quad \text{.....(3)}$$

the common boundary between layers was made to coincide after transformation. An illustrative example of a typical cross section showing prototype and model dimensions is shown in Fig. 2.

DESCRIPTION OF THE MODEL

The electric analogy model for this study consisted of several components, including the electrolytic tank, the electrical circuit, the conducting medium, the analogy boundaries, and the drawing table. A photograph of the assembly is shown in Fig. 3.

As the conducting medium was an electrolyte, a large shallow lucite tank, with dimensions 25 in. by 60 in. by 3 in., was constructed to hold the liquid. The bottom of the tank was plane and was levelled to insure a uniform depth of electrolyte. In all tests the maximum length of the tank was utilized. It was found that making a test of the largest possible size in the model minimized inaccuracies and boundary errors.

The electric circuit for the model is shown in Fig. 4. A 12.6 v 60-cycle current was connected to the electrolytic tank. The potential divider accurately divided the voltage into 1,000 subdivisions so that readings to 0.1% were possible. Visual identification of the potential at the probe position in the tank was obtained with a cathode ray oscilloscope connected to the probe and the potential divider (Helipot). When there was no potential difference between the probe and the desired potential set on the potentiometer, no current flowed through the oscilloscope.

The resistance box provided a means for establishing a wide variety of fixed potentials on electrodes in the tank. Most tests required only the limiting potentials of 0% and 100%; but to represent sloping water tables, intermediate potentials with specified differences were necessary. The box contained forty precision resistors of 150 milliohms each, connected in series. In order to avoid adjustments when intermediate potentials were being connected to the electrodes in the tank, resistances in the resistance box were made relatively small as compared to the resistance of the electrolyte in the tank. In this way only very small amounts of current were consumed at the intermediate points on the main line. The deviation by variable current from a linear distribution of potentials along the line was negligible.

Various concentrations of a copper sulfate solution as well as tap water were employed as the conducting medium for these tests. Liquid conductors are advantageous when a large number of tests with different boundaries are to be studied. Solutions could be poured into the model readily, and after each test could be drained into storage containers. Also, where a permeability ratio

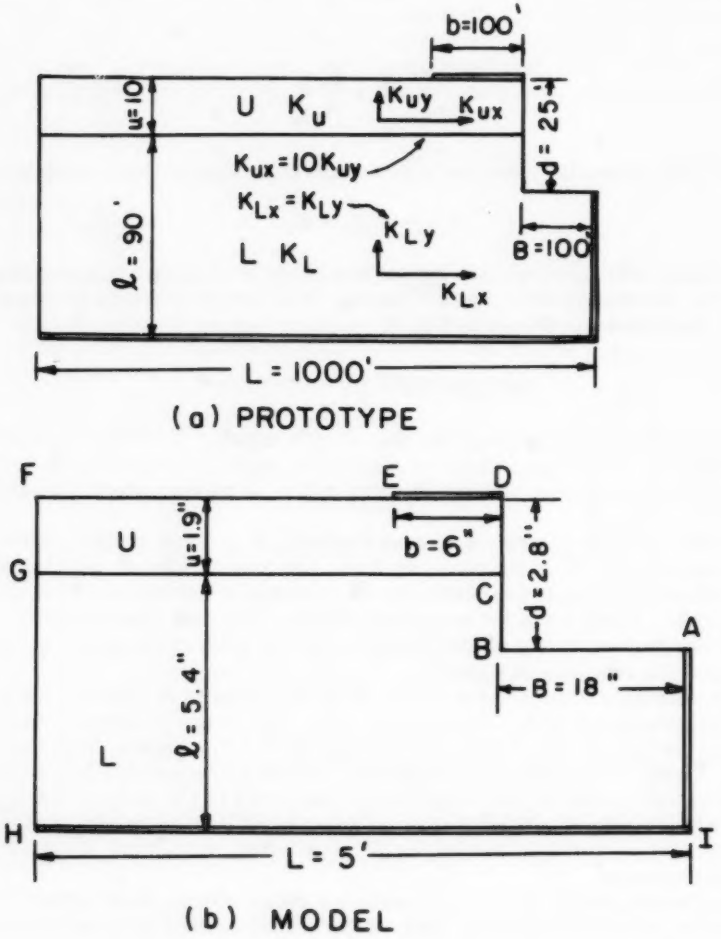

FIG. 2.—ILLUSTRATION OF PROTOTYPE AND MODEL DIMENSIONS FOR ONE CROSS SECTION

in two layers of 50:1 was under investigation, this difference was obtained by selecting solutions with a corresponding conductivity ratio. Liquid depths over the entire cross section were kept equal to about 2 in. With alternating current, copper electrodes, and a copper salt in the tank, no problems of polarization were encountered at the electrode surfaces.

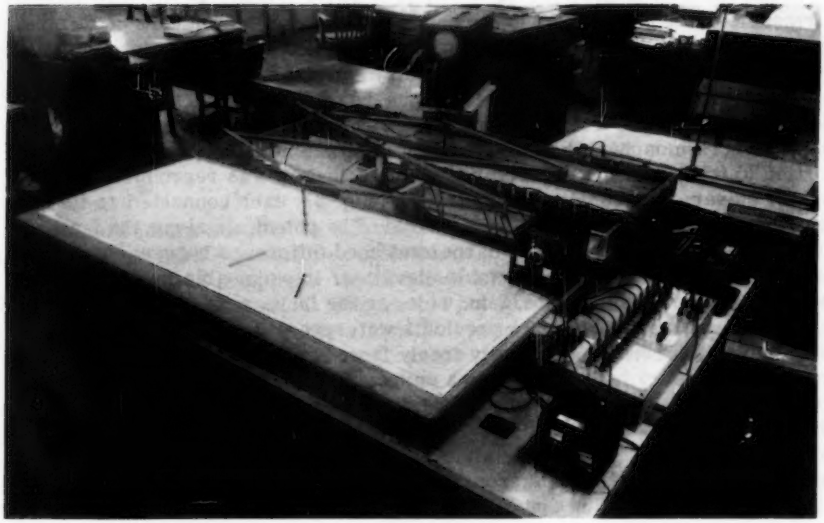

FIG. 3.—VIEW OF ELECTRIC ANALOGY MODEL

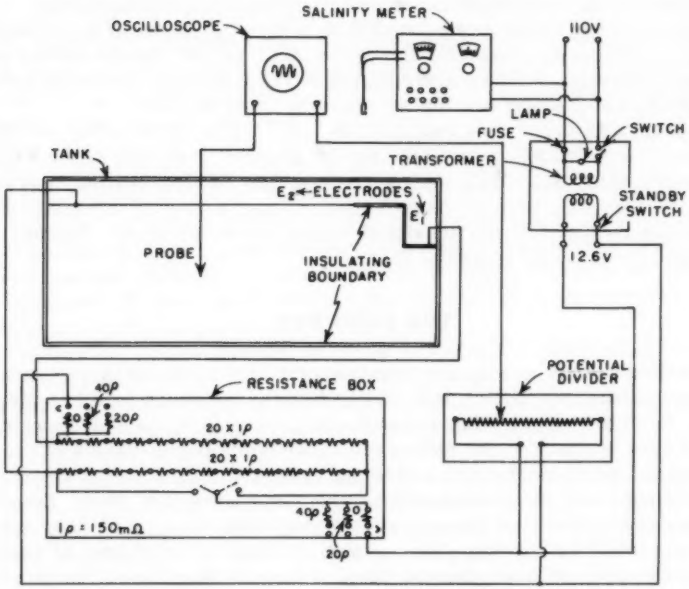

FIG. 4.—ELECTRIC CIRCUIT FOR ELECTRIC ANALOGY MODEL

Three kinds of boundaries were required in the model: permeable and impermeable outer boundaries, and inner boundaries between layers of different permeability. Permeable boundaries were made of copper strips 3 in. wide bent to fit the configuration of the boundary and carrying a given potential by means of a connection with the resistance box. For boundaries representing sloping water tables, a variable potential was required. Because the pressure is constant (atmospheric) on a water table, the potential is everywhere in proportion to the elevation. Therefore, such a boundary was reproduced by a series of closely-spaced copper electrodes (Fig. 3), each connected to its corresponding potential in the resistance box. The potentials along the boundary were expressed in percentages of the total head difference between the channel water level and the lowest water table elevation. Impermeable boundaries were nonconducting strips of lucite, 3 in. wide, or the lucite wall of the tank.

The inner boundaries had to provide a waterproof seal between the two liquids, and had to conduct electricity freely from one layer to the other, but each point on a boundary had to maintain a unique potential value. The boundary was constructed by modifying a procedure first suggested by Vreedenburgh and Stevens (22), (28). Lucite strips were notched and perforated at 3/16-in. intervals, and a short length of 1-mm diameter copper wire was inserted in each hole and bent so that the ends crossed in the notch above. All boundaries were held in place by modeling clay at the bottom.

Outer boundaries were interchanged during each test. Electrodes on permeable boundaries enabled equipotential lines of electricity and flow to be sketched, while placing electrodes on impermeable boundaries allowed streamlines to be located. Variable potential boundaries could be interchanged only after computing the redistribution of potentials along such boundaries.

Movement of the probe was recorded on a drawing paper at a 1:1 scale by means of a pantograph connecting the probe and a pencil. By connecting points of the same potential, each equipotential line was obtained. Sketching time for one set of lines of a cross section amounted to about 30 min.

In general, with proper instrumentation, any degree of accuracy can be obtained in an electric analogy model. As the present work was concerned with ground-water flow, basic data such as boundaries, permeabilities, and anisotropy ratios were only approximately known. A high degree of accuracy, therefore, was not required in the idealized model cross sections. Results were estimated to be accurate to within 5%.

THE FLOW NET

The curves $\phi(x,y)$ = constant (equipotential lines) and $\psi(x,y)$ = constant (streamlines) form two orthogonal families of curves which together form the flow net. Each two neighboring streamlines form a flow channel, in which the amount of flow is equal to the difference between the two ψ-values of the corresponding streamlines. Usually a flow net is constructed with an integer number of flow channels, each transmitting the same amount of flow. Similarly, the number of equipotential lines is chosen such that the drop of head between adjacent ones will be the same throughout. If H is the total loss of head, N_e denotes the number of equipotential drops ΔH, and N_s defines the number of stream channels with a flow rate ΔQ per unit width in each, then by Darcy's law

$$\Delta Q = K \frac{\Delta H}{b} a \cdot 1 \quad \ldots\ldots\ldots\ldots\ldots \quad (4a)$$

and

$$\frac{Q}{N_s} = K \frac{H}{N_e} \frac{a}{b} \quad \ldots\ldots\ldots\ldots\ldots\ldots \quad (4b)$$

or

$$\frac{a}{b} = \frac{Q}{K H} \frac{N_e}{N_s} \quad \ldots\ldots\ldots\ldots\ldots\ldots \quad (5)$$

in which a is the streamline spacing and b is the equipotential spacing. The ratio a/b remains constant throughout any homogeneous isotropic region.

For reasons of simplicity it was decided to draw the flow nets for the present work with $N_e = N_s = 20$. This gave a potential drop between two equipotential lines equal to 5% of the total available head H, and a flow in each flow channel equal to 5% of the total flow from the river. The total flow per unit distance along the river channel was given by

$$Q = K H \frac{a}{h} \quad \ldots\ldots\ldots\ldots\ldots\ldots \quad (6)$$

and an average of a/b from several measured "squares" was found sufficient to insure a reliable flow value. When two layers are present, the ratio a/b is different in each zone, so that

$$\frac{a_1}{b_1} = \frac{K_2}{K_1} \frac{a_2}{b_2} \quad \ldots\ldots\ldots\ldots\ldots\ldots \quad (7)$$

To draw equipotential lines, the river bank and bed [ABCD in Fig. 2(b)] were connected to the 100% electrical potential, and the ground-water level and the end of the model [EFGH in Fig. 2(b)] were connected to the 0% electric potential. The impervious base of the levee (ED), the impervious bottom (HI), and the right edge of the model which is a line of symmetry (IA) were made of non-conductive lucite. From a theoretical standpoint the line FH should have been infinitely distant from the channel, but the error introduced by assuming it to be about 1,000 ft to 2,000 ft from the channel is negligible. For these boundaries and a given K_U/K_L ratio, the equipotentials were drawn.

For drawing streamlines, impermeable and fixed potential boundaries were interchanged. At the same time the conductivities of the two layers were interchanged.

The flow net drawn directly from the isotropic model is an orthogonal one. The prototype itself is anisotropic; therefore, the actual flow net is not orthogonal. When the drawing is reduced by distorted scales, that is, the horizontal reduction differs from the vertical, the resulting drawing is also a non-orthogonal flow net (see Figs. 5 and 6).

Almost all tests had an upper boundary formed by a fixed horizontal water table, the elevation of which was taken as the datum level ($\phi = 0$). This approximated conditions existing in fields adjacent to a river where drains control the water table. In this way the problem of an unknown phreatic surface was avoided; a phreatic surface can be studied in an electric analogy only by trial and error. However, in some field cases of interest the controlled steady water table is not horizontal, but slopes away from the river with a gradient of from about 1:500 to 1:1500. Two tests were performed with sloping water

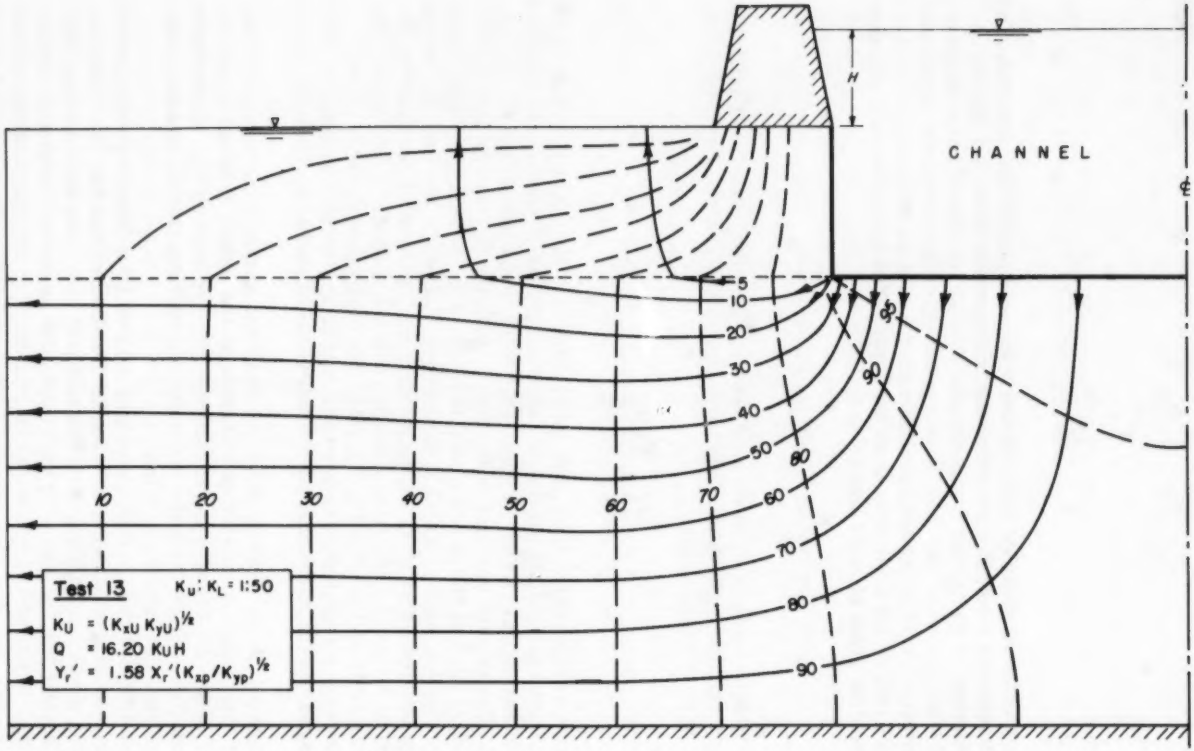

FIG. 5.—FLOW NET WITH LOWER PERMEABLE LAYER. ANISOTROPY RATIO K_x/K_y = 0.10 FOR BOTH LAYERS

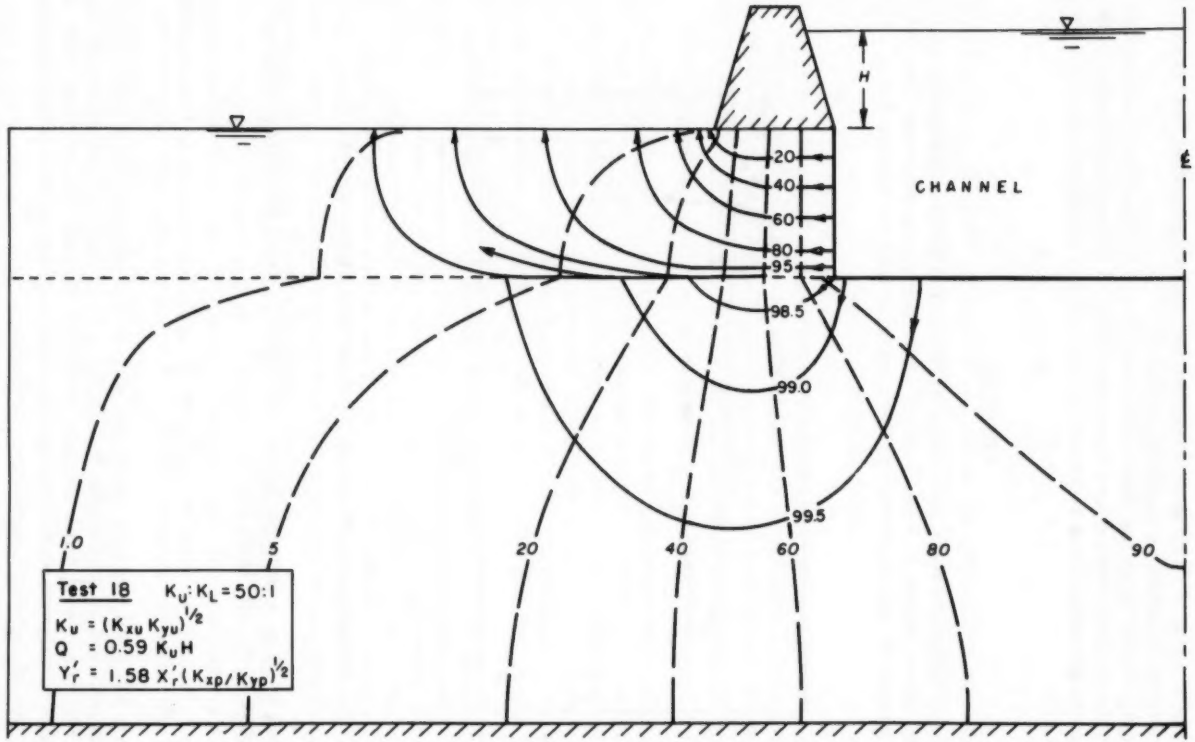

FIG. 6.—FLOW NET WITH UPPER PERMEABLE LAYER. ANISOTROPY RATIO K_x/K_y = 0.10 FOR BOTH LAYERS

tables to study these situations. The lowest point of the water table (at a distance of 3,000 ft from the center of the river) was taken as the datum level ($\phi = 0$), and a slope of 1:500 was assumed for the water table. An example giving prototype dimensions is shown in Fig. 7.

The equipotential lines for these tests were drawn by the electrical analogy, while the streamlines were drawn by constructing an orthogonal family of curves to the equipotential lines according to the rules of graphical flow net construction (3).

RESULTS

Results of the model tests were summarized in the form of plates and tables (25). Two plates, shown in Figs. 6 and 7, illustrate cross-sectional flow nets. Seepage quantities and distribution were summarized in tabular form. For

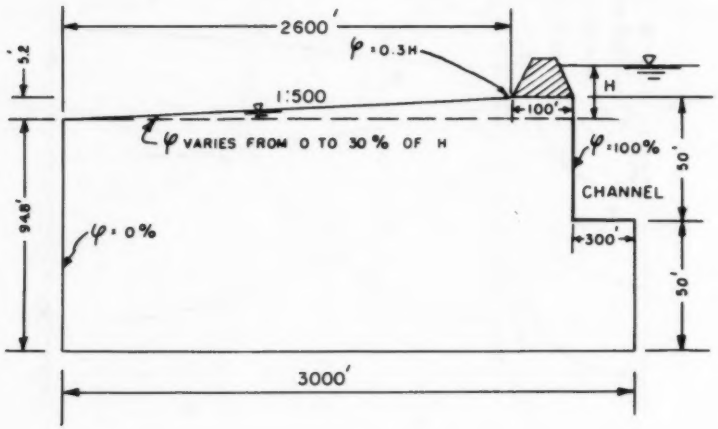

FIG. 7.—EXAMPLE OF CROSS SECTION WITH SLOPING WATER TABLE

each cross section, a seepage factor was obtained from measured values of $\frac{a}{b}$ in the upper layer, and from Eq. 6,

$$\frac{Q}{K_U H} = \frac{a}{b} \quad \ldots\ldots\ldots\ldots\ldots\ldots \quad (8)$$

Therefore, the total seepage from one side of the channel for a given cross section is obtained by multiplying the factor a/b by appropriate values of K_U and H. The fraction of total seepage emerging through the vertical side of depth d was determined as well as the distribution of seepage at ground surface as a function of distance inland from the levee.

A dimensionless scaling factor α was computed for each cross section so that the test data can be extended to other anisotropies of the upper and lower

layers. The factor is related to the permeabilities and scales by

$$Y'_{rU} = \alpha\, X'_{rU} \left(\frac{K_{xUp}}{K_{yUp}}\right)^{1/2} \quad \ldots\ldots\ldots\ldots \quad (9a)$$

and

$$Y'_{rL} = \alpha\, X'_{rL} \left(\frac{K_{xLp}}{K_{yLp}}\right)^{1/2} \quad \ldots\ldots\ldots\ldots \quad (9b)$$

in which X'_{rL}, X'_{rU}, Y'_{rU}, and Y'_{rL} denote the ratio of the figure length to the corresponding prototype distance and other terms are as previously defined.

ANALYSIS OF RESULTS

Seepage flow nets for the cross sections studied depend upon the variables: (1) channel depth, (2) channel width, (3) levee base width, (4) anisotropy, (5) arrangement and thickness of layers, and (6) water table slope. From the test results an effort was made to evaluate the effect of each factor on seepage.

Effect of Channel Depth.—Discharges as $\frac{Q}{K_U H}$ are plotted against the depth ratio d/D in Fig. 8. In general, the discharge increases with channel depth, the rate of rise being dependent upon the anisotropy ratio. For an increase in depth ratio of 0.25 to 1.00, the seepage increases 8% for an anisotropy ratio of 1:100; an increase of approximately 45% occurs for an increase in depth ratio from 0 to 0.25. For an anisotropy ratio of 1:10 the increase in discharge is 5% for an increase in depth ratio from 0.25 to 1.00 and the same for an increase in depth ratio from 0 to 0.25.

Analytic evaluations of channel depths d = 0 and d = D are discussed in Appendix I.

Effect of Channel Width.—Most of the tests were performed with a half-channel width equal to 300 ft, so that a direct observation as to this effect for the various anisotropy ratios and thicknesses of layers could not be made. However, it was apparent that a relatively small portion of the total seepage occurs through the channel bottom when the upper layer is a pervious one not extending appreciably below the channel bottom.

In tests in which the bottom of the upper pervious layer extends to well below the channel, the percentage of seepage through the bottom increases up to approximately 50%. The percentage depends upon the geometry of the cross section and the anisotropy ratio. When the upper layer is semipervious, most of the seepage takes place through the bottom unless the thickness of this layer is smaller than the depth of the channel.

The effect of channel width for a homogeneous anisotropic case was demonstrated in tests for bottom widths of 300 ft, 200 ft, and 100 ft. The resulting seepage factors were $\frac{Q}{K_U H}$ = 1.08, 1.10, and 1.15, respectively. Similarly, small differences were obtained in the analytic treatment of a zero depth channel (Appendix I).

Effect of Levee Base Width.—Because all tests were performed with a levee base width of 100 ft, no conclusions could be drawn as to the effect of this fac-

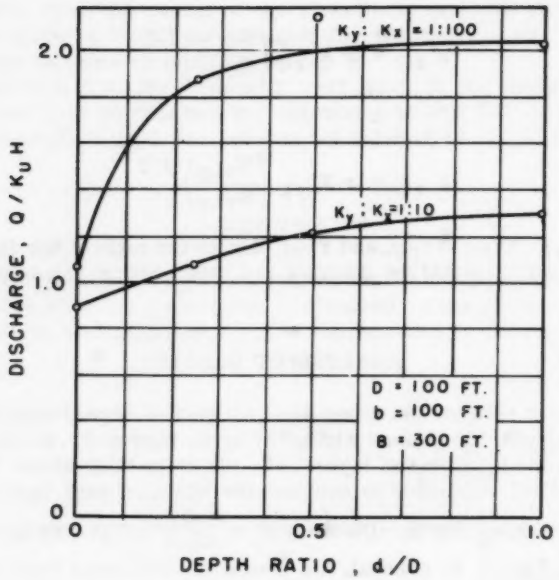

FIG. 8.—EFFECT OF CHANNEL DEPTH ON SEEPAGE DISCHARGE

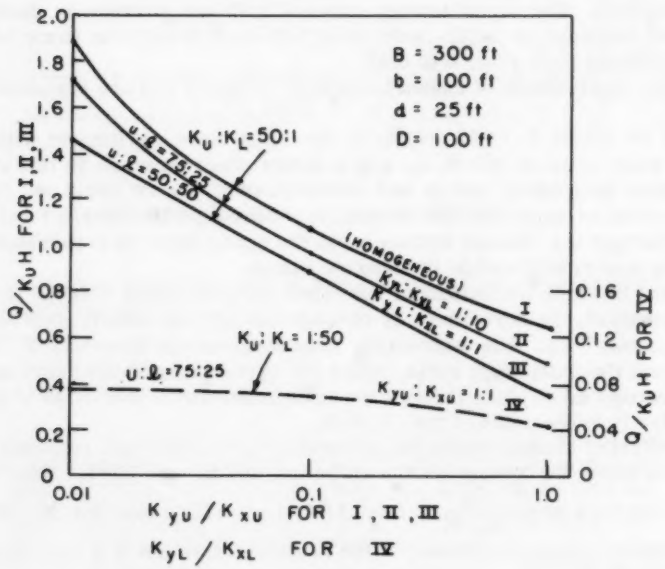

FIG. 9.—EFFECT OF ANISOTROPY ON TOTAL SEEPAGE DISCHARGE

tor. For the theoretical case of a channel with zero depth, described in Appendix I, the effect of levee base width was determined (Fig. 14). For a given B/D ratio, the discharge decreases with increasing levee base width b/D. This trend is believed to be generally true for the investigated cross sections.

Effect of Anisotropy.—Fig. 9 shows discharge as a function of the anisotropy ratio of the more permeable layer. In general, the seepage factor increases as the anisotropy ratio becomes smaller. This relation holds both for the homogeneous cases (Curve I) and for two-layer cases (Curves II, III, and IV).

It was apparent that flow in the semipervious layer, when it is the upper layer, is mainly vertical so that its anisotropy ratio is unimportant. Also, whenever the semipervious layer lies below the pervious one, the flow transmitted through it is very small so that the effect of its anisotropy is again negligible.

The distribution of seepage through the side of the channel depends upon the anisotropy ratio. For both the homogeneous and the layered cases with the more permeable layer on top, the percentage of seepage through the banks increases as the anisotropy ratio decreases. When the less permeable layer is on top, the fraction of seepage through the banks increases with an increase in the anisotropy ratio. Trends are shown on Fig. 10; in some cases the effect is negligible.

The distribution of seepage with landward distance from the levee is shown in Fig. 11 for three tests with homogeneous cross sections and for three tests with isotropic semipervious layers on top. Although data are limited by model dimensions required for transformations, these demonstrate that seepage is distributed further inland as the anisotropy ratio decreases.

Effect of Arrangement and Thickness of Layers.—In comparing the effect of the position of the relatively permeable layer to that of the relatively impermeable layer, it was noted that the discharge is greater when the more permeable layer is on top. For the same situation, a greater amount of seepage appears near the levee.

The effect of the relative thicknesses of the two layers is shown in Fig. 12 for selected tests. These show, for different anisotropies, that the discharge decreases as the thickness of an upper permeable layer decreases [Fig. 12(a)], but the converse is true if the upper layer is the relatively impermeable one [Fig. 12(b)].

Effect of Water Table Slope.—The effect was studied in two tests. In both cases the water table slope away from the levee was 1:500, but the total drop (in feet) represented different percentages of the total head H. A direct comparison between the two tests could not be made; however, individual comparisons were possible between these tests and a test having a similar cross section with a horizontal water table. Compared to a discharge of 1.08 K H for the horizontal water table, discharges of 1.3 K H (for a water table drop of 0.3 H) and 3.88 K H (for a water table drop of 0.6 H) were obtained. Slope of the water table also affects seepage distribution landward from the levee. Seepage is distributed farther inland with water tables sloping away from the levee than for horizontal water tables. The larger the portion of the total available head above the lowest point of the slope, the greater the inland extent of seepage.

CONCLUSIONS

Model tests demonstrated that seepage from a leveed river into adjoining low-lying lands is affected to only a minor extent by variations of channel depth

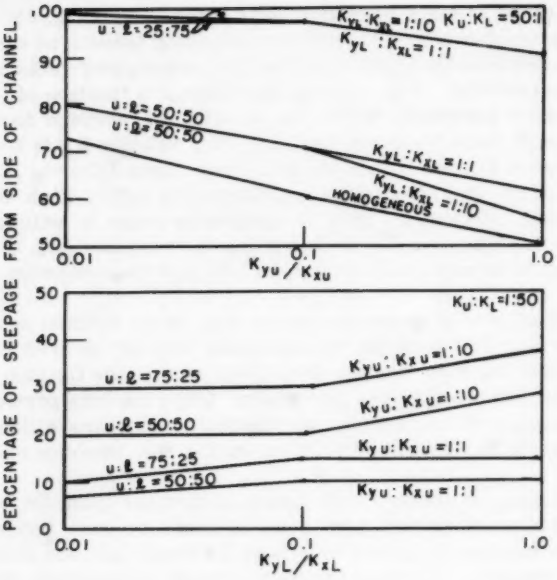

FIG. 10.—EFFECT OF ANISOTROPY ON BANK SEEPAGE

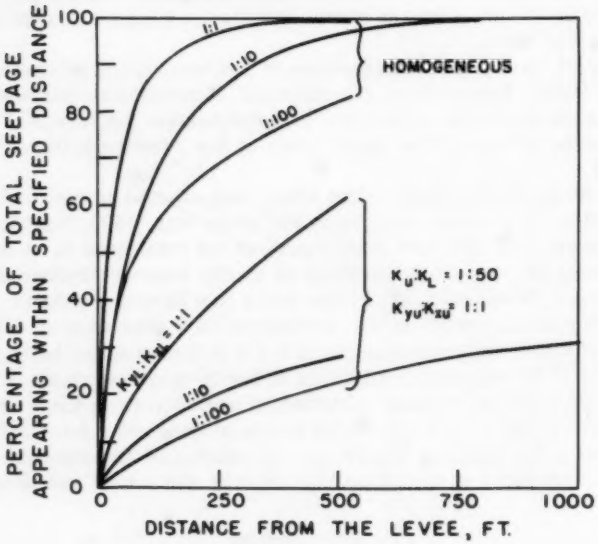

FIG. 11.—EFFECT OF ANISOTROPY ON BANK SEEPAGE DISTRIBUTION

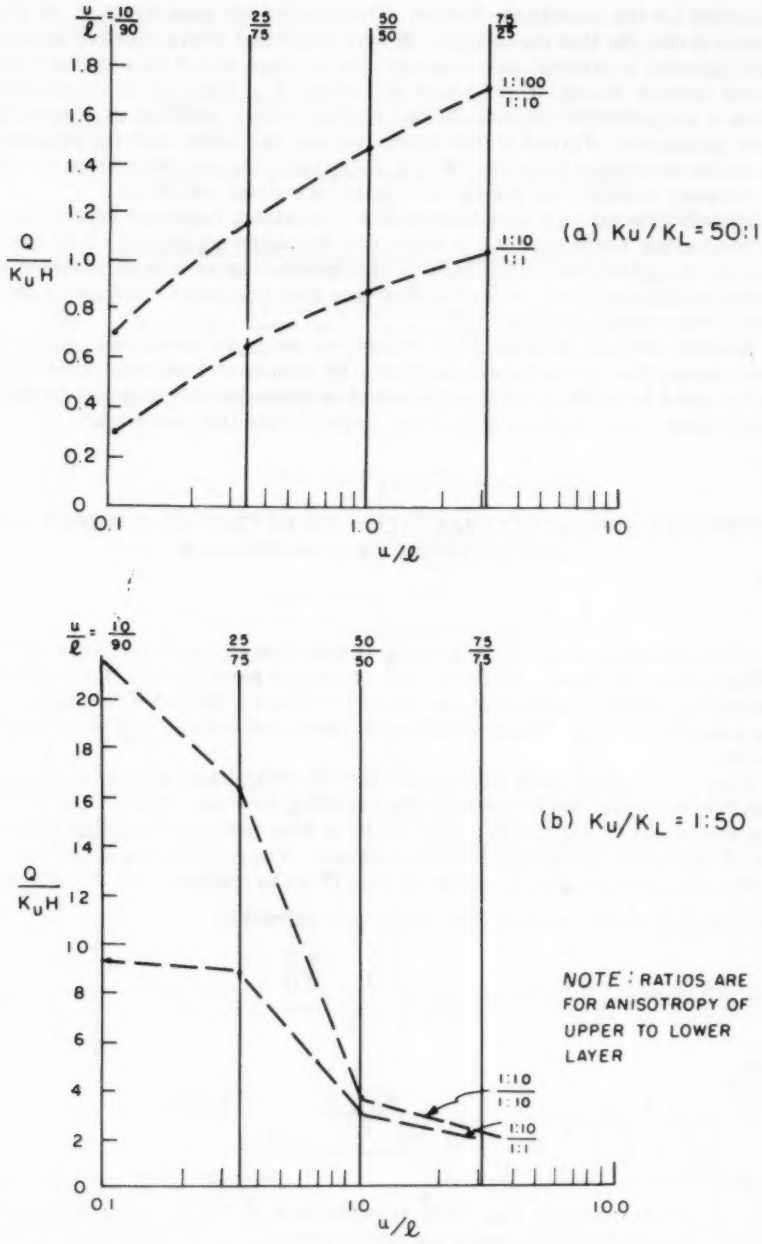

FIG. 12.—EFFECT OF THICKNESS OF LAYERS ON SEEPAGE DISCHARGE

and width for the conditions studied. The greater the base width of an impermeable levee, the less the seepage. It was found that with a smaller anisotropy ratio (greater horizontal permeability) the seepage factor was greater and extended farther inland. Only rough estimates of anisotropy are necessary to define a seepage flow pattern. In two-layered strata, seepage is greater if the more permeable stratum is the upper one and increases with the thickness of the more permeable stratum. With a water table sloping away from the river, the seepage quantity and inland movement increases with slope.

The electric analogy model was found to provide a rapid and versatile means for evaluating seepage under a variety of boundary conditions. The model is general in application, being capable of representing an infinite number of geologic conditions. Only lack of subsurface data precludes analysis of seepage from given cross sections.

Results defined seepage for a variety of geologic conditions, particularly those where two strata govern the flow. By means of a dimensionless scaling factor, good estimates can be obtained of seepage quantity and distribution for many other cross sections which only approximate test conditions.

APPENDIX I.—ANALYTIC EVALUATION OF EFFECT OF CHANNEL DEPTH ON SEEPAGE FOR d = 0 AND d = D

Analytic determination of seepage is practicable for only a very few simplified cross sections. Solutions are presented here for two isotropic cases, one with a channel depth equal to zero (d = 0) and a second with fully penetraing channel (d = D). These supplement the model results and their interpretation.

Case 1 - Channel with Zero Depth (d = 0).—Fig. 13(a) shows the cross section for this case. With regard to the resulting flow net, Figs. 13(b) and 13(c) are equivalent to Fig. 13(a). Fig. 13(c) is then used as a starting point for a set of Schwartz-Christofel transformations. The z-plane shown in Fig. 13(d) is transformed into the ζ_1 -plane of Fig. 13(e) by means of the transformation $\zeta_1 = \sin \frac{\pi z}{2D}$ and m and n in Fig. 13(e) are defined by

$$m = \frac{e^{\frac{\pi B}{2D}} - e^{\frac{-\pi B}{2D}}}{2} \quad \ldots\ldots\ldots\ldots\ldots\ldots (10a)$$

and

$$n = \frac{e^{\frac{\pi(b+B)}{2D}} - e^{\frac{-\pi(b+B)}{2D}}}{2} \quad \ldots\ldots\ldots\ldots\ldots (10b)$$

The ζ_2 -plane shown in Fig. 13(f) is equivalent to the ζ_1 -plane shown in Fig. 13(e). By this transformation the entire width (2B) of the channel is considered; accordingly, the resulting discharge will correspond to the whole chan-

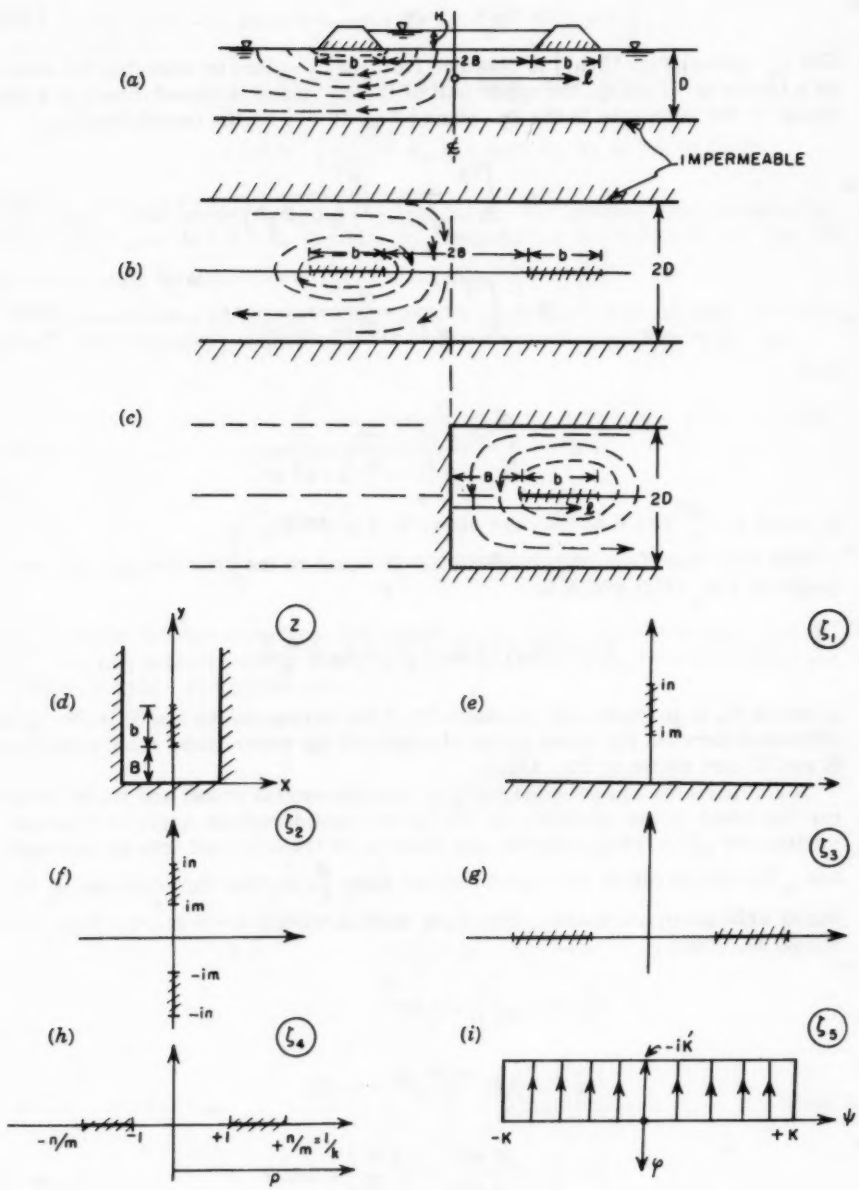

FIG. 13.—TRANSFORMATIONS OF CHANNEL WITH ZERO DEPTH

nel. The ζ_3 -plane (Fig. 13(g) is obtained from the ζ_2 -plane by rotating

$$\zeta_3 = -i\,\zeta_2 \quad \ldots\ldots\ldots\ldots\ldots\ldots \quad (11)$$

The ζ_4 -plane [Fig. 13(h)] is obtained from the ζ_3 -plane by reducing the scale by a factor m. Finally, the upper half of the ζ_4 -plane is transformed into the inside of the rectangle in the ζ_5 -plane [Fig. 13(i)] by the transformation

$$\zeta_5 = \int_0^{\zeta_4} \frac{dt}{\sqrt{(1-t^2)(1-k^2 t^2)}} \quad \ldots\ldots\ldots \quad (12a)$$

$$K = \int_0^{\zeta_1} \frac{dt}{\sqrt{(1-t^2)(1-k^2 t^2)}} \quad \ldots\ldots\ldots \quad (12b)$$

and

$$i\,K' = \int_1^{1/k} \frac{ds}{\sqrt{(1-s^2)(1-k^2 s^2)}} \quad \ldots\ldots\ldots \quad (12c)$$

in which $k = \frac{m}{n}$ and K and K' are shown in Fig. 13(i).

The total flow from the channel (2Q) is equal to the flow through the rectangle of Fig. 13(i) which is

$$2Q = (K_e)(2\,K)\left(\frac{H}{K'}\right) = K_e\,H\,\frac{2\,K}{K'} \quad \ldots\ldots\ldots\ldots \quad (13)$$

in which K_e is the hydraulic conductivity of the porous media and H is the head difference between the water in the channel and the water table. The quantities K and K' are shown in Fig. 13(i).

A comparision can be made between the theoretical result and model tests for the same cross section. As the above considerations apply to isotropic media, any given cross section has first to be transformed into an isotropic one. The discharge is determined by the ratio $\frac{K}{K'}$ so that the scale can be reduced arbitrarily. Consider the cross section where B = 6 in., b = 2 in., and D = 20 in. Then

$$\frac{B}{D} = 0.3;\ \frac{\pi\,B}{2\,D} = 0.471$$

$$\frac{B+b}{D} = 0.4;\ \frac{\pi(B+b)}{2\,D} = 0.628$$

$$k = \frac{m}{n} = \frac{e^{0.471} - e^{-0.471}}{e^{0.628} - e^{-0.628}} = 0.727$$

and from Eq. 9a

$$\sin \alpha = k = 0.727; \quad \alpha = 46^\circ 40'; \quad \phi = \frac{\pi}{2}$$

$$k' = 0.686; \quad K = 1.880; \quad K' = 1.830$$

$$2Q = \frac{2 \times 1.880}{1.830} K_e H = 2.06 K_e H; \quad Q = 1.03 K_e H$$

The result of the model test was $Q = 1.06 K_e H$. For another cross section the model test gave $Q = 0.9 K_e H$ while by computation $Q = 0.935 K_e H$. Fig. 14 gives seepage discharges for various ratios of $\frac{b}{D}$ and $\frac{B}{D}$.

The distribution of seepage with distance from the levee can also be computed. The complex potential $\omega = \phi + i\psi$ for the rectangle [Fig. 13(i)] is

$$\omega = i\,\zeta_5 = i \int_0^{\zeta_4} \frac{dt}{\sqrt{(1-t^2)(1-k^2 t^2)}} = \phi + i\psi \quad \ldots\ldots \quad (14a)$$

and

$$\omega = i \int_0^{-\frac{i}{m} \sin \frac{\pi z}{2D}} \frac{dt}{\sqrt{(1-t^2)(1-k^2 t^2)}} \quad \ldots\ldots\ldots\ldots (14b)$$

Let l denote the distance from the origin in the horizontal direction [Fig. 13 (a)]. In the transformed z-plane this distance is represented by y along the imaginary axis. Along this axis

$$\omega = i \int_0^{-\frac{i}{m} \sin \frac{\pi i y}{2D}} \frac{dt}{\sqrt{(1-t^2)(1-k^2 t^2)}}$$

$$= i \int_0^{\frac{e^{\frac{\pi y}{2D}} - e^{-\frac{\pi y}{2D}}}{2m}} \frac{dt}{\sqrt{(1-t^2)(1-k^2 t^2)}} \quad \ldots\ldots\ldots\ldots \quad (15a)$$

or

$$\omega = i \int_0^{\rho} \frac{dt}{\sqrt{(1-t^2)(1-k^2 t^2)}} \quad \ldots\ldots\ldots \quad (15b)$$

in which

$$\rho = \frac{e^{\frac{\pi y}{2D}} - e^{-\frac{\pi y}{2D}}}{2m} \quad \ldots\ldots\ldots\ldots\ldots\ldots \quad (16)$$

The integral must be evaluated in three separate parts:

1. $0 \leq y \leq B$, or $0 \leq \rho \leq 1$. For this case

$$\psi = \int_0^{\rho} \frac{dt}{\sqrt{(1-t^2)(1-k^2 t^2)}} \quad \ldots\ldots\ldots \quad (17)$$

When $y = 0$, $\rho = 0$, $\psi = 0$; and when $y = B$, $\rho = 1$, $\psi = K$ (the total flow from half a channel).

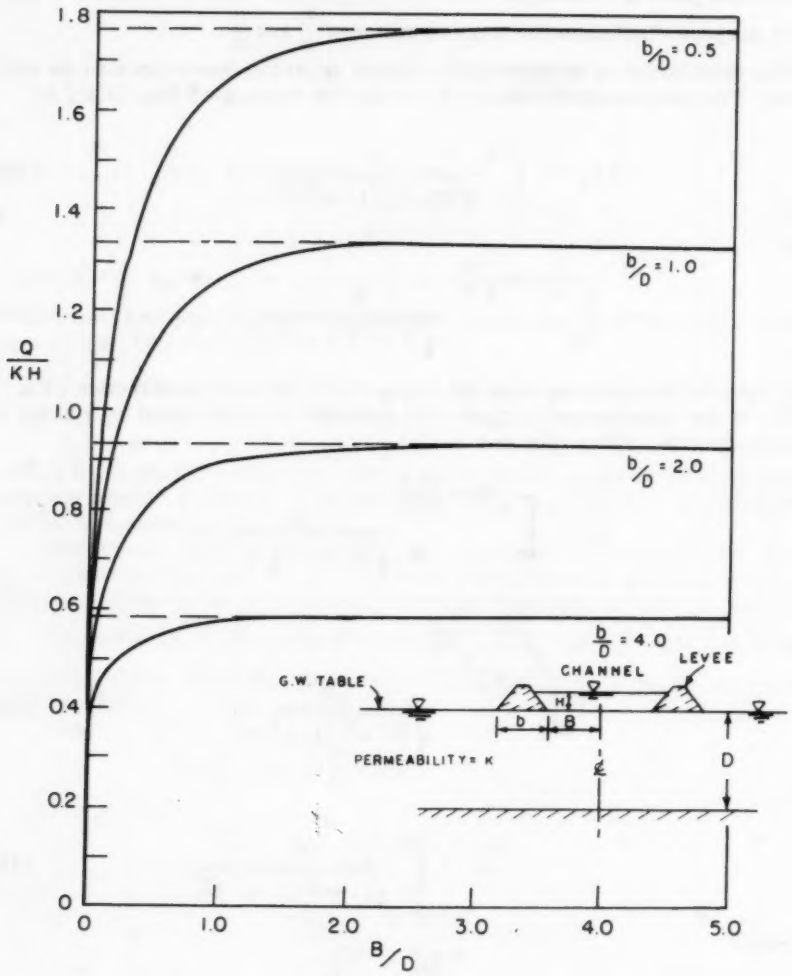

FIG. 14.—SEEPAGE FROM CHANNEL OF ZERO DEPTH AS A FUNCTION OF $b/_D$ AND $B/_D$

2. $B < y < B + b$ or $1 < \rho < \frac{1}{k}$ or ζ_5 from K to K + iK'. Along this line ψ remains constant and only the value of ϕ changes. This follows from the fact that the integral has a real part, which is the same as that of part (1), and an imaginary part which gives the change of potential along the base of the levee. In general, values for ϕ and ψ can be obtained from w; however, only the values of ψ are considered here.

3. $B + b < y < \infty$, or $\frac{1}{k} < \rho < \infty$, or ζ_5 from K + iK' to iK'. For this case

$$\psi = \text{Re} \left[\int_0^{\rho} \frac{dt}{\sqrt{(1-t^2)(1-k^2t^2)}} \right] \quad \ldots\ldots (18a)$$

$$= \text{Re} \left[\int_0^1 \frac{dt}{\sqrt{(1-t^2)(1-k^2t^2)}} - i \int_1^{1/k} \frac{dt}{\sqrt{(t^2-1)(1-k^2t^2)}} + \int_{1/k}^{\rho} \frac{dt}{\sqrt{(1-t^2)(1-k^2t^2)}} \right] \quad \ldots\ldots\ldots (18b)$$

$$= \int_0^1 \frac{dt}{\sqrt{(1-t^2)(1-k^2t^2)}} - \frac{1}{k} \int_{1/k}^{\rho} \frac{dt}{\sqrt{(t^2-1)\left(t^2-\frac{1}{2}\right)}} \quad \ldots\ldots (18c)$$

where both integrands (and also the integrals) are real in their intervals. Evaluation by tables yields

$$\psi = K - F(\alpha, \phi) \quad \ldots\ldots\ldots\ldots\ldots\ldots (19)$$

in which

$$\sin \phi = 1/k \sqrt{\frac{1 \rho^2 k^2}{1 - \rho^2}} \quad \ldots\ldots\ldots\ldots (20a)$$

and

$$\sin \alpha = k \quad \ldots\ldots\ldots\ldots\ldots\ldots (20b)$$

Thus, for $y = 0$, $\psi = 0$; for $y = B$ and $y = B + b$, $\psi = k$; and for $y = \infty$, $\psi = 0$.

The following example shows how the preceding analysis can be applied for determining the distribution of seepage.

Example.—At 100 ft from the levee in the same cross section described above, y = 10 in. Width 2 m = 0.978,

$$\rho = \frac{e^{\pi/4} - e^{-\pi/4}}{0.978} = 1.775$$

$$k = 0.727; \quad \frac{1}{k} = 1.372; \quad K = 1.880$$

$$\sin \phi = 1.375 \sqrt{\frac{1 - (1.775)^2 (0.727)^2}{1 - (1.775)^2}} = 0.762$$

$$\phi = 49.6°$$

From Eq. 9a

$$\sin \alpha = k = 0.727; \quad \alpha = 46.7°$$

$$F(0.727;\ 49.6°) = 0.92$$

$$\psi = 1.88 - 0.92 = 0.96$$

As a percentage the value of ψ equals $\frac{0.96}{1.88} \times 100 = 51.2\%$ as compared to approximately 53% obtained by the model.

Case 2 - Fully Penetrating Channel ($d = D$).—A sketch of this cross section appears in Fig. 15. After a series of transformations, similar to those described for Case 1, the following results can be written (25)

$$K = \int_0^1 \frac{dt}{\sqrt{(1 - t^2)(1 - k^2 t^2)}} \quad \ldots\ldots\ldots (21a)$$

and

$$iK' = \int_1^{1/k} \frac{ds}{\sqrt{(1 - s^2)(1 - k^2 s^2)}} \quad \ldots\ldots (21b)$$

The total discharge (for one side) is

$$Q = K_e \frac{2H}{2K} K' = K_e H \frac{K'}{K} \quad \ldots\ldots\ldots\ldots (22)$$

The seepage distribution can be obtained in a similar way to that described for Case 1.

Fig. 15 shows the relationship between the discharge $\left(\text{expressed as } \frac{Q}{K_e H}\right)$ and the width of the levee $\left(\text{expressed as } \frac{b}{D}\right)$.

Cases 1 and 2 lead to the following conclusions:

1. Increasing the width of the channel increases the discharge very rapidly at first, but has almost no effect for $\frac{B}{D} > 2$.
2. For a fixed ratio of $\frac{B}{D}$, the discharge increases as the ratio $\frac{b}{D}$ decreases.
3. For a fully penetrating channel, its width has no effect on the discharge. The discharge from the channel increases as the length of the base of the levee decreases.

Although these conclusions were obtained from the theoretical cases of a channel with no depth and a fully penetrating channel, it is believed that these trends remain true also for the cross sections investigated in the model. The analytic study was based on an aquifer of infinite extent, whereas the model

tests of necessity presupposed an aquifer of limited extent. Comparison of results by the two methods reveal that differences were negligible, thus justifying the model work.

In general, the theoretical approach described previously is applicable only to a limited number of simplified cross sections in a homogeneous aquifer. Even for these cases, the determination of the complete flow net requires many

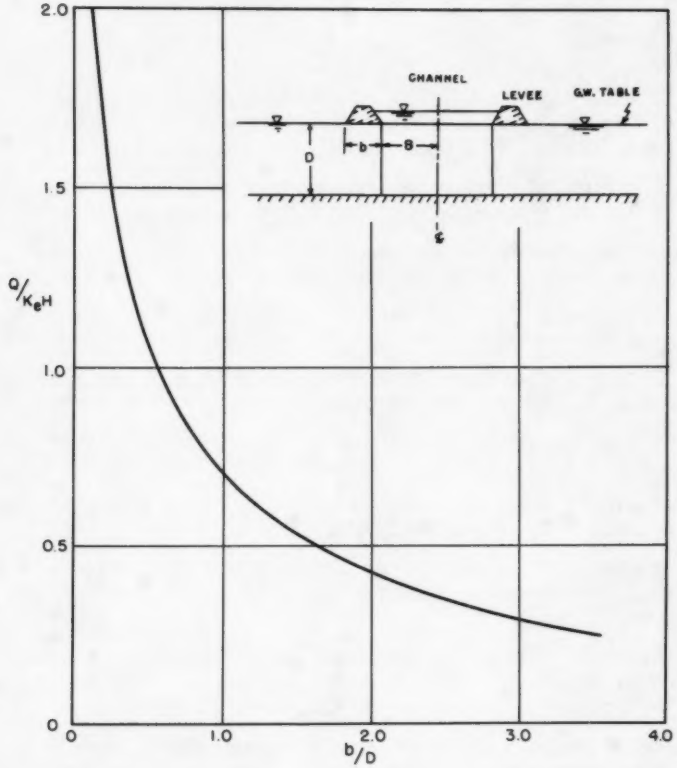

FIG. 15.—SEEPAGE FROM A FULLY PENETRATING CHANNEL AS A FUNCTION OF b/D

hours of claculation for each case. From a practical point of view, therefore, the electric analogy model was essential to investigate the seepage through cross sections approximating field conditions.

ACKNOWLEDGMENTS

The investigation presented in this paper covers one portion of a continuing research program in ground water hydrology sponsored by the Water Resources Center of the University of California. The study was conducted in the Hydraulic Laboratory of the College of Engineering at Berkeley, California. In-

formation on field seepage conditions was supplied by the California Department of Water Resources and the U. S. Geological Survey. G. de Josselin de Jong furnished advice on the theoretical computations.

APPENDIX II.—BIBLIOGRAPHY ON SEEPAGE THROUGH RIVERS AND NATURAL CHANNELS

1. "The Effect of a Slightly Pervious Top Blanket on the Performance of Relief Wells," by R. A. Barron, Proceedings, Second Internatl. Conf. on Soil Mech., Vol. 4, 1948, pp. 324-328.
2. "The Effect of Blankets on Seepage Through Pervious Foundations," by P. T. Bennett, Transactions, ASCE, Vol. 111, 1946, pp. 215-252.
3. "Seepage Through Dams," by A. Casagrande, Journal, New England Water Works Assoc., Vol. 51, 1937, pp. 131-172.
4. "Seepage Through Foundations Containing Discontinuities," by E. E. Esmiol, Proceedings, ASCE, Vol. 83, No. SM1, January, 1957.
5. "Seepage Losses from Irrigation Canals," by H. Y. Hammad, Proceedings, ASCE, Vol. 85, No. EM2, April, 1959.
6. "Uplift and Seepage under Dams on Sand," by L. F. Harza, Transactions, ASCE, Vol. 100, 1935, pp. 1352-1406.
7. "Tables of Functions with Formulae and Curves," by E. Jahnke and F. Emde, 4th Ed., Dover Publ., New York, 1945.
8. "Seepage Forces in a Gravity Dam by Electrical Analogy," by H. A. Johnson, Proceedings, ASCE, Vol. 81, Proceedings-Separate No. 757, July, 1955.
9. "Sacramento River Seepage and Erosion Problems," Joint Committee on Water Problems of the California Legislature, Sixth Partial Report, San Francisco, Calif., 1953, pp. 22-29, 40-45.
10. "Investigation of the Sacramento-San Joaquin Delta Water Supply and Water Utilization on Medford Island," by S. Kabakov, Report 2, California Water Project Authority, Sacramento, 1956.
11. "Security from Under Seepage, Masonry Dams on Earth Foundations," by E. W. Lane, Transactions, ASCE, Vol. 100, 1935, pp. 1235-1351.
12. "Electrical Analogy Applied to Study Seepage into Drain Tubes in Stratified Soil," by S.D.L. Luthra and G. Ram, Journal, Central Board of Irrig. and Power, India, Vol. 11, 1954, pp. 398-405.
13. "Soil Anisotropy and Land Drainage," by M. Maasland, in "Drainage of Agricultural Lands," J. N. Luthin, ed., Amer. Soc. of Agronomy, Madison, Wis., 1957, pp. 216-285.
14. "The Use of Rheoelectrical Analogies in Aerodynamics," by L. C. Malavard, AGARDograph 18, NATO Advisory Group for Aeronautical Research and Development, Paris, France, 1956.

15. "Control of Under Seepage, Mississippi River Levees, St. Louis District," by C. I. Mansur and R. I. Kaufman, Proceedings, ASCE, Vol. 82, No. SM1, January, 1956.

16. "Investigation of the Sacramento-San Joaquin Delta Ground Water Geology," by C. R. McClure, et al., Report 1, California Water Project Authority, Sacramento, 1956.

17. "Relief Wells for Dams and Levees," by T. A. Middlebrooks, Transactions, ASCE, Vol. 112, 1947, pp. 1321-1402.

18. "The Flow of Homogeneous Fluids Through Porous Media," by M. Muskat, McGraw-Hill Book Co., New York, 1937.

19. "Motion of Water under Dams," by N. N. Pavlovsky, 1st Congress on Large Dams, Stockholm, Sweden, Vol. 4, 1933, pp. 179-192.

20. "Seepage Conditions in Sacramento Valley," by C. E. Plumb, et al., California Div. of Water Resources, Sacramento, 1955.

21. "Predicting Seepage under Dams on Multi-Layered Foundations," by P. F. Shea and H. E. Whitsett, Proceedings, ASCE, Vol. 84, No. SM3, August, 1958; Discussion by H. F. Cedergren, Vol. 85, No. SM1, February, 1959.

22. "Electrical Determination of the Line of Seepage and Flow Net of a Groundwater Flow Through Joint Regions with Different Anisotropy," by O. Stevens, De Ingenieur in Ned. Indie, Vol. 9, 1938, pp. 205-212.

23. "Ground-Water Flow in Relation to a Flooding Stream," by D. K. Todd, Proceedings, ASCE, Vol. 81, Proceedings-Separate No. 628, February, 1955.

24. "Ground Water Hydrology," by D. K. Todd, John Wiley & Sons, New York, 1959.

25. "River Seepage Investigation," by D. K. Todd and J. Bear, Water Resources Center Cont. No. 20, Univ. of California, Berkeley, 1959; Engrg. Societies Library, New York.

26. "Relief Well Systems for Dams and Levees," by W. J. Turnbull and C. I. Mansur, Transactions, ASCE, Vol. 119, 1954, pp. 842-878.

27. "On the Steady Flow of Water Percolating Through Soils with Homogeneous-Anisotropic Permeability," by C. G. J. Vreedenburgh, Proceedings, Internatl. Conf. on Soil Mech. and Foundation Engrg., Vol. 1, Harvard Univ., Cambridge, Mass., 1936, pp. 222-225.

28. "Electric Investigation of Underground Water Flow Nets," by C. G. J. Vreedenburgh, Proceedings, Internatl. Conf. on Soil Mech. and Foundation Engrg., Vol. 1, Harvard Univ., Cambridge, Mass., 1936, pp. 219-222.

Journal of the
HYDRAULICS DIVISION
Proceedings of the American Society of Civil Engineers

FISH PASSAGE THROUGH HYDRAULIC TURBINES[a]

By Glenn H. Von Gunten,[1] F. ASCE

SYNOPSIS

One of the major problems in connection with water resource development in the Pacific northwest of the United States has been safe fish passage at dams. Particular concern has been felt in regard to fish safety at dams 100 ft or more high. This concept has been perhaps the greatest factor in establishment of the basic plan for development of the Lower Columbia and Snake Rivers. Also, it may be that the apparent safety accorded to dams under 100 ft high has been an adverse factor in migratory fish protection. There is now promising evidence that successful passage can be achieved through hydraulic heads of several hundred feet, and that the hydraulic characteristics of the water passageways are far more significant than heights of dams.

This paper reviews basic concepts of fish passage through dams and their significance with particular reference given to passage through turbines. Test procedures and summarized results of fingerling survival in passing through high speed model turbines and a prototype turbine under a 450 ft hydraulic head are furnished. The numerous data presented demonstrating a correlation of fish survival with various turbine characteristics show promise of leading to the achievement of successful passage through high head turbines.

INTRODUCTION

Anadromous fish have had and will probably continue to have a great influence on water resources development in the Pacific northwest. Hydro-

Note.—Discussion open until October 1, 1961. To extend the closing date one month, a written request must be filed with the Executive Secretary, ASCE. This paper is part of the copyrighted Journal of the Hydraulics Division, Proceedings of the American Society of Civil Engineers, Vol. 87, No. HY 3, May, 1961.

[a] Presented at the August 1960 ASCE Hydra. Div. Conf. in Seattle, Wash.

[1] Chf., Planning and Reports Branch, U.S. Army Engr. Dist., Corps of Engrs., Walla Walla, Wash.

electric power developments, primarily on coastal streams and in the middle Snake River area, have been extensively curtailed due to the concern of maintaining commercial and sport fisheries dependent on those streams as spawning grounds and migration passageways to and from the ocean. Curtailment of such development has been an exceedingly controversial issue, primarily because of the great economic potential for power development and the lack of evaluation of the effects such developments would have on the migratory fish population.

The various species of salmon spawn in fresh-water streams. The young fingerlings move from their hatching grounds to the sea where they live until maturity. After maturing in the ocean, they return to the the streams to spawn and die, thus completing their life cycle. Steelhead trout follow a similar life cycle but of a less definable pattern and do not necessarily die when spawning.

Dams without adequate fish passage facilities obstruct the natural passageways of the migrants. A structure developing a hydraulic head of only a few feet may create a barrier to upstream adult migrants, and reservoir impoundments often submerge their spawning grounds. Downstream migrants may be exposed to severe physical stresses in passing through hydraulic structures.

UPSTREAM MIGRANTS

In the past much stress has been placed on the question of the ability of upstream migrant adults to negotiate fish ladders. However, during recent years the question of upstream passage has been resolved to the extent that any one of several methods appear to be feasible. This advance has been largely due to the Fisheries Engineering Research Program financed and sponsored by the Corps of Engineers, and the activities of other agencies. It appears that the primary problem associated with upstream passage is the ability to intercept or attract the migrants through the entrances by providing proper locations and hydraulic conditions, rather than the ability of the migrants to negotiate a ladder once found and entered.

DOWNSTREAM MIGRANTS

Young fingerling migrants move to the sea with the current. At dams they are involuntarily swept through spillways, turbines, or outlet works. In the Columbia River, fingerlings vary from 2 in. to 5 in. long, except for steelhead trout which vary from 5 in to 9 in. Under natural conditions they migrate without being exposed to major pressure changes. In being swept through hydraulic structures at a dam, they are at the mercy of the prevailing forces. The extreme turbulence and pressure changes of spillways and turbines inflict severe stresses on fish passing through them. Some conditions unquestionably cause injury and death, but for the most part, specific correlation of these conditions to distress has not yet been defined.

There is considerable evidence derived from various research programs which indicates or substantiates the following statements:

1. Static pressures associated with hydraulic heads of several hundred feet are not fatal. Although under certain conditions distress is evident, no lasting injury is apparent.

2. The apparent mortality in passing over or through spillways at dams of relatively low head is minor. High free-fall spillways discharging into a plunge pool also appear to provide relatively safe passage.

3. Negative pressures cause distress and may or may not cause permanent injury and death. In turbine passage and in laboratories negative pressures apparently have caused distress, and in some cases, death. Most observations indicate that, under conditions prevailing at dams, lasting ill effects are not apparent except in areas of extreme hydraulic turbulence or areas of pressure at or near the point of vaporization. The length and nature of exposure to both temperature and pressure changes and the degree of vacuum, may all be factors of significance.

4. Exposure to an area of vaporization and cavitation causes death.

5. Mechanical injury may be experienced by fish passing through turbines with small clearances between blades in relation to size of fish. The physical injury apparently varies with the relative dimensions and speed. Under prototype conditions, indications are that if blade clearances are greater than the length of fish, the mechanical injury is not significant at normal turbine speeds.

DOWNSTREAM MIGRANT PASSAGE THROUGH TURBINES

The mortality tests which have been performed at McNary, Big Cliff, Baker, Elwha, and Bonneville dams were primarily designed to evaluate the extent of, and not to explore the cause of, death. Intensive review of those test results and the research data, failed to reveal factual evidence of correlation between mortality and either high static hydraulic pressures or negative pressures normally experienced throughout the major portion of hydraulic passageways in a power plant. Because of this, the Walla Walla District, Corps of Engineers, initiated investigations toward evaluating mortality in relationship to physical conditions. The purpose was to find a means of safely passing downstream migrants through turbines. The possibility of studying mortality in passing fish through small-scale turbine performance models was investigated, and findings were promising.

MODEL TURBINE TESTS

In June 1959, exploratory tests were made at the S. Morgan Smith (now Allis-Chalmers) Hydraulic Turbine Test Laboratory at York, Pennsylvania, to determine the feasibility of investigating mortality in model turbines.

A low-head turbine performance test stand (Fig. 1) was used to conduct the tests. The closed hydraulic system was capable of providing turbine operating heads up to 50 ft. Hydraulic control and performance calibration of the model is excellent, as this test stand has been used extensively for turbine design research and acceptance tests for many years. The McNary 12-in diameter Kaplan model runner (Fig. 2), intake, scroll case, wicket gates and draft tube were used for the tests.

A 4-in diameter pipe 42 in. long, with a flap valve at the lower end and a screw cap and air line fitting at the upper end, served as a fish lock to move fish into the model. A 4-in pipe, extending downward from the lock, led the fish to a release point approximately midway in the vertical opening of the center intake opening. Nylon bobbinet material was used to construct a net to capture the fish after they passed through the turbine (Fig. 3).

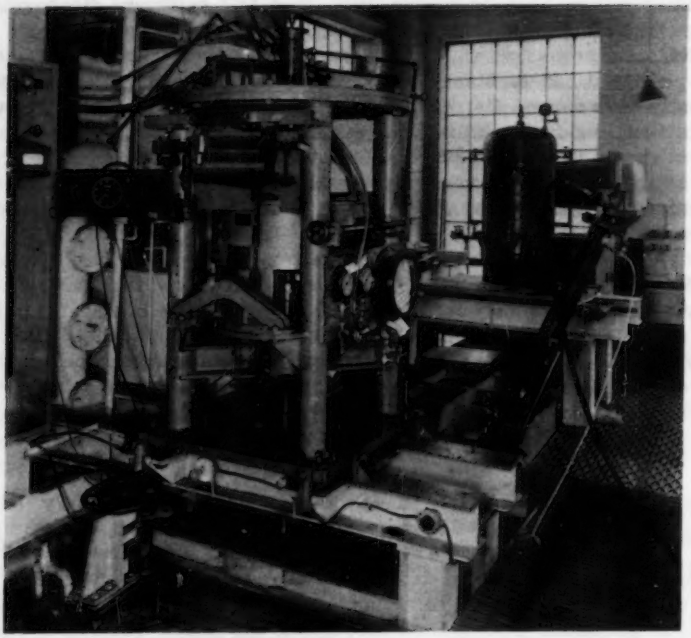

FIG. 1

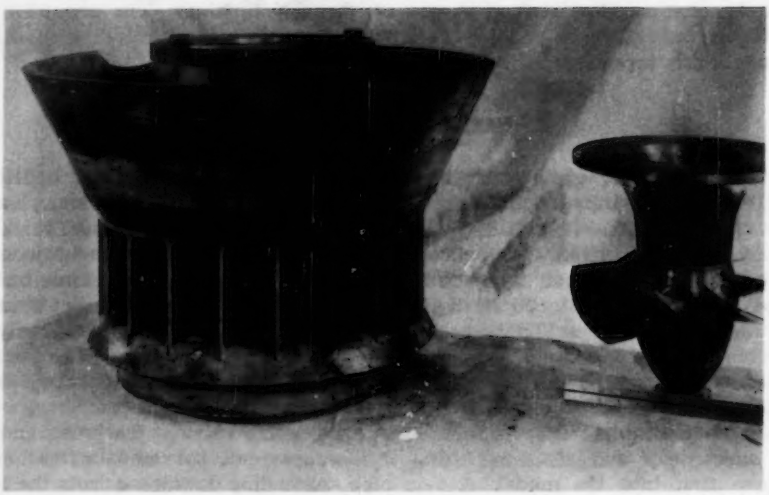

FIG. 2

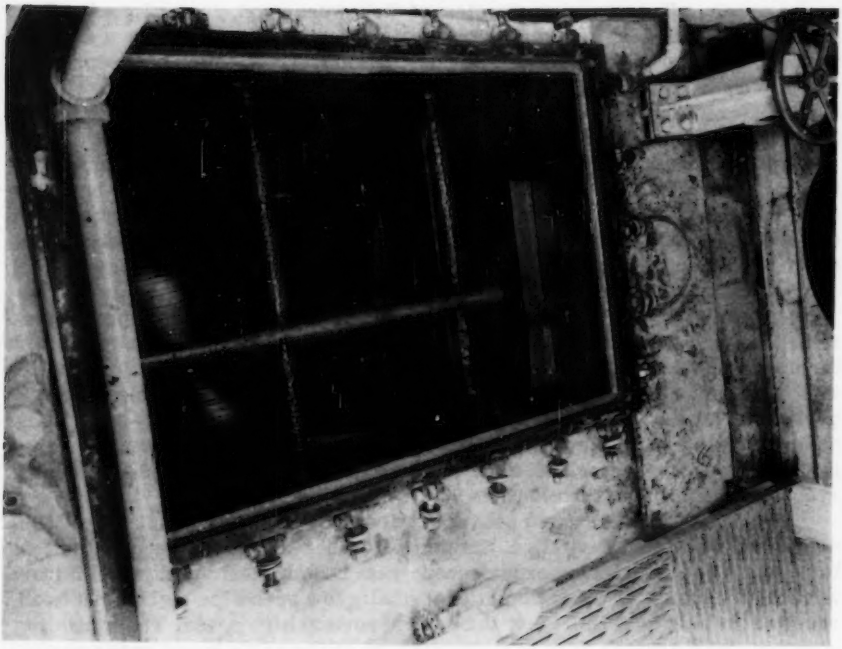

FIG. 3

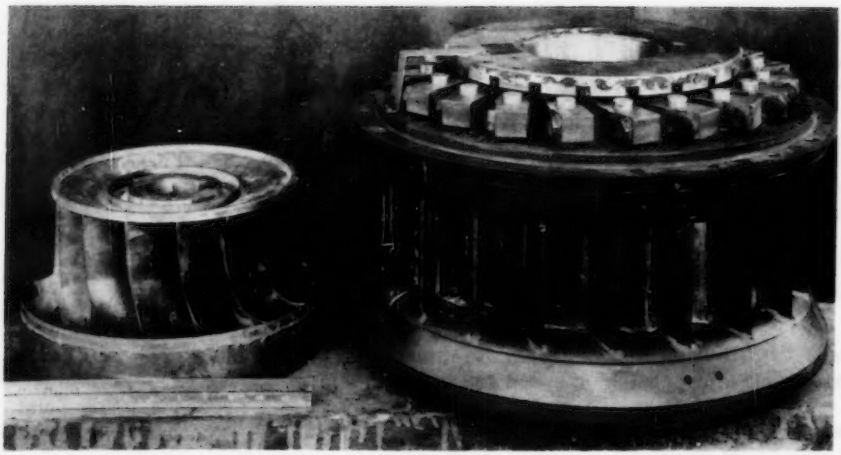

FIG. 4

In nearly all tests, two species of fish were used, generally a hundred fish of each species. A similar group of each species, utilized as a control, was subjected to the same water, transportation, and handling conditions, but did not pass through the turbines. Primary species used were largemouth bass (Micropterus salmoides) and fathead minnows (Pimephalus notetus), both ranging from 1.5 in to 2.4 in. long.

Fish and various services were obtained from the Pennsylvania Fish Commission. The fish were held at the Commission's Pleasant Gap hatchery and delivered each testing day to the hydraulic laboratory at York, Pa. At the finish of each day's testing, both test and control fish were returned to the hatchery and placed in hatching troughs for holding and recording of delayed reactions. A pathologist of the Pennsylvania Fish Commission examined test fish at the hydraulic laboratory to record types of injuries sustained by the test fish under different test conditions. Injuries detected in turbine-passed test fish seemed to fall into two categories: strictly mechanical injuries caused by turbine blades, and internal injuries caused by rapid pressure changes. Mechanical injuries ranged from a slight nick some place on the body, to complete decapitation or severance of body. Pressure-caused injuries were characterized most often by internal hemorrhages, protruding eyeballs, and deflated air bladders.

In general, with the runner setting at tailwater level and normal operational conditions free from cavitation, the mortality increased in direct relationship to speed. The mortality experienced was largely due to physical injury. Artificial braking, or operation at abnormally low speed for a given net head, resulted in less total mortality than at the normal high speed. The mortality, however, was greater than that experienced at the same speed under normal design conditions. Similar tests at the same net heads and speeds, but with the turbine runner set at a high level in reference to tailwater, resulted in high mortality. The high negative draft tube pressures and associated extreme cavitation conditions caused extensive pressure injuries fatal to nearly all survivors of mechanical injury. A summary of the test results is given in Table 1(a) and shown graphically in Fig. 5. In September 1959 the Martin power plant Francis-type runner (Fig. 4) was substituted for the McNary runner. No significant differences in pressure or death due to mechanical injury were experienced at normal speed. However, abnormal low speeds resulted in a greater increase in mortality than was experienced with the Kaplan runner. Apparently, the Kaplan blades simulated conditions in closer proximity to normal speed than could be simulated with the Francis-type runner. A summary of the test results using the Francis runner is given in Table 1(b) and shown graphically on Fig. 6.

The tests were highly successful in demonstrating that the research on fingerling mortality in passing through turbines is practicable. In addition, the tests appeared quite conclusive in respect to the following:

1. With a small model turbine, 12 in. in diameter, having blade clearances less than the length of test fish specimens, wide variations in survival could be achieved, depending on speed and tailwater elevation.
2. Mechanical injury could be distinguished from pressure injury, and was apparently directly proportional to speed, that is, exposure to physical contact with blades.
3. Sufficient survival from mechanical injury was achieved to allow analysis of pressure injury.

TABLE 1.—TURBINE MODEL TESTS

Experiment No. (1)	Headwater Elevations (2)	Tailwater Elevation ± Centerline Of Runner (3)	Net Head In Ft (4)	Speed[c] In Revolutions per Minute (5)	Percent Total Survival (Test Fish) (6)
		(a) Kaplan Runner[a]			
A1(K) 12 OCT 59	+ 6.10	+ 0.80	+ 5.30	500(n)	76
C1(K) 13 OCT 59	+ 6.10	+ 0.75	+ 5.35	500(n)	85
D2(K) 25 JUN 59	+ 5.60	+ 0.60	+ 5.00	500(n)	78
D3(K) 14 OCT 59	+ 6.40	+ 0.95	+ 5.45	500(n)	76
A2(K) 12 OCT 59	+ 6.10	+ 0.80	+ 5.30	95(r)	96
B3(K) 13 OCT 59	+44.30	- 0.30	+44.60	1400(n)	49
C3(K) 14 OCT 59	+44.60	+ 0.30	+44.30	1400(n)	28
C1(K) 23 JUN 59	+46.20	+ 0.70	+45.50	1400(n)	21
B2(K) 13 OCT 59	+44.00	- 0.50	+44.50	500(r)	59
D1(K) 14 OCT 59	+45.55	- 0.10	+44.65	500(r)	47
B1(K) 12 OCT 59	+10.80	-22.80	+33.60	1400(n)	17
C2(K) 13 OCT 59	+11.30	-21.70	+33.00	1400(n)	11
D1(K) 25 JUN 59	+ 9.09	-23.88	+32.97	1400(n)	19
D2(K) 14 OCT 59	+30.50	+ 0.50	+30.00	1200(n)	38
E1(K) 15 OCT 59	+30.00	-27.20	+57.20	500(r)	1
E2(K) 15 OCT 59	+23.00	-22.40	+45.40	500(r)	10
E3(K) 15 OCT 49	+11.30	-22.50	+33.80	1400(n)	4
E4(K) 15 OCT 59	- 1.90	-17.50	+15.60	1300(n)	7
		(b) Francis Runner[b]			
A1(F) 20 OCT 59	+ 5.80	+ 0.80	5.00	313(n)	88
C2(F) 21 OCT 59	+ 5.41	+ 0.16	5.25	313(n)	95
A2(F) 20 OCT 59	+44.60	+ 0.20	44.80	939(n)	46
C3(F) 21 OCT 59	+45.10	+ 0.10	45.00	939(n)	49
A3(F) 20 OCT 59	+11.81	-26.00	37.81	939(n)	6
B3(F) 21 OCT 59	+14.40	-26.00	40.40	939(n)	2
B1(F) 20 OCT 59	+44.85	+ 0.20	44.65	322(r)	21
D1(F) 21 OCT 59	+45.40	+ 0.10	45.30	322(r)	30
D2(F) 21 OCT 59	+46.20	+ 0.00	46.20	322(r)	23
B2(F) 20 OCT 59	+14.00	-26.20	40.60	315(r)	6
C1(F) 21 OCT 59	+18.95	-26.90	45.25	313(r)	1
F1(F) 22 OCT 59	+31.45	+ 1.00	30.45	768(n)	69
F2(F) 22 OCT 59	+ 3.50	-26.70	30.20	768(n)	23
E3(F) 22 OCT 59	+ 6.00	+ 0.80	5.20	313(n)	95
E1(F) 22 OCT 59	+44.60	+ 0.25	44.35	939(n)	49
D3(F) 22 OCT 59	+12.60	-26.45	39.05	939(n)	13
E2(F) 22 OCT 59	+15.95	-26.70	42.65	313(r)	15

[a] (McNary Model. 12 in. Diameter. 6 Adjustable Blades. Size Relationship of Model to Prototype = 1 to 24)

[b] (Martin Dam Model. 12 in. Diameter. 15 fixed Blades. Size Relationship of Model to Prototype = 1 to 15)

[c] n - normal speed
r - reduced speed

4. Extremely high mortality prevailed where adverse hydraulic conditions resulted in cavitation.

The marked increase in mortality associated with increases in negative pressures at low heads, together with lack of any evidence that the positive head was influential in mortality, encouraged extending the research to a high-head prototype installation.

HIGH-HEAD TURBINE TEST

The Fishery agency members of the Corps of Engineers' Fisheries Engineering Research Technical Advisory Committee expressed an interest in the results of the model tests and gave support to continued study, which

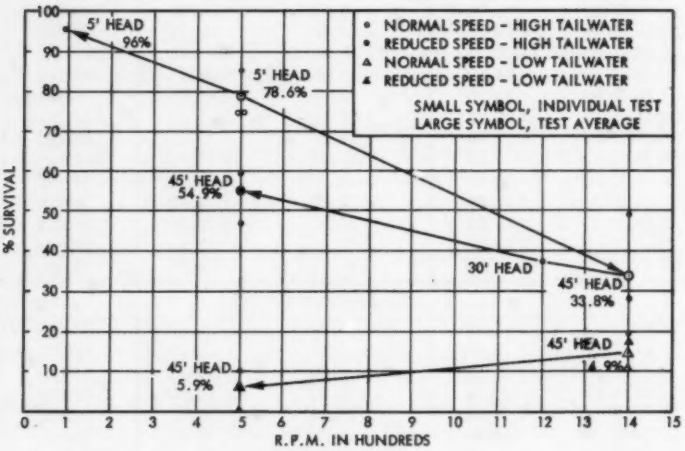

FIG. 5.—KAPLAN RUNNER

led to prototype experiments at a high head power plant. After a comprehensive study of power installations in the Pacific northwest, it was decided that the city of Tacoma's (Washington) Cushman No. 2 hydroelectric plant was the most suitable project at which to investigate the effects of tailwater, partial loadings, and the possibility of successful passage of fingerlings through high-head turbines. Following this investigation a project under the Corps of Engineers, North Pacific Division, Fisheries Engineering Research Program was established and conducted by the Walla Walla District. Fig. 7 is a view of the Cushman penstock, looking down toward the power plant from a point just below the surge tanks.

The Cushman Project has a hydraulic head of approximately 460 ft. Efficiency of the units is within the range of normal practice and cavitation characteristics are considered normal or possibly subnormal. The turbine runner diameter is 76 in, developing 37,500 hp at 300 rpm with a 440-ft head.

The runner has fifteen blades. The blade clearance varies from approximately 15 in. at the inlet side to 3 in. to 3 1/2 in. at the inner discharge side. The draft tube is vertical, discharges into a rectangular chamber, and is provided with a discharge hydraucone. The turbine used in the tests is served by a 10.5-ft diameter penstock at a net hydraulic head of approximately 450 ft. The turbine discharge is approximately 800 cfs at design head and rated output.

A series of marks (tattoos) for the fish used in the tests were set up to provide a certain mark for each of the twelve combinations of tailwater elevation and wicket gate opening so that, regardless of when a fish was captured, the conditions under which it passed through the turbine would be known.

Fingerling test fish were inserted in a penstock at El.-402 msl under approximately 70 ft of static head through a pressure lock (Figs. 8 and 9). The test specimens were collected by a large net at the draft tube exit, which

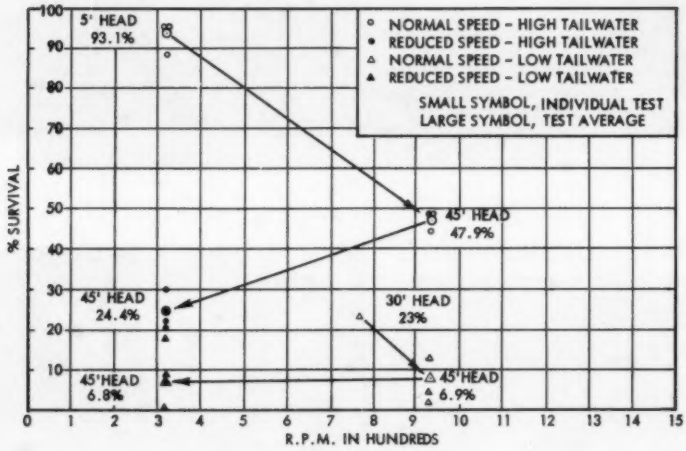

FIG. 6.—FRANCIS RUNNER

screened the entire discharge exclusive of minor leakage around the net anchorage frame (Fig. 10). The average recovery of all test specimens placed in the penstocks was 90%. The average recovery of all control fish released at the center of the net entrance was 82%. Pertinent power plant data are given in Table 2, and test results are summarized in Table 3. Although test procedures preclude refined evaluation, variations in results of duplicate tests appear to be relatively small. Where variations of individual test results appear significant, it is attributed to the fact that catches from one test sometimes overlapped those of similarly marked fish from an identical test. The fish were furnished, marked, handled and examined by personnel of the Washington Department of Fisheries and the U.S. Fish and Wildlife Service.

Under the more favorable tailwater and hydraulic conditions of normal turbine operation at best efficiency, and average survival of more than 75% was experienced, as adjusted by mortalities experienced with control fish.

FIG. 7

FIG. 8

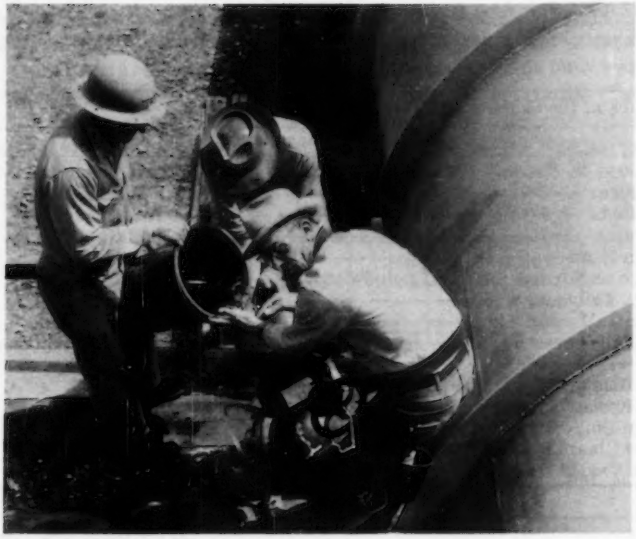

FIG. 9

FIG. 10

TABLE 2.—PHYSICAL PLANT DATA CUSHMAN NO. 2 HYDROELECTRIC PLANT UNIT NO. 33

Plant Location	
North Fork of the Skokomish River near Potlatch, Wash.	
Turbine:	
Type	Francis
Manufacturer	Allis-Chalmers
Normal Head	450 ft
Rated Output	37,500 hp
Maximum Head	485 ft
Discharge at Normal Head and Rated Output	800 cfs
Maximum Tailwater Elev.	+12.00 msl
Minimum Tailwater Elev.	0.0 msl
Draft Tube	Vertical with Hydraucone
Speed	300 rpm
Turbine Runner Inlet Diameter	83 in.
Turbine Runner Discharge Diameter	76 in.
Maximum Guide Vane Opening	5 1/4 in.
Minimum Clearance Between Runner Vanes Varied from	3 in. - 3 1/2 in.
Penstock	
Diameter	Varies from 10'6" to 8'0"
Length - Total	1,310 ft
Length - Lock to Scroll	1,260 ft

TABLE 3.—TEST FISH SURVIVALS CUSHMAN NO. 2 HYDROELECTRIC PLANT UNIT NO. 33[a]

Gate Opening (1)	High Tailwater (2)	Medium Tailwater (3)	Low Tailwater (4)
40%	59.0%	44.6%	52.2%
65%	77.3%	70.9%	65.5%
80%	75.0%	73.7%	55.1%
100%	73.5%	69.1%	63.8%

[a] Average of all tests.

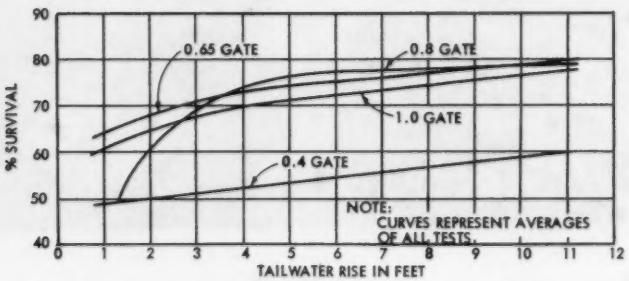

FIG. 11.—1960 CUSHMAN NO. 2 TESTS, UNIT NO. 33

Under the most adverse conditions of partial turbine loading and low tailwater, the survival was reduced to approximately 45%. Figs. 11, 12, and 13 show relationship of survival to turbine characteristics and tailwater elevations. The only apparent significant variables in test conditions were turbine output and elevation of tailwater. The tailwater designations (Table 3) are averages of generalized categories associated with high, low, and medium tides. Tailwater elevations were further influenced by the discharge of other units; consequently, detailed correlation of survival to each of the variables

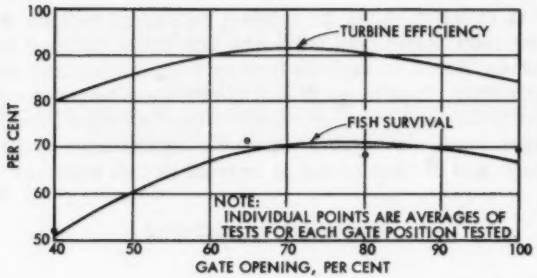

FIG. 12.—1960 CUSHMAN NO. 2 TESTS, UNIT NO. 33

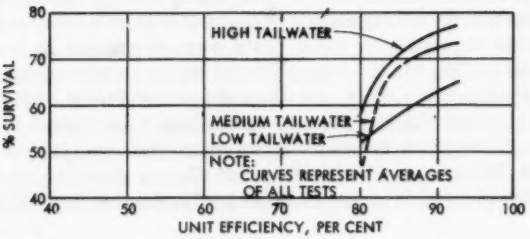

FIG. 13.—1960 CUSHMAN NO. 2 TESTS, UNIT NO. 33

cannot be made. Variations in survival of 10% or more were experienced with each of the variables individually.

SUMMARY

The exploratory tests on survival rates of fish passing through model and prototype turbines have definitely demonstrated that turbine performance characteristics are important, and possibly have a greater influence on survival than all other factors. In all test programs, high mortalities have been observed in passing of fish through turbines operating at low efficiencies and through cavitating conditions. Since the extent of cavitation zones in the water passages can be highly influenced by design and operational considerations, the prospects of improving survival are promising.

The exploratory research to date (1961) has indicated definite avenues of future study, and also gives much promise that passage through turbines may be made relatively safe. The investigations in the future should be aimed at three problem areas:

1. Structural design of turbines to reduce mechanical injury.
2. Physical setting of the runner in relationship to tailwater conditions to reduce negative pressures.
3. Scheduling of turbine operation to obtain optimum hydraulic conditions throughout the water passages.

Walla Walla District plans to conduct additional turbine model tests with fish in October 1960. Additional tests are also being planned for the spring of 1961 at Cushman No. 2 to explore further both mechanical and pressure injuries and, possibly, to achieve direct correlation between model and prototype results as related to both pressure and mechanical injuries. The primary purpose of these tests will be to evaluate the significance of fish size, turbine blade clearance, and turbine speed as related to fish survival.

ACKNOWLEDGMENTS

The following organizations and personnel have made major contributions in cooperative efforts toward formulating and carrying out the test program. Excellent cooperation was given by all individuals and organizations.

For the studies utilizing model turbines, Allis-Chalmers Manufacturing Company made available their Hydraulic Laboratory at York, Pa., and worked closely with the Corps of Engineers both during the planning and test periods. Fish and various services for these tests were furnished by the Pennsylvania Fish Commission. For the studies utilizing the prototype installation at Cushman No. 2 hydroelectric plant, the Department of Public Utilities of Tacoma made this plant available for the experiments and furnished a variety of services. Fish and services were obtained from the Washington Department of Fisheries and Washington Department of Game. Service of pathologists to examine fish for type of injuries was obtained from the U. S. Fish and Wildlife Service.

Appreciation is expressed to Edwin C. Franzen, F. ASCE, Chief, Engineering Division; Berton M. MacLean, Chief, Fish and Wildlife Section; and Frederick K. Cramer, Fisheries Research Biologist; all of the Walla Walla District Corps of Engineers, who made major contributions toward the success of the program, for their assistance and guidance.

Journal of the
HYDRAULICS DIVISION
Proceedings of the American Society of Civil Engineers

AERATED FLOW IN OPEN CHANNELS

Progress Report
Task Committee on Air Entrainment in Open Channels
Committee on Hydromechanics

FOREWORD

The purpose of the Task Force on Aerated Flow in Open Channels is to investigate the status of present (1961) knowledge of the phenomena of aerated flow in open channels and to prepare a report on the subject. The personnel of the Task Force and a brief record of its activities are presented under the heading "Acknowledgments."

The reason for the interest in the phenomena of aerated flow as a mechanical mixture is involved with the proper design of steep channels or chutes. As air is entrained in the flow, the mixture increases in volume of "bulks." The bulking of aerated flow requires higher side walls than non-aerated flow. Thus, the phenomenon has important economic aspects in the design of chute spillways for earth dams, chutes for wasteways of irrigation canals, and high overflow spillways.

The process of air entrainment in chutes is inextricably involved in the mechanism of the generation of turbulence. The actual presence of large quantities of air in the form of bubbles, no doubt, affects the decay of turbulence. The complete problem is related to the problem of suspended sediment, except that solid particles tend to settle toward the bottom where turbulence is generated and air bubbles rise to the surface.

Although much has been learned of the mechanism of the phenomenon by experimentation, a rational solution has not been accomplished, in the knowledge of Task Force members. The objective of this Report is to include empirical relationships which should be helpful to engineers in preparing an economical design of a channel to carry aerated flow. Reliable empirical

Note.—Discussion open until October 1, 1961. To extend the closing date one month, a written request must be filed with the Executive Secretary, ASCE. This paper is part of the copyrighted Journal of the Hydraulics Division, Proceedings of the American Society of Civil Engineers, Vol. 87, No. HY 3, May, 1961.

design criteria are not known to have appeared in the technical literature published in the United States.

HISTORICAL RESUME

A full account of the history of development of the knowledge of aerated flow is not within the scope of this Report, nor would it serve any useful purpose except for historians. A brief historical resume, however, is of value to afford the engineer a perspective of the problem, as well as to recognize outstanding contributions to the advance of the general information on the subject. A short list of references appears as Appendix I, followed by a more extended bibliography in Appendix II.

Three significant events have come to the attention of the Task Force members. The first important event concerns pioneer research in Germany, about 1925. The next two events involve the initiation of important research in the United States and a published symposium on entrainment of air in flowing water. The occurrence of the last two events were stimulated in no small measure by the interest of the original Committee on Hydraulic Research which preceded the organization of the Hydraulics Division of ASCE.

The Committee on Research of the Hydraulics Division inherited the functions of the old committee, upon organization of the Division. In 1957, the name of the Committee on Research was changed to the Committee on Hydromechanics and a new Committee on Research was formed. It is indeed appropriate, therefore, that the sponsoring committee of this task force should maintain a continuing interest in the difficult problem of bulking caused by aerated flow.

Instruments to measure the amount of air mixed with the water form an important aspect in the advance of the technical knowledge. R. Ehrenberger (1)[1] described a simple, yet effective, device for measuring the concentration of air entrained in the flow of chutes constructed in the laboratory at Versuchsanstalt fur Wasserbau, Vienna, Austria. His apparatus was simply a tube, pointing into the flow, and communicating through an elbow to a vertical glass tube of much larger diameter. The Pitot-like tube was rated in unaerated flow with a known velocity by measuring the time to fill a known volume of the vertical tube. The operation was repeated in aerated flow where the air bubbles rose to the surface in the vertical tube. By the increased time to fill the tube in aerated flow, Ehrenberger calculated the air concentration in the air-water mixture.

The Ehrenberger apparatus produced results which have been questioned because of the lack of similitude of flow into the Pitot-like tube in aerated and in unaerated flow. The apparatus was definitely crude compared with the modern electronic method, but ingenious, nonetheless.

Ehrenberger published empirical relationships defining air concentration as follows:

$$P_w = 0.42\ R^{-0.05}\ (\sin \alpha)^{-0.26} \quad \text{for } \sin \alpha < 0.476$$

$$P_w = 0.30\ R^{-0.05}\ (\sin \alpha)^{-0.74} \quad \text{for } 0.476 < \sin \alpha < 0.707$$

---

[1] Numerals in parentheses refer to corresponding references in Appendix I.

in which P_w is the percentage of water in the toal air-water mixture, R denotes the hydraulic radius, and α is the angle of the channel slope with the horizontal. Ehrenberger considers his formulas valid for $R < 0.30$ (0.98 ft). The width of his wood chute was 0.25 (0.82 ft). No doubt a substantial portion of the air was entrained by turbulence generated at the side walls. Therefore, the formulation of his results would not be applicable to a chute of different width.

Experimental work was initiated in the United States about 1939. During that year J. C. Stevens, F. ASCE, was chairman of the original Committee on Hydraulic Research. Upon the recommendation of ASCE, the Engineering Foundation made a small grant to Lorenz G. Straub, F. ASCE, Director, St. Anthony Falls Hydraulic Laboratory. ASCE had intended that this would be "seed" money, to stimulate other sponsorship, which indeed it proved to be. Later the funds were supplemented by support from the University of Minnesota, the United States Navy, and other sponsors.

The early adjustable metal flume at St. Anthony Falls was 1 ft wide. In an effort to achieve true two-dimensional flow, with no sidewall effect on the air entrainment, the flume was rebuilt to a width of 18 in. in 1950.

The most important advance in the science of aerated flow research at St. Anthony Falls Hydraulic Laboratory was the development of better methods of measuring the concentration of entrained air. The early method of measuring the entrained air volumetrically was to give way to an electronic method in 1950. This apparatus was described in a paper by O. P. Lamb and J. M. Killen (2). Essentially it involved a pair of electrodes set in the line of the flow direction. The electrical resistance of the laboratory water without entrained air was measured, in effect. The concentration of air in aerated flow could then be calculated by measuring the increase of resistance across the electrodes.

Two series of experiments were conducted with the wide flume and the electrical resistance apparatus. Results of a series with the smooth steel wall were in an unpublished report by Straub and A. G. Anderson (3), for the United States Navy in 1955. The results of the test series on walls roughened with granular particles were reported by Straub and Anderson (4) in 1958. Significantly, Straub was awarded a Research Prize by ASCE in 1958 for his work on aerated flow.

A Symposium on the Entrainment of Air in Flowing Water was published in the Transactions of ASCE in 1943. The paper by L. Standish Hall (5) reported on field tests of three chutes operated by the Pacific Gas and Electric Company. He also included field test data on the Kittitas chute by the Bureau of Reclamation, United States Department of the Interior (USBR). For reasons of large width and a mimimum amount of vertical and horizontal curvature, the Kittitas results proved the most desirable for later analysis.

The tests on the Kittitas chute were made by C. W. Thomas and reported to the USBR in 1938 (6). Thomas measured the water-surface profiles as well as the mean velocity by the salt-velocity method. With a known water discharge, the quantity of entrained air could be estimated.

PRESENT STATUS OF KNOWLEDGE

Narrow Chutes.—For purposes of this Report, a narrow chute is defined as one which has a width less than five times the depth. Air entrainment can

ordinarily be considered to be a relatively simple two-dimensional problem for wide chutes. Three boundaries, the bottom and two sides, contribute to the generation of turbulence which causes air entrainment in narrow chutes. It is probale that the effect from one side wall reaches nearly to the opposite wall, thus compounding the air-entrainment effect in narrow chutes. Fig. 1 demonstrates development of the side-wall effect of the Uncompaghre Chute very clearly. Much of the data reported by Hall (5) fall in the category of narrow chutes. The discussions of this paper embraced attempts to generalize the results for the calculation of air concentration and the resultant bulking of the flow.

FIG. 1.—AIR ENTRAINMENT FROM SIDE-GENERATED TURBULENCE

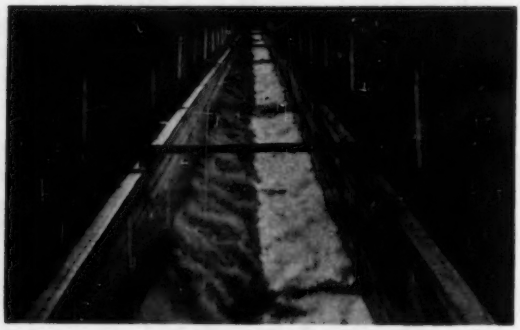

FIG. 2.—AIR ENTRAINMENT CAUSED BY SIDE-WALL EFFECT IN NARROW CHUTES

In later years, other attempts at generalization of the air-entrainment phenomena were based on the Hall paper. Although these empirical conclusions were roughly applicable to narrow chutes, they lead to over-design of spillway chute side walls when applied to wide chutes. Fig. 2 shows the side-wall effect of the USBR Kittitas Chute.

Wide Chutes.—Maintaining the definition for a narrow chute expressed previously, a wide chute is considered to be one which has a width greater than five times the depth. An example of a wide chute may be seen in Fig. 3, which shows the Ft. Peck spillway. Close scrutiny of the water surface during operation led to the conclusion that there was a negligible amount of bulking from air concentration. Such an observation was impressive when contrasted with a high air concentration indicated by previous empirical criteria based on narrow chute operation.

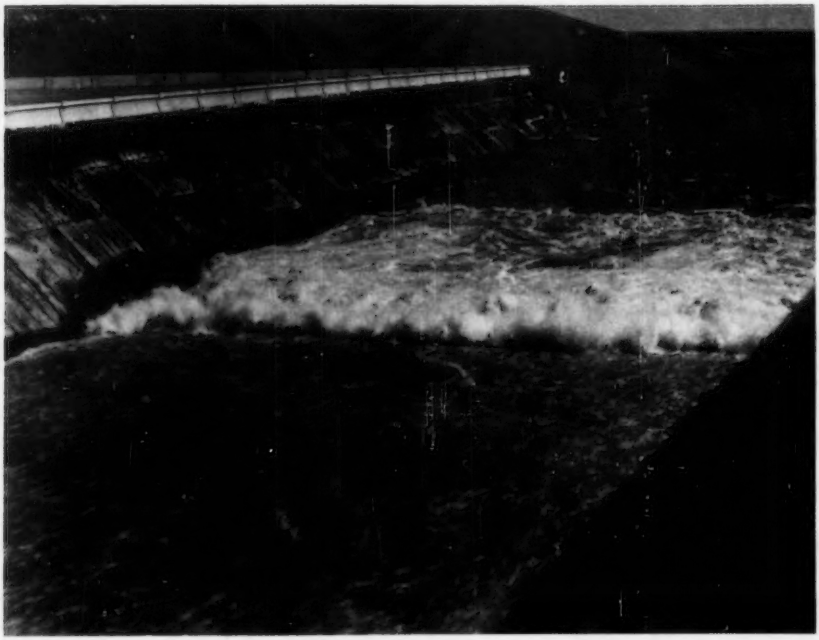

FIG. 3.—LOW AIR ENTRAINMENT FROM BOTTOM-GENERATED TURBULENCE IN A WIDE SPILLWAY CHUTE

Hydraulic design engineers have been concerned that the use of design criteria based on unselected field data for narrow chutes had influenced the tendency toward costly over-design of side walls. In recent years, engineers of the United States Army Waterways Experiment Station, Vicksburg, Miss., (WES), analyzed the smooth-channel data obtained at St. Anthony Falls (3) in combination with selected Kittitas field observations. The Kittitas data were selected on the basis of the observations with depths less than one-fifth of the width.

Straub and Anderson had found the air concentration, c, in two-dimensional smooth channel to be a function of $S/q^{2/3}$, in which S is the sine of the slope and q is the unit discharge.

The WES issued a hydraulic design criteria chart in June, 1957, based on the foregoing analysis of the Straub and Anderson smooth-channel results. The curve of best fit was

$$\bar{c} = 0.38 \log_{10}\left(\frac{S}{q}\right)^{2/3} + 0.77 \quad \ldots\ldots\ldots\ldots\ldots \quad (1)$$

This chart presented a much more economical basis for the design of wide chute spillway walls than did previous criteria from unselected narrow chute results.

As mentioned previously, Straub and Anderson (4), presented the results of tests on rough channels in December, 1958. They concluded that for an artificially roughened channel, air concentration was a function of $S/q^{1/5}$. This function of slope and unit discharge was based on an empirical relationship between $\bar{c}$ and V^*/d_t in which V^* is the shear velocity and d_t is a so-called transition depth as defined therein. The new Straub and Anderson data on rough channels were also analyzed in comparison with selected Kittitas field results. The large unit discharge of the prototype chute at Kittitas produced small values of $S/q^{1/5}$, and consequently small concentrations of air. The curve of best fit for the combined laboratory and field data was determined by use of a digital computer and is shown in Fig. 4. The standard error for air concentration was $\sigma_c = 0.061$. The Task Force believes that this relationship offers a realistic basis for the design of wide chute spillways within the limitations of the present status of knowledge.

Overflow Spillways.—The relationship represented by the curve in Fig. 4 is believed applicable to wide ungated overflow spillways, although no prototype observations are yet available for verification. A laboratory study by W. J. Bauer (7) made at the State University of Iowa, Ames, Iowa, covered an investigation of the development of the turbulent boundary layer on an overflow spillway. His observations were not carried beyond the point on the profile where the turbulent boundary layer reached the surface. It is at this part where the phenomenon of air entrainment begins.

The Task Force is not aware of any research which deals with the effect of spillway crest piers on air entrainment. Examination of the operation of overflow spillways in the field indicate that the turbulence generated at the pier noses can cause substantial air entrainment. Indeed, it is believed that for modern spillways with a large design head compared with the width of the gate bay, the pier disturbance has a greater effect on air entrainment and its resultant bulking, than does the bottom turbulence alone. The effect of piers on air entrainment at the Chief Joseph Dam on the Columbia River may be seen in Fig. 5.

NEED FOR FUTURE RESEARCH

This Report has presented an empirical criterion as a guide to the judgment of the engineers in the design of wide steep channels. Nevertheless, much remains to be learned of the basic mechanics of the generation of turbulence, its energy as the water surface is approached, and of the actual phenomenon of air entrainment.

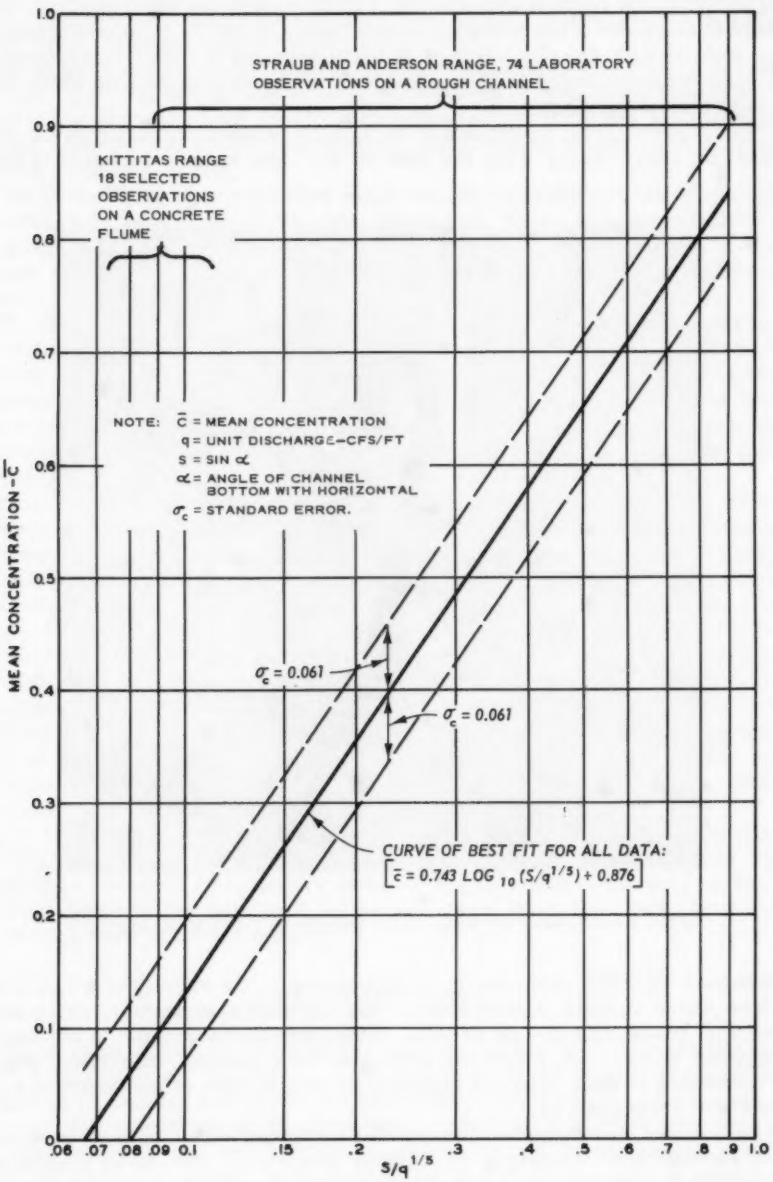

FIG. 4.—AIR ENTRAINMENT BASED ON TESTS OF A ROUGH LABORATORY CHANNEL AND FIELD TESTS

Theory.—The problem is related to the more fundamental one of the generation of turbulence at the boundary, its diffusion upward through the liquid, and the action of the vertical components of turbulence at the water surface. More needs to be known of the reflection or dissipation of the vertical components at the surface with various degrees of turbulence and the actual piercing of the surface by turbulence cells. It is undoubtedly the latter phenomenon which gives rise to air entrainment.

The present (1961) knowledge of turbulence is based primarily on the great mass of observations with the flow of air. The work in aeronautics is not

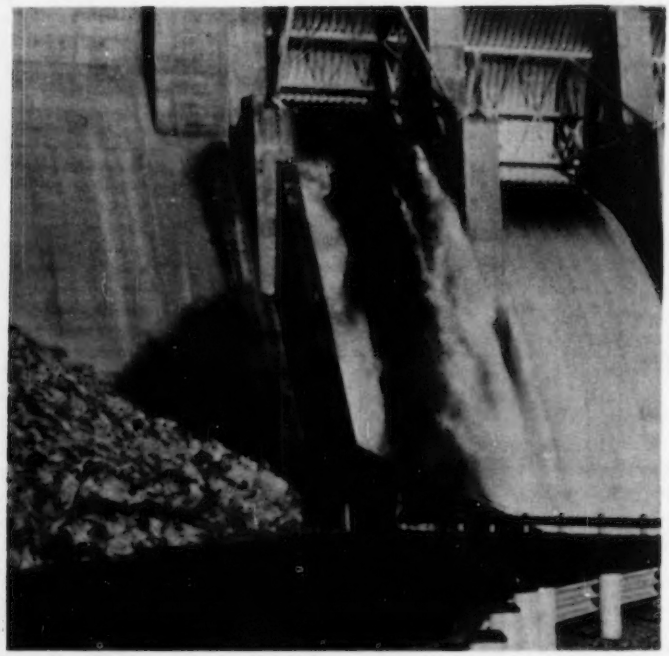

FIG. 5.—EFFECT OF SPILLWAY PIERS ON AIR ENTRAINMENT

concerned with the phenomenon of turbulence in the vicinity of a liquid with a free water surface. Unfortunately, the hot wire anemometer, which is the principal measuring device in wind tunnel turbulence studies, is not readily adaptable to use with air-water mixtures. Nevertheless, theoretical studies of turbulence in open channels should start with a study of the theory and test results of aerodynamics.

Laboratory Equipment.—Although the combined effect of both side walls and bottom are important in certain structures, the more simple two-dimensional problem of a wide channel should be approached first. A disadvantage of studying wide channels with steep slopes is that large discharges are needed to obtain substantial depth. The fundamental problem of turbulence

in open channels can be studied with fairly light slopes. Practically uniform flow can be obtained with a reasonable channel length, if the bottom is artificially roughened. A fairly wide channel with a rough bottom and smooth side walls would then have very little side-wall effect.

More laboratory work is needed to perfect instruments which will measure, at least, the longitudinal and vertical components of turbulence velocities in water. The Hubbard-Ling hot-film anemometer (8)(9) is one approach and several laboratories have experimented with pressure transducers mounted on stream-lined supports.

The three-dimensional problem could well be investigated by first studying the side-wall effect, alone. A wide laboratory flume is again indicated to minimize reflection from the opposite wall. The experimenter would probably choose to roughen only one wall and maintain the bottom and opposite wall smooth.

The behavior of the turbulence from discrete wall protuberances, whether knobs or vertical strips, as the disturbance reaches the surface needs to be studied. Little is known of the effect of joint offsets in channel walls. The effect of piers on overflow spillways belongs to this class of problems. The Task Force believes that the fundamental research could best be performed in the laboratory, where the geometrical variables may be changed with little expense.

Field Tests.—More observations on existing prototype structures should be made and publicized, if only to alert the profession to the important design problems involved. The problem of holding measuring instruments in high velocity flows of the prototype is severe in itself. Provisions for measurement of such a rudimentary variable as velocity are badly needed in the prototype. Velocity observations would yield information for friction-loss studies as well as for basic information on high velocity turbulent flow. The provision for high-velocity measurement must normally be done during construction, by embedded metal which can hold a support at the bottom or a span for attaching the support from above. Embedded metal has been installed for the attachment of instrument piers to the bottom of the Ft. Randall chute spillway. Observations at this installation must await the availability of test flows, which is a common problem with all field tests.

Air entrainment caused by the disturbances of crest piers on overflow spillways may be a critical condition for the design of side walls of this type of spillway. General field observations of the pier effect may well serve as a useful guide in the design of future spillways, until more basic work can be accomplished in the laboratory.

ACKNOWLEDGMENTS

The interest of the Committee on Hydromechanics (the Hydraulics Division's "old" Committee on Research), subsequent to World War II, began at the Minnesota International Hydraulics Convention at Minneapolis on September 3, 1953. At that convention, J. M. Robertson, a committee member, presided at an open meeting on the subject of "Research Needs on Aerated Flow."

At the following meeting of the Committee in 1954, a proposal to establish a Task Force on Aerated Flow in Open Channels was discussed. However, it was not until October 27, 1955, that the Task Force was officially established.

The original task force membership was:

W. J. Bauer
D. Colgate
J. P. Lawrence
W. W. DeLapp, Chairman
F. B. Campbell, Contact Member from Committee on Research.

J. P. Lawrence subsequently resigned from the task force and was replaced by A. G. Anderson.

The task force arranged a technical session for the Jackson, Miss., ASCE Convention on February 18, 1957. W. W. DeLapp presented a progress report on the activities of the Task Force and F. B. Campbell made some formal remarks on the design problems involving air entrainment. The following papers were presented:

"Experiments on Self-Aerated Flow in Open Channels," by L. G. Straub and A. G. Anderson.

"Entrainment of Air by Flowing Water in Circular Conduits with a Downgrade Slope," by J. C. Kent.

The paper by Straub and Anderson was subsequently published in the Journal of the Hydraulics Division, Vol. 84, No. HY7, December, 1958, Paper 1890.

The Task Force met at Minneapolis on May 28, 1957. The members enjoyed the privilege of counsel with L. G. Straub, Director, St. Anthony Falls Hydraulic Laboratory, during the meeting. A bibliography was prepared soon thereafter.

On account of the urgency of other professional business, W. W. DeLapp and W. J. Bauer each requested to be relieved of their duties on the Task Force.

The sponsoring Committee on Hydromechanics met at Iowa City, Iowa, on June 14, 1958. The committee invited retiring member F. B. Campbell to assume chairmanship of the Task Force on Aerated Flow in Open Channels. The reconstituted Task Force met in Kansas City, Mo., on April 25, 1959, and agreed on an outline for the foregoing report.

Respectfully submitted,

W. Douglas Baines
Frederick R. Brown
Emmett M. Laursen
E. Roy Tinney
Norman H. Brooks, Chairman,
Committee on Hydromechanics

A. G. Anderson
D. Colgate
F. B. Campbell, Chairman, Task
Force on Air Entrainment in
Open Channels

APPENDIX I.—LIST OF REFERENCES

1. "Wasserbewegung in steilen Rinnen mit besonder Berucksichtigung der Selbstbeluftung" ("Flow in Steep Chutes, with Special Reference to Self-Aeration"), by R. Ehrenberger, Oesterreichischer Ingenieur-und Architektverein No. 15/16 and 17/18, 1926. Translated by E. F. Wilsey, U.S. Bur. of Reclamation.
2. "An Electrical Method for Measuring Air Concentration in Flowing Air-Water Mixtures," by O. P. Lamb and J. M. Killen, St. Anthony Falls Hydr. Lab., Tech. Paper No. 2, Series B, 1950.
3. "The Distribution of Air in Self-Aerated Flow in Smooth Open Channels," by L. G. Straub and A. G. Anderson, St. Anthony Falls Hydr. Lab. Project Report No. 48, July, 1955.
4. "Experiments on Self-Aerated Flow in Open Channels," by L. G. Straub and A. G. Anderson, Proceedings, ASCE, Vol. 84, No. HY7, December, 1958.
5. "Entrainment of Air in Flowing Water (Symposium): open Channel Flow at High Velocities," by L. S. Hall, Transactions, ASCE, Vol. 108, 1943, p. 1394.
6. "Progress Report on Studies of the Flow of Water in Open Channels with High Gradients," by C. W. Thomas, U. S. Bur. of Reclamation, Hydr. Lab. Report HYD 35, July 27, 1938.
7. "Turbulent Boundary Layer on Steep Slopes," by W. J. Bauer, Transactions, ASCE, Vol. 119, 1954, p. 1212.
8. "Constant-Temperature Hot-Wire Anemometer with Application to Measurements in Water," by P. G. Hubbard, Doctoral Dissertation, State Univ. of Iowa, Iowa City, Iowa, 1954.
9. "Measurement of Flow Characteristics by the Hot-Film Technique," by S. C. Ling, Doctoral Dissertation, State Univ. of Iowa, Iowa City, Iowa, 1955.

APPENDIX II.—BIBLIOGRAPHY ON AERATED FLOW IN OPEN CHANNELS[a]

201. "The High Velocity Flow of Water in a Small Rectangular Channel," by W. W. DeLapp, Ph.D. Dissertation, Univ. of Minnesota, Minneapolis, 1947.

[a] Filed in Engineering Societies Library, New York, October, 1959.

202. "The Flow of Water in Channels Under Steep Gradients," by W. F. Durand, Transactions, Amer. Soc. of Mech. Engrs., January, 1940, pp. 9-14.

203. "Wasserbewegung in steilen Rinnen (Schusstennen) mit besonder Berucksichtigung der Selbsteluftung" ("Flow in Steep Chutes, with Special Reference to Self-Aeration"), by R. Ehrenberger, Osterreichischer Ingenieur-und Architektverein, No. 15/16 and 17/18, 1926. Translated by E. F. Wilsey, U. S. Bur. of Reclamation.

204. "Open Channel Flow of Water-Air Mixtures," by H. A. Einstein, Transactions, AGU, Vol. 35, No. 2, April, 1954, pp. 235-242.

205. "Head Loss and Air Entrainment by Flowing Water in Steep Chutes," by Ante Frankovic, Proceedings, Internatl. Hydr. Convention, St. Anthony Falls Hydr. Lab., Minneapolis, Minn., 1953, pp. 467-476.

206. "An Experimental Study of Bubbles Moving in Liquids," by W. L. Haberman and R. K. Morton, Proceedings, ASCE, Vol. 80, Proceedings-Separate No. 387, January, 1954.

207. "The Measurement of Concentrations and of Velocities in a Current of Air and Water Mixed," by G. Halbronn, La Houille Blanche, May-June, 1951, pp. 394-405.

208. "Air Entrainment in Steeply Sloping Flumes," by G. Halbronn, R. Durand, de Lara, and G. Cohen, Proceedings, Internatl. Hydr. Convention, St. Anthony Falls Hydr. Lab., Minneapolis, Minn., 1953, pp. 455-466.

209. "Entrainment of Air in Flowing Water (Symposium): Open Channel Flow at High Velocities," by L. S. Hall, Transactions, ASCE, Vol. 108, 1943, p. 1394.

210. "The Influence of Air Entrainment on Flow in Steep Chutes," by L. S. Hall, Univ. of Iowa Studies in Engrg., Bulletin 31, Iowa City, 1946, pp. 298-314.

211. "Air Entrainment on Spillway Faces," by G. H. Hickox, Civil Engineering, Vol. 15, No. 12, December, 1945, p. 562.

212. "Entrainment of Air in Flowing Water and Technical Problems Connected with It," by V. Jevdjevich and L. Levin, Proceedings, Interntl. Hydr. Convention, St. Anthony Falls Hydr. Lab., Minneapolis, Minn., 1953, pp. 439-454.

213. "An Electrical Method for Measuring Air Concentration in Flowing Air-Water Mixtures," by Owen P. Lamb and John M. Killen, SAF Tech. Paper No. 2, Series B, 1950.

214. "An Electronic Equipment for Measurement of Air Entrained in Flowing Water," by Owen P. Lamb and John M. Killen, Annual Report (Tech.), Research Publication No. 18, Central Water and Power Research Sta., Poona, 1952, pp. 75-76.

215. "An Experimental Channel for the Study of Air Entrainment in High-Velocity Flow," by Owen P. Lamb, SAF Project Report No. 34, November, 1952.

216. "Recent Studies on Flow Conditions in Steep Chutes," by E. A. Lane, Engineering News-Record, January 2, 1936, p. 5.

217. "Entrainment of Air in Swiftly Flowing Water, Observations of the Flow Over Spillways Yield Conclusions of Interest to Hydraulic Engineers," by E. A. Lane, Civil Engineering, February, 1939.

218. "Notes on the Flow Mechanics of Water-Air Mixtures," by Leon Levin, La Houille Blanche, Vol. 10, No. 4, August-September, 1955, pp. 555-557; Applied Mechanics Reviews, April, 1956, p. 160.

219. "Some Prototype Observations of Air-Entrained Flow," by V. Michels and M. Lovely, Proceedings, Internatl. Hydr. Convention, St. Anthony Falls Hydr. Lab., Minneapolis, Minn., 1953, pp. 403-414.

220. "Field Tests on High Velocity Flow and its Air Content," by A. Okada and K. Fukuhara, Tech. Research Inst. of Electric Power Industry, Japan. Presented at Eighth Congress, Internatl. Assoc. for Hydr. Research, Montreal, Canada, August, 1959.

221. "Flow of Water Mixed with Air in Channels and on Spillways," by Dorin Pavel, Hydr. Proceedings, No. 2, Budapest, Hungary, 1951, pp. 168-171.

222. "Air Entrainment in Chute Spillways," by M. S. Priest, Tech. Annual Report, Govt. of India, Central Water and Power Research Sta., Poona, Research Publication No. 19, 1943, pp. 114-122.

223. "Air Entrainment by Water in Steep Open Channels," by M. S. Priest, Tech. Paper No. 3, Engrg. Inst. of Canada, 1951.

224. "The Distribution of Air in Self-Aerated Flow in a Smooth Open Channel," by L. G. Straub and A. G. Anderson, SAF Project Report No. 48, July, 1955.

225. "Experiments on Selff-Aerated Flow in Open Channels," by L. G. Straub and A. G. Anderson, Proceedings, ASCE, Vol. 84, No. HY7, December, 1958.

226. "Velocity Measurements of Air-Water Mixtures," by L. G. Straub, J. M. Killen, and Owen P. Lamb, Transactions, ASCE, Vol. 119, 1954, p. 207.

227. "Experimental Studies of Air Entrainment in Open Channel Flow," by L. G. Straub and Owen P. Lamb, Proceedings, Internatl. Hydr. Convention, St. Anthony Falls Hydr. Lab., Minneapolis, Minn., 1953, pp. 425-438.

228. "Progress Report on Studies of the Flow of Water in Open Channels with High Gradients," by C. W. Thomas, USBR Hydr. Lab. Report HYD 35, July 27, 1938.

229. "Ricerca Sperimentale Sulle Correnti Rapide," by Michele Viparelli, Univ. of Naples, Instituto di Idraulica e Construzioni Idrauliche, Tech. Paper No. 64, 1951.

230. "The Flow in a Flume with 1:1 Slope," by Michele Viparelli, Proceedings, Internatl. Hydr. Convention, St. Anthony Falls Hydr. Lab., Minneapolis, Minn., 1953, pp. 415-424.

231. "Study of Air Entrainment in Chute Spillways," by Michele Viparelli, Annual Report (Tech.), Research Publication No. 18, Central Water and Power Research Sta., Poona, India, 1952, pp. 71-74 (30° slope). (1954 Report, No. 20, pp. 284-293 for 45° slope.)

232. "Fast Water Flow in Steep Channels" ("Ecoulement d'eau rapide dans les canaux a forte pente"), by Michele Viparelli, AIRH Ville Congress, Lisbon, Portugal, Section D, 1957, La Houille Blanche, January-February, 1958, p. 95.

233. "Correnti Rapids," by Michele Viparelli, L'Energia Elettrica, No. 7, 1958.

Journal of the
HYDRAULICS DIVISION
Proceedings of the American Society of Civil Engineers

FORMS OF BED ROUGHNESS IN ALLUVIAL CHANNELS[a]

By D. B. Simons,[1] M. ASCE, and E. V. Richardson,[2] A.M. ASCE

SYNOPSIS

Laboratory experiments in a large recirculating flume, in addition to field studies, have established that resistance to flow and sediment transport in alluvial channels are related to the form of bed roughness. The forms of bed roughness that have been observed in the laboratory flume and in natural alluvial channels can be divided into two regimes of flow, on the basis of their shape, resistance to flow, and sediment transport. These divisions are the lower flow regime and the upper flow regime. Between the two regimes there is a transition zone. The bed forms are ripples and dunes in the lower flow regime and plane bed, standing waves, and antidunes in the upper flow regime. The bed form in the transition zone is variable, ranging from that which is typical of the lower flow regime to that for the upper regime.

Resistance to flow in the lower flow regime is relatively large and sediment transport is relatively small. Conversely, in the upper flow regime the resistance to flow is relatively small and sediment transport is large. In the transition zone both resistance to flow and sediment transport vary appreciably.

The variables that determine the form of bed roughness are the slope of the energy grade line, the depth of flow, fall velocity or effective fall diameter of the bed material, and the shape of the channel. The fall velocity is a function of the size of bed material, the shape factor of the sediment, the mass density of the sediment, the mass density and the viscosity of the water-sediment mixture.

Note.—Discussion open until October 1, 1961. To extend the closing date one month, a written request must be filed with the Executive Secretary, ASCE. This paper is part of the copyrighted Journal of the Hydraulics Division, Proceedings of the American Society of Civil Engineers, Vol. 87, No. HY 3, May, 1961.

[a] Publication authorized by the Dir., U. S. Geol. Survey, Dept. of Interior.

[1] Hydr. Engr., U. S. Geol. Survey, Colorado State Univ., Fort Collins, Colo.
[2] Hydr. Engr., U. S. Geol. Survey, Colorado State Univ., Fort Collins, Colo.

Laboratory and field studies indicate that the change in resistance to flow that occurs when the form of the bed roughness changes from dunes to plane bed or standing waves, accounts for the discontinuity observed in stage discharge relationships on those streams that flow in both regimes during a runoff event.

INTRODUCTION

Flow in alluvial channels is complicated by the fact that the form of the roughness elements and, hence, the resistance to flow and the sediment transport are functions of the characteristics of the fluid, flow, bed material, and channel. Because of the limited scope of most studies and the interdependency and the number of variables involved there are many conflicting statements in the literature. This was brought out by Norman H. Brooks,[3] A.M. ASCE and those who discussed his paper. However, a clearer insight into the alluvial channel problem results when the various forms of bed roughness that can occur in an alluvial channel, the factors that affect the form of bed roughness, and the variation of resistance to flow and sediment transport with forms of bed roughness are known.

Herein is described the bed configurations that have been observed in a large recirculating laboratory flume with a sand bed and in alluvial channels in the field; the magnitude of resistance to flow and sediment transport associated with these bed forms; the variables that influence the bed configuration and, where known, how these variables influence the bed form. A possible relationship that may prove useful in predicting the configuration of the bed is introduced and one field situation for which the change in bed form is of prime importance is described.

This analysis is an outgrowth of a continuing study of alluvial channels by the United States Geological Survey, Dept. of Interior (USGS) at Colorado State University, Fort Collins, Colo. The investigation is conducted primarily in a recirculating flume 150 ft long, 2 ft deep, and 8 ft wide. Slope can be varied from 0 ft per ft to 0.01 ft per ft and discharge from 2 cfs to 22 cfs. To supplement the large flume a recirculating flume 2 ft wide, 3 ft deep, and 60 ft long is also used.

The depth of sand bed in the flumes was approximately 0.6 ft. With shallower depths of sand the dunes could not fully develop and portions of the flume floor were exposed. The 0.45 mm data quoted in this report were previously

---

[3] "Mechanics of Streams with Movable Beds of Fine Sand," by Norman H. Brooks, Transactions, ASCE, Vol. 123, 1958, pp. 526-549.

published[4] and the 0.28 mm data are included herein (Table 1). A more detailed description of the facilities and methods of collecting the data are available.[5]

REGIMES OF FLOW

It is commonly recognized that four regimes of flow occur in open channels with rigid boundaries.[6] Two of these regimes frequently occur in natural alluvial channels. These are the tranquil-turbulent flow and rapid-turbulent flow regimes. Tranquil and rapid flow are adequately defined by either the specific energy diagram or the Froude number, F. When $F < 1$, the flow is tranquil and when $F > 1$, the flow is rapid. The Froude number is defined as

$$F = \frac{V}{\sqrt{g\,D}} \quad \ldots\ldots\ldots\ldots\ldots\ldots (1)$$

in which V is the velocity of flow, in feet per second; g denotes the gravitational acceleration, in feet per second squared; and D refers to the depth in feet.

Normally the mean velocity V and average depth D are used to compute the Froude number. However, it is important to recognize that with the extreme variability of flow conditions that occur in the cross section of an alluvial channel it may be advantageous to consider local values of velocity and depth and the corresponding Froude number to help explain observed phenomenon. It is not uncommon to be confronted with a situation where the Froude number, based on average V and D, is less than unity and yet in the same cross section, the local Froude number may exceed unity.

The absolute magnitude of the Froude number in either the tranquil or the rapid flow regime depends on the scale of the system and is only quantitatively significant for the system under consideration. For instance, in the large recirculating flume which is 8 ft wide, the dunes only occurred when $0.3 < F < 0.6$, whereas in a large deep river, dunes can occur when $F \ll 0.3$. Also in the large flume, the beginning of motion occurs at a $F \approx 0.15$, whereas, in a very small flume using the same bed material and width-depth ratio, the beginning of motion may occur at $F > 1.0$.

If $F < 1$ the water accelerates over the artificial or natural humps on the stream bed and decelerates over the depressions or troughs. This is illustrated in Figs. 1(a) and 1(b). Fig. 1(a) also illustrates a separation zone and the existence of strong circulation in the trough area of a dune bed and the fact that boils appear on the water surface just downstream of the crests of the sand waves. The separation and the turbulence generated dissipates considerable energy which increases the resistance to flow.

When $F > 1$, the water decelerates over the humps and accelerates in the troughs as illustrated in Figs. 1(c) and 1(d). Fig. 1(c) illustrates symmetrical sand and water waves of sinusoidal form that have been described mathematically with limited accuracy by the writers. In flumes these sand and water

---

4 "Resistance to Flow in Alluvial Channels," by D. B. Simons and E. V. Richardson, Proceedings, ASCE, Vol. 86, No. HY 5, May, 1960.

5 "Studies of Flow in Alluvial Channels; Flume Studies Using Medium Sand," by D. B. Simons, E. V. Richardson, and M. L. Albertson, Water Supply Paper 1498A, U. S. Geol. Survey, 1961, in press.

6 "On the Four Regimes of Open-Channel Flow," by J. M. Robertson and Hunter Rouse, Civil Engineering, March, 1941.

waves are commonly observed in the rapid flow regime. There is little separation and circulation in the rapid flow regime when plane bed and standing waves exist. In these cases, the dissipation of energy reflected by resistance to flow is primarily the result of shear on the bed and the formation of waves.

TABLE 1.—BASIC VARIABLES FOR RUNS WITH 0.28 mm SAND IN THE 8 FT FLUME

Run	Slope x 10^2 per ft	Discharge cfs	Depth, in ft	Velocity, in ft per sec	Viscosity x 10^5 ft^2 per sec	Temperature in °C	Total load, in ppm	Bed Forms
(1)	(2)	(3)	(4)	(5)	(6)	(7)	(8)	(9)
6	0.005	3.79	0.90	0.53	1.46	9.0	0	Plane
7	0.007	6.61	1.01	.82	1.27	13.9	0	Plane
8A	0.011	7.76	1.00	.97	1.34	11.9	-	Plane
8B	0.023	7.76	1.01	.96	1.38	10.9	3.3	Ripple
10	0.041	4.16	.59	.88	1.23	15.1	1.0	Ripple
5	0.045	10.73	1.00	1.34	1.19	16.5	12	Ripple
13B	0.062	13.46	1.00	1.68	1.19	16.4	75	Ripple
4	0.069	10.73	0.86	1.56	1.25	14.6	51	Ripple
11	0.073	4.92	0.59	1.04	1.23	14.9	20	Ripple
33	0.090	15.74	1.06	1.86	1.15	17.6	330	Dune
1[a]	0.100	12.70	0.88	1.80	1.18	16.7	405	Dune
12	0.108	7.19	0.57	1.58	1.20	16.0	150	Ripple
14	0.116	8.61	0.62	1.74	1.21	15.6	298	Dune
20	0.120	18.14	1.05	2.16	1.21	15.6	506	Dune
2[a]	0.131	15.19	0.92	2.06	1.21	15.8	664	Dune
21	0.131	20.39	1.07	2.38	1.19	16.5	732	Dune
19	0.134	9.90	0.65	1.90	1.23	14.9	563	Dune
16[a]	0.134	17.23	1.02	2.11	1.21	15.8	549	Dune
23	0.134	22.02	0.91	3.02	1.21	15.6	1230	Trans.
17[a]	0.136	10.01	0.65	1.92	1.24	14.7	505	Dune
3[a]	0.136	15.28	0.88	2.17	1.22	15.2	733	Dune
18	0.141	11.96	0.61	2.45	1.24	14.7	1040	Trans.
30	0.142	15.68	0.64	3.06	1.25	14.5	1370	Trans.
34	0.150	5.50	0.44	1.56	1.26	14.1	480	Dune
22	0.153	14.92	0.60	3.11	1.31	12.7	1540	Plane
15[a]	0.158	12.87	0.75	2.14	1.30	13.0	789	Dune
24	0.172	21.98	0.82	3.35	1.21	15.7	2350	Trans.
25	0.199	21.85	0.72	3.79	1.24	14.7	2710	Plane
28	0.229	15.72	0.55	3.57	1.23	15.1	2760	Plane
29	0.278	15.70	0.52	3.77	1.22	15.4	3120	Plane
26	0.328	15.51	0.50	3.88	1.23	15.0	5060	Antidune
32	0.470	21.76	0.58	4.69	1.38	10.8	10500	Antidune
27	0.533	15.47	0.43	4.50	1.23	15.1	11500	Antidune
31	0.593	21.34	0.56	4.76	1.40	10.2	13000	Antidune
35	0.815	21.33	0.54	4.93	1.38	10.9	27600	Antidune
37	0.820	8.34	0.30	3.48	1.35	11.6	19900	Antidune
38	0.930	15.26	0.40	4.77	1.37	11.1	36100	Antidune
36	1.007	21.38	0.57	4.69	1.36	11.5	42400	Antidune

[a] Slope poorly defined.

With antidunes the resistance to flow is related to the shear on the bed, the formation of waves, and the energy dissipated in the breaking waves.

FORMS OF BED ROUGHNESS

The forms of bed roughness observed in the flumes and in alluvial streams are illustrated in Fig. 2. These forms of bed roughness were described and divided into the tranquil and rapid flow regimes.[4] Additional laboratory studies by the writers and a field investigation,[7] indicate that it is more logical to classify forms of bed roughness into a lower and upper regime connected by a transition zone than to work with the tranquil and rapid flow regimes that are defined by the Froude number.

The lower and upper flow regime classification is based upon magnitude of resistance to flow, bed, and water surface configuration, and mode and magnitude of sediment transport. In the lower regime the bed roughness is ripples

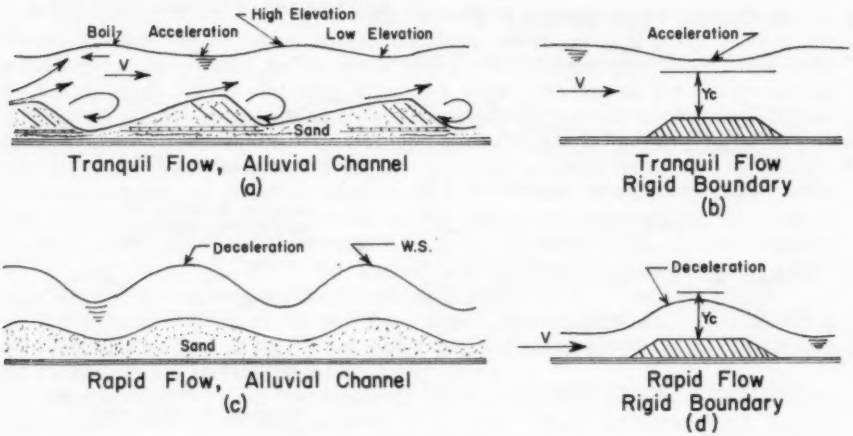

FIG. 1.—RELATION BETWEEN WATER SURFACE AND BED CONFIGURATION IN THE TRANQUIL FLOW AND RAPID FLOW REGIMES

or dunes or both, the resistance to flow is large and the bed material load is relatively small. The majority of the bed material load moves close to the bed over the backs of the ripples or dunes and at the crest of these roughness elements some of the bed load avalanches down the faces of the ripples or dunes where it is temporarily stored causing the ripples and dunes to advance downstream. The other part of the bed material load is carried onward, some to the surface in the boil areas.

When the bed is plane or when standing waves and antidunes develop the resistance to flow is small, the bed material transport is relatively large and is nearly continuous in motion. With ripples and dunes bed load is closely related to the velocity of the roughness elements. With plane bed, standing

[7] Personal communication with D. R. Dawdy.

waves, or antidunes the bed load is closely related to the velocity of the individual grains moving in contact with the bed. In the transition region which connects lower and upper flow regimes there is a discontinuity in the resistance to flow and sediment transport relations.

There are reports in the literature of a plane bed with bed material movement which develops before ripples in the lower regime of flow. Based upon experimentation, this seems to be a small flume phenomenon. In the large flume whenever general movement of bed material occurred ($d < 0.5$ mm) ripples or dunes ultimately formed.

Ripples are usually spaced on the order of 0.5 ft to 1.5 ft and have amplitudes of 0.01 ft to 0.1 ft. The spacing of the dunes is usually greater than 2 ft, and their amplitudes range from 0.10 ft to many feet depending on the depth of

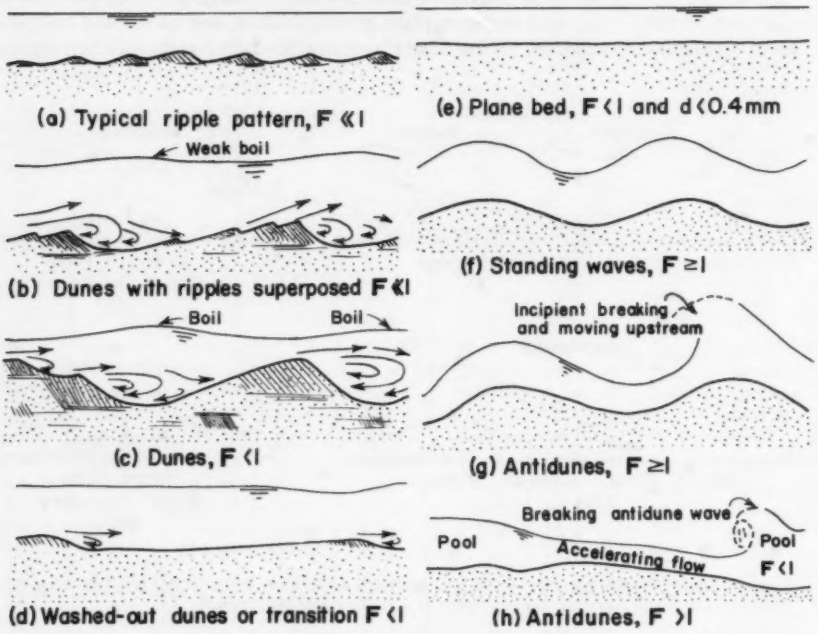

FIG. 2.—FORMS OF BED ROUGHNESS IN ALLUVIAL CHANNELS

flow and the characteristics of the bed material. For example, in small alluvial channels the dunes may be 0.5 ft to 1 ft high with a spacing of 5 ft to 20 ft, whereas, in the Mississippi River sand waves of dune form have been recorded by W. C. Carey, F. ASCE and M. D. Keller,[8] A.M. ASCE which have lengths of several hundred feet and amplitudes as large as 40 ft. Dunes as defined here are frequently referred to as bars.

In the transition zone for the same boundary shear the bed configuration may range from plane bed to fully developed dunes depending primarily on antecedent conditions. Generally, the bed consisted of long dunes of small amplitude that decreased in amplitude as the boundary shear was increased. However, when the bed form consisted of dunes, slope or depth could be in-

[8] "Systematic Changes in the Beds of Alluvial Rivers," by W. C. Carey and M. D. Keller, Proceedings, ASCE, Vol. 83, No. HY 4, August, 1957.

creased to relatively large values before the bed form changed to the plane bed or standing waves of the upper flow regime. Conversely if the bed was plane, the slope or depth could be decreased significantly before dunes developed.

A plane bed developed in the flume experiments following the transition zone with the 0.28 mm sand. With the 0.45 mm sand a plane bed did not develop following the transition. Instead, standing waves developed. The standing sand and water waves that occurred with the 0.45 mm sand and that did not occur with the 0.28 mm sand were of sinusoidal form, in phase, and did not move either upstream or downstream with time to any great extent. The amplitude and spacing of these waves depended upon the size of the flow system and the characteristics of the fluid and the bed material. The amplitude of the water waves increased with depth and were 1.5 to 2 times the amplitude of the sand waves.

The antidunes are very similar to standing waves except some of the sand and water waves continued to grow in amplitude until they broke. Antidunes have been observed in natural streams in which the median diameter of the bed materials have ranged in size from fine sand to coarse gravel. In the flume studies the breaking of the antidune waves usually occured when the amplitude of the water waves were about twice the amplitude of the corresponding sand waves. At this time, the water surface in the trough was at approximately the same elevation as the crests of adjacent sand waves. These sand and water waves moved upstream prior to breaking. Either one or two waves broke at one time or a train of several waves broke more or less simultaneously. After the antidune waves broke, a new train of waves developed and the antidune cycle repeated itself or the waves subsided without developing to their break point and then reform to break or abate again. As indicated by W. B. Langbein,[9] F. ASCE the Froude number, where antidunes first form, increases with increasing size of bed material.

In the large flume at the steeper slopes, the antidune activity was in the form of chutes and pools. Flow was rapid and accelerated in the chutes and flow was tranquil in the pools, as in Fig. 2(h).

When antidunes break they resemble the hydraulic jump and can be analyzed with some success as such, particularly with two-dimensional flow. Large quantities of sediment are carried into suspension in the breaking antidune wave.

In the breaking wave and immediately downstream, the velocity is relatively small. The storage of water in the short reaches where the waves are breaking causes the discharge to vary with time and this action tends to set up slug flow. In Mendano Creek, which is located in the San Luis Valley of Colorado, antidunes set up slugs of water that had a depth about twice average depth and traveled down the channel spaced at intervals of about 350 ft at nearly 10 fps. At the time of this field observation, the average discharge was approximately 120 cfs, the median diameter of the bed material was 0.3 mm, and the channel slope was 1.67%.

VARIATION OF RESISTANCE TO FLOW WITH BED ROUGHNESS

The variation of resistance to flow, as measured using the Darcy-Weisbach f, with the form of bed roughness and the influence of size of bed material

[9] "Hydraulic Criteria for Sand Waves," by W. B. Langbein, Transactions, Amer. Geophysical Union, 1942, pp. 615-618.

and slope on the form of the bed roughness, resistance to flow, and sediment transport are illustrated in Fig. 3 and Table 2.

The resistance to flow is relatively small for plane bed prior to beginning of motion. However, resistance to flow is larger for this case than it is for the

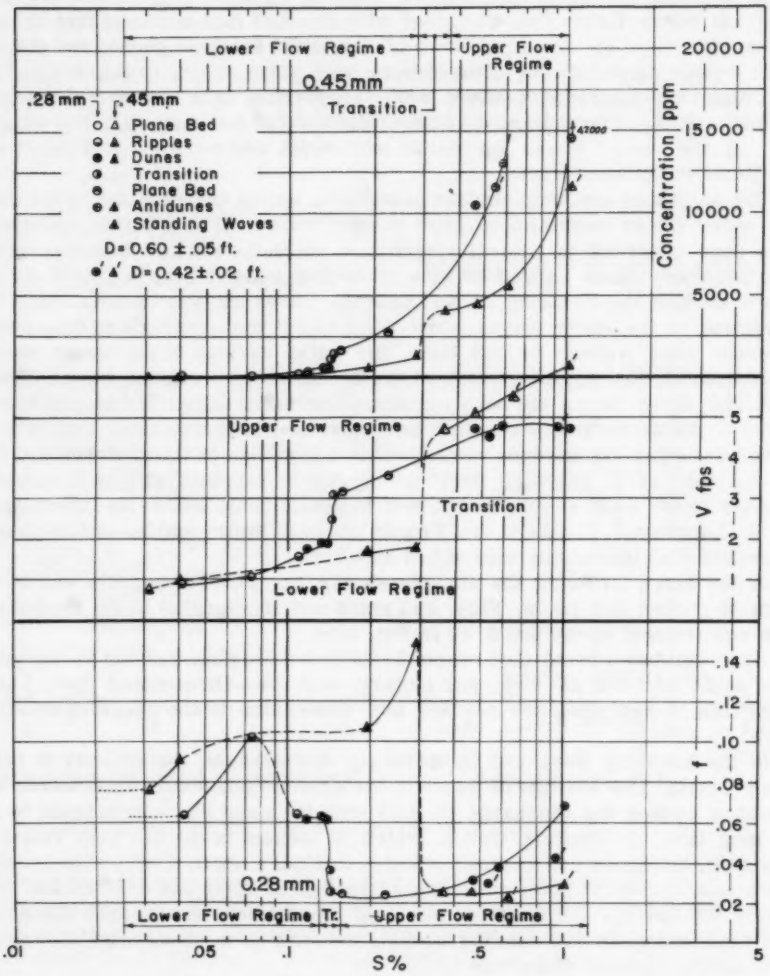

FIG. 3.—VARIATION OF f, V, AND CONCENTRATION WITH S AT CONSTANT DEPTH

plane bed or standing wave case where there is motion of bed material. This is understandable because, in the first case, resistance results from grain roughness that is fixed; whereas, in the second case the grain roughness is not fixed but moving and a form of rolling friction exists.

TABLE 2.—VARIATION OF FACTORS WITH REGIMES OF FLOW AND FORMS OF BED ROUGHNESS

	Forms of Bed Roughness	Total Load Concentration ppm --	0.28 mm sand f -	0.28 mm sand n ft1/6	0.28 mm sand Fr --	0.28 mm sand Sx10^2 ---	Total Load Concentration ppm --	0.45 mm sand f -	0.45 mm sand n ft1/6	0.45 mm sand Fr --	0.45 mm sand Sx10^2 ---
Lower Flow Regime	Plane	0	0.0301	0.016	0.17	0.011	0	0.0359	0.016	0.18	0.015
	Ripples	1	.0635	.02	.17	.023	1	.0521	.020	.14	.016
		to	to	to	to	to	to	to	to	to	to
		150	.1025	.027	.37	.11	100	.1330	.028	.28	.11
	Dunes	150	.0612	.021	.32	.09	100	.0489	.019	.28	.06
		to	to	to	to	to	to	to	to	to	to
		800	.0791	.026	.44	.16	1,200	.1490	.033	.65	.30
Transition		1,000	.0250	.014	.55	.13	1,400	.0415	.016	.61	.37
		to	to	to	to	to	to	to	to	to	to
		2,400	.0344	.017	.67	.17	4,000	.0798	.022	.92	.49
Upper Flow Regime	Plane	1,500	.0244	.013	.71	.15					
		to	to	to	to	to	---	---	---	---	---
		3,100	.0262	.014	.92	.28					
	Standing Waves	---	---	---	---	---	4,000 to 7,000	.0200 to .0406	.011 to .015	1.0 to 1.6	.36 to .62
	Antidunes	5,000	.0281	.014	1.0	.33	6,000	.0247	.012	1.4	.66
		to	to	to	to	to	to	to	to	to	to
		42,000	.0672	.022	1.3	1.0	15,000	.0292	.014	1.7	1.0

As general motion of the bed material was initiated by increasing the boundary shear, ripples formed that caused a large increase in resistance to flow. With sufficient increase in slope, and depth constant, dunes formed, and with further increase in slope transition conditions developed. The ripples formed from the 0.28 mm bed material had a slightly larger resistance to flow than the ripples formed of 0.45 mm bed material. Conversely, the dunes formed from 0.45 mm bed material had a greater resistance to flow than the dunes formed of 0.28 mm bed material (Table 2).

In the transition zone, because the bed form was unstable, the resistance to flow was extremely variable. In general, the magnitude of the resistance to flow was between that for fully developed dunes and a plane bed. The variation in resistance to flow in the transition zone was larger for the 0.45 mm bed material than for the 0.28 mm bed material. Also note that the transition zone occurred at a much flatter slope when using the 0.28 mm sand.

With still further increase in boundary shear the upper flow regime was reached. In this regime of flow the bed roughness was plane bed, standing waves, antidunes or some combination of these. Resistance to flow was a minimum for a given bed material throughout the plane bed or standing wave range or both. As antidunes develop, the resistance to flow increased slightly and continued to increase with further increase in boundary shear. The rate of increase in resistance to flow was much more rapid for the finer sand and was reflected directly by increased antidune activity.

VARIATION OF BED MATERIAL LOAD AS A FUNCTION OF BED FORM

The large flume studies indicated that the bed material transport varied with form of bed roughness and size of sand, as shown in Fig. 3 and Table 1. The transport for the ripples reached a maximum of 150 ppm for the 0.28 mm bed material and 100 ppm for the 0.45 mm bed material. With dunes as the form of bed roughness, the maximum concentration of bed material transport was about 800 ppm and 1200 ppm, respectively, for the 0.28 mm sand and the 0.45 mm sand.

For the 0.28 mm sand, the bed material load in the upper flow regime ranged from 1500 ppm for the plane bed to 42,000 ppm with antidunes. The range in concentration of bed material discharge for the 0.45 mm sand was from 4,000 ppm with standing waves to 15,000 ppm for the antidunes.

The bed material load in the transition zone was unpredictable but varied, for both sands, from slightly greater than the maximum concentration for the dunes to a concentration that was characteristic of that for the plane bed or the standing waves.

FACTORS INFLUENCING FORM OF BED ROUGHNESS

The variables that fix the form of bed roughness in alluvial channels are

$$\text{Form of bed roughness} = \phi\left[D, S, d, \sigma, \rho, g, w, S_f, f_s\right] \quad \ldots\ldots\ldots (2)$$

in which

$$w \text{ or } d' = \phi\left[d, \rho_s, \rho, g, S_p, \mu\right] \quad \ldots\ldots\ldots\ldots (3)$$

and D refers to the depth, S denotes the slope of the energy grade line, d defines the median diameter of the bed material, σ is a measure of the size

distribution, ρ refers to the mass density of the water-sediment mixture (normally taken as that for water unless considerable fine sediment is present), ρ_s is the mass density of the bed material, g denotes the acceleration of gravity, w is the fall velocity of the bed material, f_s describes the seepage force, S_f is a shape factor of the cross section, S_p is a shape factor of the particle, μ defines the viscosity of the water-sediment mixture, and d′ refers to the effective median fall diameter of the bed material. In addition to temperature, μ also depends on the concentration of fine sediment.

The full significance of all of these variables has not been revealed (as of 1961) because the investigations have not been broad enough to include all conditions. However, the effect of some of the variables are at least qualitatively known and in the following paragraphs they are summarized. Referring to Eq. 1, velocity or bed material load can be substituted for bed roughness.

Slope S.—The effect of slope was illustrated in Fig. 3. With depth constant a change in slope increases the boundary shear. With sufficient increase in shear the form of the bed roughness changes. To develop a given form of bed roughness in alluvial channels that has the same bed material, the slope must be large if the discharge is small if the discharge is large.

Depth D.—The effect of depth is not well defined because the range in depth which has been studied is small. However, in the experiments conducted in the large flume the variation in depth has been adequate to indicate that a change in depth can change the bed form. In natural alluvial channels in which slope is essentially constant bed form changes have been reported that have resulted from changes in depth.[10,11,12] However, there appears to be combinations of slopes and sizes of bed material where the bed form will not change with a large change in depth.

In addition to the changes in bed form that can occur with changes in depth, there are the uncertain effects of changes of depth on bed material load and resistance to flow when the bed form does not change. With ripples there is a relative roughness effect. The resistance to flow decreases with increase in depth. Whereas with dunes, the flume data indicate that resistance to flow increases with increase in depth. However, it has not been verified that resistance to flow with a dune bed form increases continuously over a large range of depths.

Bed material load is also affected by changes in depth of flow. Based upon a recent study of available field data, B. R. Colby[13] has shown that because velocity increases with depth and concentration decreases with depth, a peculiar but logical relationship exists between sediment load, depth of flow, and velocity. Within a certain range of velocities, if velocity is held constant, the bed material load increases with increasing depth, within another range of velocities, bed material load decreases with increasing depth.

---

10 "Discontinuous Rating Curves for Pigeon Roost and Cuffawa Creeks in Northern Mississippi," by B. R. Colby, ARS 41-36, U. S. Dept. of Agric.

11 Discussion by J. K. Culbertson and C. F. Nordin of "Discharge Formula for Straight Alluvial Channels," by Hsin-Kuan Liu and Shoi-Yean Hwang, Proceedings, ASCE, Vol. 86, No. HY 6, June, 1960.

12 "Studies of Flow in Alluvial Channels; Depth-Discharge Relation of Alluvial Streams," by D. R. Dawdy, Water Supply Paper 14896, U. S. Geol. Survey, 1961, in press.

13 Personal Communication.

The effect of the combination of depth and slope in the shear term, γDS, has been studied by I. A. Shields,[14] R. A. Bagnold[15] and Hans A. Einstein, F. ASCE, and Ning Chien, M. ASCE,[16] to mention a few. All have indicated that shear is an important parameter, whereas Brooks[3] stated "that for the laboratory flume it was found that neither the velocity nor the sediment discharge concentration could be expressed as a single-value function of the bed shear stress, or any combination of depth and slope . . . ." It is apparent in Fig. 3 that what Brooks states is true for the transition zone. However, in the upper and lower flow regimes shear is closely related to velocity and sediment concentration.

Size of Bed Material.—The effects of the physical size of bed material on the bed form are (1) its effect as a grain roughness, and (2) its influence on the fall velocity or the effective fall diameter, which is a measure of the mobility of the particle. The mobility of the particle, when related to the fluid forces, is of the utmost importance in determining whether the bed form is ripples, dunes, plane bed, standing wave, or antidunes.

In the second effect the physical size of the bed material, as measured by fall diameter[17] or sieve diameter, is important only as it is related to the other variables in Eq. 3. However, fall diameter has the advantage of eliminating the shape factor and density of the particle as variables. Knowing the fall diameter, the fall velocity or effective fall diameter of the particle, in any fluid at any temperature, can be computed if the fluid's density and viscosity are known.[18]

The importance of size of bed material on the form of bed roughness was indicated by the experiments using the 0.45 mm and the 0.28 mm sands. The length of the dunes (crest to crest or trough to trough) observed while experimenting with the 0.28 mm sand were much longer than the dune lengths for the 0.45 mm sand. Although the amplitude of the dunes for the two sands were the same, their shapes were different. The dunes formed of 0.45 mm sand were more angular. The large spacing between the dunes and the smaller separation zone and turbulence in the troughs accounts for the fact that some ripple runs exhibited a larger f value than the dune runs where the 0.28 mm sand was used. The flow over the relatively long plane backs of these dunes was quite efficient, reducing the over-all resistance to flow to a value less than that computed for the ripple case. The dunes, using the 0.45 mm sand, had much larger f values than the ripples in the same sand or the dunes in the 0.28 mm sand because of the closer spacing of the dunes, the large separation zone in the dune troughs, and the greater magnitude of turbulence. The increase in resistance to flow that occurred with an increase in sand sizes

---

14 "Application of Similarity Principles and Turbulence Research to Bed-Load Movement," by I. A. Shields, 1936, Trans. from German by W. Poh and J. C. van Vehelin, U. S. Soil Conservation Service, Coop. Lab., Calif. Inst. of Tech., Pasadena, Calif.

15 "The Flow of Cohesionless Grains in Fluids," by R. A. Bagnold, Philos. Trans., Royal Soc. of London, Vol. 249, No. 964, 1956, pp. 235-297.

16 Discussion by H. A. Einstein and N. Chien of "Mechanics of Streams with Movable Beds of Fine Sand," by N. H. Brooks, Transactions, ASCE, Vol. 123, 1958, pp. 553-562.

17 "Measurement and Analysis of Sediment Loads in Streams, Some Fundamentals of Particle Size Analysis," Inter-Agency Report 12, U. S. Govt. Printing Office, Washington, D. C., 1957.

18 "The Effect of Fine Sediment on the Mechanics of Flow in Alluvial Channels," by W. L. Haushild, thesis presented to Colorado State Univ., at Fort Collins, Colo. in 1960, in partial fulfillment of the requirements for the degree of Master of Science.

is different from the trend reported by L. B. Leopold, F. ASCE, and T. Maddock, F. ASCE.[19]

The change from lower to upper flow regime occurred at a much smaller shear value, and the rate of change was faster for the finer sand. Also, using the fine sand the form of bed roughness changed from dunes to a plane bed when $F \approx 0.4$, and the bed remained plane as the boundary shear was increased until $F \approx 1$, then antidunes developed. Using the coarser sand, the dunes decreased in amplitude with increasing boundary shear when $F \approx 0.6$ and transition conditions persisted until $F \approx 1$, then standing waves developed.

That a plane bed developed with tranquil flow with the 0.28 mm sand and not with the 0.45 mm sand is attributed to the greater mobility of the finer sand and the limitations of the experimental equipment. The boundary shear required to eliminate the dunes was sufficiently small for the more mobile finer sand so that the change could occur at a depth and slope such that the $F < 1$. Whereas, with the coarser sand the discharge capacity of the flume system was not sufficient to eliminate the dunes at a depth and slope where the change would occur with $F < 1$. Field observations indicate that streams with 0.45 mm or coarser bed material, but having large depths and flat slopes may have a plane bed form of bed roughness when $F < 1$.

Fall Velocity and Effective Fall Diameter.—As indicated in the preceding section, the fall velocity or the effective fall diameter of the bed material is of major importance in determining the bed form, resistance to flow, and sediment transport. Because the size concept is so entrenched in the literature, effective fall diameter is used in preference to fall velocity. Effective fall diameter of a sediment particle is defined as the diameter of a sphere having a specific gravity of 2.65 and a fall velocity in quiescent distilled water of infinite extent at a temperature of 24°C equal to the fall velocity of the particle falling alone in any quiescent stream fluid at stream temperature. This definition neglects the unknown effect of turbulence on fall velocity.

The effect of the various factors given in Eq. 3 on fall velocity are well known although they are often overlooked. For instance, it is known that viscosity and mass density of a fluid varies with temperature and affects the fall velocity, but the fact that fine sediment affects the viscosity[18,20,21] and the mass density of the fluid are often overlooked. An increase in concentration of suspended fine sediment (wash load) or a decrease in temperature increases the viscosity and specific density of the liquid and decreases the fall velocity and effective fall diameter of the bed material. Particles of different physical diameter have the same effective fall diameter if their fall velocities are the same. With the same effective fall diameter the forms of bed roughness, resistance to flow, and bed material load should be approximately the same in spite of the difference in physical size.

With respect to temperature effect there have been conflicting statements in the literature. Vito A. Vanoni, F. ASCE, and Brooks[22] reported that with an increase in temperature there is a decrease in resistance to flow; whereas,

---

19 "The Hydraulic Geometry of Stream Channels and Some Physiographic Implications," by L. B. Leopold and T. Maddock, Jr., Prof. Paper 252, U. S. Geol. Survey.

20 "Fluidity and Plasticity," by E. C. Bingham, Mc Graw-Hill Book Co. Inc., New York, 1922.

21 "Flow Properties of Disperse Systems," J. J. Hermans, ed., North-Holland Publishing Co., Amsterdam, The Netherlands.

22 "Laboratory Studies of the Roughness and Suspended Load of Alluvial Streams," by V. A. Vanoni and N. H. Brooks, Report No. E-68, Calif. Inst. of Tech., Pasadena, Calif.

D. W. Hubbell[23] reported that with an increase in temperature there is an increase in the resistance to flow. These two apparently contradicting statements, that show the effect of temperature variation, are easily explained by considering the forms of bed roughness which existed in the alluvial channels in question, and the effect of temperature change on the fall velocity and, hence, effective fall diameter of the bed material particles.

A decrease in temperature increases the viscosity of the water and decreases the fall velocity of the sand. Thus, a decrease in temperature decreases the effective fall diameter of a given sand. Consequently, if a sand bed is covered with ripples and the temperature of the water is decreased, the mobility of the particles is increased due to the decrease in effective fall diameter of the sand, larger ripples form, and resistance to flow increases. On the other hand, if the form of bed roughness is near to or in the transition zone and there is a reduction in temperature, the reduction in effective fall diameter causes the dunes to shear out to a greater extent or perhaps causes the bed to become plane, which (in either event) is accompanied by a decrease in resistance to flow. Both of these phenomena are reversible. These two variables (temperature and fine sediment) have been studied by the USGS.

Seepage Force.—In an alluvial channel there is usually either inflow or outflow from the channel through the bank and bed material that causes seepage forces because there is a loss of head. Although the effect of seepage forces on bed form has not been studied it is known that if there is inflow, the seepage force acts to reduce the effective weight of the sand. If there is outflow from the channel, the seepage force acts in the direction of flow and increases the effective weight of the sand. With inflow in the extreme case, the seepage forces can be large enough to set up a quick-sand condition and the weight of the material is in equilibrium with the seepage forces. The seepage force reduces or increases the effective size of the bed material in contact with the bed by changing the effective weight of the sand on the bed. Once a particle of sand loses contact with the bed, the seepage forces no longer have a direct effect on it.

Gradation of the Bed Material.—The comments concerning the effect of the size of the material, fall velocity, and seepage force indicate that the bed material can be adequately described by a fictitious diameter. This obviously is not the case. Although, extensive studies into the effect of gradation of bed material on form of bed roughness, and resistance to flow have not been made, it would appear that an alluvial stream with a bed material composed of only one size would not react to fluid forces the same as if the bed material had the same median diameter but a large range of sizes.

Vanoni and Brooks[22] investigated the effect of gradation of bed material on bed material load and concluded that for a given median diameter of bed material the load increases as the range of sizes or gradation increases. Einstein[24] also recognized the importance of the gradation of bed material.

Shape Factor of the Cross Section.—The effect of channel shape is rather nebulous. However, wide shallow channels have been simulated and under certain conditions two or more forms of bed roughness have developed simultaneously, for example, small dunes on part of the cross section and plane

[23] "Investigations of some Sedimentation Characteristics of a Sand Bed Stream," by D. W. Hubbel et al., Open-File Report, U. S. Geol. Survey, Lincoln, Nebr.

[24] "The Bed Load Function for Sediment Transportation in Open Channel Flows," by H. A. Einstein, Tech. Bulletin 1026, U. S. Dept. of Agric., 1950, 70 pp.

bed, standing waves or antidunes on the other. The resistance to flow is variable and difficult to evaluate when there is multiple roughness. The resistance to flow is dependent on the percent of the bed covered with each bed form. Multiple roughness and the variable resistance to flow associated with this condition has been observed in alluvial streams by the writers.

Current (1961) studies of resistance to flow and sediment transportation indicates that the forms of bed roughness for given alluvial bed material may be quite different in flumes of different size, other conditions being essentially the same.

Using the large flume, the forms of bed roughness observed in the two regimes of flow were as illustrated in Fig. 2. These forms of bed roughness seem to agree with field conditions. Using the 0.45 mm bed material in the small flume the observed bed configurations were different. When bed movement began, ripples did not form in the small flume. In fact, ripples never developed in this flume with this size of bed material. When bed shear in the small flume was increased sufficiently, the plane bed was replaced by dunes. These dunes were more two dimensional than those which occur in the large flume and these dunes never, at any time, had a ripple roughness superposed on them as was the case in the large flume.

In the rapid-flow regime, conditions were quite similar in both flumes. However, the resistance to flow in the small flume was much greater because flow was more nearly two dimensional which caused the total width of the flume to be occupied by the waves and antidunes that developed.

The results of this comparison indicate the many problems that the experimentor faces who tries to effectively utilize the data collected by various investigators from their flumes of different size and design.

PREDICTION OF FORM OF BED ROUGHNESS

Thus far, no completely adequate method of predicting form of bed roughness has been developed. M. L. Albertson, F. ASCE, and others presented[25] a method suitable for predicting bed forms for the laboratory case, but it was not completely satisfactory for the field case. Similarly R. J. Gardi[26] presented a figure relating Shield's parameter $\gamma DS/\Delta \gamma d$, the Froude number, F, and the form of bed roughness. This figure was not as satisfactory for the laboratory case but was superior for the field case. As another possibility Fig. 4 was developed which is a modification of the figure by Hsin-Kuan Liu, M. ASCE for ripple formation.[27] Fig. 4 separates the bed forms for the various sand sizes for both streams and flumes, fairly well. Because the fall velocity is used, it also takes into account all viscous and gravitational forces that appear to affect the bed form. However, Fig. 4 may not separate the bed forms when larger depths are studied. Until additional data are available that cover an adequate range of depth, it will be difficult to develop the criterion necessary to predict form of bed roughness in alluvial channels with confidence.

---

[25] Discussion by M. L. Albertson, D. B. Simons, and E. V. Richardson of "Mechanics of Sediment-Ripple Formation," by Hsin-Kuan Liu, Proceedings, ASCE, Vol. 84, No. HY 1, February, 1958.

[26] "Total Sediment Transport in Alluvial Channels," by R. J. Gardi, thesis presented to Colorado State Univ., at Fort Collins, Colo., in 1960, in partial fulfillment of the requirements for the degree of Doctor of Philosophy.

[27] "Mechanics of Sediment Formation," by Hsin-Kuan Siu, Proceedings, ASCE, Vol. 86, No. HY 5, May, 1957.

In the meantime, the possibility of predicting the bed configuration based upon the mechanics of surface waves and the appearance of the water surface should be considered. This method is not applicable to design but is extremely useful for analysis. However, some training is required on the part of the individual before he can apply it effectively.

Whether the flow is rapid or tranquil can be determined by observing the direction of travel of an artificially induced surface wave using the wave celarity concept. If the disturbance generated to oppose flow moves upstream with respect to a fixed point of observation, flow is tranquil, and if it is swept downstream, flow is rapid.

It is also usually possible to determine form of bed roughness and whether the lower or upper flow regime exists in an alluvial channel by observing the

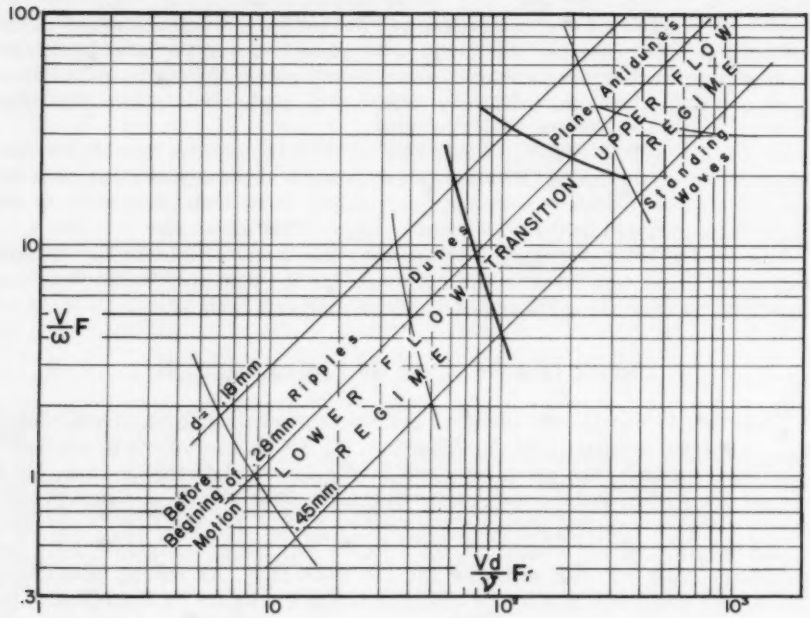

FIG. 4.—FORMS OF BED ROUGHNESS IN ALLUVIAL CHANNELS

condition of the water surface. In the upper flow regime, the water surface is likely to appear relatively smooth and fast or there will be some evidence of standing waves and antidunes [as illustrated in Figs. 2(e), 2(f), 2(g), and 2(h)] which immediately fix the general form of bed roughness that exists. In the lower flow regime the velocity will be relatively slow and the major rises in water surface (usually boils) will be out of phase with the dunes. For a rippled bed, the water surface will be quite plane and placid except for very small depths. In this case small waves will be generated on the water surface by the sand ripples. With a dune bed configuration, there will be turbulence generated at the water surface in the form of boils downstream of the dunes.

Usually the color of the water is different in the boil area due to the large concentration of suspended sediment carried to the water surface within the boil. The strength of the boil activity is dependent on the magnitude, spacing and shape of the dunes, and the depth of flow. In the transition zone the water surface will be rather plane with minor boils appearing on the water surface.

The classification of a stream into the proper regime of flow and form of bed roughness by observing the water surface combined with some knowledge of the bed material would give some information about the transport of sediment and resistance to flow. This information could then be applied to the interpretation of stage-discharge relations and other flow phenomena.

FIELD PROBLEMS

The conditions observed in the field and in the large flume agree quite well. However, in the field the slope of energy grade line through a given reach

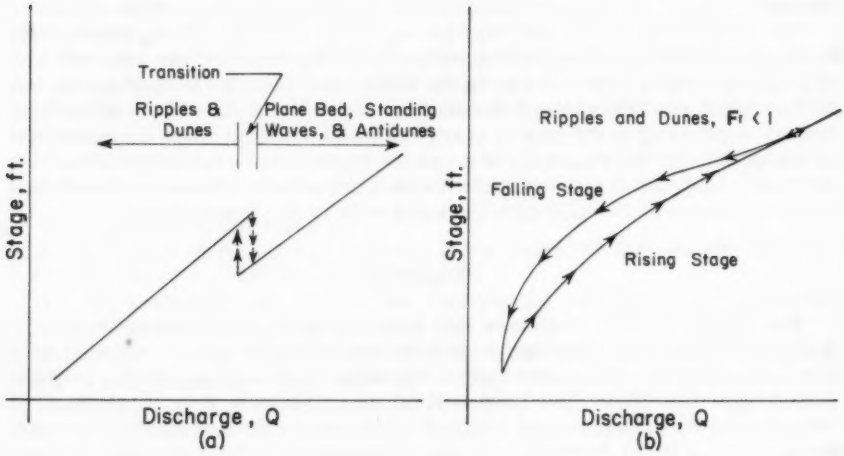

FIG. 5.—TYPICAL QUALITATIVE STAGE—DISCHARGE CURVES FOR ALLUVIAL CHANNELS

of channel varies within narrow limits and the depth varies greatly as the discharge changes; but in the flume studies the slope can be varied widely and depth variations are small due to the physical limitations of the pumping plant and the flume. There is ample evidence that a change in depth can shift the form of bed roughness from dunes to transition, plane bed, and antidunes. The reduction in resistance to flow which occurs as dunes are eliminated accounts for the discontinuity in stage-discharge relations which have been observed in the laboratory and for many natural streams.[10,11,12] Typical qualitative stage-discharge curves which illustrate the effect of change of bed roughness on stage are presented in Fig. 5. Einstein and Chien[16] in their discussion of Brook's paper[3] recognized that the depth-discharge curves

illustrated in Fig. 5 could occur. However, contrary to present evidence, they thought these curves would only rarely if ever occur in nature.

In Fig. 5(a) the break which is shown is caused by a change in bed roughness from dunes to plane bed or standing waves. The break occurs on the rising stage at a larger discharge than on the falling stage. There is usually considerable scatter in the stage discharge relation with ripples and dunes on the bed due to the wide variation of resistance to flow. Under certain circumstances, this variation can be explained. For example, in Fig. 5(b) the magnitude of resistance to flow lags the actual discharge, that is, the change of bed roughness lags the change of discharge. This results in a smaller resistance to flow and smaller depth than would normally occur for equilibrium flow. The reverse occurs on the falling stage. In this instance, at the peak discharge, assume the form of bed roughness is large dunes. As discharge decreases, the large dunes are not reduced in amplitude and spacing at a rate in keeping with the reduction in discharge, and the resistance and depth are larger than for equilibrium flow on the falling leg of the hydrograph. This results in a loop type of stage-discharge curve which resembles a hysteresis curve.

The loop curve of Fig. 5(b) may be reversed. Then the falling stage points would plot below the rising stage points or the two curves may coincide with the falling stage points plotting on the same curve as the rising stage points, or the rising and falling stage curves may cross. The form of the curve which results depends upon the rate of change of discharge with time, the magnitude of the discharge, the characteristics of the bed material, the effect of the fine sediment load, and the characteristics of the channel. Under certain circumstances, temperature could play the same role as the fine sediment.

SUMMARY

The forms of bed roughness that exist in an alluvial channel because of similarities in form, resistance to flow, and sediment transport are divided into categories of lower flow regime, transition zone, and upper flow regime. Based upon laboratory and limited field investigations, the major forms of bed roughness in the normal order of occurrence with increasing slope with depth, bed material, temperature and concentration of fine material constant are as follows:

Lower flow regime
1. Ripples,
2. Dunes with ripples superposed, and
3. Dunes.

Transition (Bed roughness ranges from dunes to plane bed or standing waves)

Upper flow regime
1. Plane bed,
2. Standing waves, and
3. Antidunes.

Resistance to flow and sediment transportation vary greatly as form of bed roughness changes. Consider the two sands with median diameters of 0.45 mm and 0.28 mm which have been thoroughly investigated in a large recirculating flume. For a dune bed configuration f varies from 0.0489 to 0.1490, and

the corresponding bed material load ranges from 100 ppm to 1,200 ppm. For the antidune condition, f varies from 0.0247 to 0.0672 and bed material load ranges from 5,000 ppm to 42,000 ppm.

The form of bed roughness depends primarily on the slope of the energy grade line, depth, fall velocity or effective fall diameter of the bed material and shape of the channel. In the transition zone the bed form also depends on the antecedent form of the bed. There are several other variables whose effect on the bed form may only be of minor importance. They are the seepage force, the gradation of the bed material, and the cohesive properties of any fine sediment in the bed, and the physical size of the sand as a grain roughness.

It has been determined that fall velocity or effective fall diameter has a significant effect on the bed form. Sands with a large difference in physical size have been found to have the same bed form, resistance to flow, and sediment transport when their effective fall diameters were the same. The factors affecting fall velocity have an important effect on the bed form. These are the size of the bed material, viscosity, and mass density of the water-sediment mixture, mass density of the bed material, and the shape of the sand particles.

Knowledge of the forms of bed roughness that develop in alluvial channels and the variables which influence bed roughness is essential to the theory of resistance to flow in alluvial channels, the design of stable channels and the refinement of sediment transport theories.

To further improve existing concepts of flow in alluvial channels it is important to proceed with the following studies:

1. The effect of depth of flow;
2. the effect of size of bed material using larger sand sizes than 0.5 mm;
3. the effect of gradation of bed material;
4. the mechanics related to the meandering and braiding of streams;
5. the effect of width-depth ratio;
6. the mechanics of flow around bends in alluvial channels to establish stability criterion and magnitude of the energy losses; and
7. the mechanics of diffusion, dispersion, and turbulence in alluvial channels.

The development of new instruments is an essential part of future work. Developing methods of measuring turbulence, instantaneous velocity profiles and boundary shear in open channels is necessary for the continued development of the theory of flow in open channels.

Journal of the
HYDRAULICS DIVISION
Proceedings of the American Society of Civil Engineers

ESTIMATING POTENTIAL EVAPOTRANSPIRATION[a]

By W. Russell Hamon,[1] A. M. ASCE

SYNOPSIS

Methods of computing potential evapotranspiration by analytical procedures have been based on the application of the turbulent-transport and energy-balance concepts. Empirical formulas, correlating some temperature function and adjusting for day-time hours, have proved valuable in practical utilization. This latter approach has been used to formulate a simple computational procedure whereby average daily potential evapotranspiration is represented as proportional to the product of day-time hours squared and the saturated water vapor concentration (absolute humidity) at the mean temperature. The day-time factor was determined from a consideration of the disparity between net radiation and temperature, latitudinally, and the fact that transpiration is restricted during darkness since the leaf stomata are closed.

Computed values of potential evapotranspiration obtained by the new procedure are compared with those obtained by the more complex Thornthwaite method (24)[2] and other methods currently employed. General applicability

Note.—Discussion open until October 1, 1961. To extend the closing date one month, a written request must be filed with the Executive Secretary, ASCE. This paper is part of the copyrighted Journal of the Hydraulics Division, Proceedings of the American Society of Civil Engineers, Vol. 87, No. HY 3, May, 1961.

[a] Sections on development and evaluation of procedure are essentially those presented in a Thesis, Dept. of Civ. and Sanitary Engrg., Massachusetts Inst. of Tech., Cambridge, February, 1960. Paper presented at the October 1960 ASCE Convention in Boston, Mass.

[1] Research Assoc., The Travelers Research Center, Inc., Hartford, Conn.

[2] Numerals in parentheses refer to corresponding items in the Appendix.

seems justified from comparisons between observed and computed values of potential evapotranspiration, both on a yearly and seasonal basis.

INTRODUCTION

The determination of evapotranspiration is of professional interest to civil engineers, hydrologists, meteorologists, and agriculturists. To these and others, the problems of water and the conservation of water supplies—in view of the "population explosion" and the increasing demand on water resources—is more than academic.

Since evapotranspiration represents the transport of water from the earth's surface back to the atmosphere—the reverse of precipitation—it assumes an important role in the hydrologic cycle and must be given careful consideration in assessing the water resources of a particular region. Given estimates of evapotranspiration then, through an appropriate accounting system of soil moisture, it becomes possible to indicate the water balance of an area.

Evapotranspiration is controlled by meteorological factors-radiation, wind, temperature, and humidity; soil moisture tension; soil moisture conditions; and plant physiological factors. Its direct measurement is difficult and climatic data have been used in a number of relations (2,7,20,24) to obtain useful estimates. These procedures rely either on the correlation between water evaporated from an open water surface and that from a vegetative area or an empirical relationship with climatic parameters and day-time hours. When soil moisture is not limiting, evapotranspiration is almost entirely dependent upon the amount of solar energy received by the surface and the resulting temperatures (27). Such a condition of optimum soil moisture results in "potential" evapotranspiration.

The concept of potential evapotranspiration was introduced by C. W. Thornthwaite (24) and is understood to represent the rate at which water would be removed from an extended area covered by an actively growing green crop, completely shading the soil, and with a non-limiting supply of water. The rate of evapotranspiration is not influenced by the advection of air that has been heated over drier areas, and the ratio of energy utilized in evaporation to that heating the air remains constant. M. A. Kohler, F. ASCE (13) has suggested that the evaporation from a large water surface must be equivalent to potential evapotranspiration. In this respect, the several methods adaptive to computing evaporation from an open water surface seem applicable in the estimation of potential evapotranspiration, provided the necessary data may be obtained. On the other hand, soil and plant factors may significantly alter the water lost by transpiration so that simpler methods based on temperature and day-time hours may be effective. The purpose of this paper is to formulate such a functional relationship.

ANALYTICAL METHODS

The turbulent-transfer approach to the determination of reservoir evaporation has received considerable attention. This method views evaporation as

equal to the flow of water vapor through the surface layer of air and determined by the product of the vertical gradient of vapor pressure and the rate of mixing of the air. The rate of mixing, expressed as a coefficient of diffusion or austauch coefficient, depends upon the rate of change with height of wind speed. Such equations as derived (22), (19), (25) could be used for the determination of evaporation over any kind of surface where the difference in surface properties is expressed through a roughness constant (22). The practical application of this approach is severely restricted due to the accuracy requirements in measurement of wind and humidity at two levels to determine the rate of change in wind and humidity with height (26).

In the extensive Lake Hefner study (29) of lake evaporation, a simple empirical formula

$$E = k\left(e_w - e_a\right) f(u) \quad \ldots\ldots\ldots\ldots\ldots\ldots \quad (1)$$

relating evaporation, E, to the difference in vapor pressure-saturated at the surface temperature, e_w, and the atmospheric vapor pressure, e_a (as Dalton formulated in 1802); adjusted by a wind factor, $f(u)$, and a proportionately constant, k, gave results comparable to those obtained by the complex mass-transfer formulas. Surface temperature is required for this simplified approach so that it is of little use since pan evaporation is usually measured whenever the water temperature is observed. The Lake Hefner study also confirmed that the energy-budget approach, when appropriate data are available, may be used successfully in estimating lake evaporation.

The problem in the energy balance approach to estimating evaporation is to measure or assess all other sources and sinks of energy and to leave evaporation as the only unknown. The complete energy balance of a crop volume has been expressed by C. B. Tanner (23) but it may ordinarily be considered as consisting of net radiation, R_n; heat flux to the soil by conduction, S; heat flux to the air by convection, A; and the heat of vaporization of water, E; expressed as

$$R_n = S + A + E \quad \ldots\ldots\ldots\ldots\ldots\ldots \quad (2)$$

Usually the soil heat flux is neglected but may be measured directly such as the net radiation while the sensible and latent heat terms can be separated using the Bowen ratio method (23).

There has been considerable discussion of the validity of equating the constants of the heat and vapor transport equations in the Bowen ratio and apparently such an assumption is only valid for conditions over a water surface. In using the energy budget under conditions of restricted soil moisture, as forced in estimating evapotranspiration, Ray K. Linsley, F. ASCE (15) states that the Bowen ratio is no longer useful as a means of eliminating the sensible heat exchange from consideration.

In determining the evapotranspiration from an irrigated plot, Maurice H. Halstead (8) has illustrated that a combination of both the turbulent-transfer and energy approach is required. To evaluate the "oasis-effect," Halstead recast turbulent-transfer equations so that they employed temperature and humidity differences between the surface and one height, and introduced another aerodynamic equation to indicate the height to which the influence of the oasis extends (8). Assuming conditions of net radiation, vertical wind gradient, roughness, temperature, and humidity such that the evaporation

from a 6-ft tank, when surrounded by a completely dry area, was 0.45 cm per hr; then, by increasing the size of the "oasis" to a 1-mile field, the computed evaporation rate was reduced to less than 1/3 that of the 6-ft tank. This extreme example demonstrates that actual evaporation can exceed that resulting from net radiation by a considerable amount, depending upon the size of the field and the difference between moisture conditions of the field and its surroundings. Even for a field of cotton extending 10 miles upwind, observations confirm that energy was gained from some drier area upwind (14).

H. L. Penman (20) has successfully combined the energy budget and aerodynamic approaches to compute open water evaporation. For the energy balance estimate, Penman neglected net heat flux to the water and considered the Bowen ratio to remain constant; and by assuming identity in the heat transfer and vapor transfer coefficients in the aerodynamic relations, the need for knowing the surface temperature was eliminated. Conversion factors have been applied to these hypothetical open water evaporation values to estimate what is termed potential evapotranspiration, obtained by comparing tanks with turf and water; and for a 2-yr period of observation they were found to range from 0.6 during the winter to 0.8 in the summer, at Rothamsted, England. The dominant factor in determining the seasonal cycle of the conversion factor is the range in day-time hours which leads to bigger summer values and smaller winter values in more northerly latitudes but to only a small annual range at low latitudes (21). Such coefficients only convert pan evaporation to an equivalent area of well watered vegetation and, therefore, cannot represent potential evapotranspiration due to the "oasis" effect that increases with the aridity of a locality. Besides, the Bowen ratio takes on larger values in arid climates (23) and the empirical aerodynamic relation varies with climate. Even so, important generalizations about potential evapotranspiration still hold, as stated by Penman (21):

1. "For complete crop covers of different plants having about the same colour, i.e., the same reflection coefficient, the potential transpiration rate is the same, irrespective of plant or soil type." (Physiological responses of the plant, particularly at high temperatures, may alter this response.)
2. "This potential transpiration rate is determined by prevailing weather."
3. "The transpiration of a short-green cover cannot exceed the evaporation from an open water surface exposed to the same weather."

EMPIRICAL RELATIONS

A number of empirical methods have been advanced to estimate actual and potential evapotranspiration, all employing some temperature function. Early work by Hedke (11) produced an equation wherein the seasonal estimated consumptive use (evapotranspiration) was considered proportional to the "effective" heat expressed in day degrees and taken as the difference between the monthly temperature and germinating temperature for each crop. Using yearly data in the same fashion, Robert L. Lowry and Arthur F. Johnson, F. ASCE (17) found a high correlation between consumptive use, under conditions where soil moisture was not limiting, and accumulated degree days with a base of 32°F.

H. F. Blaney, F. ASCE, and W. D. Criddle, M. ASCE (2) correlated actual measurement of consumptive use with the product of monthly mean temperature and the monthly day-time hours as a percentage of yearly day-time hours, to obtain applicable coefficients for different irrigated cropping conditions in the West. The average coefficient varies from around 0.6 for field crops to 1.2 for rice over the growth period under arid and semi-arid conditions. The coefficients, however, show a marked seasonal variation and for grapefruit in the vicinity of Phoenix, Ariz., they range from 0.55 in January to 0.75 in August (2).

A widely used method for estimating potential evapotranspiration (P.E.) is that devised by Thornthwaite (24) through correlating mean monthly temperature with evapotranspiration as determined from the water balance for valleys where sufficient moisture was available to maintain active transpiration. The equation, when obtaining 30-day month values in centimeters, takes the form

$$P.E. = 1.6\ L \left(\frac{10t}{J}\right)^a \quad \ldots\ldots\ldots\ldots\ldots\ldots \quad (3)$$

in which L represents day-time hours expressed in units of 12 hr; t is the mean monthly temperature in degree centigrade; J, a heat index obtained by the summation of the twelve monthly indices (i), in which

$$i = (t/5)^{1.514} \quad \ldots\ldots\ldots\ldots\ldots\ldots\ldots\ldots \quad (4)$$

and the value of a is obtained from a cubic function of the heat index (J), as

$$a = 0.000000675\ J^3 - 0.0000771\ J^2 + 0.01792\ J + 0.49239 \quad \ldots\ldots \quad (5)$$

In commenting on the formula, Thornthwaite (24) stated that its work-ability requires the use of nomograms and that the chief obstacle in developing a rational equation is the lack of understanding of the reason why potential evapotranspiration corresponding to a given temperature is not the same everywhere.

DEVELOPMENT OF METHOD

In seeking any new relationship to represent average potential evapotranspiration as a function of temperature, due consideration must be given to the geographical variation between temperature and radiation. Average daily temparatures in July over the eastern United States vary from 80-85° in the southern states to 65-70° over the northern tier states. In contrast, the average incoming solar radiation exhibits only a small variation (6) and for clear skies the incoming radiation is a constant quantity at the summer solstice for latitudes 25° to 50° over North America (10).

Since net radiation comprises the heat source of an area, aside from advected heat in certain localities, a relationship between temperature and net radiation is desired. Hamon (9), upon examination of limited net radiation observations and adjusting observed incoming radiation by computing total longwave nocturnal radiation, found that for monthly data net radiation could be represented as a linear function of the product of day-time hours and temperature, as

$$R_n = 5(D\ T - 27) \quad \ldots\ldots\ldots\ldots\ldots\ldots\ldots \quad (6)$$

in which R_n is the average daily net radiation in langleys (calories per square centimeter); D is the average duration of day-time hours in units of 12 hr; and T is the average daily mean temperature in degrees fahrenheit.

The need for considering wind in average estimates of potential evapotranspiration may be reckoned from the effect of wind on open water evaporation and the response of transpiring plants. For daily wind movement of 50 to 100 miles, the percent error in evaporation with percent change in wind is in the order of 0.25% in dry regions (16). Penman states (21), in reference to his formula (developed in a humid region), that it is possible to have 100% overestimate in evaporation by the aerodynamic term leading to only 10% overestimate in open water evaporation. Perhaps more conclusive in substantiating the elimination of wind as a variable under natural conditions is the response of plants. Y. Yamaoka (31), in a laboratory study of transpiration from plants exposed to constant temperature and relative humidity, found that the transpiration rate remains constant under a particular radiation intensity for wind speeds above 1 m per sec (about 2 miles per hr).

It then appears justifiable to consider wind as a constant factor in any climatological estimate of average potential evapotranspiration. For a condition, however, where an "oasis" situation exists any estimate of actual evapotranspiration would be highly dependent on advected heat and, therefore, the wind.

Adhering to the concept of potential evapotranspiration and accepting a constant Bowen ratio, we may assume that an average relative humidity exists at some height near the surface which would result in a proportionaility between the saturated vapor density at the mean surface temperature, and the average difference between the saturated vapor density at the surface and the vapor density at the reference height. Therefore, other things being equal, and referring to the turbulent transport equations, average potential evapotranspiration may be considered as proportional to the saturated water vapor density P_t at the air temperature near the surface, represented as

$$P.E. = K P_t \quad \ldots\ldots\ldots\ldots\ldots\ldots\ldots\ldots \quad (7)$$

Considering that transpiration is a daytime phenomenon due to the functioning of the leaf stomata (open only in daylight) and that turbulence occurs principally during the daytime, an adjustment for day-time hours is required. Also, the adjustment enters again to account for the disparity between net radiation and mean temperature, latitudinally.

From the preceeding considerations, it seems feasible to formulate the final simplified expression for potential evapotranspiration as

$$P.E. = C D^2 P_t \quad \ldots\ldots\ldots\ldots\ldots\ldots\ldots\ldots \quad (8)$$

in which P. E. represents the average potential evapotranspiration in inches per day; D is the possible hours of sunshine in units of 12 hr; P_t is the saturated water vapor density (absolute humidity) at the daily mean temperature in grams per cubic meter; times 10^{-2}; C = 0.55, chosen to give appropriate yearly values of potential evapotranspiration as indicated by observations reported in the literature (24), (17).

EVALUATION

Yearly values of potential evapotranspiration as obtained from the new relation (Eq. 8) for which C = 0.55, are practically identical to those obtained

by the highly complicated Thornthwaite method (Fig. 1) with a consistent departure of about 5% noted only for latitudes of southern Florida. A further evaluation on yearly data has been made by comparing average computed values of potential evapotranspiration to consumptive use data for valleys covering a wide variation in climate as obtained by Lowry and Johnson (17) and G. R. Williams, F. ASCE (30), as listed in Table 1 and shown in Fig. 2.

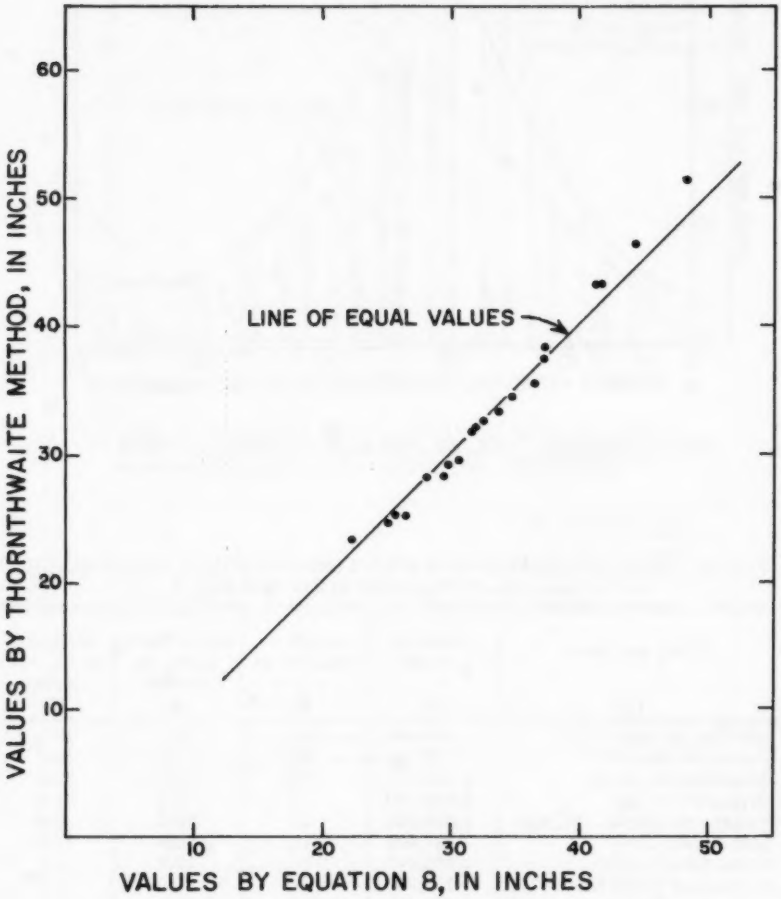

FIG. 1.—COMPARISON OF COMPUTED AVERAGE ANNUAL POTENTIAL EVAPOTRANSPIRATION

An important test of the reliability of the new relation (Eq. 8) is whether such a simplified procedure is adequate in representing the seasonal variations. Several comparisons are made.

Average monthly values of water loss from an irrigated valley, Mesilla Vally in New Mexico, are reported in the study of Lowry and Johnson (17). The

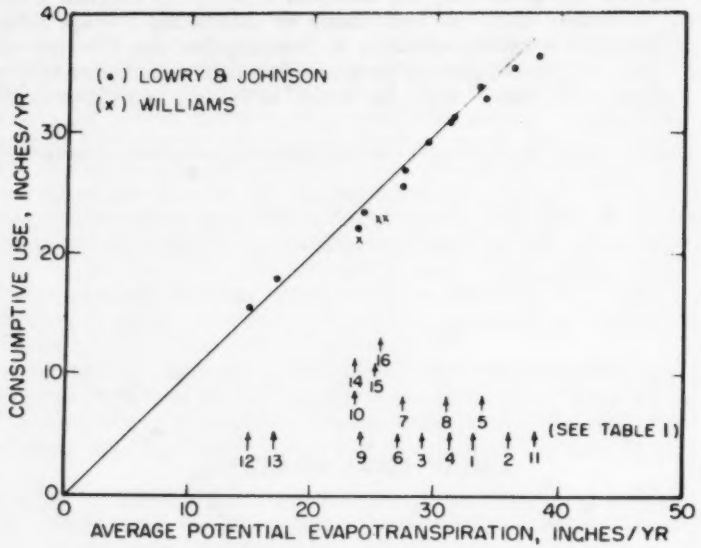

FIG. 2.—CONSUMPTIVE USE FOR BASINS COMPARED WITH COMPUTED POTENTIAL EVAPOTRANSPIRATION

TABLE 1.—DATA OF OBSERVED WATER LOSS AND COMPUTED AVERAGE POTENTIAL EVAPOTRANSPIRATION FOR FIG. 2

Valley and State (1)	Area, in acres (2)	Length of Record, in years (3)	Mean Water Loss, in inches (4)	Estimated by Eq. 8, in inches (5)
1. Mesilla, N. Mex.	109,000	13	34.0	33.4
2. Pecas, N. Mex.	37,850	18	35.3	36.3
3. Sangamon River, Ill.	1,640,000	16	29.2	29.3
4. Green River, Ky.	5,000,000	6	31.4	31.4
5. Tallapoosa River, Ala.-Ga.	1,060,000	13	33.0	34.0
6. Mad River, Ohio	307,000	13	25.8	27.3
7. Skunk River, Iowa	1,890,000	16	27.0	27.6
8. N. Fork of White River, Mo.	755,000	14	31.0	31.1
9. N. Platte, Wyo.-Neb.	462,000	9	23.8	24.1
10. Black River, Wisc.	494,000	13	22.2	23.9
11. Cypress Creek, Tex.	545,000	13	36.2	38.3
12. Wagon Wheel Gap, Colo.	222	14	15.6	15.0
13. Mich.-Ill., River, Colo.	43,000	3	18.0	17.2
14. West River, Vt.		8	21.5	23.9
15. Lake Cochituate, Mass.		30	23.2	25.1
16. Swift River, Mass.		15	23.1	25.5

correspondence of these observed values of actual water loss to computed average potential evapotranspiration is satisfactory as seen in Fig. 3.

Estimates of the average water loss for periods of adequate water supply has been obtained by W. F. Fox, F. ASCE (5) for basins in Wisconsin by the

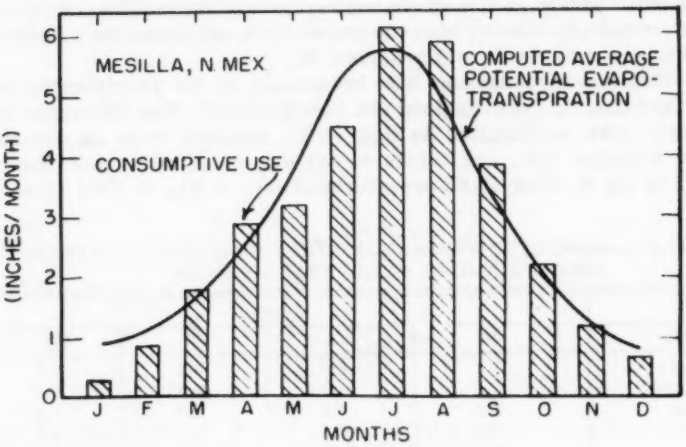

FIG. 3.—SEASONAL DISTRIBUTION OF CONSUMPTIVE USE AND POTENTIAL EVAPOTRANSPIRATION

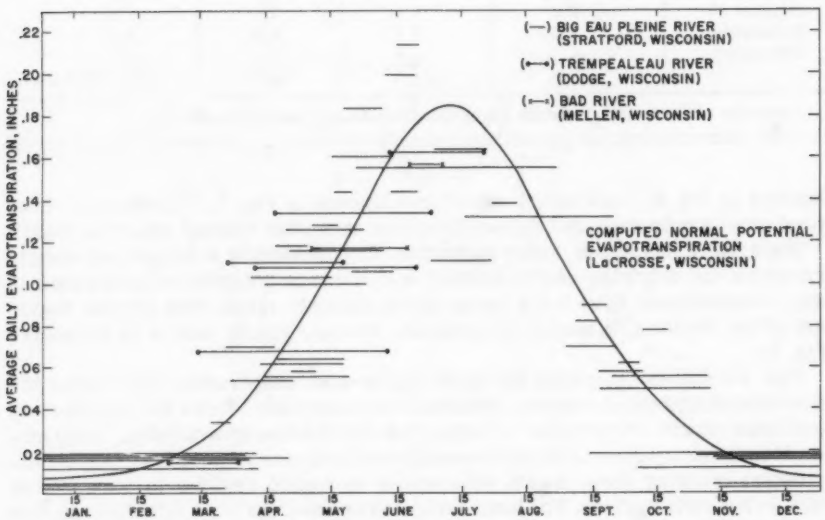

FIG. 4.—POTENTIAL EVAPOTRANSPIRATION FROM WATER BALANCE FOR BASINS

water-balance method. His determined average values of water loss and the computed curve of average potential evapotranspiration compare favorably as shown in Fig. 4.

Both Penman and Blaney (4) have computed estimates of evapotranspiration by their respective methods for Asheville, N. C., and for the climate of this location should approximate potential evapotranspiration. In addition, computations by the Thornthwaite method and by Eq. 8 have been listed in Table 2. Results from the new procedure are fully satisfactory in comparison with the other widely used methods and succeeds in correcting a short-coming of the Thornthwaite method wherein winter-time estimates are considered too low and mid-summer values excessive (18).

An extensive investigation has been made of the yearly water loss and lake evaporation in New England and New York (12). The difference between the yearly lake evaporation in this study, obtained by an adaptation of the Penman equation (16), and values of average potential evapotranspiration, obtained by Eq. 8, show small departures as seen in Fig. 5. This close corre-

TABLE 2.—COMPUTED AVERAGE MONTHLY EVAPOTRANSPIRATION FOR ASHEVILLE, N. C., BY SEVERAL METHODS

Month	Inches			
	(a)	(b)	(c)	(d)
January	1.1	0.7	0.3	0.7
February	1.1	1.1	0.4	0.9
March	2.0	2.0	1.0	1.4
April	2.4	2.7	2.1	2.3
May	3.7	4.0	3.5	3.5
June	4.8	4.8	4.9	4.7
July	5.1	4.8	5.4	5.1
August	4.7	4.0	4.9	4.4
September	3.4	2.4	3.6	3.1
October	2.2	1.7	2.1	1.8
November	1.3	0.8	0.8	1.0
December	1.1	0.6	0.4	0.7
	32.9	29.6	29.4	29.6 (Totals)

Methods: Blaney (a), Penman (b), Thornthwaite (c), and by Eq. 8 (d).

obtained by Eq. 8, show small departures as seen in Fig. 5. This close correspondence is only expected in humid regions where the "oasis" effect is small.

Since Eq. 8 has shown every indication of representing a unique and simple procedure for obtaining useful estimates of average potential evapotranspiration, computations have been made using monthly mean data for the region east of the Rockies. A map of generalized average yearly values is presented (Fig. 6).

The conditions required for potential evapotranspiration eliminates the advection of air heated over surrounding drier areas and allows for equilibrium conditions where evaporation is proportional to the energy available. Evaporation losses from pans or soil tanks are always in excess of potential evapotranspiration—ranging from small differences in humid regions to excesses of 100% in hot-arid regions. For large irrigated areas or valleys this discrepancy is practically eliminated. Under non-irrigated conditions, the actual evapotranspiration depends upon the available soil moisture and the potential evapotranspiration may be adjusted for its estimation.

The decrease in evapotranspiration in relation to soil moisture is viewed differently by various investigators. Thornthwaite (18) has adopted a system

FIG. 5.—DEPARTURE OF ANNUAL POTENTIAL EVAPOTRANSPIRATION FROM LAKE EVAPORATION, IN INCHES

FIG. 6.—COMPUTED AVERAGE ANNUAL POTENTIAL EVAPOTRANSPIRATION IN INCHES

that decreases evapotranspiration on a direct function of the remaining soil moisture on the basis of field data that showed the fraction of available energy used in evaporation as proportional to soil moisture. From data of C. H. Wadleigh (28), the suppression of plant growth and the soil moisture above the permanent wilting point are seen to vary in the same fashion with soil moisture stress. This indicates that the adjustment to potential evapotranspiration to obtain actual evapotranspiration should be made proportional to the plant available moisture under conditions where soil moisture is limiting. Whether or not soil moisture is "limiting" depends upon the soil and soil aeration, the plant, and meteorological factors.

CONCLUSIONS

The equation developed to estimate average potential evapotranspiration (Eq. 8) adheres to the desirable features of requiring only readily available mean temperature data-converted to saturation water vapor density and daytime hours, expressed in an easily computable fashion. General applicability seems justified in view of the close correspondence between observed and computed values of average potential evapotranspiration, both on a yearly and seasonal basis for widely scattered localities.

APPENDIX.—READING REFERENCES

1. "Monthly Consumptive Use Requirements for Irrigated Crops," by H. F. Blaney, Proceedings, ASCE, Vol. 85, No. IR1, March, 1959.
2. "Determining Water Requirements in Irrigated Areas from Climatological and Irrigation Data," by H. F. Blaney and W. D. Criddle, U.S. Dept. of Agric., Soil Conservation Service, Washington, D.C., 1950.
3. "Evaporation and Evapotranspiration Investigations in the San Francisco Bay Area," by H. F. Blaney and D. C. Muckel, Journal, Amer. Geophysical Union, Vol. 36, No. 5, October, 1955, pp. 813-820.
4. Discussion by H. F. Blaney of "Estimating Evaporation," by H. L. Penman, Transactions, Amer. Geophysical Union, Vol. 37, No. 1, February, 1956, pp. 46-48.
5. "Computation of Potential and Actual Evapotranspiration," by W. E. Fox, U.S. Weather Bur., Washington, D.C., 1946.
6. "Average Solar Radiation in the United States," by S. Fritz and T. H. MacDonald, Heating and Ventilating, July, 1949.
7. "The Derivation of an Equation for Potential Evapotranspiration," by M. H. Halstead, Johns Hopkins Univ. Pub. in Climatology, Vol. 4, No. 5, Seabrook, N. J., 1951, pp. 10-12.

8. "Some Meteorological Aspects of Evapotranspiration," by M. H. Halstead and W. Covey, Proceedings, Soil Sci. Soc. of America, Vol. 21, No. 5, September-October, 1957, pp. 461-468.

9. "Estimating Potential Evapotranspiration," by W. R. Hamon, Unpublished Thesis, Massachusetts Inst. of Tech., Cambridge, February, 1960.

10. "Insolation as an Empirical Function of Daily Sunshine Duration," by W. R. Hamon, L. L. Weiss, and T. W. Wilson, Monthly Weather Review, Washington, D.C., June, 1954.

11. "Consumptive Use of Water in Irrigation," Progress Report of the Duty of Water Committee of the Irrigation Division, Transactions, ASCE, Vol. 94, 1930, pp. 1349-1399.

12. "Average Annual Runoff and Precipatation in New England-New York Area," by C. E. Knox and T. J. Nordenson, U.S. Geol. Survey, Hydro. Invest. Atlas HA7, Dept. of Interior, Washington, D.C.

13. "Meteorological Aspects of Evaporation Phenomena," by M. A. Kohler, Transactions, Internatl. Assoc. of Science and Hydrology, Vol. III, pp. 421-436.

14. "Some Aspects of the Relationship of Soil, Plant and Meteorological Factors to Evapotranspiration," by R. R. Lemon, A. H. Glaser, and L. E. Salterwhite, Proceedings, Soil Sci. Soc. of America, Vol. 21, No. 5, September, October, 1957, pp. 461-468.

15. "The Common Ground of Meteorology and Hydrology," by R. K. Linsley, Bulletin, Amer. Meteorological Soc., Vol. 41, No. 8, August, 1960.

16. "Hydrology for Engineers," by R. K. Linsley, M. A. Kohler, and J. L. H. Paulhus, McGraw-Hill Book Co., New York, 1958.

17. "Consumptive Use of Water in Agriculture," by R. L. Lowry and A. F. Johnson, Transactions, ASCE, Vol. 107, 1942.

18. "The Measurement of Potential Evapotranspiration," by J. R. Mather, ed., Publ. in Climatology, Vol. VII, No. 1, Johns Hopkins Univ., Lab. of Climatology, Seabrook, N. J., 1954.

19. "Some Further Consideration of the Measurement and Indirect Evaluation of Natural Evaporation," by F. Pasquill, Q. J. Royal Meteorological Soc., Vol. 76, 1950, pp. 287-301.

20. "Natural Evaporation from Open Water, Bare Soil and Grass," by H. L. Penman, Proceedings, Royal Soc. of London, Series A, Vol. 193, 1948, pp 120-148.

21. "Evaporation: An Introductory Survey," by H. L. Penman, Netherlands Journal Agric. Sci., Vol. 4, No. 1, 1956, pp. 9-29.

22. "Eddy Diffusion of Momentum, Water Vapor and Heat near the Ground," by N. E. Rider, Philosophical Transactions, Royal Soc. of London, Series A, 1954, pp. 481-501.

23. "Energy Balance Approach to Evapotranspiration from Crops," by C. B. Tanner, Proceedings, Soil Sci. Soc. of America, Vol. 24, No. 1, January-February, 1960.

24. "An Approach toward a Rational Classification of Climate," by C. W. Thornthwaite, Geographical Review, Vol. 38, 1948, pp. 55-94.

25. "The Determination of Evaporation from Land and Water Surfaces," by C. W. Thornthwaite and B. Bolzman, Monthly Weather Review, Vol. 67, 1939, pp. 4-11.

26. "Note on the Variation of Wind with Height in the Layer near the Ground," by C. W. Thornthwaite and M. H. Halstead, Transactions, Amer. Geophysical Union, 1942, pp. 249-255.

27. "The Water Budget and its Use in Irrigation," by C. W. Thornthwaite and J. R. Mather, Water, the Yearbook of Agriculture, U. S. Dept. of Agric., Washington, D.C., 1955, pp. 346-357.

28. "Soil Moisture in Relation to Plant Growth," by C. H. Wadleigh, Water, the Yearbook of Agriculture, U.S. Dept. of Agric., Washington, D.C., 1955, pp. 358-361.

29. "Water Loss Investigations: Lake Hefner Studies," Tech. Report, U.S. Geol. Survey, Professional Paper No. 269, 1954.

30. "Natural Water Loss in Selected Drainage Basins," by G. R. Williams, et al., U.S. Geol. Survey, Water Supply Paper 846, U.S. Dept. of Interior, Washington, D.C., 1940.

31. "Experimental Studies on the Relation between Transpiration Data and Meteorological Elements," by Y. Yamaoka, Transactions, Amer. Geophysical Union, Vol. 39, No. 2, 1958, pp. 249-266.

Journal of the
HYDRAULICS DIVISION
Proceedings of the American Society of Civil Engineers

ROUGHNESS SPACING IN RIGID OPEN CHANNELS

By William W. Sayre,[1] M. ASCE, and
Maurice L. Albertson,[2] F. ASCE

SYNOPSIS

A series of experiments to determine the effect of roughness spacing on open channel flow is reported. The experiments were conducted in an 8-ft wide by 72-ft-long adjustable-slope flume. Roughness elements consisting of sheet metal baffles were placed on the bed of the flume at various longitudinal and transverse spacings.

The data are analyzed in terms of the von Kármán-Prandtl concepts of turbulent flow near a rough boundary. Logarithmic flow formulas are developed in which the roughness factor is related to the size and spacing characteristics of the roughness elements.

The experimental results are compared with those of some other investigators. In addition, some observations are made on the von Kármán turbulence coefficient and the problem of depth determination in rough channels.

INTRODUCTION

Notation.—The letter symbols adopted for use in this paper are defined where they first appear, in the illustrations or in the text, and are arranged alphabetically, for convenience of reference, in the Appendix.

Note.—Discussion open until October 1, 1961. To extend the closing date one month, a written request must be filed with the Executive Secretary, ASCE. This paper is part of the copyrighted Journal of the Hydraulics Division, Proceedings of the American Society of Civil Engineers, Vol. 87, No. HY 3, May, 1961.

[1] Asst. Civ. Engr., Colorado State Univ., Fort Collins, Colo.

[2] Dir., Colorado State Univ. Research Foundation and Prof., fo Civ. Engrg., Colorado State Univ., Fort Collins, Colo.

Many important phenomena involved in the flow of water in open channels are only partially understood. One of the most basic of these is the effect of boundary roughness on the flow.

Over the years, a number of empirical roughness formulas have been developed. Almost all are based on the Chezy formula

$$V = C\sqrt{RS} \quad \ldots\ldots\ldots\ldots\ldots\ldots\ldots\ldots \quad (1)$$

in which V is the mean velocity of flow, C denotes the Chezy resistance function, R defines the hydraulic radius of the channel cross section, and S is the slope of energy gradient. Formulas developed by Manning, Ganguillet and Kutter, Bazin, and others relate C to the boundary roughness. These formulas have little or no rational foundation. They give fair results when applied over the fairly narrow range of flow conditions on which they were based, but frequently lead to results that are seriously in error when applied outside of this range. Experiments by Sayre[3], A. R. Robinson[4] M. ASCE, and Sayre and Albertson[5], show conclusively that the roughness coefficients in these formulas do not necessarily remain constant for a particular boundary roughness.

In the last few decades, the development of the boundary layer theory has opened the way toward a rational understanding of some of the flow phenomena involving boundary roughness.

Using the von Kármán-Prandtl concepts of turbulent flow near a rough boundary in addition to data from his own experiments with pipes having sand-coated interiors, J. Nikuradse[6] developed an artificial roughness standard for pipes, that is based on the diameter of the sand grains k_s constituting the roughness.

The application by G. H. Keulegan[7] and others of the Nikuradse roughness standard to open channels has been quite successful in describing grain-type roughness in wide, open channels. However, it has been found inadequate for describing certain other types of roughness in which the relative spacing in addition to the relative size of the roughness elements is an important boundary characteristic. Dune and ripple formations on the beds of alluvial channels are considered typical of the latter type of roughness.

Using square strips extending across the bed of the channel as roughness, Ralph W. Powell[8,9], F. ASCE, studied the effect of the longitudinal spacing of the strips. Robinson[10] and Robinson and Albertson[4] reported experiments in which the size of geometrically similar roughness baffles was varied, but the

---

3 "Artificial Roughness Patterns in Open Channels," by W. W. Sayre, thesis presented to Colorado State University, at Fort Collins, Colo., in 1957, in partial fulfillment of the requirements for the degree of Master of Science.

4 "Artificial Roughness Standard for Open Channels," by A. R. Robinson and M. L. Albertson, Transactions, Amer. Geophysical Union, Vol. 33, No. 6, December, 1952, pp. 881-888.

5 "The Effect of Roughness Spacing in Rigid Open Channels," by W. W. Sayre and M. L. Albertson, Dept. of Civ. Engrg., Colorado State Univ., Fort Collins, Colo., CER59 WWS31, October, 1959, 78 pp.

6 "Strömungsgesetze in rauhen Röhren," by J. Nikuradse, Forschungsarbeiten auf dem Gebiete des Ingenieur Wesens, Heft 361, Vol. 4, 1933, Berlin, pp. 1-22.

7 "Laws of Turbulent Flow in Open Channels," by G. H. Keulegan, Journal of Research, U. S. Natl. Bur. of Standards, Vol. 21, December, 1938, pp. 707-741.

8 "Flow in a Channel of Definite Roughness," by R. W. Powell, Transactions, ASCE, Vol. 111, 1946, pp. 531-566.

9 "Resistance to Flow in Rough Channels," by R. W. Powell, Transactions, Amer. Geophysical Union, Vol. 31, No. 4, August, 1950, pp. 575-582.

10 "Artificial Roughness in Open Channels," by A. R. Robinson, thesis presented to Colorado State Univ., at Fort Collins, Colo., in 1950, in partial fulfillment of the requirements for the degree of Master of Science.

ratios of longitudinal and transverse spacings to baffle height were held constant. For a particular roughness pattern they demonstrated that the Chezy resistance function depends only on the relative roughness (ratio of flow depth to baffle height), assuming rough boundary conditions.

These and other studies have contributed toward the establishment of a reproducible artificial roughness standard that will be applicable to open channels characterized by a "dune"-type roughness. It is hoped that this study will stimulate further interest toward this end.

ANALYSIS

Theoretical Analysis.—The von Kármán-Prandtl equation for velocity distribution near rough boundaries is of the form

$$\frac{v}{\sqrt{\tau \frac{o}{\rho}}} = \frac{2.30}{\kappa} \log \frac{y}{k} + C_1 \quad \ldots\ldots\ldots\ldots\ldots \quad (2)$$

in which v is the velocity at distance y from the boundary, κ defines the von Kármán turbulence coefficient, y is the distance above the bed of the channel, k denotes the measure of roughness size, C_1 defines a constant of integration, and $\sqrt{\tau_o/\rho}$ denotes the shear velocity at the boundary. Its derivation appears in many standard fluid mechanics texts. It has been verified by experiment over a wide range of conditions in pipes, in fluids moving past a flat plate, and in open channel flow provided that secondary circulation is not an important consideration.

An expression for the mean velocity can be obtained by integrating Eq. 2 over the depth of flow in the following manner

$$V = \frac{\int_o^{y_n} v \, dy}{\int_o^{y_n} dy} \quad \ldots\ldots\ldots\ldots\ldots \quad (3)$$

that results in the expression

$$\frac{V}{\sqrt{\tau \frac{o}{\rho}}} = \frac{2.30}{\kappa} \log \frac{y_n}{k} + C_2 \quad \ldots\ldots\ldots\ldots\ldots \quad (4)$$

in which y_n is the normal depth (the depth of flow occurring when slopes of energy gradient, water surface, and bed are equal), and C_2 defines an experimental constant dependent on the roughness spacing. From the Chezy and Darcy-Weisbach equations

$$\frac{V}{\sqrt{\tau_o/\rho}} = \frac{V}{\sqrt{R\,S\,g}} = \frac{C}{\sqrt{g}} = \sqrt{\frac{8}{f}} \quad \ldots\ldots\ldots\ldots \quad (5)$$

in which C is the Chezy coefficient, R denotes the hydraulic radius, S defines the slope of the energy gradient and f is the Parcy-Weisbach resistance coefficient. Eq. 4 can thus be written in the form of a genéral resistance equation such as

$$\frac{C}{\sqrt{g}} = \frac{2.30}{\kappa} \log \frac{y_n}{k} + C_2 \quad \ldots\ldots\ldots\ldots\ldots \quad (6a)$$

or

$$\frac{1}{\sqrt{f}} = \frac{0.81}{\kappa} \log \frac{y_n}{k} + 0.35\, C_2 \quad \ldots\ldots\ldots\ldots\ldots\ldots \quad (6b)$$

Equations proposed by Keulegan, Powell, and Robinson and Albertson are of the form of Eq. 6(a). The von Kármán-Prandtl equation for rough pipes is of the form of Eq. 6(b).

Because k in Eq. 3 is defined in terms of roughness size, it is logical to conclude that C_2 must be a factor dependent upon the arrangement and shape of the roughness elements. An alternate form of Eq. 6(a) would be

$$\frac{C}{\sqrt{g}} = \frac{2.30}{\kappa} \log \frac{y_n}{X} \quad \ldots\ldots\ldots\ldots\ldots\ldots\ldots \quad (6c)$$

in which X appears as a roughness parameter dependent on the size, shape and spacing of the roughness elements. In other words, X should completely describe the boundary roughness.

Two fundamental assumptions are implicit in the foregoing analysis. The first is that the boundary is hydrodynamically rough (roughness protruding above the laminar sublayer) and that consequently viscosity has negligible effect. The second is that the channel is of sufficient width, or that the bed roughness is so great relative to the side-wall roughness or both, as to eliminate any appreciable sidewall effect.

Dimensional Analysis.—The variables used in the dimensional analysis were chosen so as to represent the experimental conditions. They can be grouped under three headings.

Boundary Characteristics.—The boundary characteristics are as follows:

- B = width of channel;
- a = height of roughness baffle;
- b = width of roughness baffle;
- x = longitudinal spacing of roughness baffles;
- e = transverse spacing between roughness baffles;
- t = thickness of roughness baffle;
- σ = shape factor of roughness elements;
- X = roughness parameter describing size, spacing and shape of roughness elements, and having the dimension of length; and
- λ = shape of channel.

Flow Characteristics.—The flow characteristics are:

- V = mean velocity of flow;
- R = hydraulic radius; and
- τ_0 = boundary shear.

Fluid Characteristics.—The following comprise the fluid characteristics;

- ρ = mass density of fluid;
- μ = dynamic viscosity of fluid; and
- $\Delta\gamma$ = difference in specific weight of water and air at the fluid interface.

If X completely defines the roughness as indicated in the theoretical analysis, the relationship existing among the variables describing the roughness

can be stated

$$\frac{X}{a} = \phi_1 \left(\frac{b}{a}, \frac{x}{a}, \frac{e}{a}, \frac{t}{a}, \sigma\right) \quad \ldots\ldots\ldots\ldots\ldots \quad (7)$$

The general relationship among the remaining variables is

$$\phi_2 (V, R, \rho, B, X, \lambda, \tau_o, \mu, \Delta\gamma) = 0 \quad \ldots\ldots\ldots\ldots\ldots \quad (8)$$

Choosing V, R, and ρ as repeating variables, the Buckingham Pi-theorem yields six π-terms among which the following relationship exists:

$$\phi_3 \left(\frac{B}{R}, \frac{X}{R}, \lambda, \frac{V}{\sqrt{\tau_o/\rho}}, \frac{VR\rho}{\mu}, \frac{V}{\sqrt{R\,\Delta\gamma/\rho}}\right) = 0 \quad \ldots\ldots\ldots \quad (9)$$

In a wide channel, y_n can be substituted for R, and if there are no side-wall effects B/R can be eliminated. Because the shape of the channel remains rectangular and wide throughout the experiments, λ can also be eliminated. Eq. 9 can now be restated as

$$\phi_4 = \left(\frac{y_n}{X}, \frac{V}{\sqrt{\tau_o/\rho}}, R, F\right) = 0 \quad \ldots\ldots\ldots\ldots\ldots \quad (10)$$

in which R and F are the Reynolds and Froude numbers respectively.

By use of

$$\frac{C}{\sqrt{g}} = \frac{V}{\sqrt{\tau_o/\rho}} \quad \ldots\ldots\ldots\ldots\ldots \quad (11)$$

Eq. 10 can be simplified and rewritten as

$$\frac{C}{\sqrt{g}} = \phi_5\left(\frac{y_n}{X}, R, F\right) \quad \ldots\ldots\ldots\ldots\ldots \quad (12)$$

If the height of the roughness elements is large relative to the thickness of the laminar sub-layer, viscous effects are negligible, and R can be eliminated. The Froude number assumes importance only when appreciable surface waves or disturbances are present. Consequently, when the boundary is hydrodynamically rough and when there are no surface eaves, Eq. 12 reduces to the simple relationship

$$\frac{C}{\sqrt{g}} = \phi_6 \left(\frac{y_n}{X}\right) \quad \ldots\ldots\ldots\ldots\ldots \quad (13)$$

Turning now to the problem of roughness geometry, Eq. 7 stated that

$$\frac{X}{a} = \phi_1 \left(\frac{b}{a}, \frac{x}{a}, \frac{e}{a}, \frac{t}{a}, \sigma\right) \quad \ldots\ldots\ldots\ldots\ldots \quad (7)$$

The ratio b/a and the shape factor of the roughness elements σ were held constant and, therefore, can be eliminated. Because t is very small (approximately

0.05 in.) relative to all other roughness dimensions, t/a can be considered in effect equal to zero, and hence of negligible importance. Because the dimensions of the individual roughness baffles remain constant the ratio X/a is independent of baffle size, and can be replaced by ψ , a parameter that appears to be dependent only on the baffle spacing. Eq. 7 can now be written in a simpler form

$$\psi = \frac{X}{a} = \phi_7 \left(\frac{x}{a}, \frac{e}{a} \right) \quad \ldots\ldots\ldots\ldots\ldots\ldots \quad (14)$$

By reasoning, the roughness size and spacing dimensions can be combined into a single dimensionless density parameter $a\,b/x(e+b)$. This parameter is numerically equal to the ratio between the combined area of all the roughness

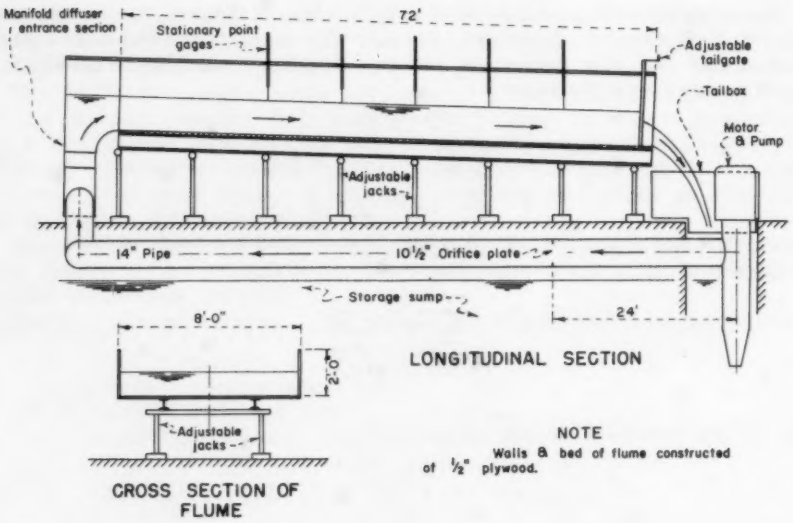

FIG. 1.—FLUME AND CIRCULATION SYSTEM

elements projected perpendicularly to the direction of flow as the numerator and the total area of the flume bed as the denominator,

$$\frac{a\,b}{x(e+b)} = \frac{\Sigma \text{ roughness area}}{\text{area of flume bed}} \quad \ldots\ldots\ldots\ldots \quad (15)$$

Another expression for the spacing parameter is then

$$\psi = \phi_8 \left(\frac{a\,b}{x\,(e+b)} \right) \quad \ldots\ldots\ldots\ldots\ldots\ldots\ldots \quad (16)$$

DESCRIPTION OF EXPERIMENTS

The experiments were conducted in an 8-ft wide by 2-ft deep rectangular flume which measured 72 ft in length. The flume and circulation system are shown in schematic form in Fig. 1.

The bed and walls of the flume were constructed of 1/2-in. plywood reinforced by 2-in. by 4-in. ribs and cross members. The flume rested on a pair of 6-in. I-beams which were supported by screw jacks at 10-ft intervals. Changes in the longitudinal slope of the flume could be accomplished by adjusting the jacks.

At the flume entrance flow was distributed and excessive local turbulence eliminated by a manifold diffuser.[12]

The water-surface level in the flume could be controlled by adjusting the vertical-slat tailgate at the downstream end of the flume. The tailbox, a 30 hp single-stage propeller pump, and a 14-in. pipeline completed the major elements of the circulation system.

The discharge was controlled by a valve in the 14-in. line. Discharge was measured by means of a 10 1/2-in. orifice plate located in the 14-in. pipe, 24 ft downstream from the pump.

Water-surface slope and flow depth were determined by five stationary point gages which were spaced over a length of 40 ft along the flume. The point gages were read with the aid of an engineer's level. An 11/32-in diameter Prandtl-type pitot tube with a tilting manometer was used to obtain velocity profiles in the vertical. The water temperature was measured with an ordinary laboratory mercury thermometer.

Sheet metal baffles measuring 6-in wide and 1 1/2-in high were used as roughness elements. As shown in Fig. 2, the baffles were placed at definite longitudinal and transverse intervals, thus forming symmetrical repeating patterns. Each baffle was centered on the space between baffles in the rows immediately upstream and downstream, hence alternate rows were the same. All patterns were symmetrical about the centerline of the flume. Half-width baffles were placed adjacent to the side walls in order to maintain the same geometry there as along the centerline. The photograph in Fig. 3 shows one of the roughness patterns. All of the patterns are shown in schematic form in Fig. 4.

In performing the experiments, the discharge, slope, and roughness pattern were the independent variables, and the normal flow depth was the primary dependent variable. Once a predetermined combination of independent variables was established, the procedure during any given run consisted essentially of manipulating the tail-gate setting until the water-surface slope equaled the slope of the flume bed. This could be done quite accurately by intentionally establishing and then interpolating between slight M_1 and M_2 backwater curves. The condition of equal slopes of the water surface and the bed defined normal flow. The depth of normal flow was then measured, and velocity profiles were obtained in at least three verticals across the flume.

Tests were conducted at discharges varying from 2 cfs to 6 cfs and at slopes of 0.001 and 0.003 for each of the six roughness patterns. A total of twenty-seven runs was made.

PRESENTATION AND DISCUSSION OF RESULTS

Data describing the overall flow characteristics and the roughness are listed in Table 1. The relationships developed in the theoretical and dimensional analysis are largely substantiated by the experimental results in the form of

12 "The Manifold Stilling Basin," by G. R. Fiala and M. L. Albertson, Dept. of Civ. Engrg., Colorado State Univ. Research Foundation, October, 1958, 32 pp.

dimensionless graphs that are presented and discussed in the following sections. In addition, information pertaining to the von Kármán turbulence coefficient, and to the problem of depth determination in rough channels is also presented.

Chezy Coefficient as a Function of Relative Roughness.—Fig. 5 is a plot of the Chezy resistance function against relative roughness based on the baffle

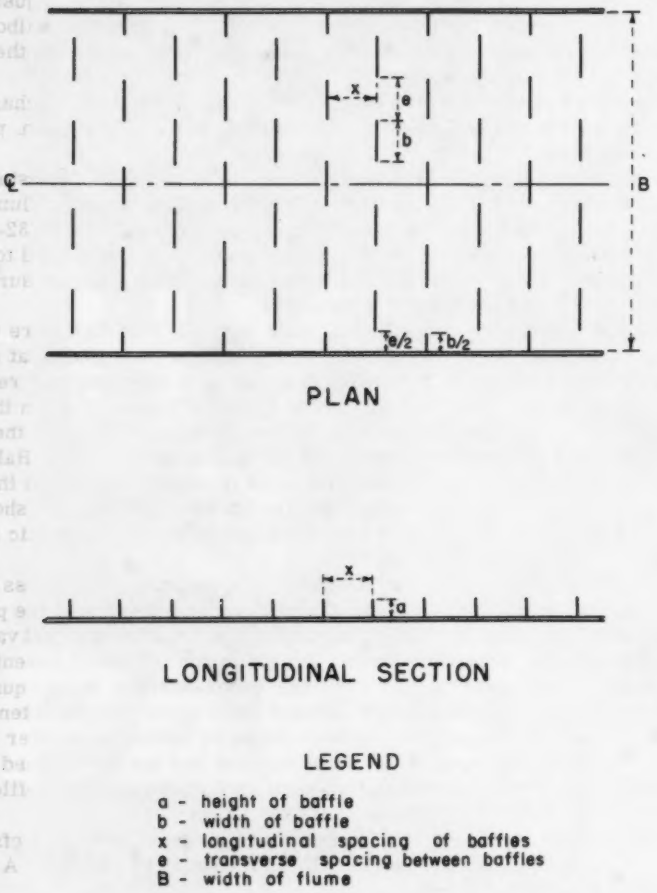

FIG. 2.—DEFINITION SKETCH OF ROUGHNESS BAFFLE INSTALLATION

height. The data fall into a family of parallel lines when plotted on semilogarithmic paper. Each line represents data obtained from experiments with a particular roughness pattern. Robinson's data[10] which are superimposed on the plot, represent experiments in which the same roughness pattern, but two different baffle sizes, were used. The roughness baffles used by Robinson were geometrically similar (b = 4a) to those used by the writers.

Data obtained by H. J. Koloseus,[11] M. ASCE, for conditions of stable flow are also plotted on Fig. 5. These tests were conducted in a 2-ft-wide flume with 3/16-in. brass cubes as roughness elements. It is interesting to note that Koloseus' data were obtained in the super-critical ($F>1$) flow range, whereas Robinson's and the writers' data all represent flow conditions well within the sub-critical range. The data are all described by the equation

$$\frac{C}{\sqrt{g}} = 6.06 \log \frac{y_n}{a} + C_2 \quad \ldots\ldots\ldots\ldots\ldots\ldots \quad (17)$$

which is similar to Eq. 6(a) given in the theoretical analysis. The constant C_2 for each line, that is each roughness pattern, is defined by extrapolation as the value of $C/\sqrt{g}$ at which $y_n/a = 1$. The writers' and Koloseus' data show

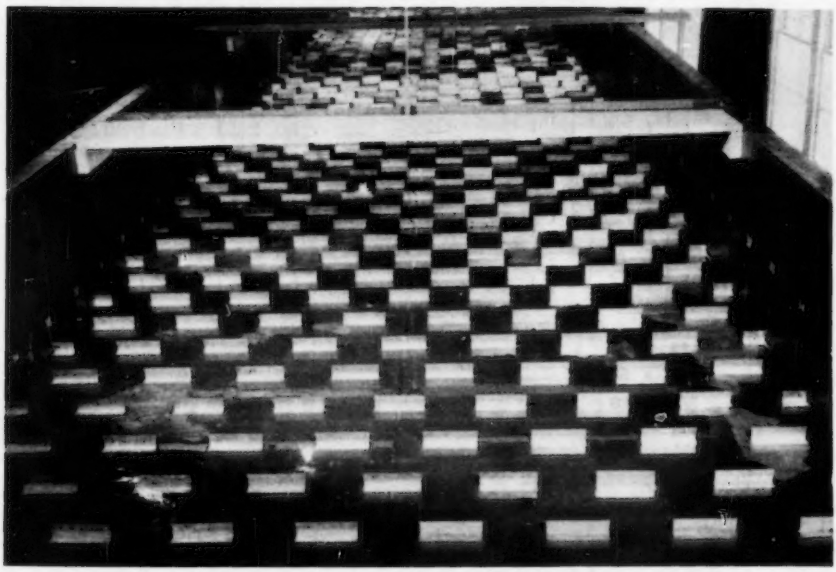

FIG. 3.—EXAMPLE OF A ROUGHNESS PATTERN

clearly that C_2 is a function of the longitudinal and transverse roughness spacing, and Robinson's data show that it is independent of absolute roughness size.

Fig. 6 is a plot of the Chezy resistance function against the relative roughness based on the roughness parameter X. Description of the boundary roughness by the single parameter X groups all the data about a single curve

11 "The Effect of Free-Surface Instability on Channel Resistance," by H. J. Koloseus, thesis presented to the State Univ. of Iowa, at Iowa City, Iowa, in 1958, in partial fulfillment of the requirements for the degree of Doctor of Philosophy.

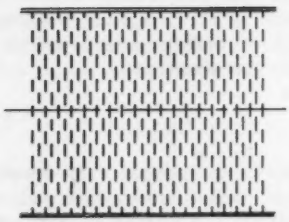

Runs 1-7
$x/a = 2$
$e/a = 3.9$

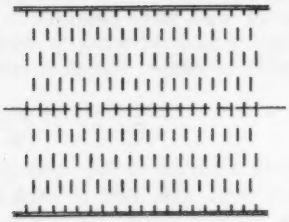

Runs 16-19
$x/a = 2$
$e/a = 11.8$

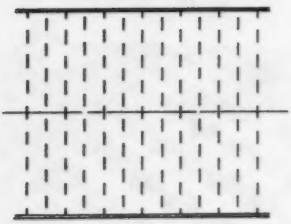

Runs 8-11
$x/a = 6$
$e/a = 3.9$

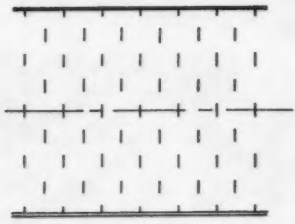

Runs 20-25
$x/a = 6$
$e/a = 11.8$

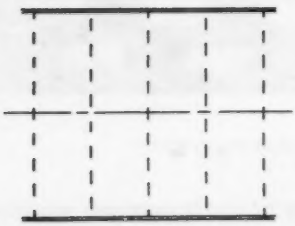

Runs 12-15
$x/a = 18$
$e/a = 3.9$

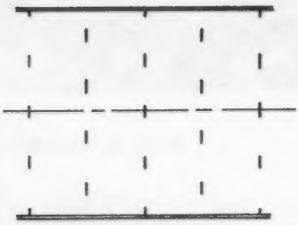

Runs 24-27
$x/a = 18$
$e/a = 11.8$

FIG. 4.—SCHEMATIC DIAGRAM OF THE SIX ROUGHNESS PATTERNS

TABLE 1.—SUMMARY OF EXPERIMENTAL RESULTS

Run	Q cfs	S	y_n ft	Temp°C	B ft	x ft	e ft	V ft/sec	R $.10^{-4}$	τ_{01} #/ft 2	τ_{02} #/ft^2	κ	κ^*	$C/\sqrt{g}$	f	n
1	4.00	0.001	0.806	10.2	7.92	0.25	0.49	0.627	3.61	0.050	0.062	0.34	0.37	3.89	0.530	0.065
2	2.00	0.001	0.591	11.0	7.92	0.25	0.49	0.428	1.85	0.037	0.026	0.45	0.37	3.08	0.844	0.078
3	5.99	0.001	0.983	10.9	7.92	0.25	0.49	0.769	5.52	0.061	0.055	0.40	0.37	4.33	0.425	0.061
4	4.01	0.003	0.634	11.1	7.92	0.25	0.49	0.799	3.72	0.118	0.142	0.35	0.37	3.22	0.770	0.076
5	2.01	0.003	0.490	11.8	7.92	0.25	0.49	0.517	1.91	0.092	0.082	0.40	0.37	2.38	1.41	0.098
6	3.00	0.003	0.566	11.7	7.92	0.25	0.49	0.669	2.53	0.106			0.37	2.85	0.986	0.084
7	6.00	0.003	0.758	11.0	7.92	0.25	0.49	1.00	5.53	0.142	0.154	0.36	0.37	3.68	0.588	0.068
8	2.00	0.001	0.512	11.0	7.92	0.75	0.49	0.493	1.85	0.032	0.034	0.37	0.39	3.84	0.544	0.061
9	6.00	0.001	0.867	10.9	7.92	0.75	0.49	0.873	5.53	0.054	0.055	0.38	0.39	5.23	0.293	0.049
10	2.00	0.003	0.402	11.3	7.92	0.75	0.49	0.629	1.87	0.075	0.095	0.34	0.39	3.17	0.800	0.071
11	5.99	0.003	0.664	11.2	7.92	0.75	0.49	1.12	5.66	0.124	0.128	0.37	0.39	4.49	0.396	0.055
12	2.00	0.003	0.313	11.3	7.92	2.25	0.49	0.807	1.87	0.059		1.32	0.35	4.61	0.378	0.047
13	5.98	0.003	0.529	11.4	7.92	2.25	0.49	1.43	5.60	0.099		0.78	0.35	6.27	0.203	0.038
14	2.00	0.001	0.395	11.5	7.92	2.25	0.49	0.639	1.87	0.025		1.03	0.35	5.65	0.251	0.040
15	5.99	0.001	0.702	11.3	7.92	2.25	0.49	1.08	5.60	0.044		0.45	0.35	7.17	0.156	0.034
16	2.00	0.001	0.465	11.7	7.92	0.25	1.48	0.543	1.89	0.029	0.031	0.37	0.38	4.43	0.408	0.052
17	5.99	0.001	0.806	11.3	7.92	0.25	1.48	0.938	5.60	0.050	0.050	0.38	0.38	5.83	0.235	0.044
18	2.00	0.003	0.361	11.5	7.92	0.25	1.48	0.700	1.87	0.067	0.067	0.38	0.38	3.73	0.575	0.059
19	5.99	0.003	0.609	11.3	7.92	0.25	1.48	1.24	5.60	0.114	0.118	0.37	0.38	5.12	0.305	0.047
20	2.00	0.003	0.327	11.8	7.92	0.75	1.48	0.772	1.90	0.061		0.38	0.38	4.31	0.430	0.051
21	6.00	0.003	0.567	11.8	7.92	0.75	1.48	1.34	5.70	0.106		0.44	0.38	5.70	0.246	0.042
22	6.00	0.001	0.750	11.4	7.92	0.75	1.48	1.01	5.61	0.047		0.42	0.38	6.51	0.189	0.038
23	2.00	0.001	0.431	11.4	7.92	0.75	1.48	0.587	1.87	0.027		0.68	0.38	4.96	0.326	0.046
24	2.00	0.001	0.328	11.7	7.92	2.25	1.48	0.770	1.89	0.021		1.77	0.36	7.48	0.143	0.029
25	5.99	0.001	0.601	11.6	7.92	2.25	1.48	1.26	5.65	0.038		0.68	0.36	9.01	0.0986	0.027
26	2.00	0.003	0.254	11.8	7.92	2.25	1.48	0.996	1.90	0.048		2.71	0.36	6.34	0.199	0.033
27	5.99	0.003	0.449	11.7	7.92	2.25	1.48	1.68	5.65	0.034		2.77	0.36	8.07	0.123	0.029

τ_{01}- $\gamma y_n S$

τ_{02}- determined from velocity profiles for $\kappa = 0.38$

κ - determined from velocity profiles

κ^* - determined from Eq. 31

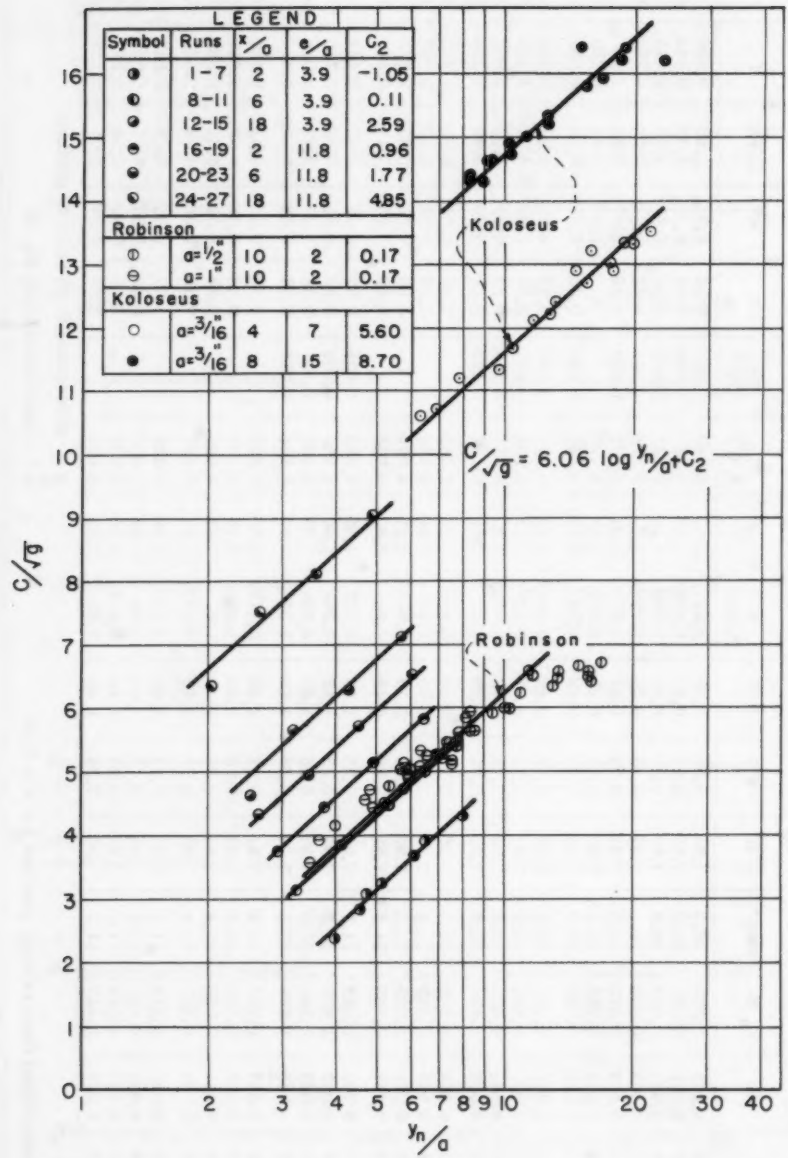

FIG. 5.—VARIATION OF RESISTANCE FUNCTION WITH RELATIVE ROUGHNESS y_n/a

described by the equation

$$\frac{C}{\sqrt{g}} = 6.06 \log \frac{y_n}{X} \quad \ldots\ldots\ldots\ldots\ldots \quad (18)$$

that is similar to Eq. 6(c) in the theoretical analysis. The parameter X has dimension of length and is a constant for a particular boundary roughness. The value of y_n extrapolated to $C/\sqrt{g} = 0$ defines X for a particular combination of baffle size and spacing. The properties of a and C_2 in Eq. 17 are combined in X according to the relationship

$$C_2 = -6.06 \log \frac{X}{a} \quad \ldots\ldots\ldots\ldots\ldots \quad (19)$$

The ratio X/a was suggested as a baffle spacing parameter ψ in the dimensional analysis.

Eqs. 17 and 18 are essentially equivalent. However, definition of the relative roughness in terms of X as in Eq. 18 appears to have a number of advantages. Grouping all of the data about a single curve is the most obvious advantage. Description of the roughness by a single term greatly facilitates the inclusion of the roughness effect in various dimensionless parameters. In addition, Eq. 18 possesses the same advantages in simplicity of application as does the Manning formula in which the single term n describes the boundary roughness.

Should it be demonstrated, however, that the coefficient 6.06 varies appreciably with roughness form or channel shape but not with roughness spacing. Eq. 17 would seem to be more significant than Eq. 18.

The empirically-determined coefficient 6.06 in Eqs. 17 and 18 is equivalent to a von Kármán turbulence coefficient of 0.38. This compares favorably with the coefficient 0.40 determined by Nikuradse[6] for turbulent flow in smooth and rough pipes, and the coefficients determined by a number of investigators in open channels.

In Figs. 5 and 6 some of the points representing observed flow conditions for the two sparsest of the writers' roughness patterns are seen to fall below the curve established by the other points. In these runs a combination of small depths and relatively high velocities occurring directly over the crests of the roughness baffles caused the formation of breaking standing waves immediately downstream from the baffles. In effect, these baffle-generated waves constituted energy sinks not accounted for by either Eq. 17 or Eq. 18. This explains the low $C/\sqrt{g}$ values obtained for these runs, and also agrees with Koloseus' results[11] for unstable flow which clearly demonstrate that channel resistance is increased in a systematic manner by free-surface instability.

The tendency of Robinson's data to drift below the curve at larger values of relative roughness is attributed to an increase in sidewall effect accompanying the increase in depth. The flume used by Robinson was only 9 in. wide, and the depth of flow in several runs approached the same magnitude.

Comparison of Chezy and Manning Formulas.—Fig. 7 compares Eq. 17 with the Manning formula. Basically it is the same plot as Fig. 5, except that it is extended over two additional log cycles of relative roughness. The straight dashed lines are extrapolations of the experimental data, each line representing a particular degree of boundary roughness. The solid curved lines represent constant values of Manning's n that were plotted on the $C/\sqrt{g}$ versus y_n/a coordinates by setting C equal to $\frac{1.49}{n}\left(\frac{y_n a}{a}\right)^{1/6}$ The line $C_2 = 10$ compares Eq.

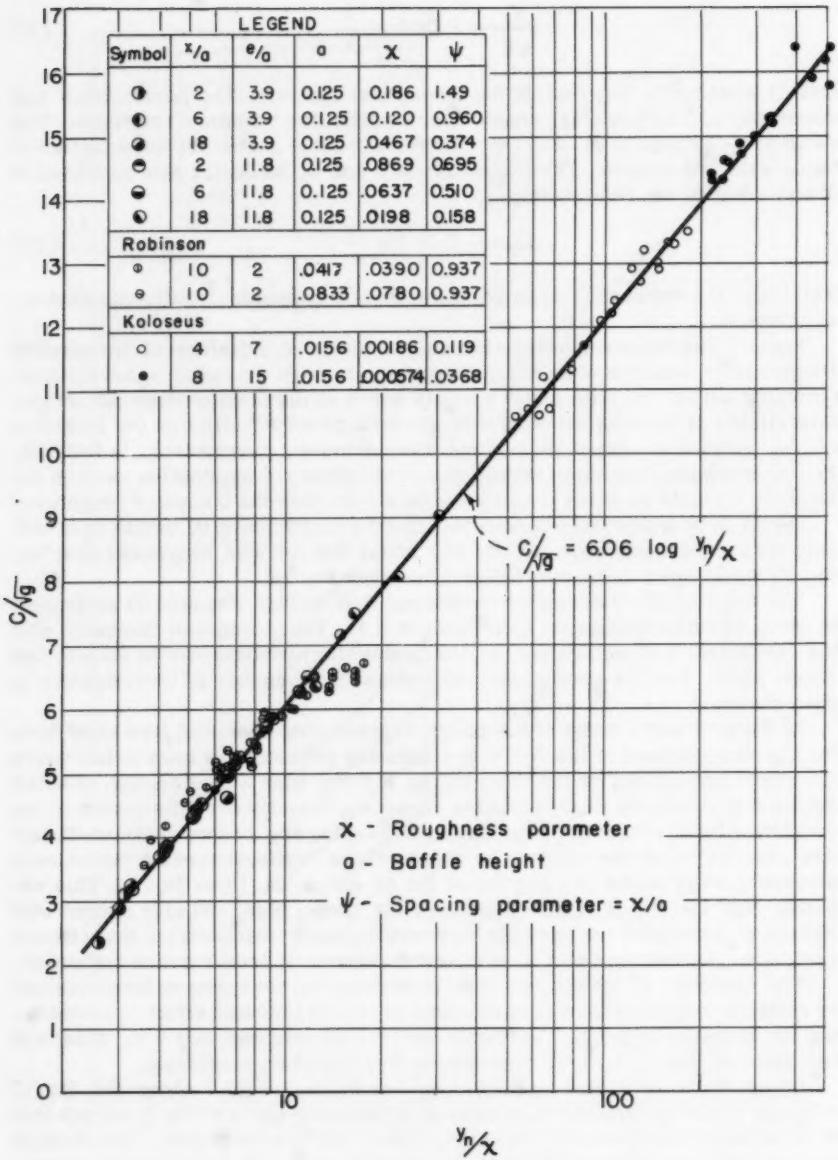

FIG. 6.—VARIATION OF RESISTANCE FUNCTION WITH RELATIVE ROUGHNESS y_n/x

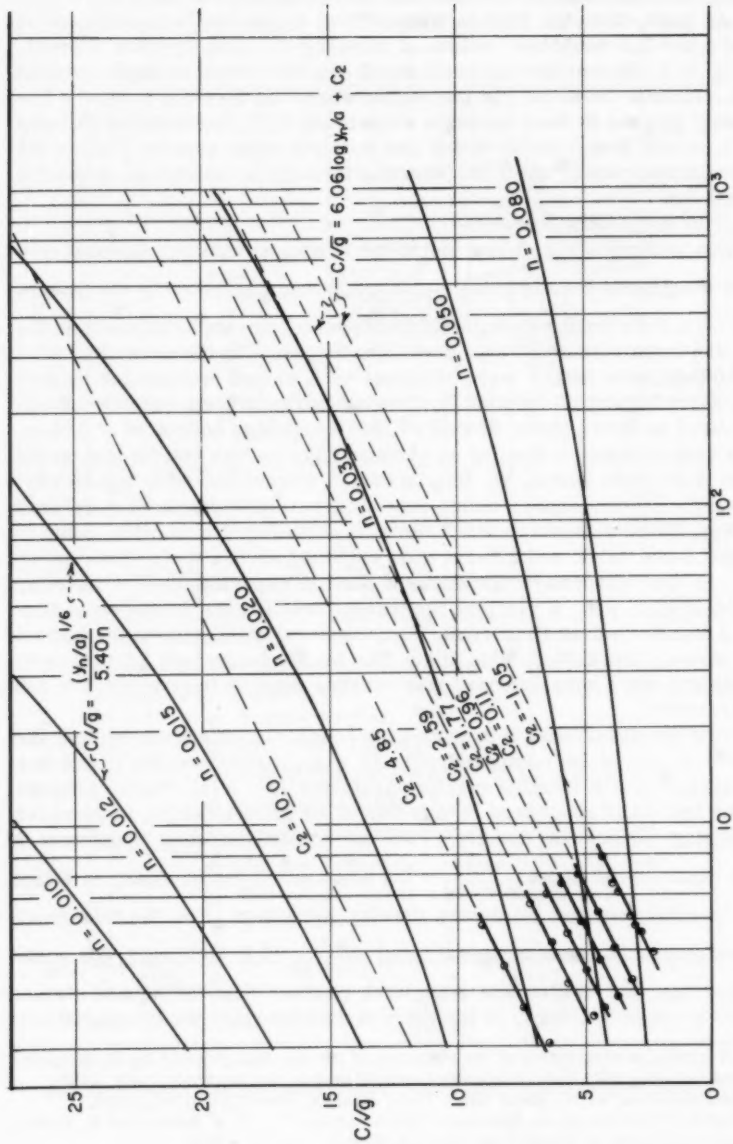

FIG. 7.—COMPARISON BETWEEN RESISTANCE BASED ON MANNING FORMULA AND ON LOGARITHMIC EQUATION

17 with the Manning formula over a range of roughness commonly encountered in practice.

Fig. 7 demonstrates conclusively that application of the Manning formula to the range of roughness included in the experiments would lead to serious error. It is seen that the boundary described by the baffle spacing ratios $x/a = 2$ and $e/a = 3.9$ would have values of Manning's n ranging from approximately 0.060 to 0.100 over the relatively small two-fold range of depth covered by the experiments. However, in the region where the Manning n curves are approximately tangent to lines having a slope of log 6.06, the Manning formula and Eq. 17 should give results which are in fairly close accord. This is the range of conditions within which the Manning formula is commonly applied to open channel flow.

Influence of Roughness Pattern.—

Resistance to Flow.—Fig. 8 is a plot of the roughness spacing parameter ψ against the roughness density ratio $\frac{a\,b}{x(e+b)}$ that was suggested in the dimensional analysis. Data from several additional sources are superimposed on the plot. Robinson's and Koloseus' data have been discussed in the preceding section. H. Schlichting's data[13] were obtained in a closed rectangular conduit measuring 4-cm high by 17-cm wide. Baffles measuring 0.3-cm high by 0.8-cm wide were fixed to the top plate. Powell's[8] 1946 roughness consisted of 1/4-in. and 1/8-in square strips extending continuously across the bottom and up the sides of an 8-in-wide flume. W. Rand's data[14] were obtained in a 2-ft-wide flume in which 1/4-in. square strips extending across the bottom were used as roughness. Bazin's experiments[15] were conducted in a 2-m-wide flume in which strips 1-cm thick and 2.7-cm wide extended across the bottom and up the sides. In the Waterways Experiment Station experiments[16] triangular ridges 0.04-ft high with a vertical upstream face and the downstream face sloped at 2 to 1 served as roughness. The ridges extended across the bottom and up the sides of the 2.08-ft-wide flume. The brushed-concrete surface upon which the ridges were superimposed was rougher than the base surface in the other experiments.

Considering the differences in roughness and channel forms it seems that the various curves should be compared only in a qualitative sense. There is a general tendency in Fig. 8 for the spacing parameter ($\psi = X/a$), that is proportional to the hydraulic roughness by a factor of roughness height, to increase with increasing roughness density. For the continuous strip roughness ψ reaches a maximum at about $\frac{a\,b}{x(e+b)} = 0.1$ after which the boundary in effect becomes smoother as the roughness density increases. For the triangular ridges, maximum roughness occurs at about $\frac{a\,b}{x(e+b)} = 0.2$. Evidently, for comparable spacings, the ridges are somewhat rougher than the square strips, particularly at close spacings. At the more distant spacings the comparitively

13 "Experimental Investigation of the Problem of Surface Roughness," by H. Schlichting, Memorandum No. 823, Natl. Advisory Committee for Aeronautics, Tech. 1937.

14 Unpublished Data, by W. Rand, State Univ. of Iowa, Iowa City, Iowa, 1952.

15 "Recherches Hydrauliques: Memoirs Divers Savants," by H. E. Bazin and H. Darcy, Science, Mathematiques, et Physiques, Vol. 19, Paris, France, 1865.

16 "Roughness Standards for Hydraulic Models Report No. 1, Study of Finite Boundary Roughness in Rectangular Flumes," Waterways Experiment Sta., U. S. Corps of Engrs., Vicksburg, Miss., Tech. Memorandum No. 2-364, 1953, 29 pp.

rough brushed-concrete surface that served as a base for the triangular ridges evidently came into play.

For the continuous roughness, it is interesting to note that the roughness density parameter reduces to a/x, because the transverse spacing e between roughness elements is zero. It seems likely that the curves representing the

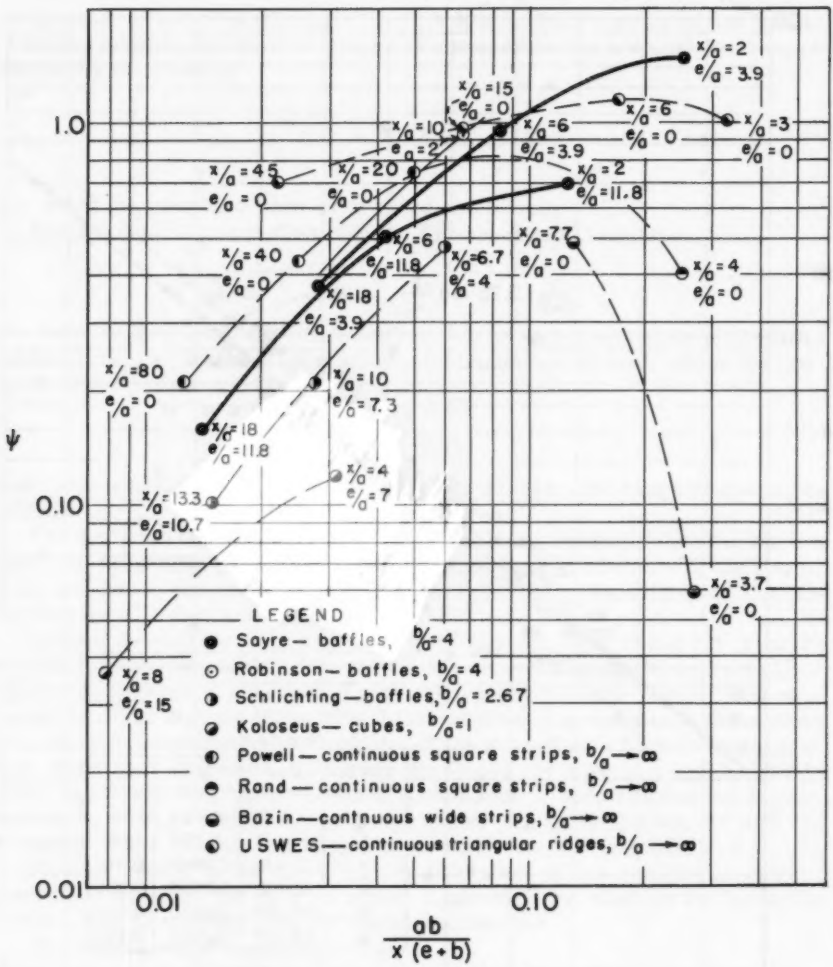

FIG. 8.—VARIATION OF SPACING PARAMETER WITH ROUGHNESS DENSITY

isolated roughness elements (baffles and cubes) also should reach maximum values of ψ, but at greater roughness densities that extend beyond the range of the data.

As would be expected, the rising limbs of the curves in Fig. 8 are arranged in order of increasing relative width (b/a) of the roughness elements as the spacing parameter ψ increases.

A plot somewhat similar to Fig. 8 which contains more complete data for continuous-strip roughness has been given by Joe W. Johnson, M. ASCE, and E. A. LeRoux.[17]

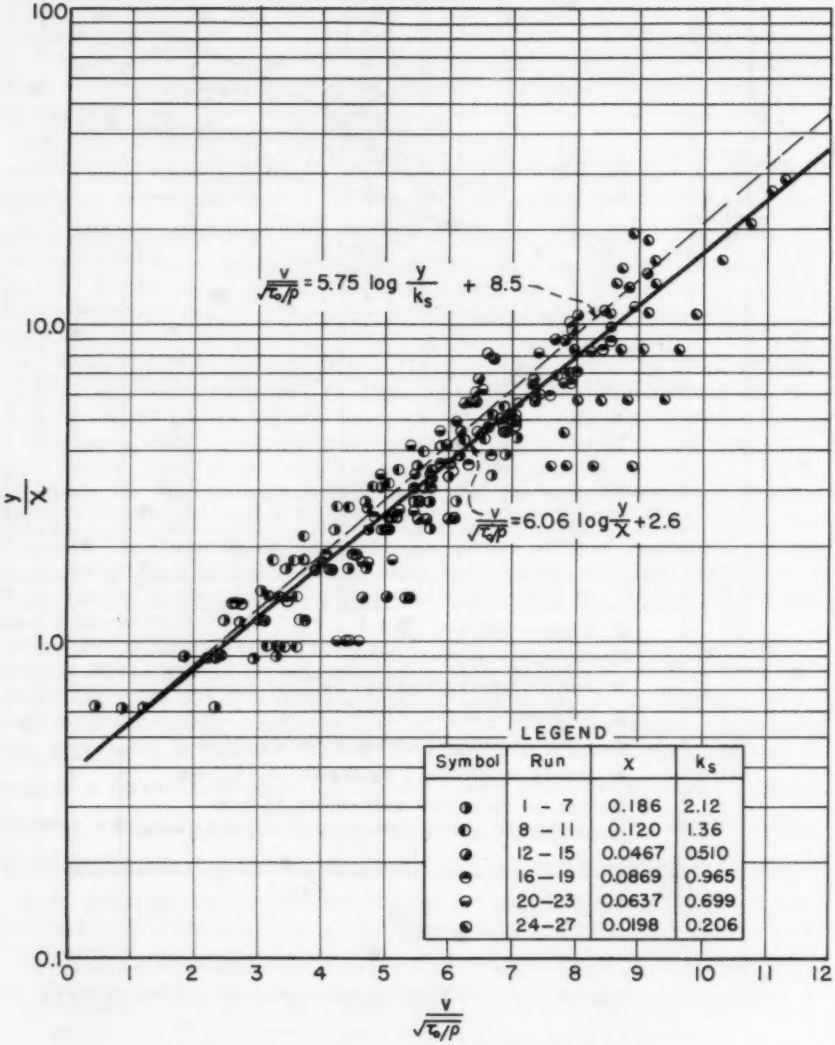

FIG. 9.—DIMENSIONLESS VELOCITY PROFILES

[17] Discussion by J. W. Johnson and E. A. LeRoux of "Flow in a Channel of Definite Roughness," by R. W. Rowell, Transactions, ASCE, Vol. 11, 1946, pp. 555-559.

Velocity Distribution.—Profiles of velocity distribution in the vertical are plotted in dimensionless form on Fig. 9. Each point represents a weighted average of at least three readings taken at the same elevation above the bed, but at different verticals across the width of the flume. The weights were assigned according to the position of the vertical with respect to the roughness elements.

The nature of the velocity profiles clearly seems to have been affected by roughness pattern, particularly by the longitudinal spacing of the baffles. Velocity profiles for the four denser roughnesspatterns are quite well represented by the equation

$$\frac{v}{\sqrt{\tau \frac{o}{\rho}}} = 6.06 \log \frac{y}{X} + 2.6 \quad \ldots\ldots\ldots\ldots\ldots \quad (20)$$

for which the constants were determined empirically.

For the sake of comparison the von Kármán-Prandtl equation

$$\frac{v}{\sqrt{\tau \frac{o}{\rho}}} = 5.75 \log \frac{y}{k_s} + 8.5 \quad \ldots\ldots\ldots\ldots\ldots \quad (21)$$

for velocity distribution in turbulent flow near a rough boundary is plotted as a broken line. The Nikuradse sand-grain roughness k_s is related to X by the nonlinear relationship

$$k_s = \frac{12.2\ X^{1.053}}{y_n^{0.053}} \quad \ldots\ldots\ldots\ldots\ldots \quad (22)$$

that corresponds approximately to $k_s/X = 11$ over the range of conditions tested.

The deviation of the points representing velocity readings taken for the two sparsest roughness patterns is attributed to the non-uniformity of the roughness and hence the turbulence in the sparse-pattern experiments. The raw velocity-profile data are available.[5]

General Resistance Diagrams for Open Channels.—Fig. 10 and Fig. 11 were plotted for the purpose of determining the order and range of hydrodynamic roughness covered in the experiments. Some available open-channel data representing other regions of the roughness spectrum are included in these plots as a means of testing the applicability of the Prandtl-von Kármán-Nikuradse type resistance diagrams, that were developed for flow in pipes, to flow in wide, rigid-boundary open channels. Assumption of wide-channel conditions, that is $y_n = R$, is justified for all data shown on Fig. 10 and Fig. 11 with the exception of the smooth-boundary data in which case R was substituted for y_n.

Fig. 10, which is an open-channel adaptation of the well-known general resistance diagram for flow in pipes, illustrates the effect of the Reynolds number, that is viscosity, on the resistance function.

The laminar-flow equation

$$\frac{C}{\sqrt{g}} = 0.577\ R^{1/2} \quad \ldots\ldots\ldots\ldots\ldots \quad (23)$$

is derived directly from the following equations describing steady, uniform, laminar flow

$$\frac{dp}{dx} = \frac{d\tau}{dy} \quad \ldots\ldots\ldots\ldots\ldots \quad (24a)$$

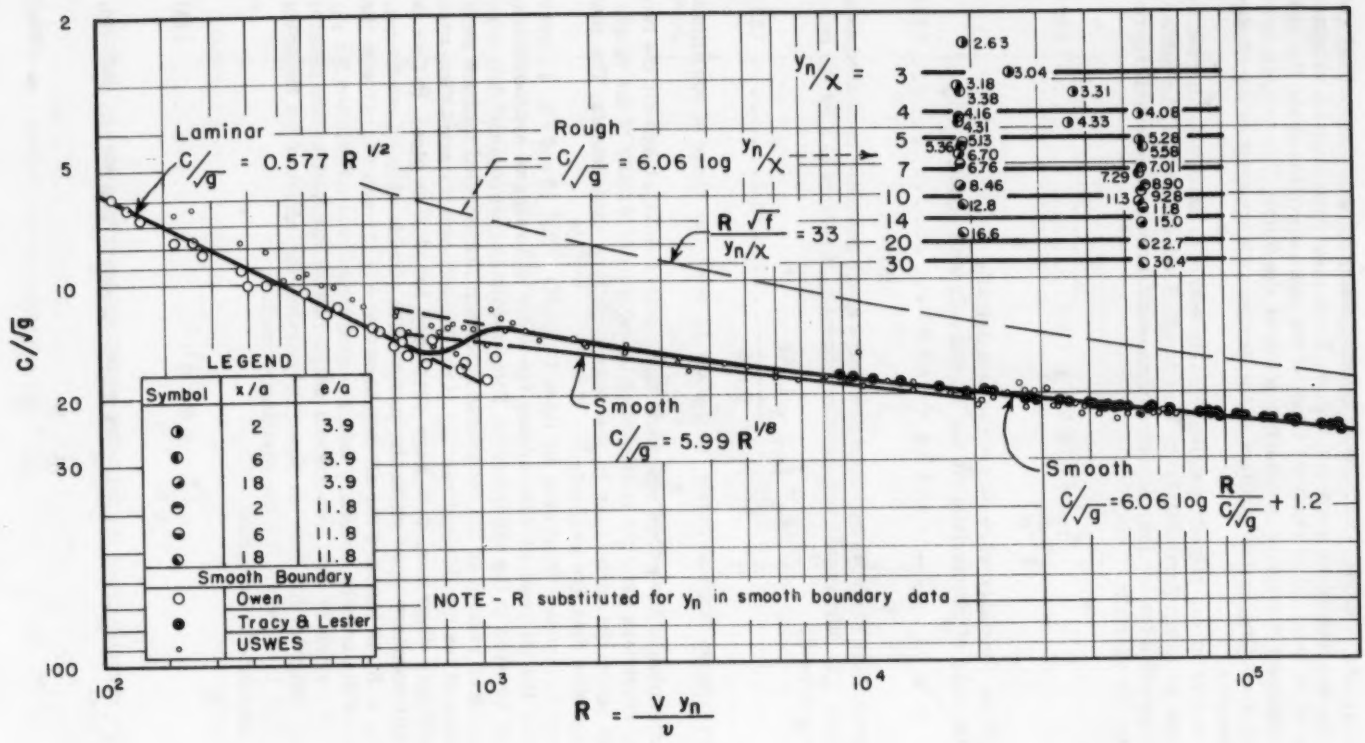

FIG. 10.—GENERAL RESISTANCE DIAGRAM FOR UNIFORM FLOW IN OPEN CHANNELS

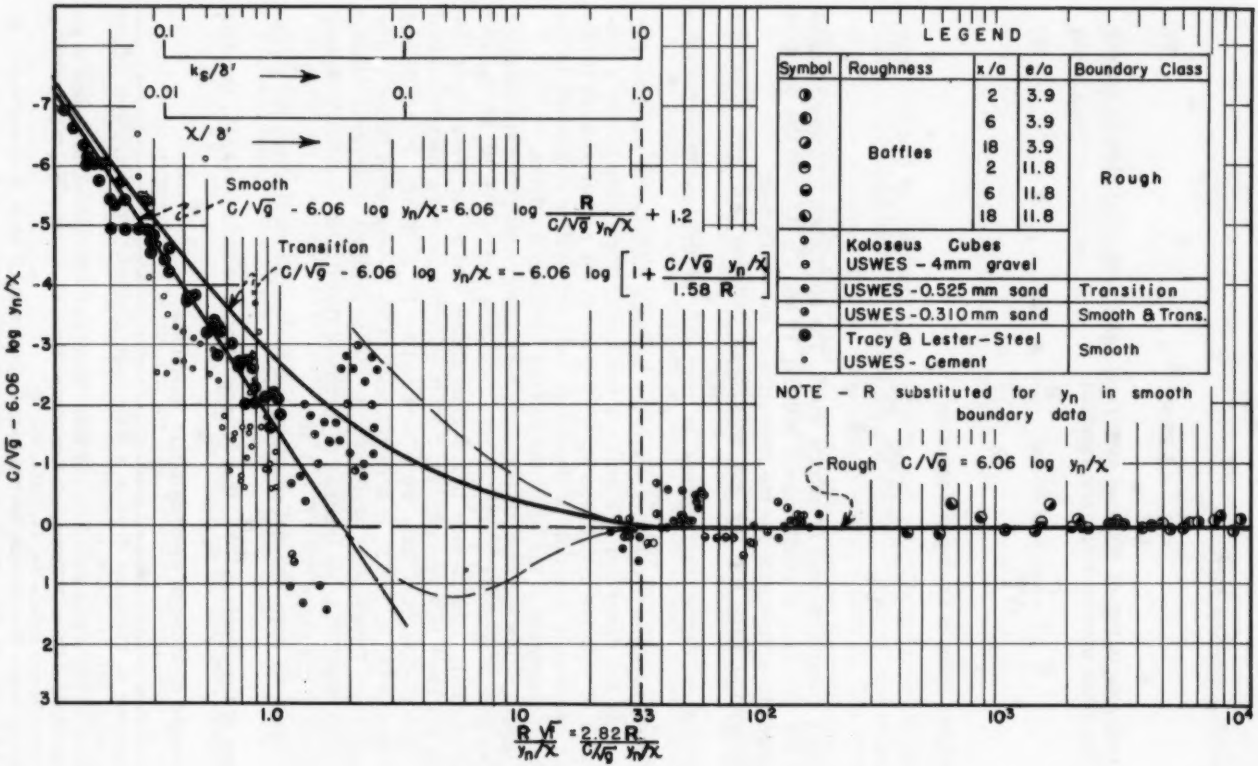

FIG. 11.—TRANSITION FUNCTION FOR UNIFORM FLOW IN OPEN CHANNELS

and $$\tau = \mu \frac{dv}{dy} \quad \ldots\ldots\ldots\ldots\ldots\ldots \quad (24b)$$

The smooth-boundary formula

$$\frac{C}{\sqrt{g}} = 5.99\, R^{1/8} \quad \ldots\ldots\ldots\ldots\ldots\ldots \quad (25)$$

is a direct adaptation of Blasius' empirical relationship for flow in smooth pipes. The other smooth-boundary equation

$$\frac{C}{\sqrt{g}} = 6.06 \log \frac{R}{\frac{C}{\sqrt{g}}} + 1.2 \quad \ldots\ldots\ldots\ldots \quad (26)$$

is a modified form of Keulegan's equation[7]

$$\frac{C}{\sqrt{g}} = 5.75 \log \frac{R}{\sqrt{\frac{C}{g}}} + 3.0 \quad \ldots\ldots\ldots\ldots \quad (27)$$

for flow in a smooth channel of infinite width. The coefficient 5.75 was changed to 6.06 for the sake of conformance with Eq. 17 and Eq. 18, and the constant was changed to compensate for the alteration of the coefficient.

Experimental data for the six roughness patterns fall well within the rough-boundary region that begins at $\frac{R\sqrt{f}}{y_n/\chi} = 33$. At this condition the ratio χ/δ' of the roughness to the thickness of the laminar sublayer is one (see Fig. 11). The data are described by a family of horizontal lines, each having a constant value of relative roughness y_n/χ. Hence, in the region covered by the data, the resistance function is dependent only on relative roughness and is therefore independent of the Reynolds number or viscous effects.

The laminar-flow and smooth-boundary data shown on the plot were obtained from a variety of sources. Laminar-flow data were obtained by W. M. Owen[18] in a rectangular, 1.50-ft-wide brass-plate flume, and by the Waterways Experiment Station[19] in a rectangular, 2.30-ft-wide flume with a smooth cement finish. Smooth-boundary data were obtained by H. J. Tracy, F. ASCE, and C. M. Lester,[20] A. M. ASCE, in a rectangular, 3.50-ft-wide steel flume and by the Waterways Experiment Station[20] in the previously described cement flume. The transition from laminar to turbulent flow for the smooth-boundary data occurs in the range $700 < R < 1{,}200$.

Fig. 11 is an open-channel adaptation of the transition function for pipes. By means of the abscissa $\frac{R\sqrt{f}}{y_n/\chi}$, that is proportional to the ratio χ/δ', the data are arranged in order of hydrodynamic roughness.

---

18 "Laminar to Turbulent Flow in a Wide Open Channel," by W. M. Owen, Transactions, ASCE, Vol. 119, 1954, p. 1157.

19 "Study of River Bed Materials and their Movement with Special Reference to the Lower Mississippi River," Waterways Experiment Sta., U. S. Corps of Engrs., Vicksburg, Miss., Tech. Memorandum No. 17, 1935, 161 pp.

20 "Experiments in a Smooth, Rectangular Open Channel," by H. J. Tracy and C. M. Lester, Administrative Report, U. S. Geol. Survey, 1959.

The smooth-boundary equation

$$\frac{C}{\sqrt{g}} - 6.06 \log \frac{y_n}{X} = 6.06 \log \frac{R}{\frac{C}{\sqrt{g}} \frac{y_n}{X}} + 1.2 \quad \ldots\ldots\ldots \quad (28)$$

is obtained merely by subtracting $6.06 \log y_n/X$ from both sides of Eq. 26. The transition equation

$$\frac{C}{\sqrt{g}} - 6.06 \log \frac{y_n}{X} = -6.06 \log \left[1 + \frac{\frac{C}{\sqrt{g}} \frac{y_n}{X}}{1.58\ R} \right] \ldots\ldots\ldots \quad (29)$$

was obtained by combining the smooth and rough-boundary equations in the manner proposed by C. F. Colebrook and White[21] for pipes, and is asymptotic to both the smooth-boundary and rough-boundary equations. The broken-line curves, indicating the extremes of the transition region, approximate the positions of the uniform and non-uniform sand roughness curves on the trnasition plot for pipes.

Data for the six roughness patterns appear at the rough end of the scale. Although most of the data representing Koloseus' two patterns also fall in the rough-boundary region, a few points representing the sparser of the patterns lap over slightly into the transition region. The Waterways Experiment Station data[19] for beds consisting of 4 mm gravel, 0.525 mm sand, 0.310 mm. sand and smooth cement, and the steel-flume data of Tracy and Lester[20] are also plotted on Fig. 11. The alluvial-bed data all represent flow conditions before the beginning of movement, so that in all cases the boundary is in effect rigid. In plotting the smooth-boundary data, it was assumed that $X = 0.00004$ ft for the smooth-cement finish, and that $X = 0.00001$ for the steel surface. Eq. 22 was used in computing X-values from the median diameters of the 0.525-mm sand ($X = 0.00019$ ft) and the 0.310-mm sand ($X = 0.00011$ ft). The 4-mm gravel data fall mostly in the rough-boundary region, overlapping into the transition region. The data for the 0.525-mm sand fall in the transition region, for the 0.310-mm sand in the transition and smooth regions, and for the smooth-cement and steel-flume surfaces, along the smooth-boundary curve.

Scattering of the data in the smooth-boundary and transition regions is not as great as it appears to be when it is remembered that the ordinate $C/\sqrt{g} - 6.06 \log y_n/X$ is a direct difference rather than a percentile deviation index. For example, considering a hypothetical point located at $C/\sqrt{g} - 6.06 \log y_n/X = -3$ and $\frac{R\sqrt{f}}{y_n/X} = 0.320$, the deviation on the ordinate scale from the smooth-boundary curve is one unit or 25%. However, based upon a $C/\sqrt{g}$ value of 15, which is about average for the data in the smooth and transition regions, deviation by one unit amounts to less than 7%.

The ratios X/δ' and k_s/δ' are plotted along the abscissa scale of Fig. 11. The ratio $k_s/X = 10$ is an average over the approximate range of relative

21 "Turbulent Flow in Pipes, with Particular Reference to the Transition Region Between the Smooth and Rough Pipe Laws," by C. F. Colebrook, Journal, Inst. of Civ. Engrs., Vol. 11, 1939, pp. 133-156.

roughness $10,000 > y_n/\chi > 1$ included in the data plotted on Fig. 11. The fact that the rough-boundary region begins at approximately $\chi/\delta' = 1$ appears to be significant. This compares with $k_s/\delta' = 6$ indicated[22] by Hunter Rouse F. ASCE, as the approximate demarcation between the transition and rough-boundary regions for pipes.

The wide band within which data may fall in the transition region can be explained on the basis of roughness spacing or size distribution or both. Where the spacing between roughness elements is large or the size of roughness elements is not uniform, isolated elements even at $\chi/\delta' << 1$ may project above the laminar sublayer in sufficient numbers to upset the turbulence pattern generated by the smooth boundary, but not in sufficient numbers to cause rough-boundary turbulence. However, when the roughness elements are densely-packed and uniform in size, smooth-boundary flow may persist at χ/δ' approaching one and the transition from smooth to rough boundary conditions would be much more abrupt.

The von Kármán Coefficient.—One of the purposes of the study was to throw some additional light on the question of how the von Kármán κ might vary, if in fact it does vary, with boundary roughness as suggested by Rand.[23]

The coefficient κ initially appeared in the literature as a "universal constant" of turbulent exchange in von Kármán's hypothesis[24] of turbulent similitude. On the basis of Nikuradse's work[6] with smooth and rough pipes, the value of κ has commonly been accepted as equal to 0.40, although Vito A. Vanoni[25] F. ASCE, in analyzing Nikuradse's data found κ-values ranging from 0.32 to 0.42 with 0.37 as an approximate average. Evidence has been mounting steadily to show that κ, as expressed in the logarithmic velocity distribution equations, is not a constant, but is systematically influenced by such factors as suspended-sediment concentration, secondary circulation, and perhaps boundary roughness.

In the experiments reported herein two methods of determining κ were used. In the first method κ was determined from analysis of the velocity-profile data through use of the relationship.

$$\kappa = \frac{2.30\sqrt{\frac{\tau_o}{\rho}}}{\Delta v} \quad \ldots\ldots\ldots\ldots\ldots\ldots \quad (30)$$

in which $\sqrt{\tau_o/\rho} = \sqrt{g}\, y_n S$ and Δv is the change in velocity over one logarithmic cycle of depth. The portions of the velocity profiles that followed most closely a logarithmic distribution were used in determining κ, and velocity measurements close to either the baffle crests or the water surface were given only secondary consideration.

The second method of determing κ was based on Eq. 6a from which it is seen that the slope of each of the lines drawn in Fig. 5 is defined by the quantity

---

22 "Elementary Mechanics of Fluids," by H. Rouse, John Wiley and Sons, Inc., New York, 1946, 376 pp.

23 Discussion by W. Rand of "Wind-Tunnel Studies of Sediment Movement," Proceedings, Fifth Hydr. Conf., State Univ. of Iowa, Bulletin 34, 1953, pp. 132-133.

24 "Mechanische Ahnlichkeit und Turbulenz," by Theodor von Kármán, Proceedings, Third Internatl. Congress for Applied Mechanics, Stockholm, Sweden, 1930.

25 "Some Effects of Suspended Sediment on Flow Characteristics," by V. A. Vanoni, Proceedings, Fifth Hydr. Conf., State Univ. of Iowa, Studies in Engrg., Bulletin 34, 1953, pp. 137-158.

$2.30/\kappa$. Best-fit lines were drawn through the data representing each roughness pattern in Fig. 5 and an average or integrated κ-value for each roughness pattern was obtained from the relationship

$$\kappa = \frac{2.30}{\frac{\Delta C}{\sqrt{g}}} \quad \ldots\ldots\ldots\ldots\ldots \quad (31)$$

in which $\Delta C/\sqrt{g}$ is the change in the resistance function over one logarithmic cycle of relative roughness.

In Fig. 12 κ is shown as a function of roughness density. Values of κ as determined by both methods are shown on this plot. The curves compare the average κ-values as determined by each method, each point on the curve representing an average value of κ determined from all the runs for a particular roughness pattern.

Fig. 12 indicates that the roughness pattern is instrumental in causing the apparent variation in κ. The principal significance of Fig. 12, however, lies in the comparison between the average κ-values as determined by the velocity-profile method and the integrated method. Agreement is remarkably good for the three denser patterns, but for the two sparsest patterns there is little semblance of agreement. It is probable that the integrated method provides a more reliable index of κ than does the velocity-profile method, and that the large apparent κ-values obtained by the velocity-profile method for the sparse patterns are indicative of large-scale local vortices set up by the isolated roughness baffles, rather than such large variations in κ. This is to be expected, however, because the κ- theory was originally developed for cases of wake-interference flow in pipes, where the turbulence, close to the boundary, is essentially random in nature. Extension of this theory to the isolated-roughness case, where the flow is three dimensional or the roughness is non-uniform, or both, is, therefore, neither logical nor justified.

This being the case, the portion of Fig. 12 drawn as a solid line appears to justify the adoption of an average value of κ for the range of conditions tested. In effect, selection of the constant 6.06 as the coefficient in Eqs. 17 and 18 amounted to adopting the average value $\kappa = 0.38$.

It cannot be said that the experimental results provided an entirely satisfactory answer to whether the von Kármán κ is in fact a constant for clear water in open-channel flow, or how and why κ might vary if it is not a constant. For the type of roughness studied, the velocity distribution method of determining κ proved deficient in a number of respects for the sparse patterns. Without taking a large number of velocity profiles in verticals at various positions relative to the roughness baffles, it was impossible to ascertain whether or not a truly representative picture of the velocity distribution had been obtained. Limitations in the velocity-measuring equipment and deviations from the logarithmic law close to the baffles and near the water surface added to the complications. Nevertheless, based on the experimental results, indications are that, provided the conditions of essentially wake-interference flow and uniform roughness are met, κ is a constant for steady, uniform flow of clear water.

Depth Determination in Rough Channels.—Various investigators, such as, Rand[26], have suggested that when roughness elements are closely spaced, the

[26] Discussion by W. Rand of "Artificial Roughness Standards for Open Channels," Transactions, Amer. Geophysical Union, Vol. 35, No. 4, August, 1954, pp. 649-650.

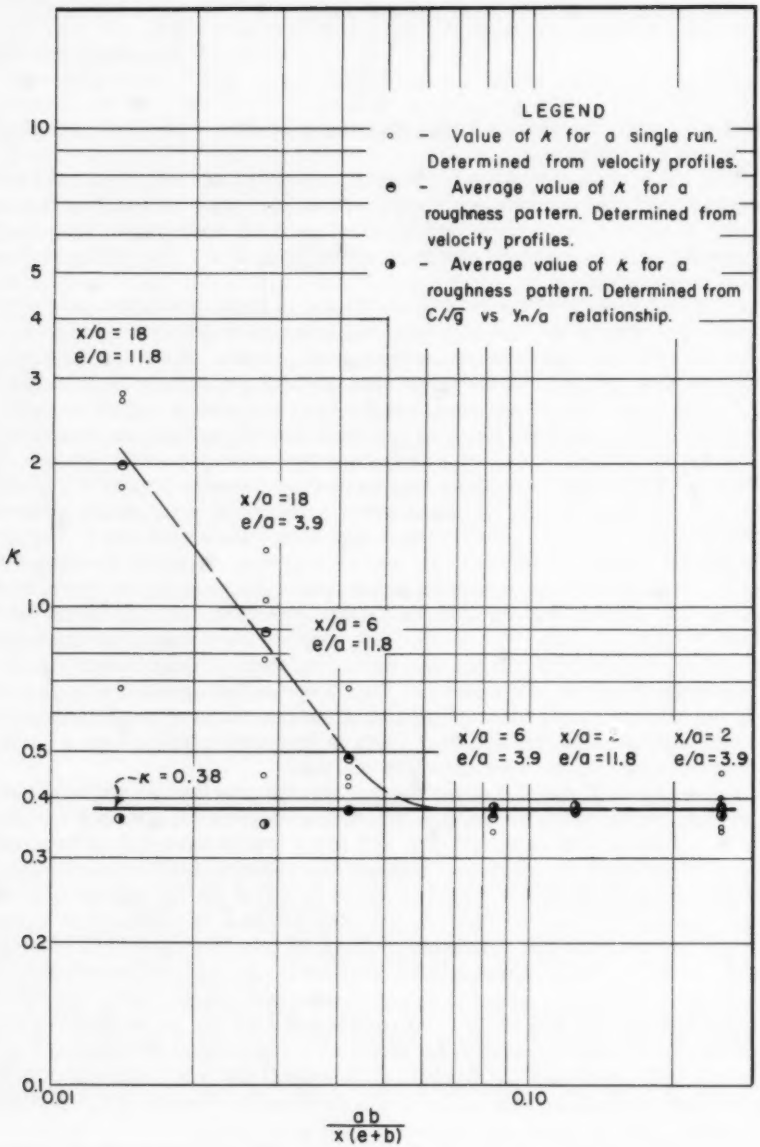

FIG. 12.—VARIATION OF VON KÁRMÁN COEFFICIENT WITH ROUGHNESS DENSITY

depth of flow should be measured from the water surface to some reference level between the crests and the troughs of the roughness elements.

As implied in the section describing the experiments, the depth of flow as measured from the water surface to the flume bed was used in the analysis. However, quite an extensive study was made of the velocity profiles obtained for the three densest roughness patterns before it was decided not to apply any depth corrections.

A detailed description of the depth-correction analysis is beyond the scope of this paper. The negative results of this analysis appear justified for quite dense roughness patterns, however, when the roughness elements consist of thin isolated baffles such as used in these experiments. This type of roughness geometry permits flow through the transverse spaces between roughness elements. In addition, because the proportion of the total bed area actually taken up by the roughness elements— $\frac{t\,b}{x(e+b)} \approx 0.008$ for the densest pattern—is extremely small, the turbulence down close to the bed level of the flume is probably not greatly inhibited. The results of turbulence flume studies by Albertson[27] reinforce these hypotheses. In these studies a staggered pattern of individual roughness baffles proved extremely effective in maintaining large sediment concentrations in suspension without appreciable deposit, whereas extensive deposits occurred at comparable concentrations when the roughness consisted of baffles extending continuously across the width of the flume. These studies have application here because of the basic similarity between the mechanisms of mass transfer and momentum transfer.

CONCLUSIONS

Analysis of the experimental data from this and other studies gives rise to the following conclusions with respect to evaluating the roughness of rigid-boundary, rough open channels:

1. The experimental results give additional evidence that the variation of the Chezy resistance function with the relative roughness is logarithmic in nature.

2. The equations

$$\frac{C}{\sqrt{g}} = 6.06 \log \frac{y_n}{a} + C_2 \quad \ldots\ldots\ldots\ldots \quad (17)$$

and

$$\frac{C}{\sqrt{g}} = 6.06 \log \frac{y_n}{X} \quad \ldots\ldots\ldots\ldots\ldots \quad (18)$$

are found to apply over the range of roughness conditions encountered in the six arrangements of roughness baffles tested. In these equations, the constant C_2 depends only on the relative spacing of roughness elements of height a, and the general roughness parameter X is a function of both the relative size and relative spacing of the baffles.

3. Eq. 17 is shown to be considerably more accurate than the Manning formula over the range of roughness and flow tested.

---

27 "Turbulence Flume to Measure Bed Load," by M. L. Albertson, Transactions, Amer. Geophysical Union, Vol. 32, No. 6, December, 1951, pp. 909-911.

4. The ratio $\frac{a\,b}{x(e+b)}$ which is equivalent to the combined area of all roughness baffles projected perpendicularly to the direction of flow divided by the total area of the bed, is found to be an adequate definition of the roughness density.

5. Distribution of velocity in the vertical direction when the roughness pattern is relatively dense is found to be similar to that described by the von Kármán-Prandtl equations for rough boundaries. The equation

$$\frac{v}{\sqrt{\frac{\tau_o}{\rho}}} = 6.06 \log \frac{y}{X} + 2.6 \quad \ldots\ldots\ldots\ldots \quad (20)$$

adequately describes the velocity distribution in such cases. A pattern consisting of sparsely-spaced, isolated roughness elements, however, gives rise to persistent horizontal and vertical vortices, and consequently considerable local variations in the turbulence pattern which cause marked deviations from the von Kármán-Prandtl type distribution.

6. The general resistance diagram, in which the resistance function is plotted against the Reynolds number, and the Colebrook-White type transition function are found to be applicable to problems of uniform flow in wide, rigid-boundary open channels.

7. Indications are that the von Kármán turbulence coefficient κ is independent of roughness pattern, provided that conditions of wake-interference flow and uniform roughness prevail. In the final analysis κ is in effect considered a constant, equal to 0.38, for the range of conditions tested in this study.

8. Negative depth corrections are found to be unnecessary for roughness systems consisting of staggered individual baffles, at least when the transverse spacing ratio $e/b \geq$ about 1, and the volume ratio $\frac{a\,b\,t}{a\,x(e+b)}$ is small.

ACKNOWLEDGMENT

This paper is based largely on a thesis submitted by W. W. Sayre[3] in partial fulfillment of the requirements for an M. S. degree in Irrigation Engineering at Colorado State Univ., Fort Collins, Colo. The study was carried out under the general supervision of M. L. Albertson who served as advisor and major professor. All of the experiments were conducted in the hydraulics laboratory of Colorado State Univ.

APPENDIX.—NOTATION

The following symbols, adopted for use in this paper, conform essentially with "American Standard Letter Symbols for Hydraulics" (ASA Z10.2-1942),

prepared by a committee of the American Standards Association with Society representation, and approved by the Association in 1942:

Symbol		Definition	Dimensions
a	=	Height of roughness baffle.	L
B	=	Width of flume.	L
b	=	Width of roughness baffle.	L
C	=	Chezy discharge coefficient.	$L^{1/2}/T$
C_1	=	Constant of integration.	
C_2	=	Experimental constant dependent on roughness spacing.	
e	=	Transverse spacing between roughness baffles.	L
F	=	Froude number.	
f	=	Darcy-Weisbach resistance coefficient.	
g	=	Acceleration of gravity.	L/T^2
k	=	Measure of roughness size.	L
k_s	=	Equivalent sand roughness (Nikuradse).	L
n	=	Roughness coefficient (Manning).	$L^{1/6}$
Q	=	Flow discharge.	L^3/T
R	=	Hydraulic radius.	L
R	=	Reynolds number.	
S	=	Slope of energy gradient.	
t	=	Thickness of roughness baffle.	L
V	=	Mean velocity of flow.	L/T
v	=	Velocity at distance y from boundary.	L/T
x	=	Longitudinal spacing of roughness baffles.	L
y	=	Distance above bed of channel.	L
y_n	=	Normal depth, that is, depth of flow occurring when slopes of energy gradient, water surface, and bed are equal.	
$\Delta\gamma$	=	Difference in specific weight of the two fluids involved (water and air) at fluid interface.	F/L^3
δ'	=	Thickness of laminar sublayer.	L
		$\frac{11.6\nu}{\sqrt{\tau_o/\rho}}$.	
κ	=	von Kármán turbulence coefficient.	

λ	=	Channel shape factor.	
μ	=	Dynamic viscosity of fluid.	FT/L^2
ν	=	Kinematic viscosity of fluid.	L^2/T
ρ	=	Fluid mass density.	FT^2/L^4
υ	=	Shape factor of roughness elements.	
τ	=	Shear intensity.	F/L^2
τ_o	=	Shear intensity acting on bed of channel.	F/L^2
X	=	Roughness parameter.	L
ψ	=	Spacing parameter.	

Journal of the
HYDRAULICS DIVISION
Proceedings of the American Society of Civil Engineers

EDDY DIFFUSION IN RESERVOIRS AND PIPELINES

By Frank L. Parker,[1] A. M. ASCE

SYNOPSIS

Previous studies have shown that the ocean eddy diffusion coefficient is a function of eddy size. Reservoir tests with radioactive tracers confirm this. Tests of eddy diffusion in pipelines are analyzed and compared with Taylor's theoretical solution. The pipeline coefficients are greater, as expected, because of obstructions and curved sections in the pipe.

INTRODUCTION

Diffusion in ponds and pipelines is a combination of molecular and eddy diffusion.[2,3,4,5] Molecular diffusion is the result of the heat motion of individual molecules and is extremely slow in liquids and gases, because the mean free path of molecules is so short. Eddy or turbulent diffusion, while fundamentally the same process as molecular diffusion, is the mass transfer

Note.—Discussion open until October 1, 1961. To extend the closing date one month, a written request must be filed with the Executive Secretary, ASCE. This paper is part of the copyrighted Journal of the Hydraulics Division, Proceedings of the American Society of Civil Engineers, Vol. 87, No. HY 3, May, 1961.

[1] Engrg. Leader, Oak Ridge Natl. Lab., Union Carbide Corp., U. S. Atomic Energy Comm., Oak Ridge, Tenn.

[2] "Modern Developments in Fluid Dynamics," by S. Goldstein, Clarendon Press, Oxford, England, Chapter 5, 1938.

[3] "Turbulent Diffusion," by G. K. Batchelor, Lecture Series, No. 4, Univ. of Maryland, College Park, 1960.

[4] "Introduction to Some Topics in Turbulence," by F. N. Frenkiel, Lecture Series, No. 3, Univ. of Maryland, College Park, 1960.

[5] "Statistical Theory of Turbulence," by S. Goldstein, Lecture Series, No. 6, Univ. of Maryland, College Park, 1960.

of molecules in eddies of various sizes. Essentially, molecular diffusion is submicroscopic in movement, while turbulent diffusion is macroscopic. Eddy diffusion has been found to vary from 1,000 to 1,000,000 times greater than molecular diffusion in open bodies of water.[6] Therefore, molecular diffusion will be ignored in the computations.

Turbulent diffusion may be taking place in numerous ways within the same area. Large-scale eddies and small-scale eddies within them induce various rates of mixing. The complete randomness of the eddy diffusion process makes it a difficult phenomena to formulate, and it is only recently with the application of statistical methods to the problem that some ideas of the fundamental nature of the process are being uncovered. At present, (1961), it is only possible to approximate the magnitude of the diffusion rate.

HISTORY OF DIFFUSION STUDIES

The earliest work on turbulent diffusion was that of Osborne Reynolds who differentiated in turbulent flow between the primary and secondary characteristics of the motion. The separation of turbulent velocity into two components is accomplished by assuming the mean velocity along the direction of travel as the primary component and a superimposed turbulent velocity having a temporal mean velocity of zero as the secondary component. This can be carried to an extreme by taking the time and length scales small enough so that even laminar flow would appear to be turbulent.

Prandtl advanced turbulence theory by relating the intensity of turbulent flow to a parameter of distance. The "mixture length" of Prandtl represents the average distance a small mass of fluid will travel before it loses its increment of momentum to the region into which it comes.[7] The work of Prandtl, however, bore no close relationship to the physical nature of turbulence. G. I. Taylor next applied the concept of the transfer of vorticity rather than momentum, but still retained the concept of mixture length which represents the transverse path in the vorticity transfer. This formulation accorded better with experimental results. Theodor von Kármán, Hon. M. ASCE, attempted to improve these efforts with his thesis of turbulent similitude based on the assumptions that the mechanism of turbulence is independent of viscosity, except in the immediate neighborhood of the flow boundaries and that the pattern of secondary flow is statistically similar from point to point, varying only in time and length scales. These assumptions lead to equations of the same form as Prandtl's and Taylor's but with the mixture length a function of the velocity distribution of the mean flow. A difference between momentum transfer and vorticity transfer is that in momentum transfer the eddy coefficient is a function of a mixing length and the transverse velocity of the stream, while in vorticity transfer the eddy coefficient is independent of the secondary velocity.

These methods lead to relatively simple and semi-empirical solutions which are widely used in engineering applications. For more adequate theoretical treatment and closer representation of the physical reality, they are

---

6 "The Oceans," by H. U. Sverdrup, M. W. Johnson, and R. H. Fleming, Prentice-Hall, New York, 1942, p. 91.

7 "Fluid Mechanics for Hydraulic Engineers," by H. Rouse, McGraw-Hill Book Co., Inc., New York, 1938, p. 186.

not sufficiently accurate to enable fundamental research into turbulent flow to proceed. The fundamental problems of turbulence are best approached through statistical analysis. Taylor produced the first study of turbulence by statistical methods. The notions introduced by Taylor in the investigation of isotropic turbulence were the study of the correlation between two fluctuating quantities in the turbulent flow, the study of the decay of turbulence, and the study of the spectrum of turbulence (that is, the distribution of energy among eddies of different sizes). The foregoing devices are means to solve the main question of the joint probability distribution of the displacement of any "n" marked particles.

The theoretical work in the field continues at an ever-eccelerating rate by such physicists and applied mathematicians as Heisenberg, Chandrasekhar, Onsager, Von Weizacker, von Kármán, Batchelor, Townsend, Dryden, Goldstein, de Feriet, Loitsiansky, Taylor, and Kolmogoroff. This research has been mainly concerned with laminar flow in the boundary layer, the initial stages of transition from laminar to turbulent flow, and the theory of nonviscous compressible and incompressible flow. As Dryden wrote[8] in 1952:

> "Progress of knowledge in fully developed turbulent flow processes has been at a more moderate rate, and our present methods (of solution) are still semi-empirical in character."

The most frequent formulations used by engineers continue to be some form of the mixing length equations.

MATHEMATICAL THEORY OF DIFFUSION

Semi-empirical formulations of the mixing-length type will be used in this study. Recognizing that the diffusion rate is a function of the size of the eddies possible, an average size of eddy and the corresponding empirical is obtained. It should be noted that in the ocean or a reservoir there are many sizes of eddies operating within one another to increase the transfer area so that a constant concentration is attained. Because of the random nature of the eddies, the concentration distribution in the ocean or reservoirs cannot follow an exact mathematical law, but must be treated in the statistical sense. That is, if enough tests are conducted the averages will tend to stabilize. Therefore, single tests must be approached warily.

The diffusion equation used is of the form

$$\alpha^2 \frac{\partial^2 c}{\partial x^2} = \frac{\partial c}{\partial t} \quad \ldots\ldots\ldots\ldots\ldots\ldots (1)$$

for the elementary case of no convection in one dimension, in which, c is the concentration, α^2 denotes the eddy diffusion coefficient, x is the length, and t represents time.

The coefficient α^2 is the constant of proportionality between the rate of diffusion across a plane area and the concentration gradient normal to that area; it is analogous to thermal conductivity in heat flow. Eq. 1 is equivalent to the general equation of conduction in heat flow. The vast amount of litera-

8 "Fluid Mechanics Supports Tasks of Civil Engineering," by H. L. Dryden, Civil Engineering, Vol. 22, No. 5, 1952, p. 329.

ture on heat transfer is thus available for the more involved studies of diffusion. The most important source of solutions of heat-conduction problems has been the text by H. S. Carslaw and J. C. Jeager.[9]

PREVIOUS STUDIES OF EDDY DIFFUSION COEFFICIENTS IN OCEANS

Among the early investigators, H. U. Sverdrup, M. W. Johnson, and R. H. Fleming have tabulated previous results for eddy diffusion coefficients.[10] Their values for horizontal diffusion are 2×10^3 to 4×10^5 ft sq per sec and for vertical diffusion 10^{-3} to 1 ft sq per sec. This would imply that vertical diffusion can be ignored when compared to horizontal diffusion. They note that the eddy diffusion coefficient is a function of the size of the eddy.

Later, Sverdrup, assuming diffusion to be a function of average velocity and of mixture length (that is, the dimension of the eddy) and independent of the depth, hazarded a guess at the values of diffusion coefficient.[11] For eddies of radius of 3×10^3 ft, 3×10^4ft, 3×10^5 ft, and 3×10^6 ft, the diffusion coefficients were estimated to be of the order of magnitude of 2.0, 5×10^2, 5×10^3, and 5×10^4 ft sq per sec, respectively. Sverdrup suspected that these values might be too large.

TABLE 1.—BURKE'S EDDY DIFFUSION COEFFICIENTS

Test Number	Diffusion coefficient, in ft sq per sec	Diffusion coefficient, in ft sq per sec	
		Eddy radius = 100 ft	Eddy radius = 200 ft
	(a) Ignoring the size of the eddies[a]	(b) Taking into account the size of the eddies	
1	0.116	0.045	0.090
2	0.052	0.322	0.645
3	0.033	0.322	0.645
4	0.069	0.258	0.516
5		0.742	1.485
6		0.678	1.356

[a] The diffusion coefficient equals a constant.

After this, C. J. Burke, in a series of tests[12] off the coast of California where he photographed dye-diffusion patterns from an airplane, arrived at the eddy diffusion values shown in Table 1.

The values of the diffusion coefficients obtained in this test were used to estimate the spread of the contaminant for "Operation Crossroad" (the 1946 Atomic Energy Commission tests in the Pacific Ocean).

9 "Conduction of Heat in Solids," by H. S. Carslow and J. C. Jaeger, Clarendon Press, Oxford, England, 1947.

10 "The Oceans," by H. U. Sverdrup, M. W. Johnson, and R. H. Fleming, Prentice-Hall, New York, 1942, p. 484.

11 "Speculations on Horizontal Diffusion in the Ocean," by H. U. Sverdrup, Scripps Inst. of Oceanography, Oceanographic Reports No. 1, January 7, 1946, p. 1 (unpublished).

12 "Horizontal Diffusion of Dyes in the Ocean," by C. J. Burke, Scripps Inst. of Oceanography, Oceanographic Reports No. 2, September 1, 1946, p. 9 (unpublished).

W. H. Munk, G. C. Ewing, and R. R. Revelle measured the concentration of reef water at various parts of the Bikini lagoon and arrived at the following values:[13] The vertical diffusion coefficient due to wind shear is 0.2691 ft sq per sec; the horizontal diffusion coefficient for an eddy size of 10^3 ft is 0.5 ft sq per sec; and for an eddy size of 3×10^5 ft, it is 5×10^4 ft sq per sec. They present as a primary constant the eddy diffusion coefficient divided by the radius of the eddy which they found equal to 0.0065 to 0.0164 ft per sec with 0.013 ft per sec being the average. These values were obtained assuming one-dimensional flow in the analysis of the test results.

Measuring the values of α^2 for the dispersion of radioactivity following the underwater atomic blast, they arrived at a mean value of α^2 for surface spreading of 1.6×10^2 ft sq per sec for r equal to 9.83×10^3 ft. This yields a value of α^2/r of 0.0164 ft per sec. The coefficient of diffusion at a depth of 150 ft was about one-third the coefficient of diffusion at the surface.

H. Stommel, by photographing sheets of paper scattered from an airplane onto the surface of the sea at Woods Hole, Mass., found[14] a series of values of α^2 ranging from 2.252×10^{-3} to 8.256×10^2 ft sq per sec. A fairly straight line was obtained when the diffusion coefficient was plotted against the 4/3 power of distance separating the sheets of paper. The equation used is

$$F(L) = \epsilon L^{4/3} \quad \ldots\ldots\ldots\ldots\ldots\ldots (2)$$

in which L denotes the distance between the sheets or particle, and ϵ is a constant. This is the Richardson Law of "neighbor diffusivity" and $F(L) \sim 3.03\ \alpha^2$.

FIELD TESTS FOR DIFFUSION COEFFICIENTS IN RESERVOIRS

A series of tests were conducted to determine the diffusion rates in reservoirs. Radioactive tracers, because of their low cost, ease of detection, small gravimetric quantities required, and absence of density problems, were used to measure the eddy diffusion coefficients.[15] Various reaches of Reservoir No. 2 of the Metropolitan District Commission at Framingham, Mass. (Fig. 1) were used to determine the eddy diffusion coefficient in quiescent bodies of water. This reservoir is completely isolated from the potable water supply, and fishing and boating are prohibited.

Method.—The tests were run in the following manner: (a) a small cove or basin or section of the reservoir was selected; (b) transit stations allowing full view of the reservoir were established; (c) a dye and radioisotope mixture were affixed to the end of a fishpole and deposited at a predesignated spot in the reservoir; (d) the dosing apparatus was removed, and a test tube was attached to the end of the fishing pole; (e) the rowboat then circled the initial spot and water samples were taken in a series of concentric circles about the initial dosing point. Because of the action of the wind and water currents, the rate of dispersion of the tracer seldom exhibited radial symmetry about the point of dosing. The dye provided a useful guide for the selection of sampling

13 "Diffusion in Bikini Lagoon," by W. H. Munk, G. C. Ewing, and R. R. Revelle, Transactions, Amer. Geophysical Union, Vol. 30, No. 1, 1949, p. 62.

14 "Horizontal Diffusion Due to Oceanic Turbulence," by H. Stommel, Journal of Marine Research, Sears Foundation, Vol. 8, No. 3, December 30, 1949, pp. 205-214.

15 "Radioactive Tracers in Hydrologic Studies," by F. L. Parker, Transactions, Amer. Geophysical Union, Vol. 39, June 1958, pp. 434-439.

points following the period of initial sampling. At the transit stations angular measurements were taken to locate each sampling point. By intersection of the angular measurements from two stations the exact points of sampling were plotted on the map. This system allowed greater flexibility than could have been attained using a fixed set of predetermined sampling points. With the 12-ft fishing pole it was possible to approach the dye in the boat without inducing too much turbulence in the area. The dye, sodium fluorescein, was chosen only after a series of tests showed it to have the maximum visibility in low concentration of all dyes tested (eosin, picric acid, Bordeau red, scarlet

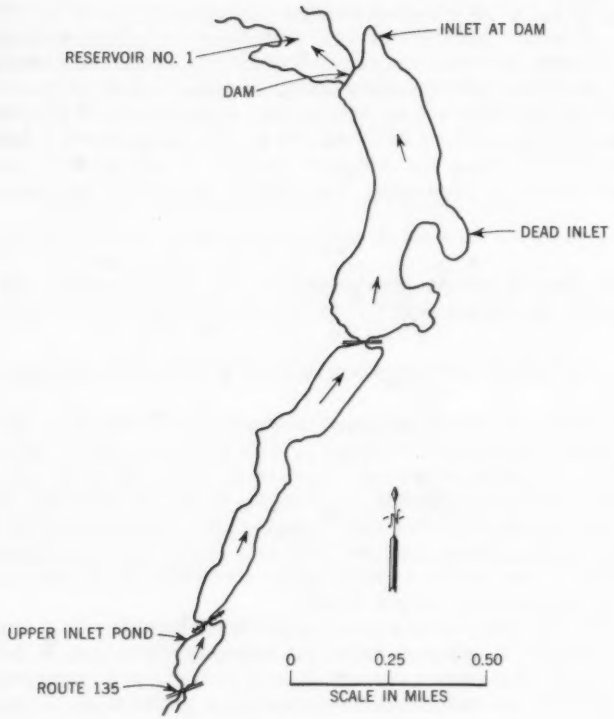

FIG. 1.—FRAMINGHAM RESERVOIR NO. 2

4R conc., acid black conc., malachite green oxalate, ecio glavcine, fuchin crystal). It is also the dye chosen for use in air-sea rescue kits. A typical reservoir test is shown in Fig. 2 and Table 2.

Analysis.—In the analysis of the test, the following mathematical model was used: A "slug" of a pure radioisotope is added at a point in a lake (of infinite expanse and constant depth) and rapidly mixed from top to bottom so as to form an instantaneous line source of constant strength. The mixing in

the water is assumed to be isotropic. Thereafter, the isotope is subject to two actions: (a) radial diffusion away from the source and (b) nuclear disin-

TABLE 2.—SAMPLING POINTS OF AUGUST 14, 1951 TEST

No.	Time After Dose (min)	Net cpm/50 ml	August 14, 1951 – Warm, sunny, no wind
			Comment
1	5	109	Extremity
2	6	613	- - - - - -
3	8	1270	Picked up bottom
4	11	52	Picked up bottom
5	13	1844	Picked up wind shift from southerly to westerly
6	17	1159	Surface wind
7	19	5159	Surface wind
8	20	34110	Surface wind
9	21	30690	Surface wind
10	22	20120	Front of path
11	24	16360	Front of path
12	26	7118	Front of path
13	27	- - -	Back of path
14	31	296	Back bottom
15	32	83	Back bottom
16	34	303	Back bottom
17	36	276	Back bottom
18	39	10770	Front of path
19	40	11670	Densest path
20	41	43	No dye
21	44	20170	Dense
22	45	13470	Densest
23	48	18	Integrated depth sample
24	50	60	Integrated depth sample
25	51	252	Integrated depth sample
26	52	223	Integrated depth sample
27	53	41	Integrated depth sample
28	54	79	Integrated depth sample
29	55	51	Integrated depth sample
30	56	324	Integrated depth sample
31	65	2944	- - - - - -
32	68	3954	- - - - - -
33	70	3674	Grab samples in path
34	73	116	Grab samples in path
35	73	39	End of path
36	76	311	In path
37	77	99	In path
38	78	52	In path
39	79	123	Dosing point
40	80	168	End of path bottom
41	81	33	End of path bottom
42	98	6	End of path bottom
43	100	0	End of path bottom
44	101	0	- - - - - -
45	---	0	- - - - - -
46	---	0	- - - - - -
47	---	0	- - - - - -

tegration together with removal by self-purification processes (precipitation and deposition, adsorption, biological uptake, etc.).

Consider (Fig. 3) an element of volume $r\,dr\,d\theta\,dz$ in the plane of diffusion, in which r is the radius from the source, $d\theta$ the angular width of the element and dz the height. The rate at which an isotope enters the element by diffusion is

$$-\alpha^2 r\,d\theta\,dz\,\frac{\partial c}{\partial r}$$

The rate at which it leaves by diffusion and die-away is

$$-\alpha^2 (r+dr)\,d\theta\,dz\,\frac{\partial}{\partial r}\left(c+\frac{\partial c}{\partial r}\,dr\right) + k\,r\,dr\,d\theta\,dz\,c$$

in which α^2 denotes the eddy diffusion coefficient reflecting the degree of mixing (length^2/tim)E), and k is the effective decay constant of the radioisotope.

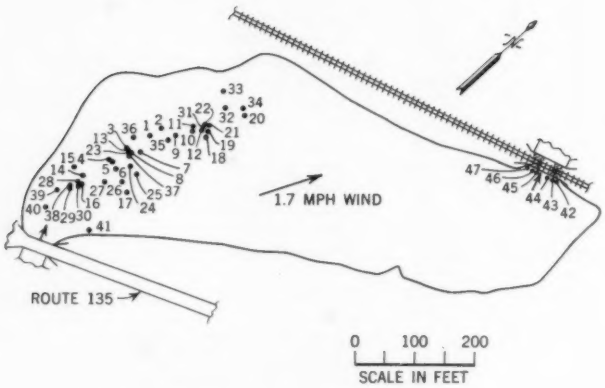

FIG. 2.—RESERVOIR TEST OF AUGUST 14, 1951

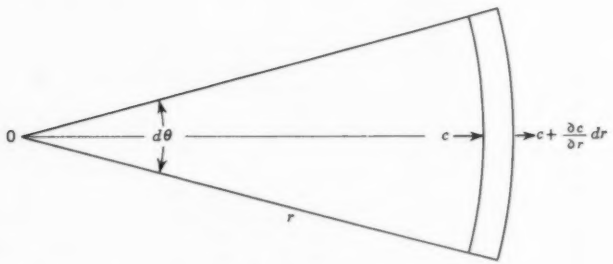

FIG. 3.—ELEMENT

Equating the difference between these two rates to the rate of accumulation of isotope within the element, one obtains

$$\frac{\partial^2 c}{dr^2} + \frac{1}{r}\frac{\partial c}{dr} - \frac{k}{\alpha^2}C = \frac{1}{\alpha^2}\frac{\partial c}{\partial t} \quad \ldots\ldots\ldots\ldots\ldots (3)$$

The appropriate solution of Eq. 3 for the boundary conditions stipulated is given by

$$c = \frac{N}{4\pi\alpha^2 t} \exp\left(-\frac{r^2}{4\alpha^2 t} - k t\right) \quad \ldots\ldots\ldots (4)$$

in which c is the concentration at any radius and at any time after the isotope is added and N represents the amount of radioactive material initially added per foot of depth. An idea of the functional relation existing between c, r, and t is given by (Fig. 4). The concentration distribution takes the form of a sym-

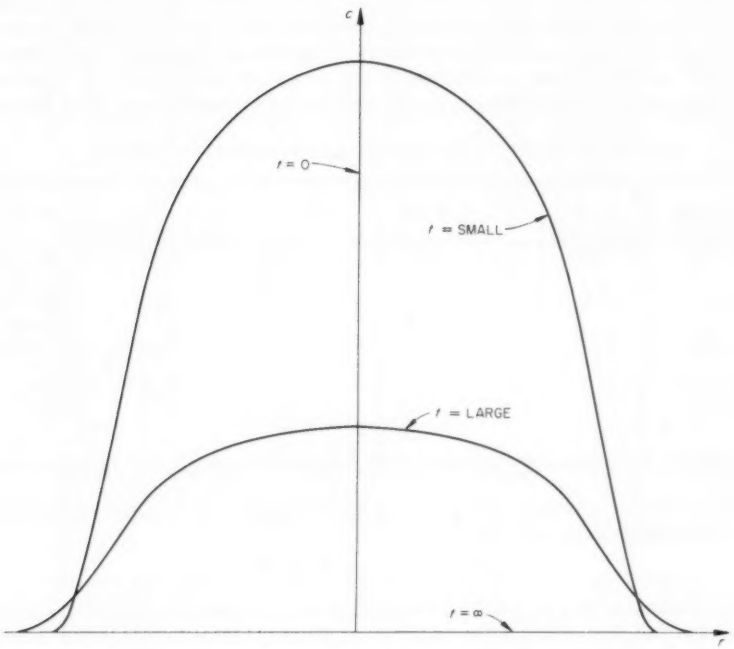

FIG. 4.—DIFFUSION FROM AN INSTANTANEOUS LINE SOURCE

metrical bell-shaped hill (Gaussian frequency distribution) with circular concentration contours. With increasing time the hill spreads out and the concentration at the center decreases; also as time goes on the volume of the hill decreases because of radioactive disintegration and self-purification.

It is instructive to consider the history of one particular concentration contour. Let r' be the radius of the circle having a concentration of c' which might correspond to a critical toxic level or tolerance concentration. From Eq. 4 it is found that

$$r' = 2\sqrt{\alpha^2 t}\sqrt{\ln\frac{N}{4\pi\alpha^2 t\, c'} - k t} \quad \ldots\ldots\ldots (5)$$

Eq. 5 indicates that the critical radius at first increases rapidly, then passes through a maximum, and with progressive disintegration recedes to zero. The recession is rapid toward the end. At any time the concentrations within the critical contour are greater than c', and outside of it they are less than c'. Of especial significance is the way the initial concentration, N, appears in the formula. A tenfold or hundredfold increase in N has a relatively small effect on r'.

Results.—The results of this type of analysis of the pond tests are shown in Table 3. These values of α^2/r are somewhat higher than those obtained by Munk. This may be explained, in part, by the circumstance that Framingham Reservoir No. 2 is relatively shallow, and uniform concentration distributions in the vertical direction were quickly established. In the ocean, however, steep concentration gradients persist for long periods following the addition of the tracer; the resulting continued downward transfer of the tracer causes a reduction in the dispersion in the horizontal directions. From the data obtained previously, eddy diffusion coefficients in oceans and ponds versus the size of the eddies are plotted in Fig. 5. Ignoring Sverdrup's estimates, it is possible

TABLE 3.—RESULTS OF FRAMINGHAM RESERVOIR TESTS

Date (1951)	r, ft	α^2, sq ft per sec	α^2/r	Initial Dose Millicuries I^{131}	Wind
Aug. 2	682	144	.21	19.3	Light and variable
Aug. 14	150	9	.06	1.8	Light and variable
Aug. 31	230	25	.10	7.4	21 mph S 25° W
Sept. 5	143	7	.05	16.2	Light
Sept. 12	52	1.3	.03	16.2	Light
			$\Sigma = 0.45$		
			$M = 0.09$		

to plot a line of average eddy diffusion coefficients versus the radius of the eddy. The equation of the line is

$$\alpha^2 = 7.5 \times 10^{-4} \, r^{1.47} \quad \ldots\ldots\ldots\ldots\ldots (6)$$

The results of this investigation indicate that Richardson's law of neighbor diffusivity obtains more than Munk's suggestion of a constant for the eddy diffusion coefficient divided by the radius of the eddy. The use of a power function, rather than a linear relationship, would accord more with the physical system where with increasing radius the diffusing surface would increase faster than linearly.

DIFFUSION IN PIPELINES

Sir Geoffrey Taylor showed theoretically and experimentally that contaminants in pipelines diffused in the following manner:[16,17]

[16] "Dispersion of Soluble Matter in Solvent Flowing Slowly Through a Tube," by Sir Geoffrey Taylor, Proceedings, Royal Soc. of London, Sect. A, Vol. 219, No. 1137, August 25, 1953, p. 186.

[17] "The Dispersion of Matter in Turbulent Flow Through a Pipe," by G. I. Taylor, Proceedings, Royal Soc. of London, Vol. 223, No. 1155, May 20, 1954, p. 446.

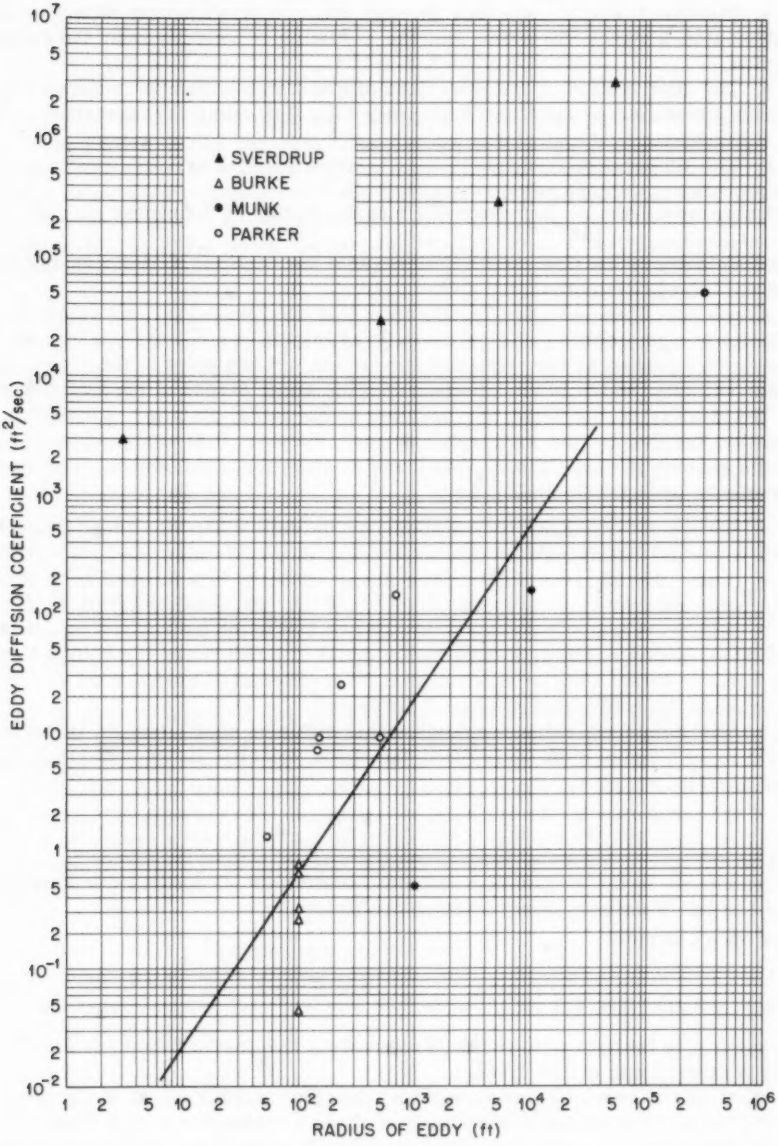

FIG. 5.—RELATIONSHIP OF EDDY DIFFUSION COEFFICIENTS TO THE SIZE OF THE EDDY

Laminar Flow.—

a. Dissolved matter spreads through the combined action of molecular diffusion in a radial direction and the variation of velocity over the cross-section.

b. The distribution of concentration of dissolved matter is centered about a mean which moved with the mean speed of the flow and is symmetrical about it.

c. The dispersion along the tube is in accord with a vertical coefficient of diffusion equal to $\frac{(r^2 \bar{u}^2)}{(48\ \alpha^2)}$ in which r is the radius of the pipe; $\bar{u}$ denotes the mean velocity of the flow; and α^2 represents the coefficient of molecular diffusion of the injected material in the fluid.

Turbulent Flow.—Taylor predicates that the universal distribution of velocity in a pipe obtains (that is, the ratio of the difference between the velocity at the center of the pipe and the velocity at any point in the pipe to the shear velocity, which is the square root of the shear stress at the wall divided by the density of the fluid, is a function of the radial distance to the point in question divided by the radius of the pipe). Further, it is assumed that Reynold's analogy is valid (that is, the transfer of matter, heat, and momentum by turbulence are exactly analogous).

a. Matter is transferred longitudinally by convection (the mean velocity) with a virtual coefficient of diffusion equal to 10.16 times the radius of the pipe times the shear velocity. The shear velocity is a function only of the Reynolds number for smooth pipes (that is, the coefficient of friction).

b. Matter is transferred longitudinally by turbulent (secondary velocities) diffusion, with a coefficient of diffusion equal to 0.052 times the radius times the shear velocity. (Taylor assumes that the coefficient of longitudinal diffusion is equal to the coefficient of lateral diffusion.)

c. The combined value for longitudinal diffusion coefficient is, therefore, equal to 10.1 times the radius times the shear velocity. In the American system of notation:

$$\alpha_L^2 = 1.785\ D\ \bar{u}\ \sqrt{f} \quad \ldots\ldots\ldots\ldots\ldots\ldots\ (7)$$

in which α_L^2 is the longitudinal diffusion coefficient, D denotes the diameter, and f is the Weisbach-Darcy friction coefficient.

For open channels

$$\alpha_L^2 = 14.28\ R^{3/2} \sqrt{2\ g\ s} \quad \ldots\ldots\ldots\ldots\ (8)$$

in which R is the hydraulic radius, g represents the gravitational acceleration, and, s is the slope of the channel.

Most of the previous theory has held that the transfer due to the superimposed turbulent component of velocity is the predominant transfer. Therefore, most theoretical formulas for eddy diffusion in pipes have been in error by a factor of about 200. This is because they have completely ignored the transfer which is dependent on the primary velocity.

d. The concentration of dissolved material in the pipe at time t and distance x is equal to

$$C = \frac{M}{2} r^{-2} \pi^{-3/2} \left(\alpha_L^2\right)^{-1/2} t^{-1/2} e^{-(x-ut)^2/4\alpha_L^2 t} \quad \ldots\ldots (9)$$

in which M is the total mass (or activity) of the dissolved material. At any given time after dosing the tracer, the concentration distribution is symmetrical and gaussian. At a fixed station downstream the curve of concentration versus time is not symmetrical due to the diffusion of the material as it passes by the measuring station. Ordinarily, skewness of the concentration-time distribution is not great when the measuring point is at a distance downstream greater than 100 diameters.

e. Numerical values of the virtual coefficient of diffusion may readily be determined by taking advantage of the fact that the Eq. 9 is the error function equation. Taylor computed α^2 from a plot of the data by scaling off one-half the distance at which the concentration exceeds 50% of the peak value. Solving the equation the following relation is obtained:

$$\alpha_L^2 = \frac{x_{0.5}^2}{4\, t \ln 2} \quad \ldots\ldots\ldots\ldots (10)$$

in which $x_{0.5}$ is one-half the distance between sections at which concentration equals 50% of the peak value, and is the maximum concentration at the measuring station.

Eq 10 may be transposed to the form

$$\alpha_L^2 = \frac{u^3 \left(t_{0.5}\right)^2}{4\, x \ln 2} \quad \ldots\ldots\ldots\ldots (11)$$

in which $t_{0.5}$ is one-half the time that the concentration is above 50% of the maximum concentration, and x is the distance from the dosing point to the measuring station.

f. Experimental work indicated that the formlation is valid for both smooth and rough pipes, since the universal distribution of velocity holds for both.

g. For curved pipe the universal distribution of velocity does not hold and, hence, the coefficient of diffusion should be expected to be greater than that computed from Eq. 6.

OTHER METHODS OF SOLUTION

Other treatments of Eq. 9 for the evaluation of α^2 are possible. Eq. 9 may be written in the form

$$\log_{10} c\, t^{1/2} = \log_{10} \frac{M}{2\left(\pi\, r^2\right)\alpha_L^2} - \frac{(x-u\,t)^2}{4\,\alpha_L^2\, t} \log_{10} e \quad \ldots (12)$$

In this form a linear relation obtains between $\log\, c\, t^{1/2}$ and $(x-u\,t)^2/t$. On a semi-log plot of $c\, t^{1/2}$ versus $(x-u\,t)^2/t$, the slope will be $\log_{10} e/\left(4\,\alpha_L^2\right)$.

Another method of linearization is obtained by writing Eq. 9 in the form

$$\log \frac{c_1\sqrt{t_1}}{c_2\sqrt{t_2}} = \left[\frac{(t_2 - t_1)x^2}{4\alpha_L^2} \frac{1}{t_1 t_2} - \frac{\bar{u}^2(t_2 - t_1)}{4\alpha_L^2} \right] \log e \quad \ldots \quad (13)$$

in which $\log\left(\frac{c_1\sqrt{t_1}}{c_2\sqrt{t_2}}\right)$ is the ordinate; $\frac{1}{t_1 t_2}$ is the abscissa; and $\frac{t_2 t_1 x^2}{4\alpha_L^2}$ is the slope of the equation.

It is also possible to evaluate the standard deviation from moments of the observed concentration-time distribution. The first two moments of the concentration-time distribution, m_1 and m_2, (Eq. 9) are

$$m_1 = \int_0^\infty t\ c\ dt = T\left(1 + \frac{2\alpha_L^2 T}{X^2}\right) \quad \ldots\ldots\ldots\ldots \quad (14)$$

and

$$m_2 = \int_0^\infty (t - T)^2\ c\ dt = \frac{2\alpha_L^2 T^3}{X^2}\left(1 + \frac{4\alpha_L^2 T}{X^2}\right) \quad \ldots\ldots \quad (15)$$

in which T is the theoretical detention period, X/u, and X represents the total length of pipe.

The second terms on the right-hand side of Eq. 4 and 5 are ordinarily small and may be neglected. If they are neglected the following equation for α_L^2 may be obtained by solving Eq. 14 and 15 for α_L^2:

$$\alpha_L^2 = \frac{X^2}{2}\frac{m_2}{(m_1)^3} \quad \ldots\ldots\ldots\ldots \quad (16)$$

A final method is the approximate formulation used by R. S. Archibald, M. ASCE, in which[18] the standard deviation of the concentration-time distribution, $2\alpha_L^2 t$, is assumed to be one-sixth the time between the first appearance and last trace of the tracer at the sampling station. The imperfection in Archibald's criterion is the determination of the time of occurrence of the last trace, since the latter is obscured by fluctuation in background activity. Therefore, this method of determining the diffusion coefficient is much less accurate than either the method of moments or the Taylor method.

DIFFUSION COEFFICIENTS COMPUTED FROM EARLY SALT-VELOCITY TESTS IN PIPELINES

The results of pipe tests reported in the literature have been analyzed, and the diffusion coefficients have been determined by the methods described. The results are presented in Table 4.

18 "Radioactive Tracers in Flow Tests," by R. S. Archibald, Journal, Boston Soc. of Civ. Engrs., Vol. 37, No. 1, 1950, p. 77.

TABLE 4.—COMPARISON OF PREVIOUS PIPE TESTS

Test	Tracer	Length, in feet	Dimension, in feet	Velocity, in feet per second	Reynolds Number	Values of the Diffusion Coefficients α^2, ft sq per sec, by Various Methods				Col. 10 / Col. 7	Col. 8 / Col. 7	Col. 9 / Col. 7
						Eq. 6	Eq. 11	Eq. 12	Eq. 16			
(1)	(2)	(3)	(4)	(5)	(6)	(7)	(8)	(9)	(10)	(11)	(12)	(13)
Delaware[a]			Diameter									
KB	Salt	118,600	15	0.58	7.2×10^5	1.67	1.65	1.14	1.42	0.85	0.99	0.69
KE	Salt	118,600	15	2.72	3.37×10^6	7.63	7.63	7.80	8.62	1.12	0.99	1.01
Delaware[b]	Salt	234,000	13.5	1.43	1.6×10^6	3.65	3.82	2.59	3.90	1.07	0.99	0.71
Allen and Taylor[c]												
Fig. Run												
4 2	Salt	355	3.33	2.93	8.0×10^5	1.85	2.31	1.78	1.86	1.01	1.25	0.96
5 2	Salt	355	3.33	3.46	9.5×10^5	2.16	2.35	2.34	2.22	1.03	1.08	1.08
5 4	Salt	355	3.33	3.46	9.5×10^5	2.16	2.35	2.00	2.11	0.98	0.93	0.93
Johnson[d]			Hydraulic Radius									
A-4	Salt	1,553	0.501	1.91	3.2×10^5	0.92	3.28	3.48	4.16	4.52	3.57	3.78
B-4	Salt	890	0.756	1.99	4.9×10^5	1.15	2.24	2.20	1.72	1.50	1.95	1.91
C-6	Salt	1,060	1.074	2.61	9.3×10^5	2.12	3.78	3.57	3.54	1.67	1.78	1.68
D-4	Salt	260	0.148	3.91	1.9×10^5	0.61	4.86	5.68	5.42	8.89	7.97	9.31
Hull and Kent[e]			Diameter									
Bonanza	Ba^{140}	72,800	0.83	2.68	2.4×10^4	0.64	1.05	1.28	1.10	1.71	1.63	2.00
Green River	Sb^{124}	227,600	0.83	2.68	2.4×10^4	0.64	1.23	1.31	1.18	1.84	1.91	2.04
Hanna		572,900	0.83	2.68	2.4×10^4	0.64	1.24	1.36	1.29	2.01	1.93	2.12

[a] "Salt Velocity Gagings of Flow in Delaware Water Tunnel," Water Works Engineering, Vol. 96, September 8, 1943, pp. 1020-1021.
[b] "Salt Velocity Gagings in 44-Mile Aqueduct Tunnel," Water Works Engineering, Vol. 98, November 14, 1945, p. 1317.
[c] "The Salt Velocity Method of Water Measurement," by C. M. Allen and E. A. Taylor, Transactions, ASME, Vol. 45, 1923, p. 291.
[d] "Determination of Kutter's n for Sewers Partly Filled," Transactions, ASCE, Vol. 109, 1944, p. 223.
[e] "Radioactive Tracers to Mark Interfaces and Measure Intermixing in Pipelines," by D. E. Hull and J. W. Kent, Industrial and Engineering Chemistry, Vol. 44, November 1932, p. 2746.

Linearization (Eq. 12) has the disadvantage that in forcing the data into a normal curve, the experimental points that do not fit into this pattern produce some scatter, and the determination of the straight line entails a strong element of subjectivity. Moreover, the physical significance of the data is lost in linearization. In the Taylor method (Eq. 11) of computing the diffusion coefficient the physical sense is retained; it is much simpler and more straight forward.

Taylor's method requires a knowledge of the mean time of flow (X/u) and, therefore, is not completely satisfactory. None of these methods give satisfactory results if instantaneous injection is not made or if an obstruction occurs in the line so as to reduce the effective diameter or if the pipeline is not straight. Taylor's method (Eq. 10 and 11) does not indicate this. Therefore, the Taylor method should be carried out in conjunction with the method of moments. The method of moments entails no bias as the mean time of flow remains unknown. Then if the proper conditions have obtained, the results of the two methods should be approximately equal.

A comparison of the values in Table 4 of the diffusion coefficients obtained by the various methods makes it evident that Taylor's formula (Eq. 11) holds for both oil and water and for pipes flowing full and partly full.

Ordinarily the coefficient of diffusion obtained experimentally may be expected to exceed the theoretical coefficients, since the Taylor formulation pertains to straight pipe. Existing pipes usually have curved sections. A few of the values in Col. 13 of Table 4 are less than unity. The discrepancy is probably due to errors in the determination of the friction coefficient of the pipe. Also, as mentioned previously, the linearization method is dependent on the choice of the line of best fit.

FIELD TESTS OF PIPELINES

A series of tests using radio-tracers was made to determine the virtual coefficient of longitudinal diffusion in pipelines. These results were then compared with similar coefficients obtained from previous pipe tests and with the coefficients computed by the Taylor formula.

The tests were run in an old water-supply pipeline made available by the Metropolitan District Commission and the Conservation Department of Massachusetts. The pipe tested was part of the conduit system between Whitehall Reservoir and Hopkinton Reservoir. These are out-of-service water-supply reservoirs and have been assigned to the Department of Consevation. The pipe is 20 in. in diameter and 6,400 ft long. The drop in the hydraulic grade between the inlet and outlet of the line is 34 ft. The method of testing was to allow the pipe to flow full long enough to establish steady state conditions and then to "slug" the pipe with a dose of radioactive tracer and dye. At the outlet of the pipe a sampler was arranged so that the outlet was sampled every 1 min. until appearance of the dye and every 1/2 min. thereafter until the dye disappeared. The sampling was continued for five or six detention periods. The concentration of the dye served as a rough check for radioactive measurements. A 50-ml volume of each sample collected was precipitated. The precipitate was dried and counted with an end window Geiger tube with suitable sealing circuits. The results were compared with a diluted sample of the initial dose.

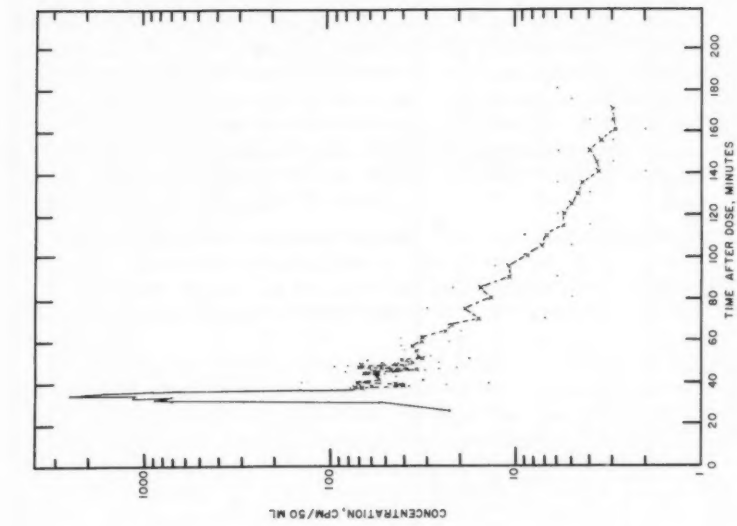

FIG. 7.—CONCENTRATION-TIME PLOT OF PIPE TEST OF DECEMBER 27, 1951

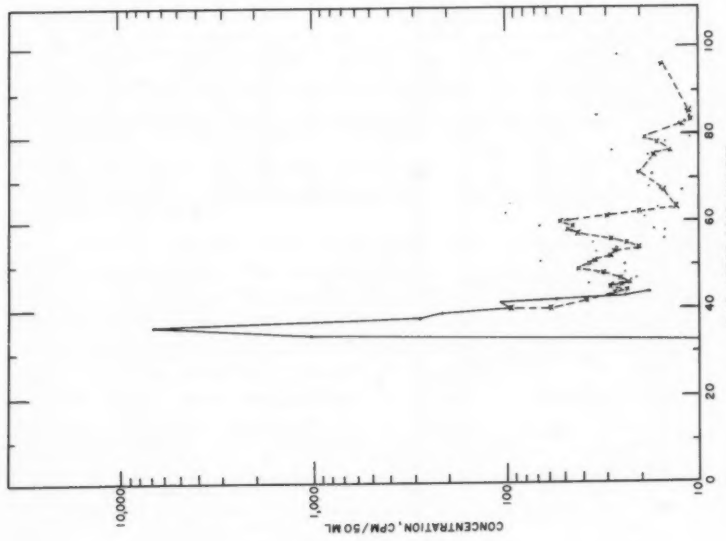

FIG. 6.—CONCENTRATION-TIME PLOT OF PIPE TEST OF JANUARY 11, 1951

TABLE 5.—RESULTS OF PIPE TESTS

Test	Tracer	Millicuries Added	Millicuries Recovered	Percentage Recovery	Length, in feet	Diameter, in feet	Velocity, in ft per sec	Reynolds Number	Values of the Diffusion Coefficients α^2, ft sq per sec, by Various Methods				Col. 13 / Col. 10	Col. 11 / Col. 10	Col. 12 / Col. 10
									Eq. 6	Eq. 11	Eq. 12	Eq. 16			
(1)	(2)	(3)	(4)	(5)	(6)	(7)	(8)	(9)	(10)	(11)	(12)	(13)	(14)	(15)	(16)
Whitehall - Hopkinton Water															
1/11/51	I^{131}	14.8	13.3	90	6400	1.67	2.77	3.82×10^5	1.3	3.5	3.91	11.7	9.0	2.69	3.0
12/27/51	P^{32}	5.8	0.8	14	6400	1.67	3.11	4.30×10^5	1.47	4.95	6.03	23.7	16.1	3.37	4.1
10/14/54	I^{131}				6400	1.67	3.46	4.80×10^5	1.55	2.30	4.14	6.58	4.25	1.48	2.7
New Bedford Sewerage															
First Test Dosed at Screen House	I^{141}														
Hudson St.					1061	10.0	0.63		2.12	3.81		14.32	6.75	1.8	
Parade Ground					3048	8.48	1.16		2.84	5.10		71.9	25.3	1.8	
Tide Chamber					4490	9.24	1.14		2.45	0.13[a]		11.15	. . .	. . .	
Second Test Dosed at Hudson St.	I^{131}														
Parade Ground					1987	8.48	1.34		2.55	2.94		7.63	2.99	1.16	
Tide Chamber					3429	9.24	1.34		3.00	2.28		10.50	3.5	0.76	

[a] Not sufficient data for computations.

The results of two of the tests are shown in Figs 6 and 7. The method of moving averages was used to compute the tails of the curves.

In Table 5, a much greater percentage of iodine passes the downstream gauging station than does phosphorus. Only a small amount of phosphorus reaches the sampling station in test 2 due to the high absorption rates of phosphorus by the bacterial slimes on the pipe walls.[19] Further credence to this theory is provided by C. C. Coffin et al., who state[20] "p^{32} uptake by plants and sooplankton is a matter of minutes or hours and not days or weeks." It will be noted in Table 5 that the coefficient of diffusion by Taylor's method (Eq. 11) and the method of moments (Eq. 16) do not agree too well.

The apparent reason for the failure of the method of moments to give results that agree with other methods is:

1. The method of moments (Eq. 16) uses "tails" of concentration-time data which are obscured by variations in background counting rate.
2. Taylor's theory is not good for those portions of the distribution-time curve at large distances from mean. This is evident from the shape of the curves.
3. The Taylor method (Eq. 11) is not good for skewed curves. The curves for the pipe test were skewed because of the air pockets which remained in the pipe. In the last test, however, the pipe was vented before the test began, and we can assume that most of the air was removed. The method of moments then gives approximately the same results as other methods.

Another series of tests were run through a sewer line at New Bedford, Mass., in co-operation with Frank Heaney, F. ASCE, of Fay, Spofford and Thorndike, consulting engineers. The sewer tested was the main collecting sewer of New Bedford, Mass. Its route is along Rodney French Boulevard and through Fort Rodman, and it discharges into Buzzards Bay (Fig. 8). The sewer is of the usual horseshoe cross section of combined sewers with a maximum width of 92 in. and a height of 84 in. The slope is approximately 0.001. In one test the activity was introduced at Hudson Street. Samples were collected with diaphragm pumps at downstream stations at the drill ground (1,987.7 ft) and at the tide chamber (3,429 ft). At these pump outlets the stream was sampled every 1 min until the dye appeared and thereafter at 20-sec intervals until the dye disappeared at which time 1-min sampling was resumed; typical curves are shown in Fig. 9.

In another test the tracer was dosed at the screen house, 1,060 ft upstream from Hudson Street. The same sampling procedure was used with an additional sampling station at Hudson Street. Due to faulty injection the activity in the test bled into the system from the screen house well slowly. This is reflected in the high values for α^2. In these conditions it should be expected and it is found that the apparent coefficient of diffusion is much larger than the theoretical value. This emphasizes the necessity for instantaneous injection into the turbulent flow. Injection into the laminar sublayer will obviously produce laminar diffusion and later turbulent diffusion as it bleeds into the turbulent flow. Attempts to measure the eddy diffusion coefficient at the outfall were

---

19 "Adsorption and Assimilation of P^{32} by Bacterial Slimes," by G. W. Reid, San. Engrg., Dept., John Hopkins Univ., Contract AT-(10-1)-498, March 20, 1950, p. 7.

20 "Exchange of Material in a Lake as Studies by the Addition of Radioactive Phosphorus," by C. C. Coffin, F. R. Hayes, L. H. Jodrey, and S. G. Whiteway, Canadian Journal of Research D, Vol. 27, 1949, p. 221.

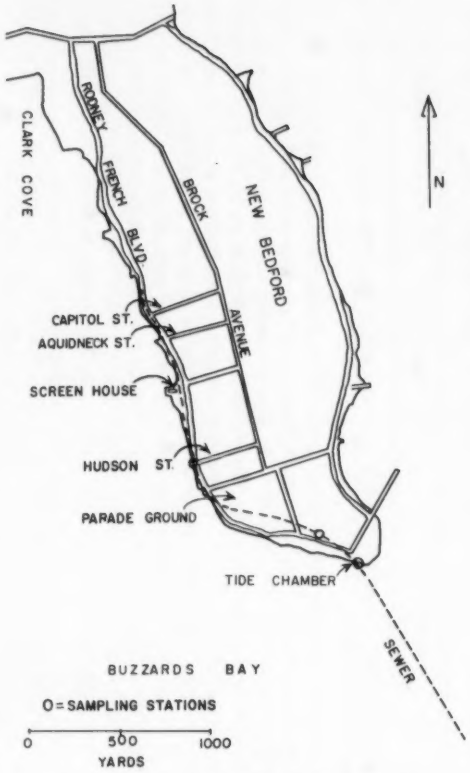

FIG. 8.—ROUTE OF SEWER IN NEW BEDFORD, MASS.

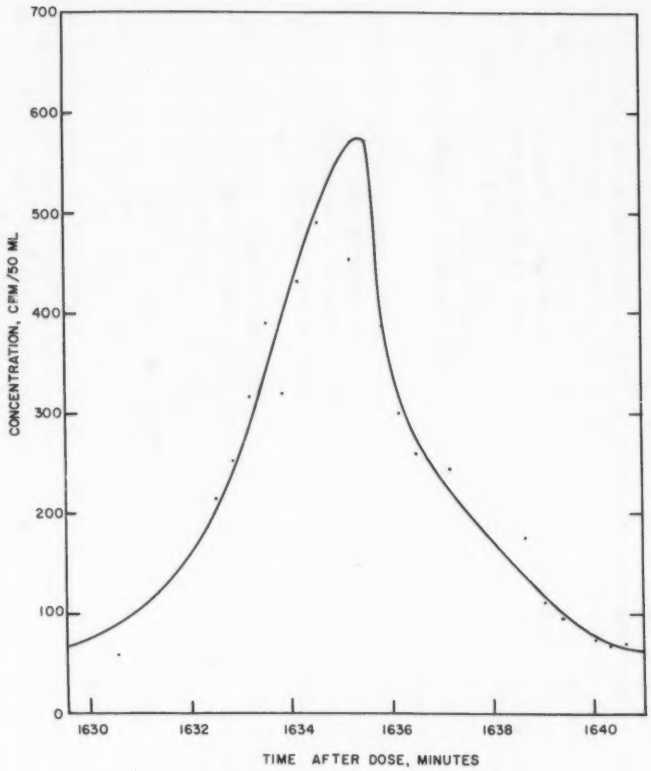

FIG. 9.—CONCENTRATION—TIME PLOT OF PIPE TEST AT TIDE CHAMBER

not successful due to the small amount of radioactive isotopes used and the high solids in sea water.

The tests in Massachusetts bear out the conclusions drawn from previous tests. With proper injection methods and measuring procedures the Taylor formulation and the method of moments give satisfactory results for circular and horseshoe pipes, full and partially flowing full pipes, and oil, water, and sewage carrying pipes.

CONCLUSIONS

It is relatively easy to determine diffusion coefficients in reservoirs and pipelines by use of radioactive tracers in comparison with most other methods heretofore used. Simple dosing and sampling devices can be used to obtain good results.

ACKNOWLEDGMENTS

The work described herein was performed under contract with the Sanitary Engineering Section of the Division of Reactor Devlopment of the AEC at Harvard University, under the direction of Harold A. Thomas, J., F. ASCE. The writer would like to acknowledge with thanks the help of Thomas in guiding the project and the participation of R. Stevens Kleinschmidt, Mrs. R. S. Kleinschmidt, Jane Maclachlan, Thomas Ostrom, M. ASCE, and Gerald Parker, in the execution of the field tests.

This paper has been submitted as part of the requirements for the Ph. D. Degree at Harvard University, Cambridge, Mass.

Journal of the
HYDRAULICS DIVISION
Proceedings of the American Society of Civil Engineers

DISCUSSION

Note.—This paper is a part of the copyrighted Journal of the Hydraulics Division, Proceedings of the American Society of Civil Engineers, Vol. 87, No. HY 3, May, 1961.

EARLY HISTORY OF HYDROMETRY IN THE UNITED STATES[a]

Closure by Steponas Kolupaila

STEPONAS KOLUPAILA.[85]—The writer feels particularly honored by the fact that three of the pioneers presented in the paper took part in the discussion: J. C. Stevens, F. ASCE, W. G. Hoyt, F. ASCE, and M. Blanchard, F. ASCE. It is not enough to thank all contributors for their valuable cooperation; let it

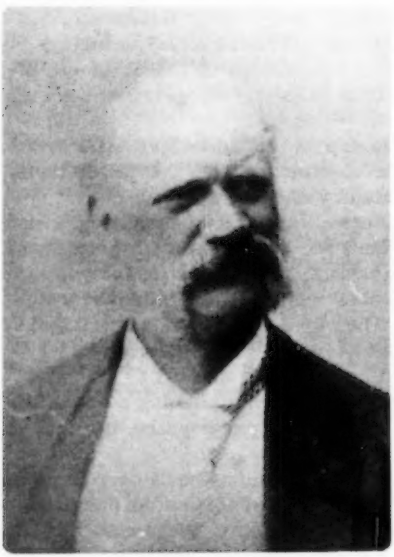

FIG. 63.—HAMILTON SMITH

FIG. 64.—LOAMMI BALDWIN

suffice to say that the writer is inspired, by the attention of his colleagues, to continue further study of the history of hydrometry.

J. W. Johnson deserves credit for recalling the "Early Engineering Center in California," a good addition to the chapter "Water in the West." Hamilton Smith is world renowned for his authoritative book[86] that is now very rare. The classical experiments carried out by Smith are mentioned in modern textbooks. The portrait of this pioneer in hydrometry (Fig. 63) is reproduced

[a] January 1960, by Steponas Kolupaila (Proc. Paper 2335).

[85] Prof. of Civ. Engrg., Univ. of Notre Dame, Notre Dame, Ind.

[86] "Hydraulics, the Flow of Water Through Orifices, Over Weirs, and Through Open Conduits and Pipes," London, 1886.

here[87] by the courtesy of K. Daugela and N. H. Bedford. Smith died while sailing down Oyster River.

Johnson mentioned in his discussion that the first of the world's long-distance high-voltage power transmission lines was built in California. In connection with this statement, G. H. Ellis, M. ASCE, insisted in a letter to the editor that the Missouri River Power Company had built a 70,000-v line extending from their Canyon Ferry plant to the town of Buthe, a distance of 63 miles, in the year 1901, thus claiming to predate the California project. The writer would like to point out, however, that the 60,000-v line running 140 miles from the Colgate plant to the city of Oakland, California, that was described by Johnson, was built in the year 1899, thus refuting Ellis' claim.

Hoyt, one of the leading pioneers in the USGS, from 1907 to 1950, recommended the inclusion of several hydrographers of that institution. It is the feeling of the writer that these persons could be more appropriately included in the modern history of hydrometry. Hoyt emphasized the manifold indirect duties of hydrometric engineers, as disseminators of public information and educators to the necessity of conserving our water resources. He expressed his opinion, as a consultant for the Senate Committee on Water Resources, concerning the future of those problems intimately affiliated with the history of hydrometry in the United States. The annual expenditure of the USGS for investigation of water resources, about 25 million dollars, demonstrates the high recognition of this important work.

E. Shaw Cole, F. ASCE, who skillfully continues the illustrious work of his father, E. C. Cole, mentioned some new developments, that, the writer feels, belong more appropriately to the modern history of hydrometry.

Blanchard, one of the distinguished pioneers of the U. S. Lake Survey, added more information on the measurements at Sault Ste Marie, and on his own work in different rivers connecting the Great Lakes.

A. H. Frazier, who inspired this study, contributed valuable improvements with which the writer agrees completely. The pioneer work of Loammi Baldwin, (Fig. 64) who has been referred to as the father of civil engineering in America, should be included in the early history of hydrometry.

The writer is grateful to Frazier for disentangling the amazing coincidence of the two Nicollets, both investigators in one part of our country, but 200 yr apart.

The first was Jean Nicolet, Canadian explorer, born in Cherbourg, France, about 1598, who immigrated to Canada in 1618, travelled across the Indian territory, at that time called New France, and was the first white man to visit Wisconsin. He did not reach the Mississippi River, however, and later returned to Quebec. He drowned in the year 1642. A river, a country, and a town in Canada bear his name.

The other was Joseph-Nicolas Nicollett, 1786 to 1843, French mathematician and cartographer, who came to the United States in 1832 and explored the upper Mississippi in the years 1836, 1838, and 1839. His report, written in French, was translated to English by J. T. Ducatel and J. H. Alexander, and published in Congressional records.[88]

The improvements to the material concerning W. H. Hall, State Engineer of California, and the portrait furnished by Frazier, are highly appreciated. While

---

87 "History of the Town of Durham, New Hampshire," 1913.

88 Report intended to illustrate map of hydrographical basin of upper Mississippi River made by J. N. Nicollet. Senate Document 237, 26th Cong., 2nd Session, 1843, Serial No. 3PO; House Document 52, Vol. 2, 2nd Session, 1845, Serial No. 464.

it is true that several methods were initiated by Hall, who published a large volume of hydrometric data collected in California,[89] and several annual reports on irrigation from 1880 to 1888, his methods were mentioned in papers by his assistant C. E. Grunsky only, and therefore were attributed to Grunsky, although Grunsky himself did not claim them personally. This information concerning Hall and Grunsky was corrected in the recently published bibliography.[90]

J. C. Stevens, the eminent pioneer in hydrometry, was particularly favorable to the writer's intentions. He recalled the origin of the widely publicized theory of hydrologic importance of our forests, that was deliberately falsified in order to further conserve the forests. This was done in connection with a comparison of droughts in the Ohio basin of 1824 and from 1925 to 1930. It was particularly interesting to know the personal opinion of one of the authors of that story. Careful hydrometric investigations carried out in experimental forest basins in different countries had thoroughly explained the true hydrologic role of forests and clearings.

I. J. Moskvitinoff presented some conclusions from his hydrometric work in Central Asia from 1914 to 1915. The extensive investigations of the accuracy of flow measurements, the best investigations known to the writer, were included in the 5th volume of the Report of the Hydrometric Department for 1914,[91] that, regrettably, was never published. Fragments of this work appeared in Bulletins of the Hydrometric Department in Turkestan in 1917.[92]

Among the many letters received by the author in connection with his paper was a humorous contribution received from George Henry Ellis, M. ASCE, who wrote:

> "Years ago, when I was swinging the current meter, there was often a group of spectators asking foolish questions. The foolish answer I sometimes gave them grew, over a period of about thirty years, into the story of the counting of the fish."

The enclosed ballad entitled "The counting of the fish" of 1946 contains verses like "fishes cannot live in water near a power plant, with kilowatts squeezed out." This excerpt is a good example of hydrometric humor.

ADDENDUM TO APPENDIX II.—SHORT BIOGRAPHICAL DATA

Loammi Baldwin, b. May 16, 1780, at North Woburn, Mass., d. June 30, 1838, at Charlestown, Mass.; 1800 graduated Harvard Univ., built dams and harbors, 1821 Union canal in Penn., 1825 in Boston, built Connecticut-Hoosac tunnel; called Father of civil engineering in America.

---

89 "Physical data and statistics of California," by W. H. Hall, Tables and memoranda of data, collected and compiled by the State Engrg. Dept. of Calif., Sacramento, Calif., 1886.

90 "Bibliography of Hydrometry," by S. Kolupaila, Notre Dame, Univ. of Notre Dame Press, 1961. See references D 17, D 157, and H 12.

91 "Bibliography of Hydrometry," by S. Kolupaila, Notre Dame Univ., Notre Dame Ind., Press, 1961. See reference Y 67.

92 "Bibliography of Hydrometry, by S. Kolupaila, Notre Dame Univ. Press, Notre Dame, Inc., 1961. See reference H 294.

FIG. 65.—JOSEPH SAXTON

FIG. 66.—E. S. NETTLETON

FIG. 67.—G. W. RAFTER

FIG. 68.—D. C. HUMPHREYS

William Hammond Hall, b. Feb. 12, 1846, in Hagerstown, Md., d. Oct. 16, 1934, (only this information was available). 1879 State Engr. of California.

David Carlisle Humphreys, b. Oct. 14, 1855, in Chatham Hill, Va., d. Jan. 10, 1921, in Lexington, Va.; 1878 graduated Washington & Lee Univ., 1879 Mo. River investigations, 1885 to 1921 Prof., 1904 Dean, Washington & Lee Univ.; 1895 to 1908 Geological Survey; 1897, James River expedition.

Elwood Mead, b. Jan. 16, 1858, near Patriot, Ind., d. Jan. 26, 1936, in Washington, D.C.; 1882 graduated Purdue Univ., 1886 Prof. of Irrig. Engrg. Colorado Agric. College; 1899 Chf., Irrig. Investigations, Dept. Agric.; 1907 to 1913 river studies in Victoria, Australia, 1913 Prof., Univ. California, 1917 Calif. State Bd. on Irrig., 1923, 1927, Cons., Palestine, 1924 to 1936 Commis-

FIG. 69.—ELWOOD MEAD

FIG. 70.—F. W. HANNA

sioner, Bur. of Reclamation, promoter of Hoover Dam; reservoir on Colorado R. was named Lake Mead in his honor.

Edwin S.(*) Nettleton, b. Oct. 22, 1831, at Medina, Ohio, d. April 22, 1901, in Denver, Colo.; ed Medina Academy and Oberlin College, Ohio, 1870 Colorado town planner, 1883 to 1886 State Engr. of Colorado. (*) Adopted initial, no middle name.

Joseph-Nicolas Nicollet, b. July 24, 1786, in Cluses, Haute-Savoy, France, d. Sept. 11, 1843, in Washington, D. C.; cartographer, 1817 Paris astronomical observatory librarian, Prof. Louis College; 1830 ruined on stock market, 1832 immigrated to U. S., 1836 to 1839 Miss. River investigations.

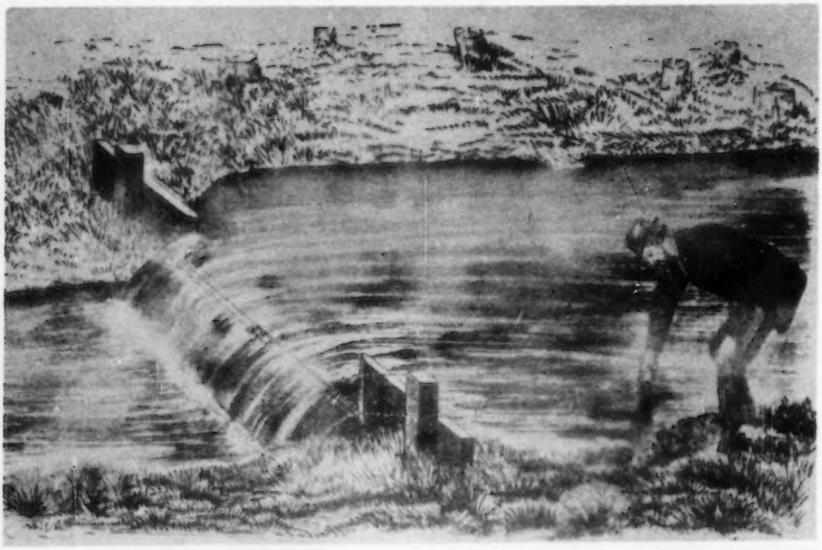

FIG. 71.—EARLY WEIR MEASUREMENT, LEFFEL, 1881

FIG. 72.—HYDROMETRIC TRAINING CAMP AT EMBUDO, N. M., 1888

Hamilton Smith, b. July 5, 1840, near Louisville, Ky., d. July 4, 1900, near Durham, N. H.; 1854 work in mining and hydraulic engrg, 1869 to 1881 in California, water supply for mining, 1881 Venezuela, London, 1892, South Africa, Alaska, mining, 1895 New York, cons. engr.

Extending cordial thanks to all contributors, the author has taken the opportunity to add several portraits located through the kind cooperation of Frazier. They are: J. Sexton, the first manufacturer of a current meter in the United States; E. S. Nettleton, State engineer of Colorado; G. W. Rafter, State engineer of New York; D. C. Humphreys, investigator of the James River (courtesy of the Washington and Lee University Library); E. Mead and F. W. Hanna, pioneers of the U. S. Bureau of Reclamation (courtesy of the Seattle Public Library). The interesting sketch of the early weir measurement[93] is also presented. (courtesy of Purdue University, Gorr Library). The historical group of the members at the first hydrometric training camp, near Embudo, New Mexico, in 1888, must also be included in the early history of hydrometry.

93 "Construction of Mill Dams," J. Leffel and Co., 1881.

GENERALIZED DISTRIBUTION NETWORK HEAD LOSS CHARACTERISTICS[a]

Closure by M. B. McPherson

M. B. McPHERSON,[25] M. ASCE.—The considered opinions, questions, arguments, clarifications, and original supplementary information presented by the thirteen engineers who contributed the nine discussions have placed the subject in much clearer perspective.

Little would be gained by reviewing the discussions point by point or by citing the multitude of statements with which the writer is in full agreement. Rather, the questions raised will be answered and clarifications offered.

Specific Details.—The writer stands corrected by Robertson on the improper use of the term "relaxation."

Constant mentions that the flows in each pipe can be checked during a network analysis by means of Eq. 6. For all of the network runs used in the paper, each junction and loop was checked to insure that the algebraic sums of all the corresponding flows and head losses were zero, with due allowance for attainable precision of meter readings. For the initial run of each network series, each and every pipe was checked via the equivalent of Eq. 6. Thereafter, on every second or third run all of the pipes were completely checked again to insure that all "fluistors" were operating properly. This is a standing operating procedure of the Philadelphia Water Department; it leaves little chance for error.

The error analysis by Constant is a valuable supplement. Some indication of relative error should have been included in the paper.

Constant contends that the procedures presented are principally applicable to field operations. Radziul and Celenza have clearly demonstrated the value of these procedures for operational purposes. However, an equally if not more important use is in the system analysis phase of design, as will be explained subsequently.

Bitoun has referred to the number of conditions required to define Fig. 4 and for determination of ϕ and n in Eq. 2. The "existing" district in Fig. 3 was studied to secure a more exact understanding of its characteristics because extensive, synchronized field tests were not practicable due to its large size. This preliminary study was of great value in subsequent studies of modifications required for future conditions. The field data were included in Fig. 4 for verification. More than one run was made for the Fig. 4 presentation to prove unequivocally that Eq. 1 was valid under the prescribed conditions. It was felt that a single run would not be adequate for that purpose with such a complex network, even though only one run is required to define K_1. It must be emphasized that a major consideration in the design of public utilities is the provision of adequate facilities for future needs. Seldom will an existing system

[a] January 1960, by M. B. McPherson (Proc. Paper 2339).

[25] Prof. of Hydr. Engrg., Civ. Engrg. Dept., Univ. of Illinois, Urbana, Ill.

be capable of handling anticipated higher future demands. Also, modern computational devices make possible more exact and realistic studies. Indeed, the inadequacy of many existing facilities can be attributed to the comparatively primitive computational procedures available and in vogue during the era in which they were designed.

Radziul and Celenza have clearly demonstrated the efficacy of using Eqs. 1 and 2 to determine the characteristics of existing prototype systems. The modifications planned for these two districts [Figs. 5 and 6(a)], either in progress or scheduled, will vastly change their existing (Tables 5 and 6) characteristics. Because variations in piping and source and storage facilities cannot be simulated under prescribed loading conditions with a prototype system, they must be simulated by means of some type of model. For this simulation one network analysis is required to define K_1 in Eq. 1 and two analyses are required to define ϕ and n in Eq. 2. Obviously, it matters not what computing device is used in analyzing a particular loading run, to paraphrase one of Lomax's observations.

Lomax states that it was "not so stated, but it is implied that the source magnitudes must be proportional as well as the load magnitudes." This would be true only in the specific instance of a network with a single source and no equalizing storage: Eq. 1 would apply for all system demands; each local demand load would be a fixed fraction of Q_d; here, because Q_p equals Q_d, the several loads would also be an equal fixed fraction of Q_p. A network fed by two sources is hydraulically quite similar to a single-storage, single-source combination (see Figs. 5 and 6) when the equalizing storage is contributing to the demand (Q_p less than Q_d). Two or more true sources, whether they be pumps or gravity storage, can be generalized by use of Eq. 2. The writer has made effective use of this procedure in the system analysis for a single-district large city that has two gravity storage reservoirs at dissimilar levels, a pumping station at a remote corner with a second station in a different quadrant needed for the future.

The system analysis of the single-source case without equalizing storage is obviously a routine matter. With multiple sources, or with single or multiple sources combined with equalizing storage, the number of hydraulic parameters that must be satisfied increase. The capacity per foot and relative water levels of storage, together with pump characteristic curves, must be reconciled with the network head loss characteristics under a variety of known or anticipated service conditions. The demonstration of storage-network-pump balancing that will be presented is a relatively simple example of a final or equilibrium phase of a system analysis. The paper was addressed to the issue of a generalization of network characteristics. In preparing the paper it was feared that a detailed treatment of system analysis would detract from and overextend the subject, but it is evident from some of the discussions that the paper should have been extended somewhat for a more firm appreciation of the potential uses of the concepts advanced.

Applicability of Proportional Load Principle to Non-Hydraulic Networks.—Trunk and Maier and Miller have clearly indicated that the proportional load principle is of little value in the analysis of gas system networks. Trunk reports (correspondence dated March 23, 1960) that prior to acquisition of a McIlroy Analyzer in 1953, his staff "resorted to the trick of thinking of a network as a single equivalent main," when a complete analysis was not warranted via manual computation. The relation between the equivalent pipe method and Eq. 1 will be discussed in a later section.

Mine ventilation networks have been investigated by means of a special McIlroy Network Analyzer by the U. S. Bureau of Mines, Health and Safety Research and Testing Center, Pittsburgh, Pennsylvania.[26] The resistance in mine airways is proportional to the square of the volume rate of flow. Although the basic procedure for analysis of mine networks is in many respects similar to that for other fluid media, loading conditions are rather unique. E. J. Harris, Acting Chief, Ventilation Group, U. S. Bureau of Mines, Pittsburgh, Pennsylvania describes the situation thusly (correspondence dated May 19, 1960):

> "We do use a form of Eq. 1; however, the application of 'proportional loading' to mine ventilation would be very limited. Where minor fan adjustments (speed or blade settings) are made with no other changes in the system a form of Eq. 1 and proportional loading would be and is applied. Where adjustments in distribution are entailed, use of Eq. 1 would be limited to major airways in which the resistance factor remains constant. Other factors would enter into the application."

As in all network analyses, accurate results can be achieved only through use of accurate pressure and quantity field survey data.

Alan C. Byers, Head, Electronics Branch, The Franklin Institute, Philadelphia, Pennsylvania (correspondence dated May 26, 1960) has carefully studied the paper:

> "My conclusion, after such a study, was that the paper does not present an analysis useful for load flow studies in power system practice. In order to avoid having this negative opinion be unchecked, engineers of the Philadelphia Electric Company were asked to study the paper also. Their electrical engineers in system planning find that there is nothing useful to them in the paper. They also had engineers from their steam and gas distribution systems, which might be thought to present closer analogies, read the paper. Here the paper was found of general interest, but not useful in any specific way. It seems that in each of these fields engineers have developed analytical methods well adapted to their problems. Doubtless, by drawing the correct analogies, the methods developed in the paper might also be used in these other fields. But there seems to be no advantage to be gained."

Reversing the orientation of these considered comments, it is apparent that the engineer engaged in water distribution network analyses should exercise caution in transferring or adapting to his use procedures or analogies that have been found satisfactory in the appraisal of electric power systems, gas, steam, or mine ventilation networks. The word "water" deliberately was not incorporated in the title of the paper because it was mistakenly assumed that Eq. 2 might prove useful in the analysis of non-hydraulic systems.

Clennon[27] has described a linear resistance analogue, and McIlroy[28] the non-linear type, for gas network analysis.

Fire Flow Analysis via Proportional Load Hydraulics.—The statement: "However, a fire load cannot be regarded as a representative proportional

---

26 "A Network Analyzer for Solving Mine-Ventilation-Distribution Problems," by G. E. McElroy, U. S. Bur. of Mines Information Circular 7704, November, 1954.

27 "Calculators Solve Flow Problems," by J. P. Clennon, Amer. Gas Assoc., October, 1951, pp. 68-70.

28 "Direct Reading Electric Analogue Computer Helps Solve Distribution Problems," by M. S. McIlroy, Gas Age, July 17, 1952, pp. 31-35.

load," was apparently misconstrued by the writers of two of the discussions. It was not intended to imply that fire flows cannot be analyzed via the proportional loading principle. Linaweaver, Geyer, and Wolff have correctly explained that a fire flow load per se is non-proportional, just as is the load imposed by elevated storage while being filled. An elementary network is shown in Fig. 10 to illustrate this point. The fire flow is termed Q_F and the head loss from Q_p to the fire flow point is termed Σh_F. The data for the four runs plotted in Fig. 10 are given in Table 8. It is apparent that Eq. 2 is appropriate for the analysis, so long as each non-fire load is a fixed proportion of the total non-fire load demand.

TABLE 8.—SUMMARY OF SIMULATED NETWORK FIRE FLOW RUNS (SEE FIG. 10)

	McIlroy Analyzer Runs			
	F-1	F-2	F-3	F-4
Q_p, mgd	7.96	12.07	14.09	15.90
Q_d, mgd	7.96	8.07	8.09	7.90
Q_F, mgd	0	4.00	6.00	8.00
$Q_d^{1.85}$	46.4	47.6	47.8	45.8
Σh_F, feet	17.9	57.6	89.8	129.1
Q_p/Q_d	1.00	1.49	1.74	2.01
$\Sigma h_F/Q_d^{1.85}$	0.386	1.21	1.88	2.82
(ϕ = 0.386 and n = 2.85)				

Using the standard fire flow extrapolation formula to anticipate run F-4 from runs F-1 and F-2:

$$Q = 4.00\left(\frac{111.2}{39.7}\right)^{0.54} = 7.0 \text{ mgd}$$

and run F-4 from runs F-1 and F-3:

$$Q = 6.00\left(\frac{111.2}{71.9}\right)^{0.54} = 7.6 \text{ mgd}$$

versus the true F-4 value of 8.0 mgd.

The elementary network given by Tong[29] will be used as a second example. In Table 9 are given the appropriate details for solution via Eq. 2. Note that the true higher fire flow is 1,000 gpm whereas for the standard formula it is 740 gpm.

These examples tend to exaggerate, to some extent, discrepancies between the standard formula and true values. Only the most remote point in the network was considered. It may be noted also that the larger the drop to the reference flow (39.7 ft, 71.9 ft and 2.3 ft) the better the formula approximation. It is understood that the National Board of Fire Underwriters (NBFU) normally requires a 10 psi drop before a fire flow sample is considered adequate

[29] Discussion of "Friction Losses in Lines with Service Connections," by A. L. Tong, Proceedings, ASCE, Vol. 86, No. 9, November, 1960, p. 160.

for rating purposes. Anderson reminds us that for adequate design, fire flows must be available under maximum day demand conditions. Whereas the standard formula yields extrapolated flows that are conservative (that is, low), the NBFU seldom extends field test data over a large increment beyond the test flows to estimate capacities at a 20 psi residual.

It should be noted that the standard formula is paradoxical, inasmuch as it is strictly applicable only when the fire flow approximates a proportional sys-

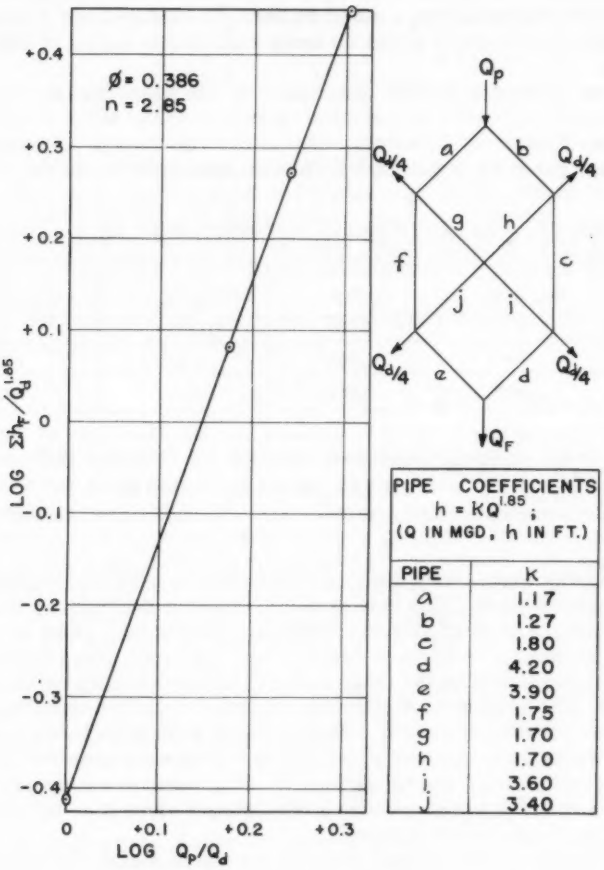

FIG. 10.—SIMULATED NETWORK FIRE FLOW RUNS (SEE TABLE 8).

tem load. This approximation is fairly exact in the extreme: when the fire flow is an insignificant part of the total system demand or when it is practically the entire system demand. The first instance is a local phenomenon because the effect of the additional system head loss attributable to the transport of the fire flow through the network is relatively small. In the second instance the fire

flow occasions the entire system loss and the standard formula is then equivalent to Eq. 1.

In the preceding two examples there is no equalizing storage. With equalizing storage there would be flow out of the reservoir(s) and the fire flow might be regarded as an additional, filling reservoir without a fixed or controlled water level. The use of Eq. 2 for fire flows with or without equalizing storage in conjunction with machine network analyses would be pointless because the design fire flow alone is required and normally can be determined directly. However, if it is evident that a field test at a given site would require extrapolation to the required flow, a standard formula extrapolated flow based on an intermediate fire demand would be more realistic in terms of ultimate NBFU rating.

Sweitzer[30] has presented a clear description of the procedure for a group hydrant flow test.

Unique Solution Feature of Networks.—Bitoun has referred to a demonstration of uniqueness given by d'Auriac.[12] The demonstration is an inferential

TABLE 9.—FIRE FLOW DATA FOR SMALL NETWORK GIVEN BY A. L. TONG

Q_d, gpm	Q_F, gpm	Q_p, gpm	Q_p/Q_d	Σh_F, feet
700	0	700	1.00	1.7[a]
700	300	1,000	1.43	4.0[b]
700	1,000	1,700	2.43	14.0[b]

[a] Computed by writer. [b] Computed by Tong. $n = 2.36$, and $\phi = 9.25 \times 10^{-6}$

$$300\left(\frac{14.0 - 1.7}{4.0 - 1.7}\right)^{0.54} = 740 \text{ gpm, versus } Q_F = 1000 \text{ gpm}$$

proof, limited to a topological consideration of boundary conditions too generally treated. It is summarized: "The unicity of the solution depends uniquely on the fact that conduit characteristics are increasing functions." This is to say that in addition to being a continuous function the head loss characteristic of pipes is bilateral, inasmuch as the magnitude of the loss is independent of the direction of flow. (The continuous, bilateral nature of resistive electrical impedances[31] makes possible the use of A.C. electrical analogues in the analysis of fluid flow networks.) A rigorous proof for $m = 2$ appears possible through use of special formulations of matrix algebra.[32] Attainment of a rigorous proof of uniqueness for network equations with a non-integer value of m is unlikely; an inductive proof of uniqueness follows.

Consider any balanced distribution network for which the flow in each main branch (both ends terminating at intersection junctions) may be described by:

$$h = k\,Q^m \quad \ldots\ldots\ldots\ldots\ldots\ldots \quad (13)$$

Because the network in question is balanced, the boundary conditions have been

30 "Basic Water Works Manual," by R. J. Sweitzer, Amer. Concrete Pipe Assoc., Chicago, 1958.

31 "Circuits in Electrical Engineering," by C. R. Vail, Prentice-Hall, Inc., New York, 1950.

32 "The Arithmetic Theory of Quadratic Forms," by B. W. Jones, Math. Assoc. of Amer., 1950.

satisfied exactly: the algebraic sum of flows at each main branch junction is zero,

$$\left| \begin{array}{l} i = f \\ \Sigma\, Q_i = 0 \\ i = 1 \end{array} \right| \quad 1, 2, \text{---}J \qquad \ldots\ldots\ldots\ldots\ldots\ldots \quad (14)$$

in which f is the number of separate flows at a junction (necessarily three or more in number) and J is the total number of junctions; the algebraic sum of head losses around each loop is zero,

$$\left| \begin{array}{l} i = b \\ \Sigma\, h_i = 0 \\ i = 1 \end{array} \right| \quad 1, 2, \text{---}L \qquad \ldots\ldots\ldots\ldots\ldots\ldots \quad (15)$$

in which b is the number of main branches in a loop and L is the total number of loops.

The combined number of loops L and junctions J in a network is equal to the total number of main branches Σb plus one. Immediately the loads are assigned values the branch flows remain the only unknowns. Because the input equals the sum of the loads the input junction equation is superfluous. The number of equations L+J=1 equals the number of unknowns Σb and, therefore, a solution is always possible.

For the balanced network under consideration Eqs. 13, 14, and 15 have been exactly satisfied. Rewriting Eq. 13

$$h = \left(kQ^{m-1}\right) |Q| = k_o |Q| \qquad \ldots\ldots\ldots\ldots\ldots \quad (16)$$

reduces its original bilateral non-linear form to a bilateral linear equivalent. The sign for each h in Eq. 15 must be determined from the sign of the corresponding balancing branch Q in Eq. 14 (note that when m = 2 the sign of h is intrinsically positive in Eq. 13). Because the magnitude and sign of $|Q|$ is fixed and k is a constant, each k_o has a singular constant value without sign, equal to the magnitude only of $\left(k\, Q^{m-1}\right)$. It follows that the transformation into linear equivalents can have no bearing on the integrity of Eqs. 14 and 15. If the equivalent linear form of Eq. 16 in k_o together with Eqs. 14 and 15 constitute a system with a unique solution; the solution for the original system of equations also must be unique.

Determinants will be used to investigate the simultaneous solution of the junction and loop equations for the balanced network with equivalent linear branches. For the j^{th} root of the solution

$$Q_j = \frac{D_j}{D} \qquad \ldots\ldots\ldots\ldots\ldots\ldots \quad (17)$$

in which Q_j is a branch flow, D_j defines the determinant containing the equation constants and D is the determinant of the equation coefficients. In D_j the constant for each loop equation would be a zero (except when a booster pump is interposed in a loop). However, loads and inputs are non-zero constants in the junction equations for an active network and consequently D_j is always unequal to zero. Because D_j is unequal to zero, the system of equations is nonhomogeneous and it is required that D be unequal to zero for a unique solution.[33] D will equal zero in this application only when any two of its rows or

[33] "The Mathematical Solution of Engineering Problems," by M. G. Salvadori and K. S. Miller, McGraw-Hill Book Co., New York, 1948.

columns have proportional elements. The order of D is $n = L + J - 1 = \Sigma b$, requiring representation for each and every branch flow in each of its rows. For a network with two or more loops a distinct and independent set of zero values characterizes each equation, precluding the possibility of proportional determinant elements, insuring a non-zero value for D (and D_j) and consequently a unique solution. The unique solution will yield a single, real value for the root characterising each branch flow. From preceding arguments the

TABLE 10.—EXAMPLE OF EQUIVALENT LINEAR NETWORK DETERMINANTS
(Balanced network of Case I, Fig. 2)

For the system of seven equations in seven unknowns, where $h = k_o|Q|$ (Eq. 16), the equations in terms of each branch are:

b	c	c'	d	d'	e	e'	Constant
$+Q_b$	$-Q_c$			$-Q_{d'}$			= 400
	$+Q_c$	$-Q_{c'}$					= 300
		$+Q_{c'}$	$+Q_d$		$+Q_e$		= 1100
			$-Q_d$	$+Q_{d'}$			= 200
					$-Q_e$	$+Q_{e'}$	= 450
	$+0.0240Q_c$	$+0.0146Q_{c'}$	$-0.0180Q_d$	$-0.0259Q_{d'}$			= 0
$+0.0016Q_b$			$+0.0180Q_d$	$+0.0259Q_{d'}$	$-0.0118Q_e$	$-0.0246Q_{e'}$	= 0

For branch b:

$$Q_b = \frac{D_b}{D} = \frac{\begin{vmatrix} 400 & -1 & 0 & 0 & -1 & 0 & 0 \\ 300 & +1 & -1 & 0 & 0 & 0 & 0 \\ 1100 & 0 & +1 & +1 & 0 & +1 & 0 \\ 200 & 0 & 0 & -1 & +1 & 0 & 0 \\ 450 & 0 & 0 & 0 & 0 & -1 & +1 \\ 0 & +0.0240 & +0.0146 & -0.0180 & -0.0259 & 0 & 0 \\ 0 & 0 & 0 & +0.0180 & +0.0259 & -0.0118 & -0.0246 \end{vmatrix}}{\begin{vmatrix} +1 & -1 & 0 & 0 & -1 & 0 & 0 \\ 0 & +1 & -1 & 0 & 0 & 0 & 0 \\ 0 & 0 & +1 & +1 & 0 & +1 & 0 \\ 0 & 0 & 0 & -1 & +1 & 0 & 0 \\ 0 & 0 & 0 & 0 & 0 & -1 & +1 \\ 0 & +0.0240 & +0.0146 & -0.0180 & -0.0259 & 0 & 0 \\ +0.0016 & 0 & 0 & +0.0180 & +0.0259 & -0.0118 & -0.0246 \end{vmatrix}}$$

From which $D_b \neq 0$, $D \neq 0$. Therefore only one value can exist for Q_b (Q_b=+1643 gpm).

corresponding solution with Eqs. 13, 14, and 15 also must be unique. Table 10 has been prepared to illustrate the non-zero, nonhomogeneous character of the determinants, using the Case I balanced network data of Fig. 2.

Only a single source has been discussed, but the proof applies as well to multiple sources with or without storage. For the special case of m = 1 the preceding proof is tacitly rigorous.

It appears that Camp and Hazen[34] were the first to adapt linear resistance electric computing boards to the analysis of water distribution networks, by means of an expression with the same meaning as Eq. 16. A trial and error procedure was used to find the set of k_o values that would satisfy the corresponding k values, using appropriate conversion factors to reduce electrical to hydraulic units. Much later, convergence procedures were developed[35,36] that vastly reduced the number of trials. Strangely, no proof of solution uniqueness was offered. Analysis by electrical analogy is based on satisfaction of Kirchhoff's laws (1845); with A.C. circuits, vector rather than algebraic sums must be used. Fich and Potter[37] give a valuable discussion on the elements of network topology and also cite special types of electronic network components that are associated with homogeneous systems of equations (a solution in indeterminate form may exist). Van Valkenburg[38] gives brief attention to resistive network analysis, but in his book and in a number of others reviewed no special effort has been made to prove general solution uniqueness, perhaps because of the comparatively small importance of purely resistive cases and emphasis on general circuit characteristics.

It may be noted in passing that electrical resistive analogues, using either linear or non-linear resistance elements, can be manipulated to satisfy different values of m for any or all pipes in the network. Reasons why the use of mixed values of m is normally unrealistic have been mentioned previously (3). Robertson has presented very convincing, comprehensive arguments for the use of a single value of m for analyses via digital computer. Lomax has called attention to the fact that laminar flow may occur in some pipes of a network, for which m = 1, but this consideration should not be critical in other than very small arterial networks or for unusually low minimum demand rates.

Bitoun's demonstration of the validity of Eq. 1 is a valuable contribution. Several decades ago one of the standard design procedures consisted of reducing a network by the equivalent pipe method to a single pipe. In order to do this all loads had to be consolidated into a single load. The method was particularly useful for small network fire flow analyses. While this equivalent pipe approach is repeatedly mentioned in the literature, it appears that J. Doland[19] was the first to suggest the simplified version of expressing the flows in each pipe as a percentage of the input. This principle has been extended without proof to multiple loads in elementary network examples in several text books. While writing the paper, the writer considered developing Eq. 1 via equivalent pipes but decided against it. In order to emphasize the fact that Eq. 2 is restricted to a single value of m and proportional loads, the simpler case without equalizing storage was offered in three levels of complexity as an introduction. Because all of the discussions relating to the equations indicate a clear understanding of these limitations, the approach used appears to have been successful. The demonstration of the validity of Eq. 1 by Bitoun could be

---

34 "Hydraulic Analysis of Water Distribution Systems by Means of an Electric Network Analyzer," by T. R. Camp and H. L. Hazen, Journal, N.E.W.W.A., Vol. 48, December, 1934, pp. 383-407.

35 "Network-Flow Analysis Speeded by Modified Electrical Analogy," by H. A. Perry, Jr., D. E. Vierling, and R. W. Kohler, E.N.R., September 22, 1949, pp. 19-23.

36 "Use of Alternating-Current Network Calculator in Distribution System Design," by M. V. Suryaprakasam, G. W. Reid, and J. C. Geyer, Journal, A.W.W.A., Vol. 42, December, 1950, pp. 1154-1164.

37 "Theory of A-C Circuits," by S. Fich and J. L. Potter, Prentice-Hall, Inc., New York, 1958.

38 "Network Analysis," by M. E. VanValkenburg, Prentice-Hall, Inc., New York, 1955.

extended to the storage case of Eq. 2. However, a boundary value approach will not lead to a full derivation of the latter. If the writer had abandoned the more complex case because his repeated attempts to arrive at a solution by direct derivation proved unsuccessful, Eq. 2 would not have been developed, albeit empirically via a similarity hypothesis.

Returning to the preceding proof of solution uniqueness, if each Q and constant in the system of simultaneous linear equations for m = 1 is multiplied by any particular non-zero constant, the solution is unchanged except that the roots are equal to the original roots times the constant. Bitoun's demonstration for Eq. 1 is indispensable for non-integer values of m.

System Analysis via Proportional Load Hydraulics.—The information in Table 11 is given in response to the request by Linaweaver, Geyer, and Wolff for a clarification of Table 4 flow ratios. The corresponding hydraulic grade

TABLE 11.—EXPLANATION OF FLOW RATIOS IN TABLE 4, ROX. H. S.[a]

Run No. (1)	Q_d, mgd (2)	Q_{PR}, mgd	Q_{SR}, mgd (two stand.)	$Q_{PR'} = Q_{PR} - Q_{SR}$ mgd	$Q_{PR'}/Q_d$ (3)	Q_{PW}, mgd	Q_{PW}/Q_d (10)	Q_{SW}, mgd (one stand.)	$Q_{SR}+Q_{SW}$, mgd
4A	26.9	9.45	-5.35	14.8	0.550	9.45	0.351	-2.65	-8.0
4B	9.2	9.45	+6.45	3.0	0.326	9.45	1.03	+3.25	+9.7
4C	17.4	6.6	-2.8	9.4	0.540	6.6	0.379	-1.4	-4.2
4D	7.9	6.6	+3.5	3.1	0.392	6.6	0.835	+1.8	+5.3
5A	26.9	—	-5.3	—	—	18.9	0.703	-2.7	-8.0
5B	9.2	—	+6.5	—	—	18.9	2.05	+3.2	+9.7
5C	17.4	—	-2.8	—	—	13.2	0.758	-1.4	-4.2
5D	7.9	—	+3.5	—	—	13.2	1.67	+1.8	+5.3
6A	26.9	18.9	-5.3	24.2	0.900	—	—	-2.7	-8.0
6B	9.2	18.9	+6.5	12.4	1.35	—	—	+3.2	+9.7
6C	17.4	13.2	-2.8	16.0	0.920	—	—	-1.4	-4.2
6D	7.9	13.2	+3.5	9.7	1.23	—	—	+1.8	+5.3

[a] (For Q_s, minus sign indicates flow out of storage and plus indicates flow into storage.) (Non-proportional load: Chestnut Hill; both series A and B, 1.2 mgd; both series C and D, 0.8 mgd.)

data for this Roxborough H.S. test series are given in Table 12. For this series, realistic water levels and storage rates were assigned for the Rox. standpipes, taken thereafter as a reference or control. The other water levels are from the network analyses, using this datum. The pump total dynamic head requirements for uniform daily pumping listed in Table 12 would be approximated quite well by the provisional pumps described at the bottom of the table [see also Figs. 5 to 7, (1a)]. The W.O.L. standpipe water levels are reasonable, realistic and satisfactory for a first phase design except for runs 6A and 6B. However, these two runs are for an outage at W.O.L.P.S. on the maximum day, an emergency condition under a rare combination of circumstances. The system layout in Fig. 7 was the first studied, and not the final arrangement adopted.

As Linaweaver, Geyer, and Wolff have emphasized, the computations presented for the Roxborough H.S. District are merely a first trial or feasibility

study, and "a thorough analysis would still be required"----"accounting for changes in levels of tanks and standpipes." The procedure for balancing that they describe could not have been applied effectively for this particular study because the proposed W.O.L. pumping station and standpipe, new pumps for the Rox. pumping station, and new major arterial mains were all unresolved design factors at the beginning of the study. It should be noted that Table 4 could be extended over a considerable number of other combinations by means of Eq. 2, for a balance study or to investigate other combinations of inputs.

Constant is of the opinion that the developments offered in the paper are of little value to the person concerned with improvements for a particular distribution system, apparently because Eq. 2 is restricted to a given loading distri-

TABLE 12.—WATER LEVELS AND PUMP REQUIREMENTS FOR TABLE 4, ROX. H. S.

Run	Rox. Standpipes (S_R), W.L. (Control) Feet	W.O.L. Standpipe (S_W), W.L. Feet	Rox. P.S. T.D.H. Feet	Rox. P.S. Disch. Hy.Gr. Feet	W.O.L. T.D.H. Feet	P.S. Disch. Hy.Gr. Feet
4A	501.5	494.2	103	504.5	167	495.1
4B	509.0	509.1	110	514.0	171	519.6
4C	512.2	509.2	109	514.0	170	510.4
4D	511.8	511.6	109	514.2	163	516.0
5A	501.5	500.7	—	—	208	525.9
5B	509.0	512.8	—	—	219	557.8
5C	512.2	512.0	—	—	198	526.0
5D	511.8	513.0	—	—	190	534.6
6A	510.5	479.3	116	514.0	—	—
6B	509.0	505.9	122	523.9	—	—
6C	512.2	501.2	116	519.0	—	—
6D	511.8	509.9	115	519.6	—	—

Provisional Pumps for Table 4 Study; Acceptable for Above, Special, and Future Demand Requirements:

	Rated Capacity, Mgd No. 1	No. 2	No. 3	Rated T.D.H., Feet	Shutoff, Feet
Rox. P.S.	7	10	10	110	160
W.O.L.P.S.	7	10	10	170	260

bution, network configuration, and set of flow coefficients. A given system design can be reduced to the hydraulic characteristics of four basic components: network, pump performance, pumping station and suction source, and storage. These must be integrated and reconciled with the design loadings. If the network proper is the only basic component subject to modification in the design, Constant's position is well taken. This would be a rather special design case. Nevertheless, Eq. 2 could still be of inestimable value in balancing final and alternative network schemes. Entirely too many designs have been based on fragmentary system studies. A comprehensive system analysis is required to insure that the benefits claimed for the design recommendations offered are physically attainable. From this standpoint it is difficult to see how "the operations end of distribution problems" can be considered independently from a

design alleged to be operable. Even in a perfunctory system analysis at least four normal consumption demand rates should be studied. Only the network analyses for two demand rates are necessary to obtain the constants in Eq. 2. The network hydraulics for other rates can then be computed using the equation, precluding the necessity for more than two runs for that particular network. Use of Eq. 2 is particularly effective when two or more basic compo-

TABLE 13.—EXAMPLE OF STORAGE-NETWORK-PUMP BALANCING USING PROPORTIONAL LOAD PRINCIPLE; BELMONT H. S.[f]

Time Interval (Starting at 6:30 am) in hours	Q_d (Ave., 9.3), in mgd	Pumping Station Suction Water Level, in Feet	Q_p (By Trial for each hour), in mgd	Storage Change, $\frac{Q_p - Q_d}{1.92}$, in feet[a]	Storage Water Level at Middle of Internal, in feet[b]	Σh via Eq. (2), ϕ=0.135, n=3.70, in feet[c]	Cal. Pump Total Dynamic Head, in feet[d]	Actual Pump Total Dynamic Head, in feet
(1)	(2)	(3)	(4)	(5)	(6)	(7)	(8)	(9)
0-1	9.6	247.5	9.15	-0.23	354.88	7.41	114.8	114.7
1-2	11.6	247.1	9.40	-1.15	354.20	5.77	112.9	112.8
2-3	11.7	246.6	9.45	-1.18	353.03	5.81	112.2	112.4
3-4	12.2	246.1	9.60	-1.35	351.77	5.69	111.4	111.3
4-5	11.7	245.6	9.60	-1.09	350.55	6.16	111.1	111.3
5-6	11.1	245.2	9.60	-0.78	349.61	6.78	111.2	111.3
6-7	11.1	244.7	9.64	-0.76	348.84	6.87	111.0	111.0
7-8	10.6	244.2	9.60	-0.52	348.20	7.36	111.4	111.3
8-9	10.2	243.8	9.52	-0.35	347.77	7.70	111.7	111.8
9-10	10.3	243.3	9.55	-0.39	347.40	7.63	111.7	111.7
10-11	10.5	242.8	9.56	-0.49	346.95	7.38	111.5	111.6
11-12	11.3	242.4	9.70	-0.83	346.30	6.80	110.7	110.5
12-13	12.3	241.9	9.85	-1.28	345.24	6.16	109.5	109.3
13-14	10.8	242.5	9.80	-0.52	344.34	7.68	109.5	109.7
14-15	9.6	243.2	9.74	+0.07	344.12	9.19	110.1	110.2
15-16	9.0	243.8	9.65	+0.34	344.32	10.18	110.7	110.9
16-17	8.4	244.5	9.57	+0.61	344.80	11.21	111.5	111.5
17-18	7.4	245.1	9.32	+1.00	345.60	12.79	113.3	113.4
18-19	6.1	245.8	8.90	+1.46	346.83	15.49	116.5	116.5
19-20	5.1	246.4	8.45	+1.74	348.43	17.81	119.8	119.8
20-21	5.1	247.1	8.37	+1.70	350.15	17.19	120.2	120.3
21-22	5.1	247.8	8.30	+1.67	351.83	16.65	120.7	120.7
22-23	5.1	248.6	8.25	+1.64	353.49	16.31	121.2	121.1
23-24	7.3	248.0	8.80	+0.78	354.70[e]	10.65	117.2	117.3

Notes: [a] For 2.0 million gal storage in 25-ft, over a 1-hr interval.
[b] Storage water level at 0 (6:30 a.m.) hours taken at El. 355.00 (Full).
[c] See Table 2.
[d] Col. (6) - Col. (3) + Col. (7).
[e] At 24 hr, El. 355.09; Q_p (ave.) for 24-hr = 9.31 mgd
[f] See Fig. 6(a) and Table 2.

nents of the system are subject to modification in the design, permitting investigation of several alternatives in the time that would otherwise be expended on only one combination.

Proof of the operability of a given design is best demonstrated by means of some sort of system balance. As noted by Linaweaver, Geyer, and Wolff, a

detailed hour-by-hour balance is not always necessary or desired. However, the more detailed the balancing the more indispensable Eq. 2 becomes, provided proportional loading can be assumed.

The use of Eq. 2 in the balancing of a system can best be illustrated by means of a detailed example. A storage-network-pump balance of the Belmont H.S. District (Fig. 6(a), Table 2) has been presented (5), but without benefit of Eq. 2. The system balancing outlined in Table 13 uses the same demands, storage, network and pump as in a previously noted example (5). To simplify the details in Table 13, the pumping station suction loss was taken as a constant (for Q_p = 9.3 mgd, that is, the ave.). In this way the clear well water level and suction loss could be combined in terms of a "pumping station suction water level." Other than this abbreviation, details are the same as previously given by the writer (5), but the balance is more exact.

Each hourly demand in Table 13 was balanced by trial in sequence. Each trial value of Q_p leads to a uniquely different value of Q_p/Q_d; approximately sixty trial combinations were needed for the preparation of Table 13. Without Eq. 2 a considerable number of network analyses would have been required for comparable exactitude. Recall that only two network analyses are needed to determine ϕ and n.

A realistic system balance is possible only when the basic system components are compatible. The Philadelphia Water Department is developing a system balance digital computer program that will incorporate Eq. 2 and subroutines for pump characteristics and pumping station suction loss. The pumping station hydraulics will be separated because pump characteristics and station losses are non-linear independent design factors. The comparative influence of diverse pump characteristics and storage capacities in the balancing for given networks will be investigated under a variety of demand schedules. The principal objective of the study is the determination of basic criteria for optimum utilization of equalizing storage and pumping facilities. The study was largely inspired by E. Shaw Cole, F. ASCE (1b). It is rather obvious that this study would not be feasible in the absence of the generalized network parameter, Eq. 2.

Corrections and Additions.—A recent article by Kincaid[39] should be added to the series given in the list of references (6).

The last equation of the paper should be corrected as stated by Constant. The word "now" should be substituted for "not" in the first line of p. 59, HY8, 1960. Inclusion of the following phrase enclosed by parentheses would clarify the sentence on page 127, HY9, 1960: "For systems without storage or with storage at or near the pumping station, proportional load hydraulics (via Eq. 1) accurately-------." Reference 19 appeared in Vol. 33, No. 2, pages 234 to 236, in February, 1941. In the line preceding Eq. 9, on page 41 of HY7 in 1960, "In any loop---" should be changed to read, "At any junction---."

39 "Value and Use of System Records in Long-Range Planning," by R. G. Kincaid, Journal, A.W.W.A., Vol. 52, February, 1960, pp. 277-283.

DRAG AND LIFT ON SPHERES WITHIN CYLINDRICAL TUBES[a]

Closure by Donald F. Young

DONALD F. YOUNG.[10]—Laursen's analysis of the results of this investigation in terms of the conventional critical tractive force is indeed interesting. Although, as noted, his analysis is speculative, it does demonstrate how lift and drag data of the type obtained may be utilized in sediment transport problems. The writer agrees that for the relatively large values of d/D used in this investigation the contraction of the flow is certainly significant, and that the study should be extended to smaller values of d/D that would be more characteristic of sediment transport problems. As pointed out in the paper, the same technique as was used in this investigation can be used to extend the range of values of the parameters. However, as the particle size becomes smaller it will become increasingly difficult to determine the conditions of impending motion.

With regard to Laursen's comment concerning the location of the lift it should be noted that as far as the equilibrium equations for the particle are concerned the resultant fluid force acting on the particle can be resolved into components at any point along the line of action of the force. The writer has arbitrarily resolved the resultant fluid force into a lift that passes through the center of the sphere and a drag that does not. It would, of course, be incorrect to arbitrarily assume that both components pass through the center of the sphere. Regardless of where the line of action of the lift is located, the condition still remains that at impending motion, in a direction normal to the pipe wall, the resultant fluid force must pass through the center of the sphere in order for rotation not to occur.

The angle β referred to by Laursen can be readily obtained from Eqs. 1 and 2 and the values of C_D and C_L given in Table 1. For impending motion $N = F = 0$ and therefore

$$\beta = \tan^{-1} \frac{C_D}{C_L} \quad \ldots\ldots\ldots\ldots\ldots\ldots (24)$$

The remarks of Indri concern the difference in flow conditions that exist between the case of solid bodies falling in a still fluid and the case of bodies held in equilibrium by a moving fluid. This is a distinction that is frequently overlooked. Certainly the velocity profile in the stream preceding the solid has an effect on the force exerted on the solid. Also, any turbulence in the approach stream is possibly significant. This is a problem that has concerned investigators working with wind tunnel models for some time.

---

[a] June 1960, by Donald F. Young (Proc. Paper 2526).

[10] Assoc. Prof., Dept. of Theoretical and Applied Mechanics, Iowa State Univ. of Science and Tech., Ames, Iowa.

For the investigation under discussion the experimental conditions utilized were similar to those normally encountered in studies related to the incipient motion of suspensions, that is, the particles were at rest and the fluid moving.

MODELS PRIMARILY DEPENDENT ON THE REYNOLDS NUMBER[a]

Closure by W. P. Simmons, Jr.

W. P. SIMMONS, JR.[17]—The clarification of concepts and nomenclature presented by Priest, Kolf, and Reitmeyer are important to those working with closed conduit flow problems. Priest correctly points out that Reynolds number applies to viscous motion and not directly to turbulent motion. Kolf and Reitmeyer likewise point out a distinction and affirm the use of Euler relationships for analyzing the model data. Chapple's contribution of a related and interesting problem well illustrates a facet of Reynolds number significance.

The paper emphasized that through an understanding of the Reynolds number, models of large closed-conduit systems, in which viscosity might be thought of as a predominant factor, may be made relatively insensitive to viscosity. This is predicated on the model being operated at Reynolds numbers greater than some critical value below which viscous effects are significant. Such models are indeed analyzed with parameters of the Euler variety that are dimensionally similar but conceptually different from the Froude ones. Thus, the statement that "...the data may be analyzed using the same relations as for models based on the Froude law" is misleading. It should be amended to read "...the data may be analyzed using Euler relations." As is pointed out, this conceptual difference involves no change in model techniques on data analysis. A point deserving further attention is that of determining Reynolds numbers high enough so viscous forces can be disregarded. By definition, **R** involves a characteristic length and flow velocity in the fluid system. These will have different significance in different systems. For example, for orifice flow in a full pipeline an **R**, based on orifice diameter and flow velocity of about 5×10^5 appears sufficient.[3] Similarly in a draft tube study an **R**, based on inlet conditions, of about 3×10^5 was satisfactory.[18] No doubt many other instances of satisfactory test results at **R**'s less that 1×10^6 can be cited. However, if minimum or near minimum values are to be used, these critical values must be determined through experiment. Unless it is worthwhile to make such tests, it seems convenient and safe to work in the range of the 1×10^6 value suggested in the paper.

---

[a] June 1960, by W. P. Simmons, Jr. (Proc. Paper 2531).

[17] Hydr. Engr., Div. of Engrg. Lab., Bur. of Reclamation, Denver, Colo.

[18] "Hydraulic Model Studies of Martin Dam Draft Tubes," by C. E. Kindsvater and R. R. Randolph, Jr., Transactions, ASCE, Vol. 120, 1955.

WATER EDDY FORCES ON OSCILLATING CYLINDERS[a]

Discussion by Donald VanSickle

DONALD VANSICKLE,[7] A.M. ASCE.—This paper is a most welcome addition to the authors' series of papers concerning wave forces on piling.[8] The accumulation of such data as they have presented is essential before design criteria can be established that correctly account for the many factors involved.

The writer is particularly interested in the relationship between drag forces on piles with tandem spacings because, in another investigation,[9] he studied this effect for H-section piles in uniform flow. It is of interest to compare the authors' test results on oscillating cylinders, their previous results on cylinders with uniform motion,[8] the writer's results on H-piles in uniform flow,[9] and the results of an NACA investigation of cylinders in uniform flow.[10]

To facilitate this comparison, the various test results are summarized in Fig. 7, in which the data are presented as ratios of the drag on the downstream pile of a tandem pair to the drag for a single pile for various center-to-center pile spacings. It was necessary to compute the ratios for the NACA tests using the given drag coefficients and a drag coefficient of 1.2 for the single cylinder. For the authors' tests on cylinders with uniform motion, the ratios were determined from the mean values of the drag coefficients for the various velocities. The results for the H-piles were already in the form of drag coefficients. The authors' results on oscillating cylinders are presented as the ratios of drag forces; however, if the depths and velocities for the tandem cylinders correspond to those for the single cylinder, the ratios of drag forces should correspond to the ratios of drag coefficients. It should be mentioned that the center-to-center spacings for the square H-piles are pile widths, whereas those for the cylinders are cylinder diameters.

An examination of Fig. 7 reveals the following points:

1. All of the curves have essentially the same shape. The ratio of drag coefficients increases with increased spacing up to about four diameters spacing. For spacings in excess of four diameters, the ratio of drag coefficients remains practically constant. It would appear, then, that a center-to-center spacing of approximately four diameters is the critical spacing as far as drag forces are concerned.

---

[a] November 1960, by Alan D. K. Laird, Charles A. Johnson, and Robert W. Walker (Proc. Paper 2652).

[7] Hydr. Engr., Turner & Collie Cons. Engrs., Inc., Houston, Tex.

[8] "Water Forces on Accelerated Cylinders," by A. D. K. Laird, C. A. Johnson, and R. W. Walker, Proceedings, ASCE, Vol. 85, No. 1, March, 1959.

[9] "An Experimental Investigation of the Drag Characteristics of a Model H-Section Bridge Pier," by Donald R. VanSickle, thesis presented to the Univ. of Texas at Austin, Tex., in 1958 in partial fulfillment of the requirements for the degree of Master of Science.

[10] "The Interference Between Struts in Various Combinations," by David Biermann and W. H. Herrnstein, Jr., NACA Report No. 468, 1933.

2. The results of the authors' previous tests on tandem cylinders with uniform motion are in substantial agreement with the results of the NACA tests. D. Biermann and N. H. Herrnstein[10] suggest that the negative drag forces at close spacings are caused by "the vortices produced by the front cylinder (which) probably encircle the rear cylinder, impinging on the back surface with sufficient force to produce a forward reaction." The directions of the eddies shown in Fig. 6 indicate that this is certainly a reasonable explanation. Both sets of test results further indicate, for spacings greater than four diameters, a leveling off of the drag coefficient for a cylinder with neighbor at from 0.25 to 0.40 the drag coefficient for a single cylinder. Biermann and Herrnstein[10] advance the hypothesis that "the boundary layer of the second cylinder is made turbulent by the rapid changes of velocity and direction of the flow behind the first cylinder." The well-known fact that the drag coefficient

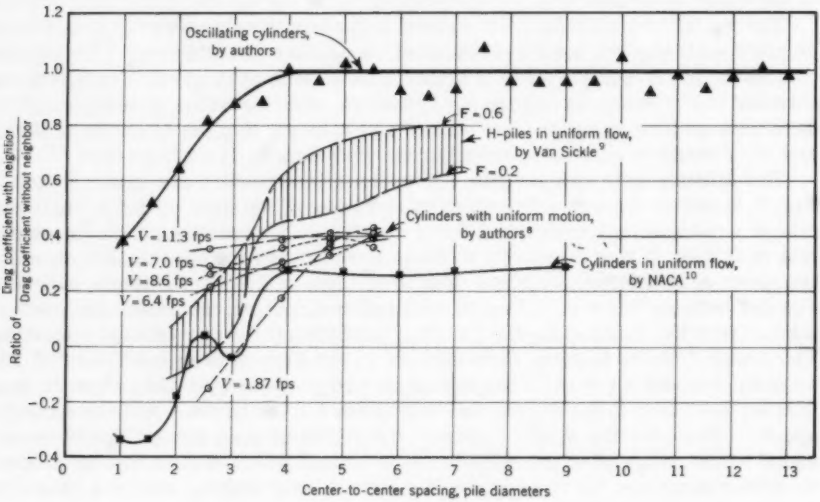

FIG. 7.—VARIATION OF DRAG COEFFICIENT RATIO WITH PILE SPACING

of a cylinder decreases to approximately one-fourth of its normal value when the boundary layer becomes turbulent[11] lends much support to this hypothesis.

3. The results of the study of tandem H-piles are shown as a shaded area in Fig. 7. The lower line of the area represents a Froude number of 0.2, and the upper line represents a Froude number of 0.6. To avoid complicating Fig. 7, the curves for intermediate values of Froude number are not shown; however, as the Froude number increases from 0.2 to 0.6, the curves shift upward in fairly uniform steps. The shape of these curves is very similar to the shape of the curves for cylinders in uniform flow. The negative drag coefficients for close spacings can be accounted for as suggested in point 2. Although, for spacings greater than four diameters, a similar leveling off of the drag coefficient

11 Hunter Rouse, ed. Engineering Hydraulics, John Wiley & Sons, New York, 1950, p. 124.

for an H-pile with neighbor occurs at values of 0.60 to 0.80 the coefficient for a single H-pile, no convenient explanation is available. The point of separation for the H-pile is essentially fixed at the sharp flange edge, and no shift downstream, with a reduction in drag coefficient, occurs when the flow becomes turbulent.

4. In contrast to these observations for tandem piles in uniform flow, the authors' data for oscillating cylinders indicate that no negative drag forces occur. Furthermore, while the drag coefficient levels off for spacings greater than four diameters, it does so at the same value as for a single cylinder. In other words, as the authors point out, for oscillating cylinders the effect of the upstream cylinder is negligible for spacings greater than four diameters.

It occurred to the writer that because the authors' results were presented as a ratio of the force on the cylinder with neighbor to the force on a single cylinder, the leveling off of the ratio at a value of 1.0 could be explained if the oscillatory motion, for some unknown reason, caused the boundary layer for the single cylinder to be turbulent. The occurrence of turbulent flow on the downstream cylinder of the tandem pair would then produce the turbulent drag force, and a drag ratio of 1.0. The authors point out, however, that "the drag coefficients corrected to infinite cylinder values were the usual 1.3 to 1.4 for the vertical cylinders extending through the water surface." Because this is the drag coefficient for laminar boundary layer conditions, it is evident that the previously described explanation cannot apply.

Another alternative is that the downstream cylinder of an oscillating tandem pair does not encounter turbulent flow conditions, whereas the downstream cylinder in uniform flow does. There would seem to be no obvious reason why such a condition should exist.

Experimental error would not seem to be a factor because the authors' previous work, using essentially the same equipment and procedures, gave results in substantial agreement with the NACA tests.

There remains the further possibility that the hypothesis advanced by Biermann and Herrnstein to explain the reduced drag on the downstream cylinder is not valid. The fact that their hypothesis cannot explain the reduced drag on the downstream H-pile adds weight to this argument. Such a conclusion, however, does not explain why piles in uniform flow have reduced drag on the downstream pile at spacings in excess of four diameters, whereas cylinders in oscillating motion do not have reduced drag for these spacings.

Do the authors know of any reason, or could they present a reasonable hypothesis, why this situation should exist?

Could they state whether or not they actually encountered negative drag forces in any of their tests on oscillating cylinders?

FISH PASSAGE THROUGH HYDRAULIC TURBINES[a]

Discussion by J. F. Muir

J. F. MUIR,[2] F. ASCE.—The research on the passage of young fish through hydraulic turbines, by Von Gunten and his associates, is one of the most important projects arising from the 3.5 million dollar fisheries-engineering research program initiated in 1951 by the Corps of United States Army Engineers.

These recent tests furnish further evidence that the Corps of Engineers' program, participated in by all the major fisheries organizations in the Pacific Northwestern states, has paid handsome dividends. A wealth of data has been published giving criteria for the safe passage of fish past dams.[3,4,5] The writer believes that this program and further research will very likely show that rivers can be developed for multi-purposes, including the preservation of anadromous fish.

The preliminary tests on the passage of fingerlings through small Francis and Kaplan runners 12 in. in diameter in the laboratory showed that cavitating conditions in a turbine will kill fish. The rate of mortality is related to the magnitude of partial vacuum present in the water passages.

The full scale tests at Cushman dam confirmed laboratory findings showing that significant mortality does not occur among young fish subjected to an abrupt reduction in water pressure from up to 200 psi to atmospheric. The tests showed a significant improvement in survival rates resulting from the reduction in cavitation in the turbine when the tailwater level rose 10 ft. The maximum mortality occurred when the turbine operated under partial loading, a condition known to result in a worsening of cavitation phenomena.

The writer had the opportunity of witnessing the Cushman tests and was particularly interested in observing the fish for evidence of the bends. Experiments at the University of British Columbia (Vancouver, B. C.) have shown that the bends are likely to occur among fish subjected to a partial vacuum of high intensity for periods of time considerably greater than the time of passage through the Cushman turbines. The writer saw no symptoms of the bends among the Cushman fish after the tests and believes that few fish were killed or seriously injured by the effects of a partial vacuum unaccompanied by cavitation.

---

[a] May 1960, by Glenn H. Von Gunten (Proc. Paper 2812).

[2] Head, Dept. of Civ. Engrg., Univ. of British Columbia, Vancouver, Canada.

[3] "Progress Report on Fisheries-Engineering Research Program," Corps of Engrs., U. S. Army, Pacific Div., November, 1956.

[4] "Progress Report on Fisheries-Engineering Research Program," Corps of Engrs., U. S. Army, Pacific Div., July, 1960.

[5] Annotated Bibliography on Fish Passing Facilities, Committee on Power Project Planning and Design, Power Div., ASCE, September, 1960.

One interesting feature of the Cushman tests was the efficiency of the large net used to trap fingerlings. The mouth of the net completely covered the draft tube exit and trapped approximately 90% of the fish passing through the turbine during the tests. Ivan J. Donaldson and his colleagues are to be commended for their pioneering work on the design of large nets for this purpose.

The research of Von Gunten and his associates points to a further program designed to solve the problem of successful passage of fish through turbines. One important aspect of this problem is the determination of relationships between turbine specific speed, the cavitation parameter sigma, and fish mortality. The Cushman turbines are placed at an elevation about 1 ft above tailwater level at high tide. In a future plant similar to Cushman, sigma could be increased more than 50% by lowering the turbines about 20 ft. One wonders about the extent of improvement in fish survival rates with such a substantial increase in the value of sigma.

In the light of the author's findings, it would be of interest if he would discuss the changes in operating conditions called for at existing plants on the Columbia River system. During the migration period, is it now standard practice to avoid turbine operation under low load conditions in plants in which young fish pass through turbines on their way to the sea?

It would also be of interest to have Von Gunten's comments on the possibility of safe passage of migrants through the Grand Coulee and Chief Joseph turbines. It would now appear that the rehabilitation of the salmon runs in the upper Columbia River is within the realm of future possibilities.

ERRATA

Journal of the Hydraulics Division

Proceedings of the American Society of Civil Engineers

"Uniform Water Conveyance Channels in Alluvial Material" by Daryl B. Simons and Maurice L. Albertson, May 1960, Proc. Paper 2484.

p. 64. Under the heading "Design Procedures: Estimating W Knowing P or Vice Versa" in lines 1 and 5 change the word wetter to wetted.